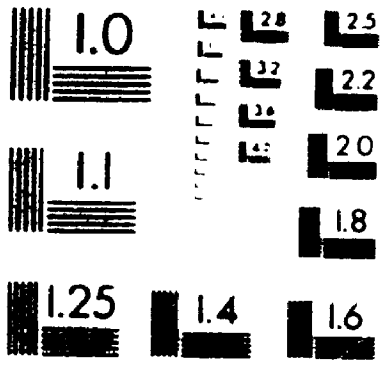
1.0
1.1
1.25
1.4
1.6
1.8
2.0
2.2
2.5
2.8
3.2
3.6
4.0

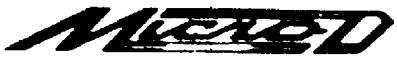

National Library of Canada
Bibliothèque nationale du Canada

Canadian Theses Service
Services des thèses canadiennes

Ottawa, Canada
K1A 0N4

CANADIAN THESES

THÈSES CANADIENNES

NOTICE

The quality of this microfiche is heavily dependent upon the quality of the original thesis submitted for microfilming. Every effort has been made to ensure the highest quality of reproduction possible.

If pages are missing, contact the university which granted the degree.

Some pages may have indistinct print especially if the original pages were typed with a poor typewriter ribbon or if the university sent us an inferior photocopy.

Previously copyrighted materials (journal articles, published tests, etc.) are not filmed.

Reproduction in full or in part of this film is governed by the Canadian Copyright Act, R.S.C. 1970, c. C-30.

AVIS

La qualité de cette microfiche dépend grandement de la qualité de la thèse soumise au microfilmage. Nous avons tout fait pour assurer une qualité supérieure de reproduction.

S'il manque des pages, veuillez communiquer avec l'université qui a conféré le grade.

La qualité d'impression de certaines pages peut laisser à désirer, surtout si les pages originales ont été dactylographiées à l'aide d'un ruban usé ou si l'université nous a fait parvenir une photocopie de qualité inférieure.

Les documents qui font déjà l'objet d'un droit d'auteur (articles de revue, examens publiés, etc.) ne sont pas microfilmés.

La reproduction, même partielle, de ce microfilm est soumise à la Loi canadienne sur le droit d'auteur, SRC 1970, c. C-30.

THIS DISSERTATION
HAS BEEN MICROFILMED
EXACTLY AS RECEIVED

LA THÈSE A ÉTÉ
MICROFILMÉE TELLE QUE
NOUS L'AVONS REÇUE

NL-339 (r. 86/06)

Canada

# Silicification in a Semiconformable Alteration Zone below the Chisel Lake Massive Sulphide Deposit, Manitoba.

by

Roger G. Skirrow

Thesis submitted to the
Faculty of Graduate Studies and Research
in partial fulfillment
of the requirements for the degree
Master of Science

Department of Geology
Carleton University
Ottawa, Ontario, Canada.

© March 1987

Permission has been granted to the National Library of Canada to microfilm this thesis and to lend or sell copies of the film.

The author (copyright owner) has reserved other publication rights, and neither the thesis nor extensive extracts from it may be printed or otherwise reproduced without his/her written permission.

L'autorisation a été accordée à la Bibliothèque nationale du Canada de microfilmer cette thèse et de prêter ou de vendre des exemplaires du film.

L'auteur (titulaire du droit d'auteur) se réserve les autres droits de publication; ni la thèse ni de longs extraits de celle-ci ne doivent être imprimés ou autrement reproduits sans son autorisation écrite.

ISBN 0-315-35854-8

The undersigned recommend to the Faculty

of Graduate Studies acceptance of the thesis

"Silicification in a semiconformable alteration zone below the Chisel Lake massive sulphide deposit, Manitoba"

submitted by

Roger G. Skirrow

in partial fulfillment of the requirements for

the degree of Master of Science.

Thesis Supervisor

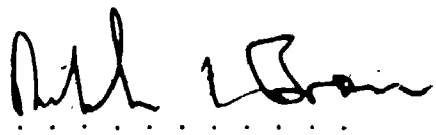

Chairman, Dept. of Geology

Carleton University

1987

## Abstract

A large semiconformable zone of silicified, Fe-metasomatized and epidotized, dominantly mafic, volcaniclastic units and flows is exposed 0.5-2 km stratigraphically beneath the Chisel Lake Zn-Cu massive sulphide deposit in the Snow Lake district, Manitoba. The alteration was metamorphosed to medium grade and is crudely zoned from distal, deeper silicification and epidotization to Fe-metasomatized, garnet-chlorite±biotite±staurolite rocks nearer the Chisel Lake deposit.

Silicification ranges from partial to complete replacement of clast margins, pillow margins and rocks adjacent to some felsic dykes by silica and sodic plagioclase, and involved intense leaching of Fe, Mg, Mn and, in places, Ca and Zn, as well as addition of Si and Na. Element fluxes during Fe-metasomatism generally were opposite to those in silicification, whereas clinozoisite-rich rocks are depleted in Na, Fe, Mg, Mn, K, Zn and Ba and enriched in Ca and Sr, relative to less altered equivalent rocks.

Almost constant ratios of Ti, Zr and Al in altered and less altered rocks indicate that these elements were essentially immobile during metasomatism, except possibly where large gradients of $P_{CO2}$, or extremely high water/rock ratios existed. Limited data suggest that HREE also were not significantly mobile during silicification.

A model of alteration is proposed in which Si supersaturated, Na-rich fluids interacted with the volcanic rocks, in places at temperatures of greater than 350°C, to produce silicification in a sub-seafloor geothermal system. A portion of the leached Fe, Mg, Mn and Zn were transported to both local and more distant sites of deposition in the lower semiconformable alteration zone, according to the model.

The detailed relationship of silicification to massive sulphide deposits in the area remains unclear, but data from this study and comparison with examples elsewhere indicate that silicification may have been directly involved in generating an ore fluid, although a more passive role in the ore-forming process can not be dismissed.

Large silicified zones, particularly in association with Fe-metasomatized rocks, provide potentially important guides for locating favourable environments of volcanic-associated massive sulphide deposition.

**Acknowledgements**

I wish to extend special thanks to Dr. J.M. Franklin of the Geological Survey of Canada, who suggested the map area, supervised the study and provided generous support in all aspects of the work.

Drs. E. Froese and J.W. Lydon of the Geological Survey of Canada and Dr. D.H. Watkinson of Carleton University are thanked for critical reviews of early drafts of the thesis, and for many hours of stimulating discussion. Grateful appreciation is extended to A. Galley and D. Ames of the Geological Survey of Canada for arranging logistical support in the field and for their warm friendship.

Discussions with Dr. A.H. Bailes, Manitoba Energy and Mines, and generous access to his regional geology work, helped greatly.

The cooperation of Hudson Bay Exploration and Development Ltd., and particularly J. Kitzler and D. Ziehlke, in permitting mapping on the property, is gratefully acknowledged.

S. Barham and L. Harnois, Carleton University, and E. Zaleski, University of Manitoba, endured the author and shared ideas.

C. Pitre ably assisted in field work.

To Ursula Johns, I extend my sincere appreciation for typing the thesis and for her encouragement and patience throughout the study.

The project was financially supported by a contract to D.H. Watkinson from the Department of Supply and Services, a National Research Council of Canada Postgraduate Scholarship (1985-86), and Carleton University teaching and research assistantships (1984-86).

## TABLE OF CONTENTS


| | Page |
|---|---|
| Abstract | iii |
| Acknowledgements | iv |
| Table of Contents | v |
| List of Tables | viii |
| List of Figures | ix |
| List of Appendices | xii |

Chapter

1. INTRODUCTION

| | | |
|---|---|---|
| 1.1 | Purpose of the study | 1 |
| 1.2 | Location and access | 2 |
| 1.3 | Previous and current work | 3 |
| 1.4 | Methods | 3 |

2. REGIONAL GEOLOGY

| | | |
|---|---|---|
| 2.1 | Stratigraphy | 8 |
| 2.2 | Intrusive rocks | 10 |
| 2.3 | Massive sulphide deposits | 10 |
| 2.4 | Regional and local structure | 12 |
| 2.5 | Metamorphism | 13 |

3. STRATIGRAPHY AND VOLCANOLOGY

| | | |
|---|---|---|
| 3.1 | Flow unit MP1: plagioclase-phyric mafic flow | 15 |
| 3.2 | Heterolithic volcanic breccia HB | 17 |
| 3.3 | Flow unit MA: aphyric mafic flows and breccia | 17 |
| 3.4 | Plagioclase-phyric flow unit MP2 and iron sulphidic mafic wacke | 19 |
| 3.5 | Felsic and mafic volcaniclastic units FMVC1 and FMVC2 | 19 |
| 3.6 | Plagioclase-phyric flow units MP3 - MP5 | 21 |
| 3.7 | Pyroxene-phyric flow units MX1 - MX5 | 22 |

3.8 Mafic volcanic siltstone, wacke and breccia: MVC . 23

3.9 Heterolithic volcaniclastic unit: HVC. . . . . 24

3.10 Pyroxene-phyric mafic flow and related breccia, and felsic and mafic volcaniclastic unit FMVC3 . . . . 26

3.11 Ultramafic and mafic intrusive rocks . . . . . 27

3.12 Plagioclase-phyric and aphyric felsic intrusions . . 28

3.13 Composite felsic-mafic dykes . . . . . 29

3.14 Fine grained quartz-plagioclase-phyric felsic dykes . 31

3.15 Quartz-plagioclase porphyry. . . . . 31

4. **ALTERATION**

4.1 Silicification . . . . . 35

4.1.1 Silicification of pillows and massive flows . 36
4.1.2 Silicification of clasts . . . . . 41
4.1.3 Silicification adjacent to felsic dykes. . . 42
4.1.4 Other forms of silicification . . . . . 45
4.1.5 Timing and depth of silicification . . . . 48

4.2 Epidotization . . . . . 50

4.3 Garnet-chlorite alteration . . . . . 52

4.4 Plagioclase-quartz-bordered fractures. . . . . 54

4.5 Iron sulphide alteration . . . . . 56

4.6 Summary of alteration distribution and timing . . . 59

5. **GEOCHEMISTRY**

5.1 Geochemistry of least altered rocks . . . . . 62

5.1.1 Mafic rocks . . . . . 62
5.1.2 Felsic rocks. . . . . 68

5.2 Geochemistry of alteration . . . . . 70

5.2.1 Alteration of pillows and massive flows. . . 71
5.2.2 Gains and losses in other types of alteration. 77
5.2.3 Effects of alteration on Ti, Zr, Al and REEs . 84

6. DISCUSSION

6.1 Origin of silicification . . . . . 89

6.1.1 Evidence for alteration origin of silicic zones in pillows . . . . . 89
6.1.2 Net gains and losses in the pillows . . . . 92
6.1.3 Porosity and permeability controls on silicification. . . . . 94
6.1.4 Metal leaching and Na addition. . . . . 96
6.1.5 Source of Si . . . . . 107
6.1.6 Precipitation of Si . . . . . 107
6.1.7 Conclusions on silicification . . . . . 115

6.2 Origin of epidotization . . . . . 116

6.3 Origin of garnet-chlorite and garnet-biotite alteration . . . . . 118

6.4 Model of alteration and comparison with other areas. 121

7. CONCLUSIONS . . . . . 124

REFERENCES . . . . . 128

APPENDICES . . . . . 140

## LIST OF TABLES


| Table | | Page |
|---|---|---|
| 1. | Stratigraphy of the Edwards Lake area | 16 |
| 2. | Summary of timing of alteration. | 61 |
| 3. | Calculation of net gains and losses in a zoned pillow. | 93 |
| 4a. | Comparison of elemental gains and losses and pH in fluid-rock experiments. | 99 |
| 4b. | Comparison of elemental gains and losses in alteration at Edwards Lake and other natural hydrothermal systems. | 100 |
| 5. | Mineral assemblages of samples analyzed for major and trace elements. | 141 |
| 6. | Plagioclase compositions. | 147 |
| 7. | Representative analyses of amphiboles | 148 |
| 8. | Representative analyses of chlorite and garnet. | 149 |
| 9. | Representative analyses of epidote-group minerals. | 149 |
| 10. | Whole rock major and trace element compositions. | 151 |
| 11. | Rare earth element abundances. | 161 |
| 12. | Routine precision of XRF and ICP analyses at the University of Ottawa and Geological Survey of Canada laboratories. | 164 |
| 13. | XRF major and trace element composition of ANRT standard DR-N. | 165 |
| 14. | Detection limits for trace elements, $H_2O$, $CO_2$ and FeO. | 166 |
| 15. | Precision or reproducibility of sample and fused pellet preparation procedures | 166 |
| 16. | Mass gains and losses (%) between less altered and altered rocks. | 168 |
| 17. | Mass gains and losses of REE. | 171 |

## LIST OF FIGURES


| Figure | | Page |
|---|---|---|
| 1. | Location of the Edwards Lake area and regional geology. | 5 |
| 2a. | Geology of the Edwards Lake area (scale 1: 2000) . . | (in pocket) |
| 2b. | Simplified geology of the Edwards Lake area. . . . | 6 |
| 3a. | Alteration in the Edwards Lake area (scale 1: 2000) . . . . . | (in pocket) |
| 3b. | Simplified alteration distribution in the Edwards Lake area. . . . . | 7 |
| 4. | Sample location map . . . . . | (in pocket) |
| 5. | Schematic representation of simplified stratigraphic sequence (a) and alteration zones (b), Chisel-Edwards Lakes area. . . . . | 9 |
| 6. | Schematic reconstruction of the pipe and lower semi-conformable alteration zones at the Anderson and Stall Lakes deposits. . . . . | 11 |
| 7. | Intensely silicified plagioclase-phyric mafic pillows, containing patches of very intense silicification and abundant concentric thermal contraction cracks. . . | 39 |
| 8. | Fragment of silicified plagioclase-phyric pillow rock in heterolithic breccia unit HB. . . . . | 39 |
| 9. | Zoned, altered aphyric mafic pillow near the base of flow unit MA. . . . . | 39 |
| 10. | Zoned alteration patches in a massive aphyric mafic flow near the base of flow unit MA.. . . . . | 44 |
| 11. | Silicified margins of aphyric pillows near the top of flow unit MA. . . . . | 44 |
| 12. | Large clast of an intact group of three silicified pillows in heterolithic breccia unit HVC. . . . . | 44 |
| 13. | Mafic volcanic wacke silicified to a mottled, light grey rock adjacent to a high - $TiO_2$ felsic dyke. . . | 47 |
| 14. | Pervasive discordant silicification of mafic volcaniclastic rock. . . . . | 47 |
| 15. | Plagioclase-quartz-bordered fractures in mafic volcanic wacke. . . . . | 58 |

16. Plagioclase (-quartz) - bordered fractures in fine grained mafic dyke. . . . . 58

17. Quartz-plagioclase porphyry dyke cross-cutting a plagioclase-quartz-bordered fracture in previously-silicified mafic volcanic wacke. . . . . 58

18. $TiO_2$ versus Zr plot of the principal rock types in the Edwards Lake area. . . . . 64

19a. AFM plot of least altered mafic flows. . . . . 65

19b. Jensen cation plot of least altered mafic intrusive rocks and composite dykes. . . . . 65

20. Jensen cation plots of less altered and altered mafic and felsic rocks. . . . . 67

21. Isocon diagram illustrating the method for calculating mass and volume changes during metasomatism. . . . 72

22. Mass gains and losses across a pillow, and the range of gains and losses in all pillows studied. . . . . 73

23. Mass gains and losses in pervasive silicification of volcaniclastic rocks, plagioclase-quartz-borders to fractures, pervasive epidotization and garnet-chlorite (-biotite) alteration. . . . . 74

24. Chondrite - normalized REE abundances of samples in an altered pillow. . . . . 78

25. Plot of Zr/Ti versus Nb/Y, comparing least altered mafic flows to silicified mafic flows. . . . . 79

26. Chondrite - normalized REE abundances in a less altered felsic volcaniclastic rock and the silicified equivalent. 81

27. Molar changes of Si versus Fe + Mg and Si + Na versus Fe + Mg + Ca during silicification of felsic volcaniclastic rock, mafic volcaniclastic rocks and pillow margins. . . . . 96

28. Comparison of the extent of mass transfer in g per 1000 $cm^3$ resulting from silicification, epidotization and Fe-metasomatism at Edwards Lake, with the extent of mass transfer of altered tholeiitic basalt from the Svartsengi geothermal system, and of epidote- and chlorite-rich altered ocean floor basalts. . . . . 104

29. Calculated solubilities of quartz in water up to 900°C at various pressures. . . . . 109

30. Solubility of quartz from 25°C to 300°C at pH values ranging from 7 to 10. . . . . 113

31. Schematic reconstruction of a cross-section through the alteration zones in the Edwards Lake area, showing generalized elemental gains and losses during alteration and spatial relationships to stratigraphy and intrusions. 123

## LIST OF APPENDICES


| Appendix | | Page |
|---|---|---|
| 1. | Mineral assemblages of samples analyzed for major and trace elements. | 140 |
| 2 | Mineral compositions. | 146 |
| 3. | Whole rock major and trace element compositions. | 150 |
| 4. | Sample preparation and analytical procedures | 161 |
| 5. | Elemental gains and losses. | 167 |

# CHAPTER 1

# INTRODUCTION

## 1.1 Purpose of the study

Recent models of volcanic-associated massive sulphide formation involve three stages in the development of a hydrothermal system: generation of a metal-bearing fluid, transport of the metals to the vicinity of a fluid-rock interface such as the seafloor, and deposition of sulphides on or immediately below this surface (e.g. Sangster, 1972; Spooner, 1977; Franklin et al., 1981; Ohmoto & Skinner, 1983; Franklin, 1986). Possibly the least understood aspect of the ore-forming process is the nature of the deep hydrothermal system beneath the deposits. At present our understanding is based on a few examples of fossil systems which display a record of fluid-rock interaction (alteration) at these levels (e.g. MacGeehan, 1978; Gibson, 1979; Franklin et al., 1981), as well as on observations and inferences from active geothermal systems (e.g. Mottl, 1983; Franklin, 1986), and on experimental and theoretical studies designed to model conditions in sub-seafloor hydrothermal systems (summarized by Mottl, 1983 and Rosenbauer & Bischoff, 1984).

Alteration at two stratigraphic positions is now recognized near volcanic-associated massive sulphide deposits. Discordant footwall alteration 'pipes' occur directly below the massive sulphide horizons and are considered to represent in part the zones through which the ore fluids moved to reach the seafloor. Less well known are the 'lower semiconformable' alteration zones (Franklin et al., 1981) which are located several hundred metres or more below the massive sulphide deposits. As well as presenting large exploration targets, these zones are genetically important because they may have constituted part of the

'reservoir zone' (Hodgson & Lydon, 1977) from which metals and sulphur in the deposits were leached (Spooner & Fyfe, 1973). In predominantly mafic volcanic terranes that formed in deep water the lower semiconformable zones near Cu-Zn and Zn-Cu deposits typically are silicified or epidotized or both (e.g. at Matagami, Quebec: MacGeehan, 1978; and at Noranda, Quebec: Gibson, 1979), whereas in shallower water felsic or mafic terranes a carbonatized lower semiconformable zone is characteristically associated with Cu-Zn and Zn-Cu deposits (Franklin, 1986).

In 1984, geologists of the Geological Survey of Canada discovered a large, well-exposed area of silicified, mainly mafic volcanic rocks in the Snow Lake area, Manitoba, several hundred metres stratigraphically below the Chisel-Lost-Ghost Lakes Zn-Cu massive sulphide deposits. The aims of the present study are to:

1. Document the spatial, temporal and chemical relationships of the silicification to volcanic and intrusive rocks and to other alteration in the area.

2. Discuss the origin of the silicification in light of recent experimental and theoretical studies of alteration, active geothermal systems and of other studies of silicification.

3. Determine the relationship of silicification to nearby massive sulphide deposits, and hence its use as a tool in exploration for these deposits.

## 1.2 Location and access

The Edwards Lake map area is situated about 9 km southwest of Snow Lake township and 1.5 km south of the Chisel Lake Mine in northern Manitoba (Fig. 1). The area is accessible from a dirt road that connects the Chisel Lake Mine and a gravel pit to the south. Hudson

Bay Exploration and Development Company (HBED) presently holds title to the property.

## 1.3 Previous and current work

The general geology of the Snow Lake area is described by Harrison (1949), Froese & Moore (1980), Walford & Franklin (1982) and Bailes (1986). Williams (1966) mapped an area centred on the Chisel Lake massive sulphide deposit, immediately to the north of the Edwards Lake map area. Concurrently with the present study, Bailes (1986) mapped stratigraphy and alteration in the Edwards Lake area at 1:15840 scale as part of the Manitoba Energy and Mines Chisel-Morgan Lakes region project. The eastern and northeastern limits of that mapping were Edwards Lake and the Chisel Lake gabbro, respectively (Fig. 1).

## 1.4 Methods

Mapping was carried out in June, July and August 1985 and for about one week in August 1986. Airphotos were photographically enlarged to a scale of 1:4000, and only the central parts were used in order to avoid distortion. Final presentation of the geology and alteration is at a scale of 1:2000 (Figs. 2a and 3a, in pocket); simplified versions of these maps (Figs. 2b and 3b) are included overleaf. Sampling of certain alteration features such as zoned pillows was accomplished with a gas-fuelled portable core drill, producing a core about 2.5 cm in diameter. Locations of analyzed samples are given in Figure 4.

Petrographic study was conducted on 144 thin sections and 30 polished sections, and the results for analyzed samples are summarized in Appendix 1. In rocks that contain fine grained untwinned plagioclase, estimation of modes was greatly facilitated by staining. Testing for K-feldspar by staining was also carried out on these samples. Mineral

compositions were determined in polished sections using the electron microprobe unit at Carleton University (analyses by P. Jones), and are presented in Appendix 2.

137 samples, were analyzed for 13 major and 12 trace elements, as well as rare earth elements in six samples. The analyses are tabulated in Appendix 3, and details of sample preparation, analytical methods, precision and accuracy are given in Appendix 4.

Densities are required in the method of mass balance calculation used in ~~this~~ study, and were determined with the use of an air picnometer and Mettler balance at the Geological Survey of Canada. The results are tabulated with the corresponding whole rock analyses in Appendix 3.

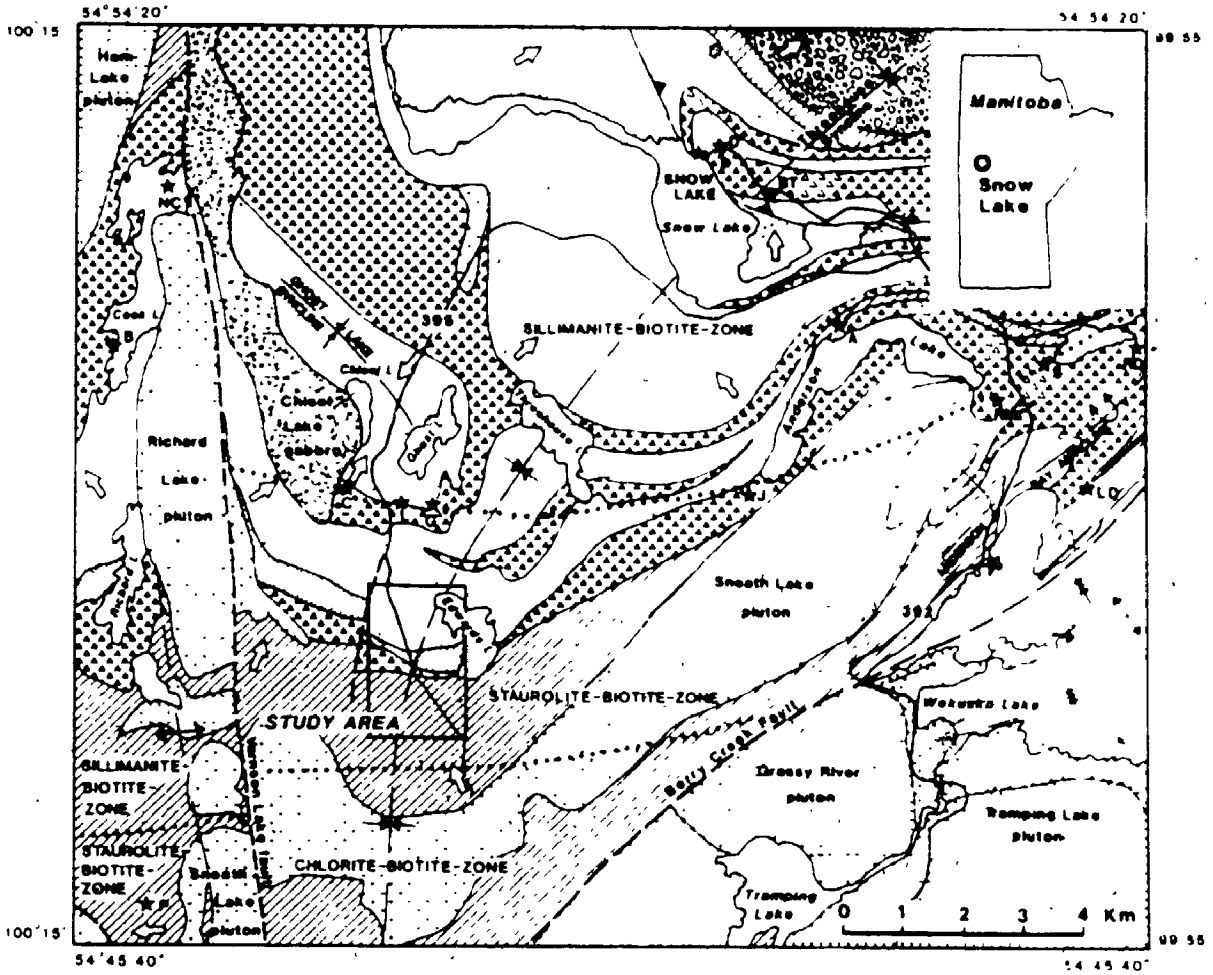


## LEGEND

### EARLY PROTEROZOIC

- Granite, granodiorite
- Gabbro

### MISSI GROUP

- Lithic arenite

### AMISK GROUP

- Greywacke, siltstone, mudstone
- Tonalite
- Felsic volcanic breccia, wacke and minor flows
- Felsic flows
- Mafic breccia, wacke and minor flows
- Porphyritic mafic flows
- Aphyric mafic flows

- Facing direction of strata
- Syncline, anticline
- McLeod Road Thrust Fault
- Fault
- M2-metamorphic isograd
- Mineral Deposit

A Anderson Lake(Cu-Zn)
B Bomber Zone(Zn-Cu)
BT Bounter Zone(Au)
C Chisel Lake(Zn-Cu)
D Dick Zone (Nor-Acme Au)
G Ghost Lake(Zn-Cu)
J Joannie Zone(Cu-Zn)
L Lost Lake(Zn-Cu)
LO Linda(Cu-Zn)
NC North Cook Lake(Cu)
P Pot Lake(Zn-Cu)
RO Rod(Cu-Zn)
RM Rem Zone(Cu-Zn)
S Stall Lake(Cu-Zn)

Figure 1. Location of the Edwards Lake area, and regional geology (after Bailes et al., 1987).

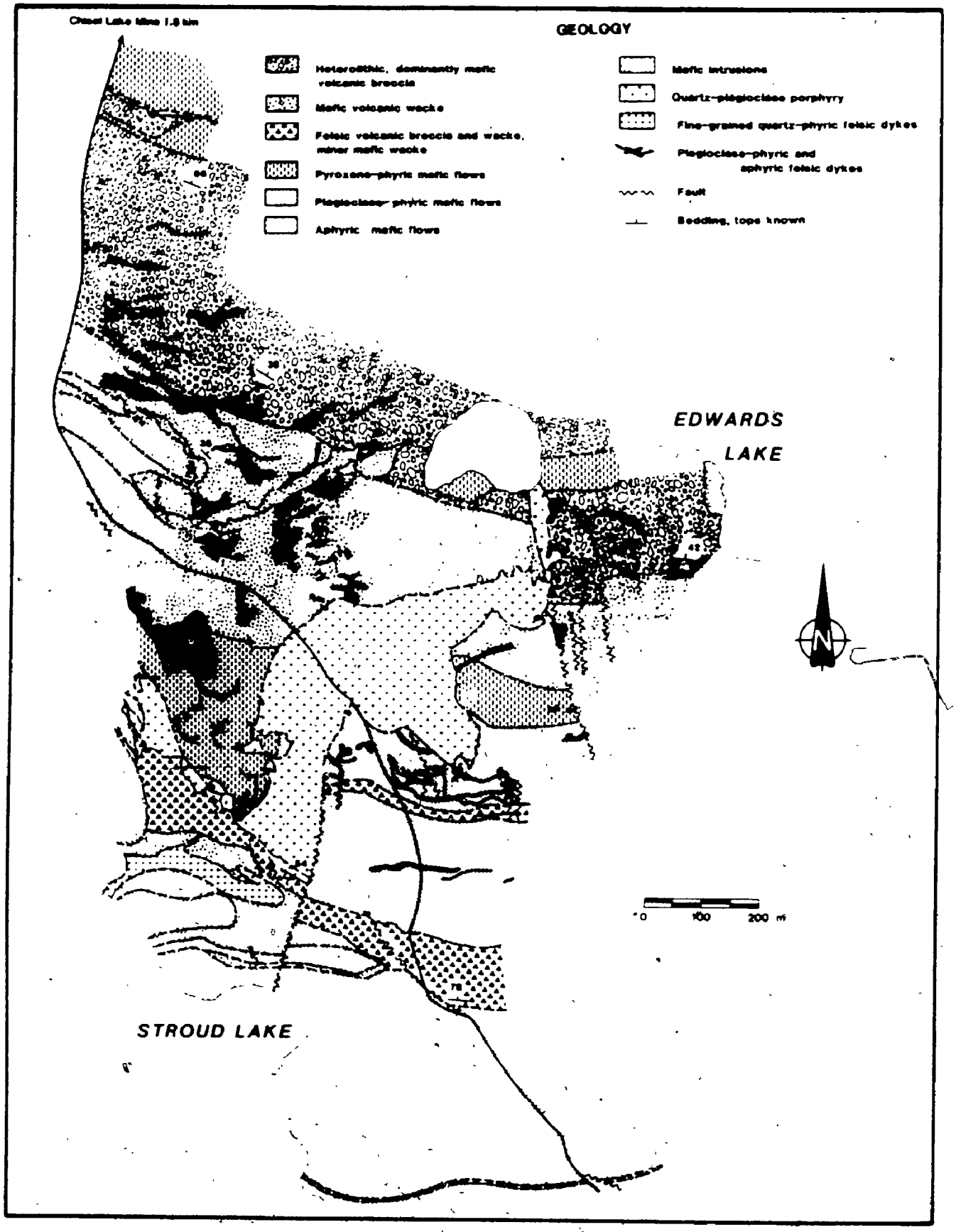


Figure 2b. Simplified geology of the Edwards Lake area.

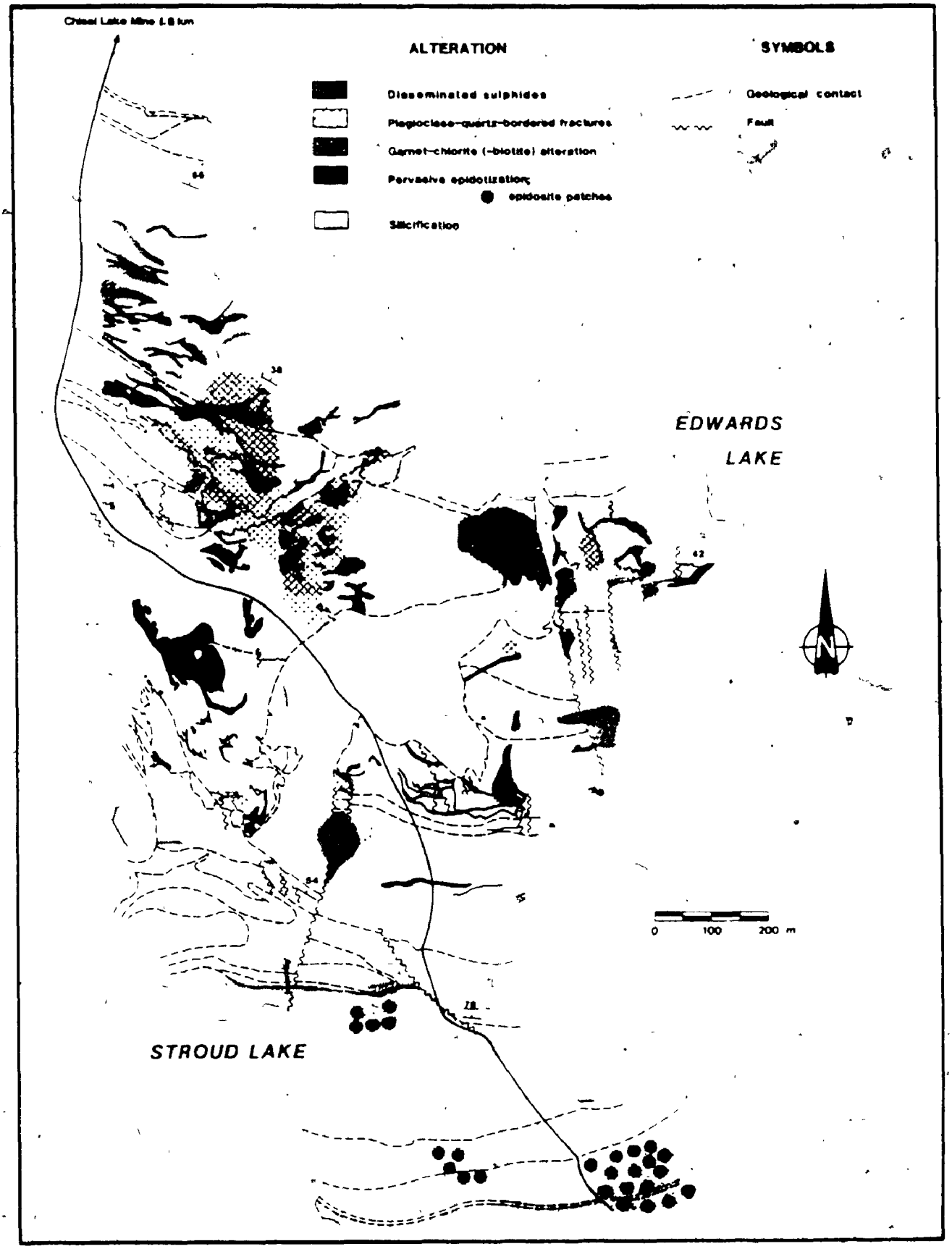


Figure 3b. Simplified alteration distribution in the Edwards Lake area.

# CHAPTER 2

# REGIONAL GEOLOGY

## 2.1 Stratigraphy

Two supracrustal sequences are recognized in the Snow Lake area (Harrison, 1949; Froese & Moore, 1980). The Amisk Group, comprising volcanic and sedimentary strata, is the lower of the two sequences and contains all of the massive sulphide deposits in the region. (All designations of the lithology of the supracrustal strata do not include the prefix 'meta', although all units are metamorphosed.) The upper sequence, the Missi Group, is comprised predominantly of thickly bedded, cross-stratified lithic arenite, with intercalated subaerial felsic and mafic volcanic rock in the Wekusko Lake region.

The Amisk Group can be subdivided into a lower portion containing mainly pillowed aphyric mafic flows, and an upper succession of thickly bedded heterolithic mafic breccia with intercalations of felsic breccia and felsic and mafic porphyritic flows (Fig. 1; Bailes et al., 1987). In the Chisel-Edwards Lakes area a 5 km thickness of north-facing, north-dipping Amisk Group rocks is exposed. A simplified stratigraphic section of this sequence is depicted in Figure 5, together with the relative positions of major base metal sulphide deposits and alteration.

Correlation between the Chisel-Edwards Lakes and Anderson Lake sections by Froese & Moore (1980), J. Kitzler (pers. comm., 1986) and Bailes et al. (1987) suggests that the Lower Mine Felsic unit which hosts the Anderson Lake, Stall Lake, Ram, Rod and Linda massive sulphide deposits is probably a more proximal equivalent of the felsic unit that hosts the barren sulphide zone near Edwards Lake, although the latter sulphides may be at a lower stratigraphic position than the Anderson

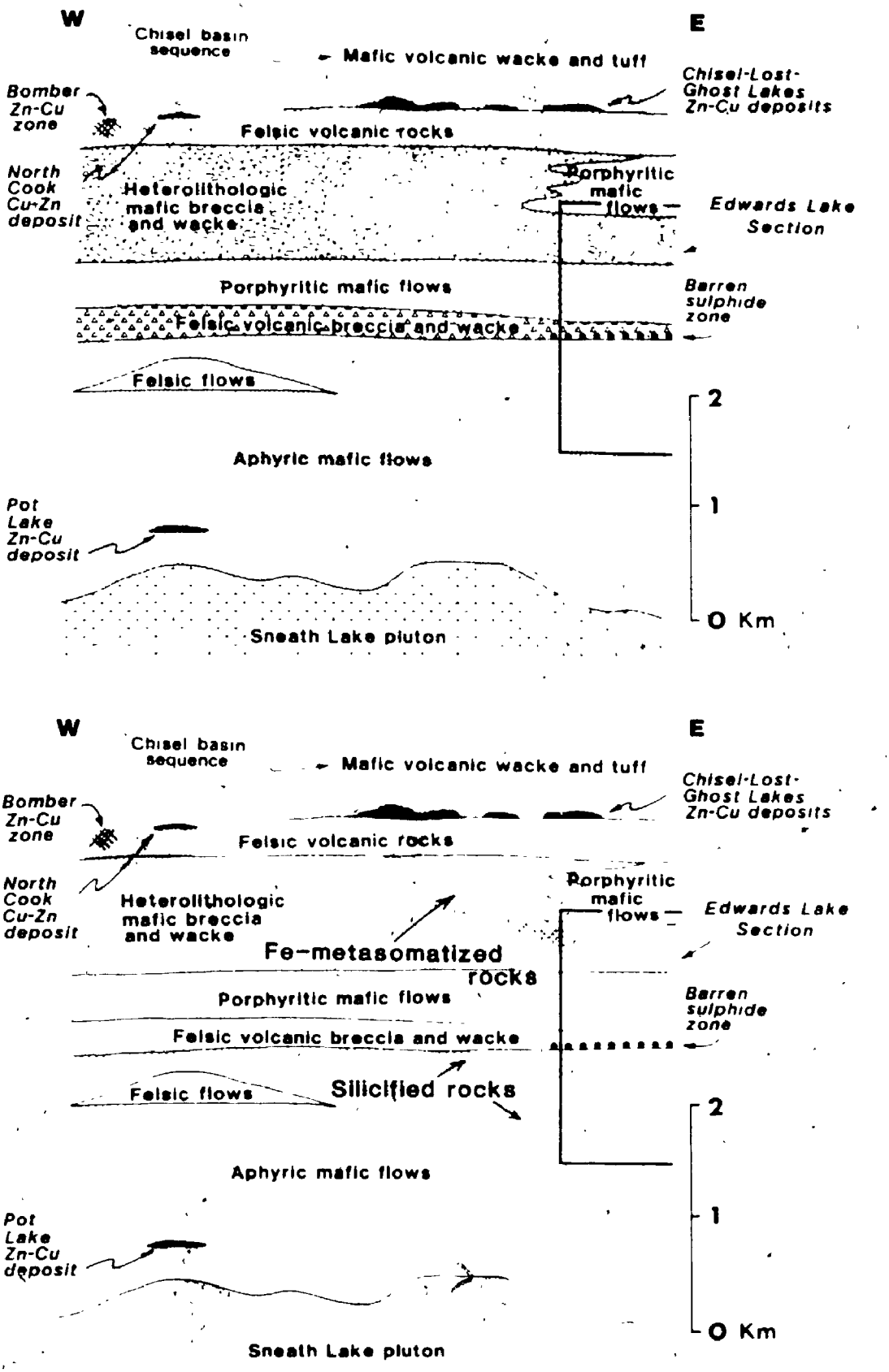


Figure 5. Schematic representation of simplified stratigraphic sequence (a) and alteration zones (b) Chisel-Edwards Lakes area (after Bailes et al., 1987).

deposit (Fig. 1). This implies that the Chisel, Lost and Ghost Lakes deposits are at a stratigraphically higher position than the Anderson Lake and nearby deposits.

Radiometric age determinations indicate that Amisk Group volcanic rocks formed during the period 1875-1832 Ma, and are thus late Aphebian in age (T.M. Gordon, pers. comm., 1987; Watters & Armstrong, 1985, and references therein).

## 2.2 Intrusive rocks

The Sneath Lake pluton is one of several polyphase, Fe-Mg-metasomatized, tonalite intrusions in the region. It is a subconcordant body of 1.5-3 km width and more than 14 km length, which stratigraphically underlies the major massive sulphide deposits in the Snow Lake area. Walford & Franklin (1982) and Bailes (1986) interpreted the Sneath Lake pluton as the synvolcanic heat source that 'drove' the massive sulphide-producing hydrothermal systems.

Several post-tectonic granitoid plutons and a differentiated intrusion of ultramafic to intermediate composition (Chisel Lake 'gabbro') are also present in the region (Fig. 1).

## 2.3 Massive sulphide deposits

The Snow Lake area contains six producing and several non-producing volcanic-associated massive sulphide deposits (Fig. 1). All of the major deposits have Fe-Mg- rich footwall alteration pipes, and the Chisel Lake deposit is enclosed in tremolite-actinolite-carbonate rock (Williams, 1966), an unusual assemblage for deposits of this type (Franklin et al., 1981; Franklin, 1986).

A lower semiconformable alteration zone is present below the Anderson Lake and Stall Lake Cu-Zn deposits, and consists of staurolite-bearing

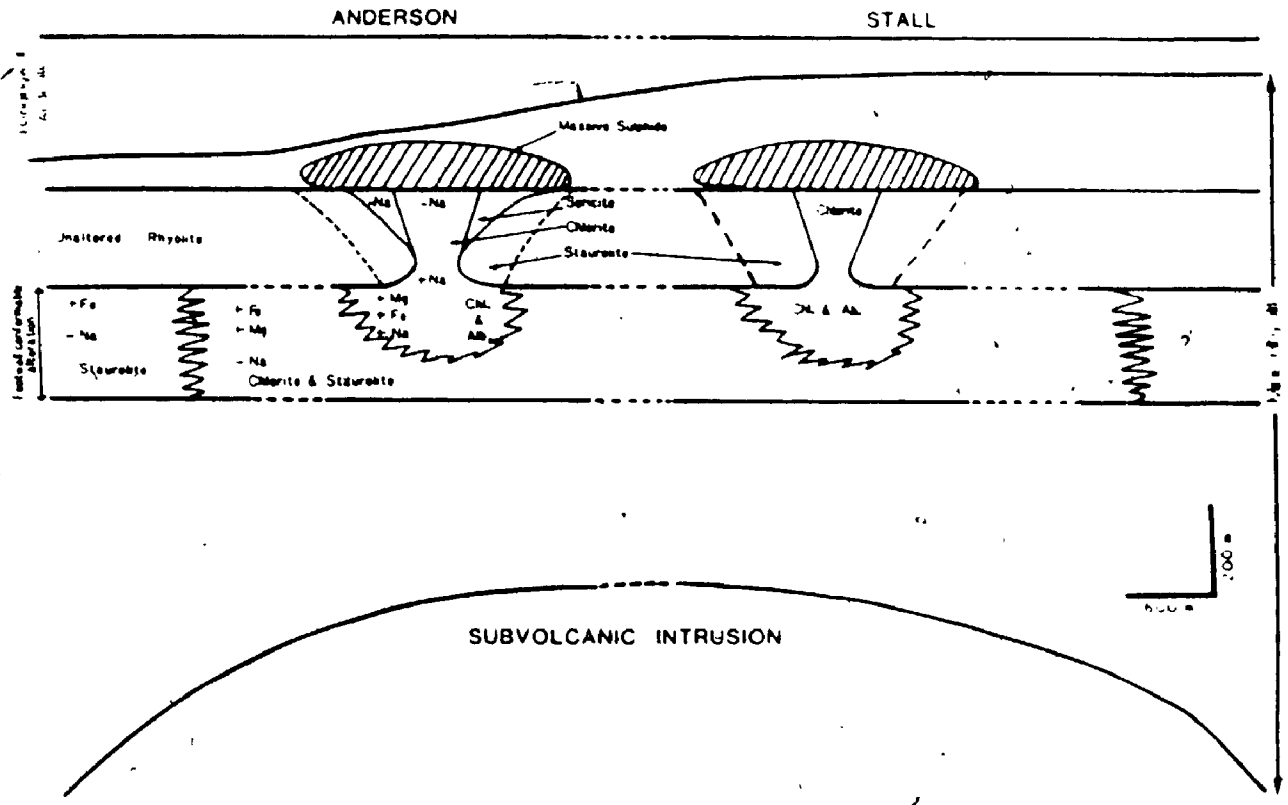


Figure 6. Schematic reconstruction of the pipe and lower semiconformable alteration zones at the Anderson and Stall Lakes deposits (from Walford & Franklin, 1982).

Fe-enriched and Na-depleted rocks except where the footwall pipes join this zone (Fig. 6; Walford & Franklin, 1982). A similar zone may exist beneath the Linda deposit in association with calc-silicate alteration (E. Zaleski, pers. comm., 1987). The results of the present study and of Bailes (1986) and Ziehlke (1982; unpublished HBED report) suggest that a lower semiconformable alteration zone is also present below the Chisel-Lost-Ghost Lakes Zn-Cu deposits, consisting of dominantly Fe-metasomatized rocks near the footwall pipe alteration, and silicification at stratigraphically deeper and more distal positions.

The Anderson Lake and Stall Lake deposits are believed to have formed as a result of expulsion of hot metal-rich fluids from the lower subconcordant zone through synvolcanic faults and fracture zones, on to the seafloor (Walford & Franklin, 1982).

## 2.4 Regional and local structure

Two phases of folding, and a third deformation event associated with emplacement of gneiss domes to the north of Snow Lake, are interpreted to have occurred in the region (Froese & Moore, 1980). The first phase of folding (F1) is characterized by megascopic and rare mesoscopic isoclinal folds, whereas the second phase of folding (F2) resulted in open, northeast-plunging, upright folds such as the Threehouse syncline (Fig. 1). The study area is situated in the closure of this structure and the sequence here has suffered relatively mild ductile deformation, as indicated by a) the open form of mesoscopic F2 folds, b) only slight flattening of clasts, pillows and amygdales in $S_1$ (subparallel to $S_0$), and c) the generally weak development of $S_2$ (cleavage trending N-NE).

Numerous facing indicators such as pillow morphology, amygdale concentrations at the top of flows, graded bedding, scours and flame structures, confirm the northwards facing of the entire sequence in the

area near Edwards Lake and, as far north as the Chisel Lake massive sulphide deposit.

North- to northwest-trending faults with displacements of up to several tens of metres are common in the study area (Fig. 2). An inferred fault to the west of the access road may account for the abrupt westwards termination of the pyrrhotitic barren sulphide horizon in the subsurface (D. Ziehlke, pers. comm., 1986). Primary volcanic features are attenuated in a northwest direction immediately to the east of this inferred fault.

## 2.5 Metamorphism

Metamorphic mineral assemblages in the Edwards Lake area are typical of the chlorite-biotite-staurolite zone (Fig. 1) that was defined in the Snow Lake area by Froese & Gasparrini (1975) and Froese & Moore (1980) on the basis of reactions in pelitic rocks. Conditions of medium grade during regional metamorphism of the Edwards Lake area are therefore indicated. For example, mafic rocks throughout the area generally contain blue-green or green hornblende, and oligoclase or andesine; cummingtonite is present locally.

Staurolite occurs with chlorite, biotite, muscovite and almandine-rich garnet in Fe-metasomatized mixed mafic and felsic breccias at 54°48'34"N, 100°05'59"W, immediately northwest of the study area, and is widespread in the breccia unit to the northwest of this location. However, staurolite is absent in muscovite-free garnet-chlorite± biotite assemblages in the study area, in spite of similar bulk compositions to the staurolitic rocks. An isograd defined by the appearance of staurolite in muscovite-free rocks, to the north of the position where staurolite appears in muscovite-bearing rocks, could explain the lack of staurolite in the study area.

Chlorite generally occurs intergrown with biotite, or as well-formed blades which are overgrown by garnet porphyroblasts in places. Thus, at least some chlorite may be of prograde origin, as suggested by Froese & Moore (1980) for rocks in the chlorite-biotite-staurolite zone elsewhere in the region.

Post-metamorphic carbonate veining is widespread in the Snow Lake area (Walford & Franklin, 1982), and is evident near Edwards Lake in calcite veinlets cross-cutting oriented hornblende blades.

## CHAPTER 3

## STRATIGRAPHY AND VOLCANOLOGY

The layered rocks in the study area form part of a homoclinal succession of submarine volcanic-sedimentary rocks striking west to northwest and dipping $30^{o}$-$80^{o}$ to the northeast. The succession can be divided into a lower sequence consisting of mafic flows, related breccias and minor intercalated felsic volcaniclastic rocks, and an upper sequence composed of dominantly mafic heterolithic volcaniclastic units (Table 1). Mafic flows and related breccias and a thin felsic volcaniclastic unit overlie the heterolithic volcaniclastic sequence near the northern limit of mapping. The section consists of about 60% by volume mafic flows, 35% mafic and 5% felsic volcaniclastic rocks. Numerous intrusions occur in the area, including pyroxenite, gabbro, basalt, basaltic andesite, tonalite-trondhjemite, and several varieties of quartz-phyric felsic intrusions.

Three texturally distinct mafic lavas are present: aphyric, plagioclase-phyric and pyroxene-phyric flows. A single flow, or a series of flows, that can be distinguished texturally from the enclosing sequence is defined here as a flow unit. Breccias that are genetically related to the flows (e.g. flow-top breccias) are also considered to be part of the flow unit.

### 3.1 Flow unit MP1: plagioclase-phyric mafic flow

An intensely silicified plagioclase-phyric pillowed mafic flow occupies the base of the section. The flow unit is betweeen 20 m and 100 m in thickness (the lower contact is not exposed). Pillows are mostly 1-2 m in diameter and the interiors weather light grey, or white

Table 1

Stratigraphy of the Edwards Lake area

| | Thickness (m) | Unit | Lithology |
|---|---|---|---|
| | limit of mapping | | |
| Mainly mafic volcaniclastic rocks | 80 | MX4 | **Pyroxene-phyric pillowed mafic flows** and pillow-fragment breccia |
| | 2-5 | FMVC3 | **Felsic volcanic breccia** and mafic wacke. |
| | 5-75 | MX3 | **Pyroxene-phyric pillowed mafic flow**; westwards facies change to HVC |
| | 200-300 | HVC | **Heterolithic, mainly mafic volcanic breccia** and lesser bedded wacke; pyroxene-phyric massive flows (MX2) and fine grained felsic intercalations in the eastern part of the unit. |
| | 250-350 | MVC | **Mafic volcanic wacke and minor breccia.** |
| Mainly mafic flows | 2-20 | MP5 | **Plagioclase-phyric pillowed mafic flow**, occurs east of the quartz-plagioclase porphyry. |
| | 40-80? | MX1 | **Pyroxene-phyric pillowed and massive mafic flows**; minor pillow-fragment breccia and bedded mafic siltstone. |
| | 70-90 | MP4 | **Plagioclase-phyric massive and pillowed mafic flows**, occur east of the quartz-plagioclase porphyry. |
| | 15 | FMVC2 | **Felsic volcanic breccia and wacke**; minor mafic wacke occurs east of the quartz-plagioclase porphyry. |
| | max. 170 | MP3 | **Plagioclase-phyric massive and pillowed mafic flows**; maximum thickness east of the quartz-plagioclase porphyry. |
| | 80-100 | FMVC1 | **Felsic volcanic breccia and wacke**; minor mafic wacke, increasing in thickness westwards. |
| | max. 40 | MP2 | **Plagioclase-phyric massive and pillowed mafic flow**; thins near road. |
| | 2-15 | | **Iron-sulphidic mafic wacke** |
| | 350-450 | MA | **Aphyric pillowed and massive mafic flows**, pillow-fragment breccia and isolated-pillow breccia |
| | 1-3 | HB | **Heterolithic volcanic breccia of silicified mafic clasts.** |
| | 15 | MP1 | **Plagioclase-phyric pillowed mafic flow** |
| | limit of mapping | | |

where most intensely silicified. Selvages weather mid-grey and are 1-5 cm in width. Numerous concentric, parallel-sided thermal contraction cracks characterize the margin and core of the pillows. Plagioclase phenocrysts are 1-3 mm in length and constitute 3-8% of the rock.

### 3.2 Heterolithic volcanic breccia HB

Flow unit MP1 is overlain by a 1-3 m thick heterolithic volcanic breccia which is laterally continuous for at least 800 m to the west.

The volcaniclastic unit is composed of subangular to angular, poorly sorted clasts up to 30 cm diameter of mainly silicified plagioclase-phyric mafic rock that is similar in appearance to the underlying pillows, and lesser amounts of fine grained mafic volcanic rock, quartz-phyric felsic rock and cherty fragments. The breccia is normally graded, has a massive base and an indistinctly-bedded top, and is clast- and matrix-supported.

Underlying pillow morphology and graded clast size in the breccia indicate a northwards facing. The breccia is interpreted as a debris flow deposit, derived mainly from fragmentation of silicified plagioclase-phyric pillows.

### 3.3 Flow unit MA: aphyric mafic flows and breccia

Flow unit MA is about 300 m in thickness and consists of approximately 60% pillowed flows, 25% massive flows and 15% breccia. Massive and pillowed parts of flows each attain a thickness of 50-80 m, and appear to be lens-, wedge- or tabular-shaped bodies. Flow contacts were identified by use of the following indicators: concentration of amygdales towards the tops of flows; decrease in the spacing of thermal contraction cracks near the contacts of massive flows; and small but significant differences in Zr and $TiO_2$ contents in some flows (Appendix

3). Pillow-fragment breccias mark some flow contacts but the existence of (minor) intraflow breccia means that not all breccias can be used to define flow contacts.

Several flows comprise a massive base and a pillowed top; the diameter of pillows steadily decreases upwards from 3-4 m ('megapillows' of Dimroth et al., 1978) to 0.5-1.5 m ('normal-size' pillows) at the top. At least one of these flows is overlain by a thick flow-top breccia unit. Other flows consist of only massive or only pillowed lava in the section exposed at the present erosional surface.

Least altered massive and pillowed aphyric flows weather olive-green, are fine grained, sparsely quartz-amygdaloidal (less than 5%) and contain sutured thermal contraction cracks up to 4 mm in width and as much as 15 cm apart which are now filled with hornblende or quartz and plagioclase. Pillow rock is slightly finer grained than massive flow rock. Small (less than 1 mm in diameter) plagioclase and hornblende pseudomorphs of pyroxene phenocrysts occur as minor components (less than 2%) of some flows. The groundmass is hypidiomorphic-granular and comprises subequal proportions of blue-green sodic hornblende (Appendix 2, Table 7) and oligoclase (Appendix 2, Table 6), minor quartz (up to 10%) and magnetite, and trace pyrite, sphene, chlorite, carbonate, apatite and epidote. Pillow selvages are almost entirely hornblende and contain rare blebs of chalcopyrite. Recrystallization during regional metamorphism has obliterated all igneous groundmass textures.

Two main types of monolithic breccia are associated with the pillowed and massive flows: isolated-pillow breccia and pillow-fragment breccia. In places, pillows grade upwards and laterally into clast-supported pillow-fragment breccia, through a zone comprising isolated, amoeboid- to pillow-shaped matrix-supported tongues of flow rock in a fine- to medium-grained hyaloclastite(?) matrix (isolated - pillow breccia). All

gradations exist between the two types of breccia. Pillow-fragment breccia also occurs as thin units (less than 2 m in thickness) at flow contacts in the lower part of MA.

In isolated-pillow breccia, dark green chilled margins enclose the lava bodies, whereas in pillow-fragment breccia only part of the margins of clasts and adjacent pillows are chilled. Apparently isolated-pillow breccia formed while the flow rock was still hot, whereas pillow-fragment breccia formed by relatively cold fragmentation of pillows, either during extrusion of the flow (i.e. flow-top breccia) or afterwards ( e.g. talus).

### 3.4 Plagioclase-phyric flow unit MP2 and iron sulphide-rich mafic wacke

West of the road, flow unit MA is overlain by 2-10 m of fine- to medium-grained mafic wacke with disseminations of pyrite and pyrrhotite. A HBED drill hole, positioned to test a geophysical anomaly, intersected 3 m of massive pyrrhotite and trace zinc, copper and lead in the mafic wacke (D. Ziehlke, pers. comm., 1986).

The sulphide-rich mafic wacke (barren sulphide horizon) is overlain by a massive and pillowed plagioclase-phyric mafic flow which pinches-out eastwards where the overlying felsic unit thickens, near the road. The flow is overlain by another fine- to medium-grained mafic wacke unit which thickens westwards from the road.

### 3.5 Felsic and mafic volcaniclastic units FMVC1 and FMVC2

FMVC1 and FMVC2 are heterolithic and monolithic felsic volcanic breccia and wacke units, and minor mafic volcanic wacke, that include about 80% of the total thickness of felsic rocks in the section. The remaining felsic component is contained in several thin units higher in the sequence, and as clasts in the thick heterolithic breccia and wacke

unit (HVC).

Individual deposits in FMVC1 are 1-20 m in thickness, lensoid to tabular in shape and typically consist of: a reversely graded base with a planar lower contact; a massive, poorly-sorted central interval of angular to subrounded clasts up to 50 cm in diameter; and a normally graded upper part capped by bedded, medium grained felsic wacke. The bedded intervals compose 10-25% of the deposits and exhibit rare cross-lamination and flame structures. The deposits are mainly clast-supported, but matrix-support occurs in some breccias and is common in the upper parts of the deposits.

Clasts in FMVC1 are mainly quartz-plagioclase porphyry, and up to 15% fine grained felsic volcanic rock and 10% biotite-rich, medium grained intermediate-composition clasts comprise the remainder. The felsic porphyry clasts contain 5-10% subhedral to euhedral quartz phenocrysts ranging in diameter from 1 mm to 10 mm; phenocrysts in a given deposit generally are of similar size. Plagioclase phenocrysts (1-5 mm in length) constitute up to 5% of the porphyry clasts, and the groundmass consists of fine grained quartz and plagioclase, 5-10% biotite, and minor hornblende and chlorite. However, some clasts, and the matrix in most felsic breccias, contain up to 40% biotite-hornblende-chlorite or hornblende-cummingtonite-garnet. The unusual abundance of Fe-rich minerals may be due largely to hydrothermal alteration, although the Fe-rich matrix also may reflect a mafic to intermediate clastic component.

By comparison with coarse clastic rocks documented in the literature (e.g. Middleton & Hampton, 1976), the felsic breccias are interpreted as subaqueous debris flow deposits, and the volcanic wacke beds probably were deposited from subaqueous turbidity currents. Sufficient water may have been entrained in the debris flows to produce water turbulence, resulting in loss of fines from the lower parts of the flows, and

grading and tractional sedimentary structures in the upper parts (Hampton, 1972). In this sense the density currents that produced these deposits may have been transitional between non-viscous and viscous (Cas & Wright, 1982), although the overall characteristics of the breccias are most similar to those of debris flows, as opposed to turbidites.

FMVC2 consists of bedded and massive quartz-phenocryst-bearing felsic volcaniclastic rocks, and 5-20% fine- to medium-grained, well-bedded and normally-graded mafic volcanic wacke. Quartz and plagioclase phenocrysts in FMVC2 are less than 2 mm in diameter and felsic clasts range from 1 mm to 10 cm in diameter. Minor muscovite is present in the predominantly quartz-plagioclase groundmass, and cummingtonite was noted in one sample of altered(?) felsic wacke. Characteristics diagnostic of either an epiclastic or pyroclastic origin for the felsic and mafic beds in FMVC2 were not observed.

### 3.6 Plagioclase-phyric mafic flow units MP3-MP5

Flow units MP3-MP5 contain pillowed and massive facies that are comprised of texturally and compositionally homogeneous plagioclase-phyric mafic lava. Massive facies grade into more voluminous pillowed facies (pillows 0.5-1.5 m in diameter) through zones of large lava lobes. Some flows may be at least 100 m in thickness - no breccias or amygdale concentrations were observed which might mark flow contacts within the flow units.

MP3-MP5 occur to the southeast and northwest of the quartz-plagioclase porphyry, but near the western contact of the intrusion the plagioclase-phyric flows are very thin. Less-altered plagioclase-phyric mafic flows weather olive-green, and contain plagioclase phenocrysts (2-4 mm in length) that constitute 5-10% of the rock. Polysynthetic twinning is generally preserved and only minor recrystallization has

affected the phenocrysts. Glomeroporphyritic texture is common. The groundmass comprises fine grained blue-green hornblende and plagioclase in subequal proportions, with minor quartz and magnetite. Aggregates of hornblende up to 4 mm in diameter and composing up to 3% of some rocks may represent pseudomorphs of ferromagnesian phenocrysts.

Two variants of the plagioclase-phyric flows occur as thin pillowed flows within MP4 and at the top of the plagioclase-phyric flow sequence. They are characterized by larger (5-8 mm in length) and smaller (0.5-1 mm in length) plagioclase phenocrysts (MP5).

### 3.7 Pyroxene-phyric mafic flow units MX1-MX5

Pillowed and massive flows (MX1) containing hornblende pseudomorphs of pyroxene phenocrysts (hereafter termed 'pyroxene-phyric' flows) occur towards the top of, and above, the plagioclase-phyric flow sequence, and also occur within the heterolithic volcaniclastic rocks in the upper part of the section (MX2-MX4). Pillow-fragment breccias are associated with particularly the uppermost pyroxene-phyric mafic flows (MX5) which also contain abundant amygdales (up to 20% by volume of the rock; quartz and carbonate filled).

The lowermost pyroxene-phyric flow unit (MX1) to the east of the quartz-plagioclase intrusion is interlayered with the uppermost plagioclase-phyric flows. It is pillowed and contains distinctive hornblende-rich, irregularly-shaped aggregates up to 2 cm in length which may be fragments of pillow selvages. Pseudomorphs of pyroxene phenocrysts constitute 5-10% and are 1-6 mm in diameter, and lesser plagioclase phenocrysts (1-5%, 1-2 mm in diameter) are also present. The groundmass consists of subequal amounts of hornblende and plagioclase. A flow with the same distinctive texture occurs to the west of the intrusion, but here it is underlain by massive, polygonal-

jointed pyroxene-phyric flow(?) rock, and overlain by massive, pyroxene phenocryst-bearing rock that is clastic in places (see Section 3.8).

A very sharp facies change from west to east across the position of the quartz-plagioclase porphyry could account for the differences in stratigraphy in this part of the section.

### 3.8 Mafic volcanic siltstone, wacke and breccia: MVC

The mafic flow sequence in the lower half of the section is overlain by, and intercalated near its top with, about 300 m of mafic volcanic siltstone, wacke and breccia. The mafic volcaniclastic rocks are subdivided into three lithologic types which, from the base of the unit upwards, are: (a) pyroxene phenocryst bearing massive wacke and breccia; (b) massive and bedded siltstone and wacke; and (c) plagioclase phenocryst-bearing massive wacke and breccia.

(a) Pyroxene phenocryst-bearing volcaniclastic rocks outcrop both to the east and west of the quartz-plagioclase porphyry, but at possibly different stratigraphic positions: in the western exposure subunit (a) overlies pyroxene-phyric flows, whereas to the east of the intrusion it occurs beneath a pyroxene-phyric flow in two intervals.

At the eastern exposure both intervals of subunit (a) are reverse-graded and grain size increases from fine at the base of the lower division to very coarse (clasts up to 10 cm in diameter) at the top of the upper division. Hornblende pseudomorphs of pyroxene phenocrysts constitute 5-15% of the rock, and fine grained, monolithic, angular mafic clasts containing quartz-filled amygdales compose 0-15%. The matrix is fine- to medium-grained and clasts are matrix-supported. Subunit (a) at the eastern exposure is interpreted as two mafic crystal-lithic lapilli tuff beds.

West of the quartz-plagioclase porphyry, subunit (a) has crude normal grading at the base and contains matrix-supported hornblende pseudomorphs of pyroxene phenoclasts up to 5 mm in diameter, angular plagioclase-phyric mafic lava clasts up to 5 cm in diameter and rare subrounded clasts of medium grained leucogabbro. The upper part of subunit (a) in this area is massive and the unit has a planar, unchilled upper contact against beds of subunit (b). It is not clear whether subunit (a) west of the quartz-plagioclase porphyry is a pyroclastic or an epiclastic deposit (e.g. a debris flow), although the diverse provenance of the clasts points to an epiclastic origin.

(b) Subunit (b) consists of laminated, bedded and massive mafic volcanic siltstone and wacke; its origin is problematic and a genetic interpretation is hindered by intense alteration in parts of the subunit.

(c) Subunit (c) is a thick-bedded to massive wacke and breccia interval consisting almost entirely of poorly-sorted, close-packed plagioclase-phyric mafic lava clasts and plagioclase phenoclasts (1-10 cm in diameter), in a matrix of finer detritus of the same flow rock. Plagioclase phenocrysts and phenoclasts are less than 5 mm in diameter.

Significant rounding, close-packing and lack of chilled margins on clasts suggest that subunit (c) is an epiclastic breccia as opposed to a pyroclastic or flow-related breccia. Subunit (c) is probably an accumulation of several mass-flow deposits.

### 3.9 Heterolithic volcaniclastic unit: HVC

A northwards increase in the variety of clasts in the breccias, particularly of felsic volcanic clasts, and an increase in the maximum size of clasts, marks the transition from the plagioclase-phenocryst- and phenoclast-rich mafic volcaniclastic rocks to the heterolithic

volcaniclastic unit HVC.

The lower parts of HVC are composed of bedded, light brown-green weathering wacke and breccia, which contrast with the darker green colour of the MVC unit. Lithic clasts are discernible in the coarser grained beds and consist of mainly plagioclase-phyric mafic lava with lesser amounts of pyroxene-phyric mafic volcanic, fine grained felsic volcanic and fine grained mafic rock. The proportion of coarse grained beds in the sequence increases northwards with maximum clast size, and is greatest in the central parts of HVC where tabular- to lens-shaped, very coarse- to medium-grained deposits occur. The deposits are normally graded, range from 10 m to 60 m in thickness and generally consist of three zones: a massive, unsorted base with a non-erosive lower contact, clast-supported or matrix-supported fabric and very coarse angular to subrounded clasts up to 50 cm in diameter (rare outsized clasts up to 3 m in diameter); a coarse grained, indistinctly-bedded interval overlying the massive portion; and a medium- to fine-grained well-bedded top which comprises 0-15% of the deposits. Scours, trough crossbeds and planar crossbeds are present in finer grained intervals throughout the HVC unit. Clast types are the same as those noted above in the lower part of HVC, with the addition of large quartz phenoclasts (5-10 mm in diameter) in the matrix of one deposit. The graded deposits become progressively thinner and finer grained towards the upper contact.

Through comparison with sections of mass-flows documented in the literature (e.g. Middleton & Hampton, 1976; Cas, 1979), the graded breccias in HVC are interpreted to be debris flow deposits with turbiditic tops. As with the felsic debris flows described earlier, the lack of matrix support in the deposits may be due to entrainment of sufficient water into the debris flows for significant loss of fluid

strength to have occurred (Hampton, 1972), resulting in crude separation of large clasts and matrix.

Phreatic explosion breccias (Dimroth & Rocheleau, 1979) share some of the features of the HVC breccias described above. However, phreatic breccias appear to be more limited in lateral extent (to within a few hundred metres of their vent), and do not display the tractional sedimentary structures that occur at the tops of the HVC breccia deposits (Dimroth & Rocheleau, 1979). Fragmentation of the volcanic rocks may nevertheless have been caused by phreatic or hydrothermal explosions (Hedenquist & Henley, 1985), with redeposition by debris flows. Another mechanism of fragmentation that could have produced non-vesiculated, boulder-sized clasts of diverse origin, is mass wasting on paleoslopes, triggered by either oversteepening or seismic activity.

Ungraded parts of HVC may be distal facies of mass-flow deposits, although a pyroclastic origin cannot be ruled out for some of the fine grained deposits.

Paleocurrent analysis of the volcaniclastics to determine transport directions was not undertaken, but a south-eastwards (lateral) fining in one part of HVC and crossbed orientations are consistent with a northwest to southeast component in the direction of mass transport.

## 3.10 Pyroxene-phyric mafic flow and related breccia units MX3 and MX4, and felsic and mafic volcaniclastic unit FMVC3

Pillowed, pyroxene-phyric mafic flows and pillow-fragment breccia are interlayered with the upper parts of HVC. The lowermost flow (MX3) thins dramatically to the west (near the road) and is overlain here by a wedge of HVC. MX3 and the HVC wedge are overlain by a 2-5 m thick volcaniclastic unit (FMVC3) consisting of three distinctive intervals: (i) a lowermost, monolithic felsic breccia composed of angular, close-

packed, non-vesiculated quartz porphyry clasts up to 20 cm in diameter, including phenocrysts of less than 1 mm diameter; (ii) a central interval containing angular felsic clasts of similar appearance to those in the underlying horizon, which are set in a fine- to medium-grained mafic clastic matrix; and (iii) an upper, dark green volcaniclastic deposit of indistinctly-bedded fine- to medium-grained mafic detritus. The felsic breccia may be of debris flow or phreatic eruption origin, and the felsic clasts in th overlying interval were probably derived from the felsic breccia and transported in mafic mass-flows.

### 3.11 Ultramafic and mafic intrusive rocks

Medium- to coarse-grained pyroxenite and melagabbro dykes intrude volcaniclastic rocks in the northwestern part of the study area. The dykes weather dark green and contain hornblende pseudomorphs of close-packed pyroxene euhedra and subhedra, as well as 5-15% interstitial plagioclase, minor carbonate and trace opaque minerals. From cross-cutting relationships the pyroxenite and melagabbro dykes are inferred to be one of the oldest intrusive rock types in the area.

Pyroxene-phyric mafic intrusions in the map area are massive, mid-grey-green-weathering bodies containing 5-15% hornblende pseudomorphs of pyroxene phenocrysts up to 5 mm in diameter, and 0-5% plagioclase phenocrysts up to 3 mm in length, in a fine- to medium-grained hornblende-plagioclase groundmass. Pods of pyroxenite reaching 50 cm in diameter occur as volumetrically minor components in some pyroxene-phyric intrusions.

At least three other types of mafic intrusive rocks are present in the area. From oldest to youngest they are: (a) fine- to medium-grained aphyric dykes - some exhibiting quartz amygdaloidal cores, thermal contraction cracks or internal banding that is symmetrically

arranged parallel to contacts; (b) plagioclase-phyric dykes containing phenocrysts of up to 8 mm length; (c) medium grained, dark-green-weathering, massive gabbroic intrusions, some of which cross-cut all other rock types. Almost all mafic dykes are less than 3 m in width, and strike between west and north.

The pyroxene-phyric mafic intrusions predate the gabbroic intrusions, and postdate the fine- to medium-grained aphyric mafic dykes. Timing of plagioclase-phyric mafic dykes relative to pyroxene-phyric mafic intrusions is not clear.

### 3.12 Plagioclase-phyric and aphyric felsic intrusions

Light-grey-weathering, sheet-like felsic intrusions, ranging in thickness from 0.5 m to more than 10 m, are present throughout the sequence to the north of FMVC1. Many of these intrusions are subconcordant and occur in two main swarms: one is located near the southeast margin of the quartz-plagioclase porphyry, and another occurs to the north of the quartz-plagioclase porphyry. More extensive intrusions of this type also outcrop immediately to the west-northwest of the porphyry and 1-2 km to the northwest of the porphyry.

The felsic intrusions predate the quartz-plagioclase porphyry and postdate all of the ultramafic and mafic intrusions described above except for some gabbroic dykes.

Intrusive contacts are sharp, but in places the felsic intrusions are difficult to distinguish from closely associated silicified host rocks (see also Chapters 4 and 5). The dykes and sills are characteristically massive, although inhomogeneities such as flow banding, angular xenoliths of host rock, sutured thermal contraction cracks and chilled margins, are not uncommon. The flow banding occurs near both contacts of the intrusions and consists of alternating hornblende-rich and

hornblende-poor zones that range in width from 5 mm to 10 cm.

The plagioclase-phyric variety of the felsic dykes contain 3-10% euhedral to subhedral oligoclase phenocrysts, ranging from 1 mm to 3 mm in length. The extent of recrystallization of phenocrysts varies considerably, even within a single thin section - relict polysynthetic twinning is preserved in some phenocrysts, whereas others are fine grained polygonal mosaics of plagioclase. The groundmass of plagioclase-phyric felsic intrusions is texturally and mineralogically identical to the aphyric felsic intrusions, and consists of 30-55% quartz, 20-50% plagioclase, 0-12% green-blue hornblende, 0-20% biotite, 0-5% garnet, 0-2% chlorite and 0-2% magnetite, with minor apatite, sphene and epidote. Hornblende and biotite generally are poikiloblastic and range in length from 0.2 mm to 2 mm. Garnet and magnetite are porphyroblastic, reach 2 mm in diameter and commonly are surrounded by a narrow (less than 1 mm in width) metamorphic corona (Spry, 1969) of fine grained polygonal quartz and plagioclase.

### 3.13 Composite felsic-mafic dykes

Several dykes in the study area are compositionally zoned and consist of dark green mafic margins (1-15 cm in width; 1-8 vol. % of dykes ) and cream-coloured to light grey silicic cores (maximum width 3 m). Mafic margins are of equal and constant width along both sides of a given dyke, and fine grained chilled contacts against host rocks are preserved in the mafic margins of some zoned dykes. However, no chilled contact is present between the mafic margins and silicic cores, and the transition from one zone to the other is gradational over a width of 5-15 mm.

Discontinuous, white-weathering bands reaching 4 mm in width and aligned parallel to the contacts occur in the mafic margin of one

composite dyke, and consist of about 65% fine grained plagioclase, 30% hornblende and 5% magnetite. The remaining, and volumetrically dominant, part of the mafic margins consists of fine- to medium-grained hornblende, 5-10% plagioclase, and 1-2% iron-titanium oxides. Phenocrysts of plagioclase (1-5%) and hornblende pseudomorphs of ferromagnesium phenocrysts (1-2%) are also present, and are slightly more abundant in the fine grained plagioclase-rich bands.

Silicic cores of the composite dykes are commonly altered to quartz-clinozoisite-carbonate-hornblende-plagioclase rock; and iron-titanium oxides are replaced by sphene where carbonate is most abundant. Plagioclase phenocrysts (2-5%) and groundmass plagioclase are partially replaced by clinozoisite and quartz.

The felsic cores and mafic margins are considered to represent separate pulses of basic, followed by silicic, magma along a shared conduit. Lack of chilling between the margin and core probably indicates that emplacement of the two magmas occurred over a relatively short time interval; that is, the dykes are composite, as opposed to multiple. Composite mafic-felsic dykes with similar characteristics have been described from the Noranda area (Thurston et al., 1985; H. Gibson, pers. comm., 1986) and in Iceland (Gibson & Walker, 1963).

An alternative origin of the zonation in the dykes may be <u>in situ</u> differentiation, as the dyke crystallized from the walls to the centre. However, Kretz et al. (1985) calculated that diffusion of cations would be too slow to cause significant differentiation within small dykes (centimetres to a few metres in width). Furthermore, the differences in composition between margin and core are probably too extreme to have resulted from <u>in situ</u> differentiation (see Section 5.1.2 and Appendix 3).

### 3.14 Fine grained quartz-plagioclase-phyric felsic dykes

Several quartz-plagioclase-phyric dykes occur to the south of FMVC2 as subconcordant cream-coloured to white-weathering bodies, 0.5-20 m in width. The dykes postdate plagioclase-phyric mafic dykes.

Quartz phenocrysts generally are less than 1 mm in diameter (rarely up to 3 mm in diameter), compose 2-5% of the dykes, and are subhedral to euhedral. Plagioclase phenocrysts are similar in size and abundance to quartz phenocrysts, although they are more recrystallized and have been replaced partially by muscovite, biotite and rarely by garnet and carbonate.

The groundmass consists of subequal proportions of fine grained quartz and plagioclase, 5-15% intergrown biotite and chlorite, up to 2% muscovite and trace garnet, sphene, opaques, epidote and apatite. One sample (036) contains about 15% hornblende but no biotite or chlorite, and disseminated garnet is common in quartz-plagioclase-phyric dykes that are located 40-80 m to the west of sample location 051. Relict spherulitic texture may be present in some dykes, as indicated by 'close-packed', circular- to ovoid-shaped patches up to 1 mm in diameter that consist of only quartz and plagioclase. Quartz-plagioclase 'coronas' also surround some phenocrysts.

The fine grain size of the groundmass and spherulitic(?) texture probably indicate high-level emplacement of the quartz-plagioclase-phyric felsic dykes.

### 3.15 Quartz-plagioclase porphyry

A white- to cream-weathering quartz-plagioclase porphyry intrusion, measuring about 1 km in longest dimension (SW-NE) and about 400 m in a SE-NW direction, occupies the central part of the map area. The quartz-plagioclase porphyry cuts all rock types observed at its contacts except

for one generation of fine grained aphyric mafic dyke. Contacts generally are steep and sharp, although parts of the northern contact are more complex due to the presence of partially-assimilated xenoliths, and an aphyric marginal phase of the porphyry which has similar appearance to some silicified rocks in the area. Most of the southern contact can be divided into NW- and NNE-trending segments of several tens of metres length. These orientations are also followed by numerous quartz-plagioclase porphyry dykes.

The intrusion contains 5-15% clear to bluish, rounded and embayed quartz euhedra, and a similar abundance of subhedral to euhedral plagioclase phenocrysts. Quartz phenocrysts range in diameter from about 3 mm to 6 mm, whereas plagioclase phenocrysts are less than 3 mm in length. Both are partly to wholly recrystallized. Plagioclase phenocrysts generally consist of a mixture of: unstrained fine grained plagioclase; sericitized plagioclase pseudomorphs of parts of the phenocrysts with preserved polysynthetic twinning; and less commonly, biotite-chlorite intergrowths with muscovite and carbonate.

Groundmass of the quartz-plagioclase porphyry is composed of subequal amounts of fine grained quartz and plagioclase and up to 5% biotite-chlorite intergrowths, muscovite, apatite and magnetite. Granophyric texture (McKenzie et al., 1982), consisting of quartz-plagioclase intergrowths arranged radially around plagioclase phenocrysts, is common.

Quartz-plagioclase porphyry dykes are most abundant to the north of the intrusion and many originate at the main body of porphyry. Dyke widths range from a few centimetres to 10 m, and almost all are texturally and mineralogically identical to the main intrusion, although some contain xenoliths of country rock and slightly greater abundances of ferromagnesian minerals, including hornblende.

An aphyric phase of the intrusion is present as a marginal zone along some parts of the northern and northeastern contacts. This zone commonly is less than 5 cm in width along the northeastern contact, but broadens in places to several metres width on the northern contact. No chilled margins are visible between the aphyric phase and either the porphyritic rock or the country rock, and the contact between aphyric and porphyritic phases is sharp. A contact metamorphic aureole in the country rock was not observed. Petrographically the aphyric rock is indistinguishable from the groundmass of the porphyritic phase.

Xenoliths as large as 6 m in length occur near the northern and northeastern contacts. The xenoliths are very similar in appearance to nearby country rock and probably represent stoped blocks. Large xenoliths of mafic volcanic wacke near 54°47'58.0"N, 100°06'21.4"W are pervasively silicified and are transected by plagioclase-quartz-bordered fractures, indicating that emplacement of the intrusion postdated both pervasive silicification and the fracture-controlled alteration at this location. Partial assimilation of some blocks is evident from the gradational nature of xenolith-porphyry contacts (over widths of several centimetres). Quartz veins cut the porphyry in several places, and one vein about 40 cm in width (at 54°47'55.6"N, 100°06'18.6"W) was tested for gold by diamond drilling (D. Ziehlke, pers. comm., 1986).

The quartz-plagioclase porphyry contains minor disseminations of pyrite near 54°47'49.5"N, 100°06'23.3"W. This sulphide may be related to a NNE-trending pyritic quartz vein structure that is exposed about 70 m to the south.

Minor chalcopyrite was intersected in a Hudson Bay Exploration drill hole, located in the eastern part of the intrusion (D. Ziehlke, pers. comm., 1986).

Classification and interpretation of the quartz-plagioclase porphyry

Modal quartz / (plagioclase + quartz) ratios (visual estimates) of the porphyry lie in the range 0.4-0.6, and the alkali feldspar to total feldspar ratio is estimated at less than 0.1. These modal abundances are typical of trondhjemite, according to the definition of Barker (1979).

Key field and petrographic features that relate to the origin of the quartz-plagioclase porphyry, and their interpretation, are given below:

(a) The quartz-plagioclase porphyry is interpreted to be premetamorphic and pretectonic in origin because it is (weakly) foliated, partially recrystallized and is cut by a metamorphosed, hornblendic mafic dyke.

(b) Fine grained groundmass and granophyric texture suggest emplacement at shallow crustal levels where cooling would be expected to be relatively rapid, especially if abundant external fluid was present. Maximum depths of emplacement are estimated to be of the order of 4-6 km, based on depths to porphyry intrusions reported in the literature (e.g. Fournier, 1968; Titley & Beane, 1981).

(c) NW and NNE trends of porphyry contacts and dykes, together with the coincident position of the western part of the porphyry with an interpreted major facies change in mafic flows, point to an important structural control on the emplacement of the porphyry. This facies change may have resulted from synvolcanic faulting, and intrusion of the porphyry could have occurred along such a zone of crustal weakness. Quartz veining and local development of iron sulphides may be related to reactivation of this structure.

(d) Garnet-chlorite alteration at the margins of the porphyry suggest that intrusion occurred prior to, or during, synvolcanic Fe-metasomatism (see also Section 4.3).

# CHAPTER 4

# ALTERATION

Field and petrographic observations of five types of alteration are presented in this chapter: 1) silicification; 2) epidotization; 3) garnet-chlorite alteration; 4) plagioclase-quartz-bordered fractures, and 5) iron sulphide alteration. The relative timing of alteration events is discussed at the end of the chapter, and the origin and significance of the alteration is discussed in Chapter 6.

Figures 3a and 3b show the distribution of alteration zones in the map area. The term 'alteration zone' is used here to refer to a mesoscopic domain of mineralogically unusual rocks that can be distinguished from more typical medium grade regionally metamorphosed rocks.

## 4.1 Silicification

An estimated 35% of rocks in the Edwards Lake section have been silicified - that is, replaced by various amounts of fine grained quartz + plagioclase to produce a white- or grey-weathering rock. Silicified rocks were identified in the field by tracing less altered flows, dykes and volcaniclastic units into the quartzo-feldspathic equivalent rock, with confirmation provided in many cases by major and trace element analyses (Chapter 5). Although the alteration contains both quartz and plagioclase the terms 'silicified' and 'silicification' are used to describe the alteration because Si is the dominant element added to the rock (see Chapter 5), and quartz generally is more abundant than plagioclase.

Much of the silicification is in the upper, volcaniclastic portion of the sequence, but also occurs in several mafic flows, lower in the volcanic pile. Silicification occurs in several well-defined sites: at pillow margins; as elongate patches in massive flows; at the margins of clasts in volcaniclastic rocks; adjacent to some felsic dykes; and, on a smaller scale, enveloping hornblende pseudomorphs of pyroxene phenocrysts. Silicification is also confined to individual beds in some volcaniclastic rocks, or is found as metre-scale discordant zones. Narrower bodies of plagioclase-quartz rock, bordering fractures, probably are of different origin and are discussed separately in Section 4.4.

Each of the types of silicification are described below.

4.1.1. Silicification of pillows and massive flows

Intense silicification of pillows occurs in plagioclase-phyric mafic flow unit MP1 and at the base and top of aphyric mafic flow unit MA. The pillows in MP1 are relatively large (up to 2 x 3 m in diameter), contain 5-10% plagioclase phenocrysts reaching 2 mm in length, and exhibit quartz-filled concentric thermal contraction cracks up to 2 mm in width. Vesicularity increases slightly towards the top of the flow (northwards) and amygdales are filled with quartz or quartz-epidote.

The pillows in MP1 (Fig. 7) are strongly zoned: (a) selvages (1-2 cm width) are mid-grey and contain fine- to medium-grained hornblende (60%), plagioclase (35%), quartz (4%), magnetite (1%) and in places minor garnet, chlorite and biotite; (b) margins (10-20 cm width) are silicified to a light grey, fine grained quartz-plagioclase-hornblende-magnetite±garnet assemblage; (c) 'inner margins' contain intensely silicified, elongate white patches (5-20 cm width) of fine grained plagioclase (30-60%), quartz (20-45%), hornblende (7-10%) and magnetite

(2%) near the top and bottom of the pillows; the patches extend around the ends of more altered pillows to form 'doughnuts' of intense silicification. Thermal contraction cracks pass through the patches without deviation, and the patches generally follow the cracks; (d) cores of pillows contain light yellowish-green patches (10-30 cm in diameter) that consist mainly of clinozoisite and quartz with minor hornblende, iron-titanium oxides and carbonate; these patches are surrounded by silicified rock that is similar to the margin zone. Plagioclase phenocrysts in the yellowish-green patches are largely replaced by clinozoisite, but in the silicified rock the phenocrysts are recrystallized to fine grained, untwinned plagioclase. No igneous groundmass textures were observed.

Plagioclase-phyric mafic flow MP1 is overlain by heterolithic breccia HB, which contains clasts of plagioclase-phyric mafic lava (Fig. 8), amongst other clast types (Section 3.2). Parts of some clasts are intensely silicified, particularly where thermal contraction cracks are abundant. The silicified patches in the clasts are truncated by the clast boundaries and the alteration does not appear to follow the clasts' peripheries. The clasts are probably fragments of previously-silicified margins of the underlying plagioclase-phyric pillows. No other plagioclase-phyric flows are known from the underlying sequence (Bailes, 1986).

The overlying aphyric pillowed flow is less silicified than the plagioclase-phyric flow, but the zonation of alteration minerals within the pillows are essentially the same (Fig. 9). In comparison with the plagioclase-phyric flow, the aphyric pillows are smaller (1-2 m in length, 0.4-0.8 m in width), selvages contain a greater proportion of hornblende (70-85%), silicic margins are more pyrrhotitic (2%) and biotitic (5%), and the least altered part of the pillows - between the

Figure 7. Intensely silicified plagioclase-phyric mafic pillows, containing patches of very intense silicification (at right side of photo) and abundant concentric thermal contraction cracks. Film canister at lower left is 5 cm in length.

Figure 8. Fragment of silicified plagioclase-phyric pillow rock in heterolithic breccia unit HB, directly overlying the pillows shown in Figure 7.

Figure 9. Zoned alteration in aphyric mafic pillow near the base of flow unit MA. Crosses mark positions of core sample used in mass-balance calculations. From right to left the crosses identify four zones: silicic rim (sample 171) immediately inside the selvage; intensely silicic patch at the pillow margin (sample 172); the least altered part of the pillow (sample 173); and the epidotized core (sample 174). Pen is 14 cm in length.

7

8

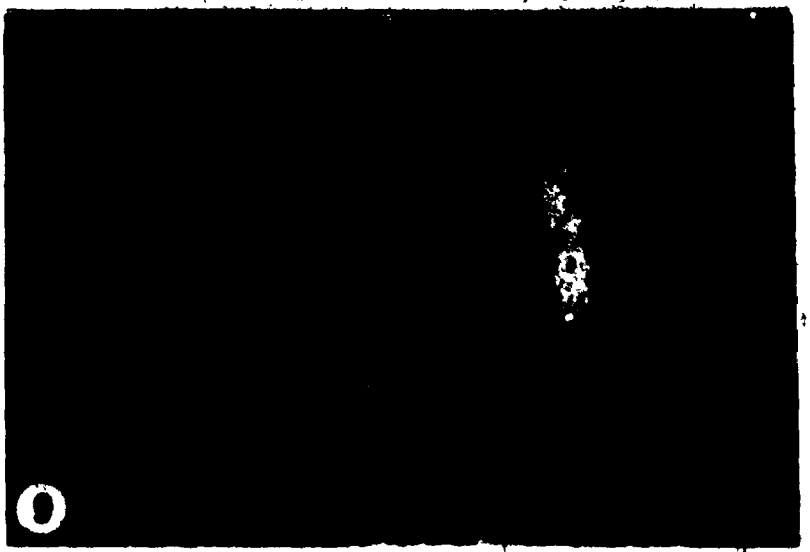
9

epidotized core and the silicic margin - approaches the mid-green colour of pillows in less altered flows. The most intensely silicified patches and the highest proportion of thermal contraction cracks (5-10% by volume of the rock) occur closer to the selvages than in the plagioclase-phyric pillows. One of these pillows was chosen for a detailed chemical study (see Chapter 5). Plagioclase compositions in the silicified rock ($An_{24}$) are similar to those in less altered flows nearby (compare samples 171 and 217 in Appendix 2, Table 6). Interpillow rock is a mixture of plagioclase, quartz, hornblende and clinozoisite.

The intensity of silicification decreases markedly in the massive flows above these pillows. The massive flows do, however, contain distinctive patches of silicification and epidotization that constitute as much as 30% of some flows. The alteration patches (Fig. 10) are generally 0.3-1.5 m in length and are elongate in the direction of thermal contraction cracks (i.e. subparallel to the lower flow contact). Most patches are concentrically zoned from a hornblendic, dark green periphery to an inner, light grey, quartz-plagioclase-hornblende-magnetite silicic zone, and finally a light yellowish-green core of clinozoisite-quartz (minor sphene and carbonate). Some alteration patches are connected and appear to form an anastomosing network. Less altered aphyric massive flow rock is green and consists of subequal amounts of hornblende and plagioclase, and minor magnetite; less than 5% quartz is present. Thermal contraction cracks are filled with mainly hornblende, but where they pass through the silicic zones of the alteration patches the cracks are filled with quartz and plagioclase.

The alteration near the base of the Edwards Lake section is laterally extensive: the zone of very intense silicification of plagioclase-phyric pillows is concordant and extends at least 800 m to the west.

The alteration zone that is characterized by patches of clinozoisite-quartz and by silicic rock is also concordant but grades westwards into less altered massive flow rock, so that about 300 m strike length of alteration is exposed. Silicification of pillows in this part of the section occurs over a stratigraphic thickness of 20-100 m, and the intensity of silicification decreases upwards in the sequence in a step-wise fashion - each flow has a characteristic intensity of alteration. The clinozoisite-quartz patches within silicic envelopes occur mainly in one massive flow that is about 20 m thick.

Pillows in the upper 50-60 m of aphyric flow unit MA are also strongly silicified, and display very similar alteration to the pillows in MP1 and at the base of MA (Fig. 11).

### 4.1.2 Silicification of clasts

Clasts throughout most of the heterolithic breccia unit HVC either have white-weathering quartz-plagioclase-rich margins, or are completely altered to quartz-plagioclase rock. The alteration is more easily discerned in the mafic volcanic than in the felsic volcanic clasts due to the contrast between the less altered grey-green cores of some mafic clasts and their light coloured silicic margins. Plagioclase phenocrysts are clearly visible in both the altered margins and the less altered cores of many mafic clasts. At 54°48'02.1"N, 100°05'57.7"W pyroxene-phyric and aphyric mafic volcanic clasts show a greater tendency to be silicified than plagioclase-phyric clasts. Also at this location, some clasts contain an additional concentric zone of quartz-plagioclase rock a few centimetres from the marginal silicified zone. The matrix is partly silicified except where Fe-metasomatism has affected the unit (Section 4.3).

Figure 12 illustrates the complete silicification of three pillows that form an outsize clast in a debris flow deposit, about 1.5 km northwest of the study area in HVC. By analogy to silicified clasts in unit HB, the three silicified pillows, and probably some other clasts in HVC, may have been silicified prior to deposition in the breccia. However, the great abundance of clasts displaying silicified margins suggests that silicification of mass-flow deposits in the HVC unit also occurred after its deposition.

4.1.3 Silicification adjacent to felsic dykes

Plagioclase-phyric and aphyric dykes at several localities (e.g. 54°48'04.0"N, 100°06'24.9"W; 54°48'06.3"N, 100°06'28.3"W) have aureoles of silicic rock, ranging in width from 10 cm to 2 m. In each case the dyke intrudes mafic or mixed mafic and felsic heterolithic volcanic wacke or breccia. The silicic aureoles consist of irregular, light grey patches (up to a few centimetres diameter) of quartz-plagioclase-hornblende-magnetite± biotite rock which form a mottled pattern where alteration is of low intensity (e.g. Fig. 13), and coalesce into massive quartz-plagioclase rock where silicification is intense. The dykes apparently are not silicified, although their felsic character could mask weak alteration. No dykes were observed that cut fractures with silicic aureoles, so the possibility that the dykes were emplaced along pre-established fractures, bordered by silicification, is unlikely.

In addition to the relatively small-scale silicification zones adjacent to individual felsic dykes, pervasive intense silicifiction of mafic volcaniclastic rocks occurs as a northwest-trending, subconcordant zone measuring about 400 x 150 m, located to the north of the quartz-plagioclase porphyry (Fig. 3). This zone coincides spatially with an areally more extensive swarm of felsic dykes and sills, of which the

Figure 10. Zoned alteration patches in a massive aphyric mafic flow near the base of flow unit MA. Central parts of the light patches are epidosite, which are enveloped by silicified rock and a dark, hornblendic peripheral zone. Pen is 14cm in length.

Figure 11. Silicified margins of aphyric pillows near the top of flow unit MA. The cores of pillows on the left are epidotized. Pen is 14 cm in length.

Figure 12. Large clast of an intact group of three silicified pillows in heterolithic breccia unit HVC. The matrix of the breccia contains chlorite, garnet, biotite and, in places, staurolite. Located 800m south-southwest of the Chisel Lake deposit.

10

11

12

four examples mentioned above are members. Mafic dykes are also abundant, and as much as 50-60% of the outcrop exposure near the alteration zone is occupied by intrusions. Not all felsic intrusions have silicic aureoles. Intensely silicified mafic volcaniclastic rocks in the subconcordant zone generally are darker than the felsic intrusions, are more distinctly mottled, have gradational contacts with less silicified rocks, and contain discernible clasts in places.

The spatial coincidence of the subconcordant intense silicification zone with the felsic dyke swarm, and the textural and mineralogical similarities between the small- and larger-scale silicification, suggest that the subconcordant zone is comprised of both overlapping and separate aureoles of silicification that are spatially, and probably temporally, associated with the felsic intrusions.

### 4.1.4 Other forms of silicification

A small discordant zone of silicification at 54°48'0.8"N, 100°05'51.4"W demonstrates the replacement character of the alteration (Fig. 14). The host rock is a well-bedded chloritic mafic volcaniclastic unit that is dark grey-green where less altered. The silicified zone is cream-white, about 1 m in width and at least 3 m in length, and cuts bedding at almost 90°. No medial fracture was observed along the alteration zone. Bedding and soft-sediment deformation structures can be clearly traced from less altered rock into the silicified zone. No dilation or compression of the beds is apparent across the alteration zone contact. The silicified rock contains about 45% plagioclase ($An_{21}$-$An_{27}$; Appendix 2, Table 6, # 284), 40% quartz, 15% biotite and minor iron-titanium oxides. Figure 14 also illustrates the selective replacement of finer grained beds and laminae in the mafic volcaniclastic rock by quartz and plagioclase. Similar examples occur

Figure 13. Mafic volcanic wacke (dark grey) silicified to a mottled, light grey rock adjacent to a high-$TiO_2$ felsic dyke (white with darker border phase, lower part of the photo). Both the dyke and associated silicification are cut by plagioclase-quartz-bordered fractures (white, narrow linear features). The silicified aureole is representative of larger alteration zones associated with a felsic dyke swarm, of which the dyke in this photo is a member.

Figure 14. Discordant silicification of mafic volcaniclastic rock. Note the persistence of individual beds and laminae from less altered rock (left) into the silicified zone (right). Some finer grained beds and laminae on the left are also silicified. Pen is 14 cm in length.

13

14

at 54°47'58.5"N, 100°05'55.4"W; 54°47'54.3"N, 100°06'07.5"W; and 54°48'03.5"N, 100°05'51.9"W. White-weathering silicified beds commonly pass laterally into less altered, darker grey or green rock, or the silicified zones in places transgress the bedding to follow a fracture.

Finally, silicification of pyroxene-phyric mafic dykes and volcaniclastic rocks is manifested by white-weathering quartz-plagioclase 'haloes' around hornblende pseudomorphs of pyroxene phenocrysts, or by silicic bands adjacent to thin hornblendic veins. The 'haloes' reach 1 cm in width and coalesce in places; they are much wider than metamorphic coronas around garnet and magnetite porphyroblasts in rocks from the Edwards Lake area. Some 'haloes' are in contact with the pyroxene phenocrysts, whereas others are separated from the phenocrysts by a narrow zone (up to 5 mm in width) of apparently less altered rock. In some cases the 'haloes' themselves are concentrically banded in shades of white to dark grey or green.

### 4.1.5 Timing and depth of silicification

The incorporation of previously silicified fragments of pillows into a breccia that directly overlies the inferred source of the pillow fragments suggests that this silicification occurred at or very near the water-rock interface.

Silicification of HVC and mafic volcaniclastic units, however, may have commenced at a considerably later time and at greater depths below the water-rock interface. Silicification of mafic dykes, and the inferred contemporaneity of some felsic dykes and accompanying silicified aureoles, place the alteration process at minimum depths below the water-rock interface of about 0.3 km (i.e. the stratigraphic extent of the dyke swarm above the alteration). The aphyric and plagioclase-phyric felsic dykes with silicified aureoles are similar

both in immobile element composition (see Chapter 5) and texture to felsic volcaniclastic rocks that occur in the immediate footwall of the Chisel Lake massive sulphide deposit, located 1-2 km stratigraphically above the silicification (Figs. 1 and 5). The felsic dykes are interpreted as feeders to the Chisel Lake felsic volcaniclastic rocks, suggesting that silicification temporally and spatially associated with the felsic dykes formed at sub-seafloor depths of at least 0.3-2 km. Maximum depth limits of the silicification are probably in the order of 4-6 km, estimated from the maximum depth of emplacement below the water-rock interface of the synvolcanic quartz-plagioclase porphyry which cuts silicification in the volcaniclastic units (Section 3.15).

The timing of silicification in the volcaniclastic rocks is constrained by the following additional observations: (a) the margins of clasts in the HVC unit are silicified; (b) pyroxene-phyric mafic dykes are silicified; (c) silicification is cut by fractures with plagioclase-quartz borders (see Section 4.4), and by the quartz-plagioclase porphyry intrusion; and (d) garnet-staurolite-chlorite-biotite alteration overprints silicification in HVC near the Chisel Lake deposit (see Section 4.3). Because large areas of silicification in HVC apparently are not spatially associated with felsic dykes it is not known whether all silicification in the volcaniclastic rocks occurred at the same time. However, the observations listed above are consistent with the hypothesis that silicification was approximately coeval with emplacement of aphyric and plagioclase-phyric felsic dykes and deposition of felsic volcaniclastic rocks beneath the Chisel Lake deposit.

The timing of silicification relative to other types of alteration is discussed in suceeding sections.

## 4.2 Epidotization

Epidote*-rich rocks occur in two main zones in the Edwards Lake area (Fig. 3): one forms an arcuate domain around the northeastern and eastern sides of the quartz-plagioclase porphyry, adjacent to silicification, and the other is a poorly-defined area in aphyric mafic flow unit MA and plagioclase-phyric flow unit MPl. The latter zone consists of scattered ovoid patches of clinozoisite-quartz rock, up to 1 m in length, at the centre of pillows and in zoned alteration patches in massive flows - these are described in Section 4.1.1 above.

The arcuate epidotization zone near the porphyry is discordant to bedding and is largely confined to mafic rocks. Where epidotization occurs in the heterolithic breccias (minor) it is restricted to mafic clasts. Two forms of epidotization that are common in both the mafic flows and mafic volcaniclastic rocks are patches of epidote-quartz (epidosite), and disseminations of epidote. Epidosite patches in plagioclase-phyric mafic flows differ from those in silicified flows further south by their lack of associated silicic rock, their non-confinement to pillow cores and the inclusion of small (1-5 cm diameter), plagioclase-phyric, less altered remnants of flow rock. However, the patches are similar in size, texture and colour, and those in the arcuate alteration zone contain clinozoisite, quartz, minor hornblende, plagioclase, sphene, iron-titanium oxides and carbonate.

Incipient epidotization of plagioclase-phyric pillows is characterized by replacement of phenocrysts by clinozoisite, the

---

* 'Epidote' refers to any member of the epidote-group of minerals, which range in composition from clinozoisite, which commonly has the composition $Cz_{94}$ - $Cz_{85}$ (Cz represents the mole fraction of the component $Ca_2Al_3Si_3O_{12}(OH)$ in the solid solution with $Ca_2Fe_3Si_3O_{12}(OH)$), to epidote (sensu stricto), which commonly has the composition $Cz_{85}$ - $Cz_{67}$ (Holdaway, 1966).

appearance of fine grained quartz patches in the groundmass, and replacement of the rims of iron-titanium oxide grains by sphene. Enlargement of the clinozoisite, quartz and sphene aggregates, and epidote veining, may represent an intermediate stage of alteration prior to massive clinozoisite development. Untwinned plagioclase commonly occurs in a narrow zone (less than 0.2 mm in width) between clinozoisite and quartz aggregates, suggesting that it was also part of the alteration assemblage, although this texture alternatively may have developed during regional metamorphism. Carbonate, on the other hand, partially replaced some hornblende blades, having grown apparently after the peak of regional metamorphism.

The other form of epidotization in the arcuate alteration zone is disseminated clinozoisite. The 'bleached', pale green-yellow colour of pervasively altered mafic rocks in this zone is due not only to the presence of clinozoisite (5-30%; Appendix 2, Table 9, #280) but also to the low abundance of hornblende, and the large amount of plagioclase + quartz (40-60%) together with colourless to pale green tremolite-actinolite (0-25%; Appendix 2, Table 7, #280) and carbonate (0-3%). Iron-titanium oxides are completely replaced by sphene. As in the epidosite patches, clinozoisite generally occurs in plagioclase phenocryst sites, and with tremolite-actinolite in both the groundmass of volcanic rocks and the matrix of breccias and wacke. Pyroxene phenocrysts are replaced by tremolite-actinolite. Essentially the same sequence of alteration events is envisaged for the disseminated clinozoisite type of alteration as for the epidosite patches, except that massive clinozoisite is not present.

No cross-cutting relationships were observed between epidotization and silicification, but each postdates emplacement of pyroxene-phyric dykes and both are cut by the quartz-plagioclase porphyry.

## 4.3 Garnet-chlorite alteration

Almost all garnet-chlorite rocks in the map area occur in volcaniclastic units, particularly in those of heterolithic character. Two small (less than 70 m in length) but intensely altered zones of garnet-chlorite-biotite rock occur in the eastern part of the area 54°47'54.4"W, 100°05'56.4"W. One of these is confined to an 8-12 m interval of dominantly mafic volcaniclastic rock containing clasts up to a few centimetres in diameter. The underlying fine- and medium-grained mafic wacke, and the overlying heterolithic, mainly mafic breccia are not altered to garnet-chlorite-rich rock.

A major zone of garnet-chlorite alteration occurs in heterolithic breccia unit HVC near the northwestern limit of mapping. Garnet and chlorite abundances generally increase from southeast to northwest in HVC, and also increase towards the centre of the unit, mimicking the increase in clast size in the breccias. In the Edwards Lake area, garnet and chlorite are mostly restricted to the matrix of the breccias and to some beds in the mafic wackes. A positive correlation is observed between the extent of silicification of the clasts and the intensity of garnet-chlorite alteration in the matrix of the breccias.

Almandine porphyroblasts (0.5-10 mm in diameter; Appendix 2, Table 8) constitute up to 50% of the matrix in some places, and the remainder is a mixture of fine- to medium-grained chlorite (5-50%), biotite (5-30%), hornblende (0-20%), plagioclase + quartz (10-30%) and minor iron-titanium oxides. Chlorite in the garnet-chlorite alteration is iron-rich (Appendix 2, Table 8).

Patches of very intense garnet-chlorite alteration are more common to the northwest in HVC, outside the map area, and at 54°48'34"N, 100°05'59"W staurolite appears with garnet, biotite, chlorite and muscovite. Increased intensity of alteration is manifested by partial

to almost complete replacement of the clasts as well as the matrix in the breccias by these minerals. Areas of up to several tens of metres in diameter of massive staurolite, garnet, chlorite and biotite are common in the HVC unit to the southwest of the Chisel Lake massive sulphide deposit, and in the felsic volcaniclastic pile between the deposit and HVC (Bailes, 1986). Drilling from the deepest levels of the mine (D. Ziehlke, pers. comm., 1986) has indicated that at least 1000 m of garnet-chlorite-biotite-staurolite rocks are present beneath the deposit in a southwest direction. This footwall zone may join the rocks with garnet-chlorite-biotite-staurolite alteration in the HVC unit.

Garnet-chlorite alteration also occurs in veins up to 20 cm in width in bedded volcaniclastic rocks, aphyric and plagioclase-phyric felsic dykes, and in the quartz-plagioclase porphyry. The veins are locally folded. Chlorite-garnet veins in the porphyry are approximately linear, trend north to northeast and occur near the margins of the intrusion. These veins are of low abundance and are relatively small structures (up to 10 cm in width, and 2 m in length).

Timing of garnet-chlorite alteration

The intimate association of garnet-chlorite alteration in the matrix of breccias with silicified clasts, described above, may be a consequence of simultaneous, or near-simultaneous, alteration processes. Nearer the Chisel Lake massive sulphide deposit, however, garnet-staurolite-chlorite-biotite alteration has progressively overprinted silicification of the clasts in HVC to produce intensely Fe-metasomatized rocks. The contention that Fe-metasomatism continued after silicification of the volcaniclastic rocks is supported by the presence of garnet-chlorite veins cutting silicified mafic volcaniclastic rocks and aphyric and plagioclase-phyric felsic dykes.

Fe-metasomatism continued after intrusion of the quartz-plagioclase porphyry, although is is not clear whether garnet-chlorite veins in the porphyry represent the effects of the same Fe-metasomatism event that altered the volcaniclastic rocks. Walford & Franklin (1982) and Bailes (1986) suggested that the Fe-Mg-metasomatized Sneath Lake, Richard Lake and other tonalite intrusions in the region, were synvolcanic plutons, based on the general similarity of the alteration mineralogy to that in footwall alteration zones below massive sulphide deposits.

## 4.4 Plagioclase-quartz-bordered fractures

Fractures bordered by plagioclase-quartz rock are distributed in several small (less than 20m diameter) zones close to the quartz-plagioclase porphyry, and in a large zone to the north of the intrusion (Fig. 3). The latter zone is roughly triangular in shape, with one apex of the area located near the porphyry contact. Measuring about 500 m length by 300 m maximum width, this alteration zone coincides spatially with intensely silicified mafic volcaniclastic rocks and with an areally more extensive swarm of aphyric and plagioclase-phyric felsic dykes. The plagioclase-quartz-bordered fractures extend further to the northeast than the silicified rocks but their southwestern limits are approximately coincident.

Plagioclase-quartz-bordered fractures form networks and ladder-like arrays, trend dominantly to the north and northwest and dip steeply. Fracture densities are higher in felsic dykes and intensely silicified rocks than in less altered mafic volcaniclastic units. Less altered domains between individual alteration structures characteristically are centimetres to metres in diameter (Fig. 15). The plagioclase-quartz-rich borders are 1-10 cm in total width and are weakly to strongly zoned: a thin (0.5-2 mm) quartz or plagioclase-biotite $\pm$ quartz $\pm$ garnet

vein is common along the centre, and is bordered by fine grained plagioclase ($An_{28}$ - $An_{40}$, Appendix 2, Table 6, #307,308), quartz and minor biotite and iron-titanium oxides. The abundance of iron-titanium oxides is moderately constant throughout, but biotite content increases towards the outer (sharp) contact of the silicic alteration. In some places there is a more distal envelope of biotitic alteration which grades into less altered hornblendic rock, and the biotitic envelopes of different plagioclase-quartz-bordered fractures may overlap to form brown-grey-weathering domains.

A less common variant of fracture-controlled alteration consists almost entirely of fine grained oligoclase alteration ($An_{20}$ - $An_{21}$, Appendix 2, Table 6, #141) adjacent to thin veins of oligoclase and hornblende (Fig. 16). Millimetre-width banding, defined by minor amounts of hornblende and biotite, is present in places. Near the intersections of the medial veins in Figure 16, for example, the banding is parallel to the curved outer contacts of the alteration, indicating that the less altered domains between the banded structures are remnants of dyke that have not been replaced by the feldspathic assemblage.

Other textural evidence of a replacement origin for the plagioclase-quartz borders to fractures is the preservation of plagioclase and quartz phenocrysts in the alteration where the host rock is porphyritic.

## Timing and interpretation

Timing of the plagioclase-quartz-bordered fracture alteration is constrained by the following observations.

a) The plagioclase-quartz structures cut: silicification adjacent to felsic dykes and at clast margins; a quartz-plagioclase porphyry dyke at 54°48'02.6"N, 100°06'22.5"W; and the garnet-chlorite alteration in heterolithic breccias.

b) Plagioclase-quartz borders to fractures are cut by the main body of quartz-plagioclase porphyry and by most porphyry dykes (Fig. 17). These relationships indicate that at least some plagioclase-quartz bordered fractures formed after silicification and before porphyry emplacement, but the alteration may have continued after the period of porphyry dyke activity in areas further (particularly northwards) from the main intrusion.

The alteration zone is interpreted to have formed by fracturing of relatively competent and impermeable silicic rocks adjacent to, and mostly above, the quartz-plagioclase porphyry, as a result of porphyry emplacement. Fracturing may have been caused by: a) fluid 'overpressure' beneath a silicic 'cap rock' (e.g. Hedenquist & Henley, 1985; Fournier, 1985) which may be represented in this case by the zone of felsic dykes and attendant silicification, or b) intrusion-related tectonic activity. The involvement of a fluid during or after fracturing, or both, is suggested by the presence of alteration adjacent to the fractures. Also, the in situ positions of blocks between the fractures is a feature that is shared by certain hydraulically fractured rocks, such as the 'jigsaw puzzle' breccias described by Hedenquist & Henley (1985) in the Waiotapu geothermal system, New Zealand.

## 4.5 Iron sulphide alteration

Several small zones of rusty-weathering, mainly pyrrhotite-bearing rocks occur in the Edwards Lake area (Fig. 3). The zone near 54°47'41.5"N, 100°06'18.6"W, in mafic volcanic wacke and siltstone, may be the surface expression of a thin, massive pyrrhotite horizon intersected by a RBED drill hole located about 150 m to the northwest (D. Ziehlke, pers. comm., 1986). This horizon is possibly stratigraphically equivalent to the Anderson Lake - Joannie massive

Figure 15. Plagioclase-quartz-bordered fractures in mafic volcanic wacke.

Figure 16. Plagioclase (-quartz)-bordered fractures in fine grained mafic dyke. Note banding within the alteration and curvature of the alteration fronts near intersections of medial fractures/veins. Pen is 14 cm in length.

Figure 17. Quartz-plagioclase porphyry dyke (left to right in photo) cutting a plagioclase-quartz-bordered fracture (top to bottom) in previously-silicified mafic volcanic wacke (light grey). Less altered volcaniclastic rock is darker grey (left one third of photo). Pen is 14 cm in length.

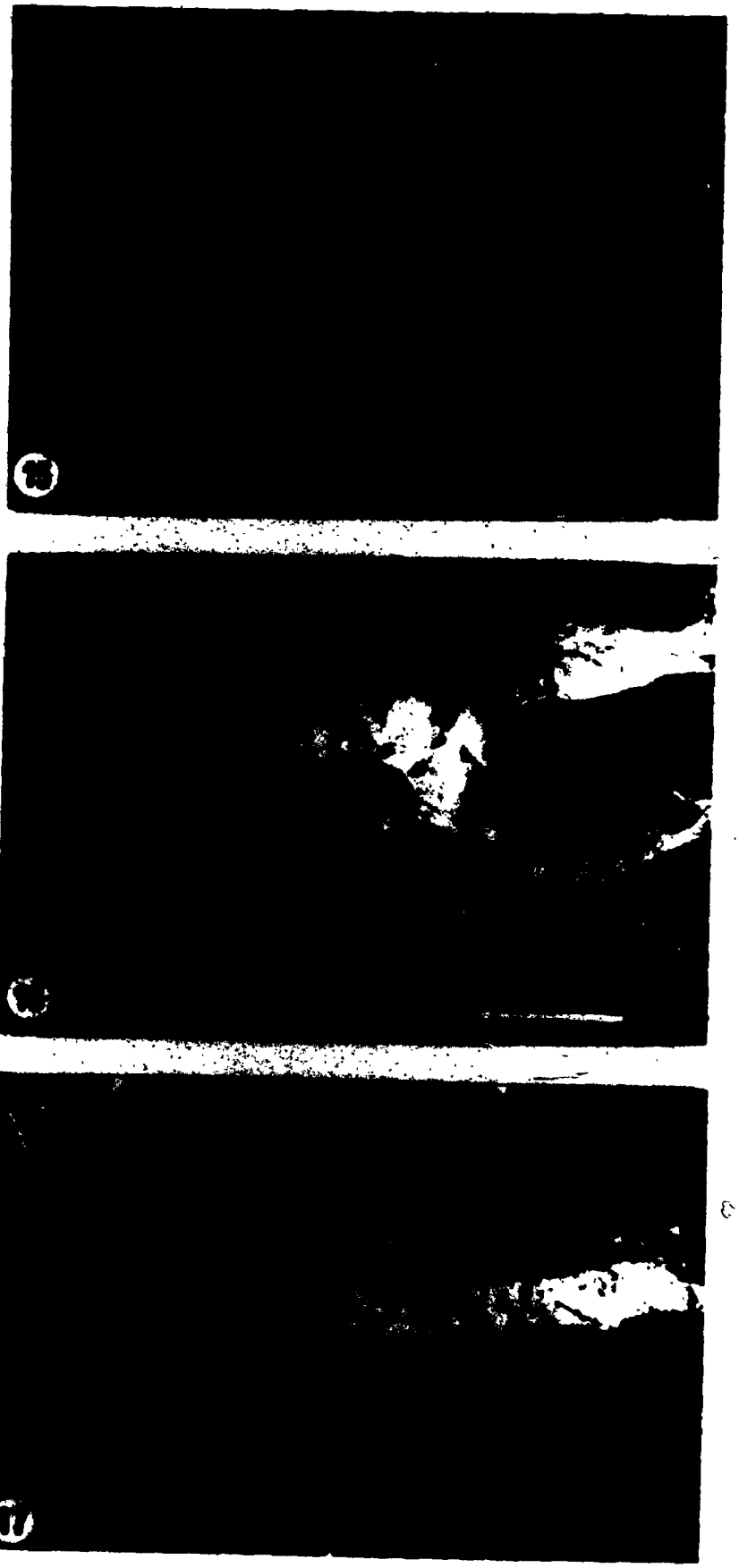

sulphide deposits (J. Kitzler, pers. comm., 1986).

Pyrite in the quartz-plagioclase porphyry near 54°47'49.5"N, 100°06'23.3"W, and with muscovitic rock adjacent to a 40 cm wide quartz vein 70 m to the south of this location, may be related to faulting. No other significant alteration was observed near this structure.

## 4.6 Summary of alteration distribution and timing

Silicification of pillows and massive flows is restricted to aphyric mafic flows and one thin plagioclase-phyric flow (MP1) at the base of the Edwards Lake section. The silicification and associated epidosite patches probably formed at nearly the same time, very soon after extrusion of the flows, and close to or at the water-rock interface (Table 2).

Other forms of silicification, epidotization and garnet-chlorite alteration are largely confined to mafic volcanic wacke and heterolithic, mainly mafic volcanic breccia in the upper part of the Edwards Lake section. A crude zonal arrangment of alteration is apparent: pervasive epidotization occurs in mafic volcaniclastic rocks beneath the heterolithic unit in the eastern part of the area; silicification is characteristic of the whole heterolithic breccia unit, and the zone extends into the mafic wacke unit near spatially and temporally-related felsic dykes; garnet-chlorite alteration increases in intensity along strike to the northwest in the heterolithic unit, reaching a maximum beneath the Chisel Lake massive sulphide deposit.

Silicification, epidotization and Fe-metasomatism of the volcaniclastic rocks may have initially been synchronous or near-synchronous, but Fe-metasomatism evidently continued after silicification and quartz-plagioclase porphyry emplacement (Table 2). Limited data suggest that silicification adjacent to felsic dykes was

approximately contemporaneous with the felsic volcanism that led to deposition of felsic volcaniclastic rocks in the immediate footwall to the Chisel Lake massive sulphide deposit. Silicification elsewhere in the volcaniclastic rocks preceded quartz-plagioclase porphyry emplacement but postdated or overlapped the period of intrusion of pyroxene-phyric mafic dykes. The timing of the commencement of this silicification is problematic.

Plagioclase-quartz-bordered fractures occur mainly to the north of the porphyry intrusion and postdate silicification. They are interpreted to have formed in response to porphyry intrusive activity.

Table 2

**Summary of timing of alteration events in the Edwards Lake area**

| **Alteration type** | Time: Cooling of mafic flows | Deposition of volcaniclastic rocks (MVC,HVC) | Pyroxene-phyric mafic dykes | Hi-$TiO_2$ felsic dykes | Chisel L. massive sulphide deposition? | Qtz-plag porphyry emplace-ment | Defor-mation regional metamor. |
|---|---|---|---|---|---|---|---|
| Silicification and epidoti-zation in flows | - - - - - - - - - - | | | | | | |
| Silicification of volcani-clastic rocks | | ? - - - - - - | - - - - - - - - | - - - - - - ? | | | |
| Pervasive epi-dotization | | ? - - - - - - | - - - - - - - - | - - - - - - ? | | | |
| Fe-metasomatism | | ? - - - - - - | - - - - - - - - | - - - - - - | - - - - - - | - - - - ? | |
| Plagioclase-quartz-bordered fractures | | | | | | ?- - - - - -? | |

# CHAPTER 5

# GEOCHEMISTRY

A prerequisite to quantitatively assessing mass transfer in the fossil hydrothermal system at Edwards Lake is to document the chemical composition of the least altered rocks. Within this framework the gains and losses of components that occurred during alteration can be estimated for domains of hand specimen to outcrop scale. The results for least altered rocks are presented and discussed in the first part of the Chapter, and are followed by a consideration of the geochemistry of alteration.

## 5.1 Geochemistry of least altered rocks

Least altered samples were carefully selected to avoid pillow selvages, weathering crusts, veins, high abundances of amygdales and thermal contraction cracks, or other compositional heterogeneities.

Following Syme (1985), classification of the volcanic rocks is based on $SiO_2$ content (by weight): basalt = 46-54%; andesite = 54-62%, dacite = 62-70%; rhyolite = 70-78%. The $SiO_2$ class limits were determined by adding and subtracting one standard deviation from the average $SiO_2$ contents listed for these rocks by Le Maitre (1976). High alumina basalts are arbitrarily defined as those containing more than 17% $Al_2O_3$.

### 5.1.1 Mafic rocks

The mafic flow rocks form three main compositional groups on the basis of $SiO_2$ content: basalt, basalt-andesite and andesite, corresponding respectively to pyroxene-phyric, plagioclase-phyric and aphyric flows (Appendix 3). The three groupings are discriminated on a

plot of $TiO_2$ vs Zr (Fig. 18), and appear to form a coherent trend of increasing Zr and $TiO_2$, but are not as clearly distinguished on AFM and Jensen cation diagrams (Figs. 19 and 20). All of the mafic volcanic rocks are assigned to the tholeiitic series, based on the criteria of Irvine and Baragar (1971) and Jensen (1976).

Mafic intrusions have compositions that are generally similar to the andesite, basalt-andesite and basalt flows (Appendix 3).

A limited number of least altered mafic volcanic wackes were analyzed, and most have high alumina tholeiitic basalt compositions. They are therefore chemically unlike any of the underlying mafic flows in the Edwards Lake area, which is surprising in view of their textural similarity to the plagioclase-phyric flows.

It is interesting to note that the flow sequence in the study area is compositionally 'inverted', beginning with andesites, overlain by basalt-andesite and capped by basalts. Walford and Franklin (1982) describe an analogous sequence in the hangingwall of the Anderson Lake massive sulphide deposit where more fractionated andesites underlie basalts.

The andesites in the Edwards Lake area are very similar in composition to andesites in the immediate hangingwall of the Anderson Lake massive sulphide deposit (Walford & Franklin, 1982), although Zr abundances are substantially lower than those of the Anderson Lake andesites. As noted by Walford and Franklin (1982) the andesites are similar to Archean andesite (Goodwin, 1977) but contain significantly less $TiO_2$, $K_2O$, Zr, Cr and Ni, and more CaO.

Basaltic flows in the Edwards Lake area differ from the high alumina Threehouse Basalt (Moore, 1977; Walford & Franklin, 1982) which occurs above the Hangingwall Andesite at the Anderson Lake deposit, in their lower $Al_2O_3$ and much lower Zr contents (~10 ppm Zr in #063; av. 42 ppm

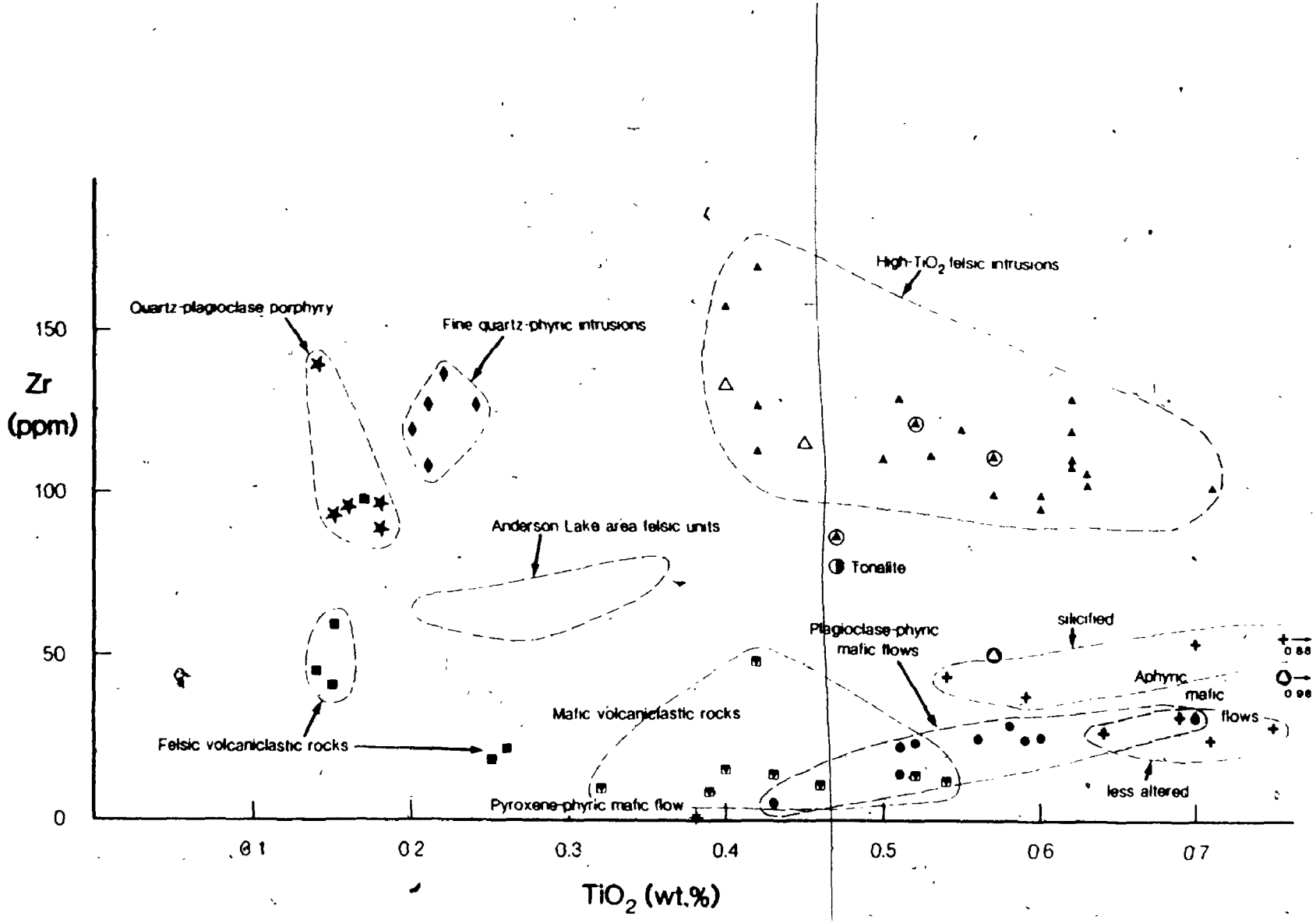


Figure 18. $TiO_2$ versus Zr plot for the principle rock types in the Edwards Lake area. ◐ = mafic margin of composite dyke; ● = felsic core of composite dyke; Δ = felsic volcaniclastic rock from footwall of the Chisel Lake massive sulphide deposit. Data from the Anderson Lake area, including 'tonalite', are plotted for comparison (Walford & Franklin, 1982).

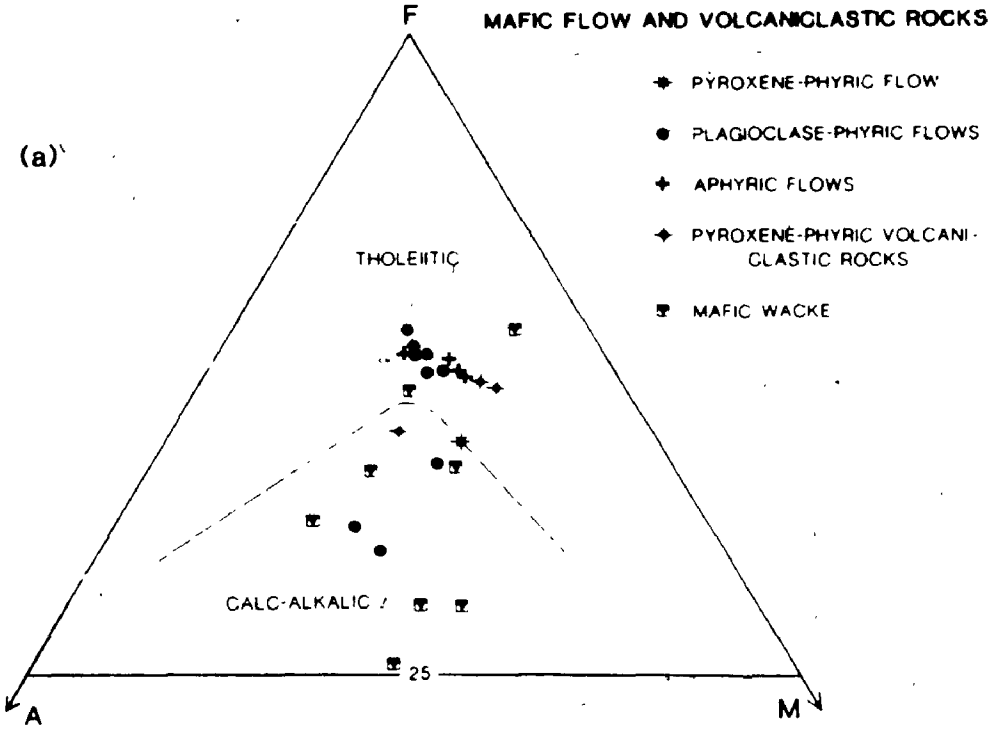


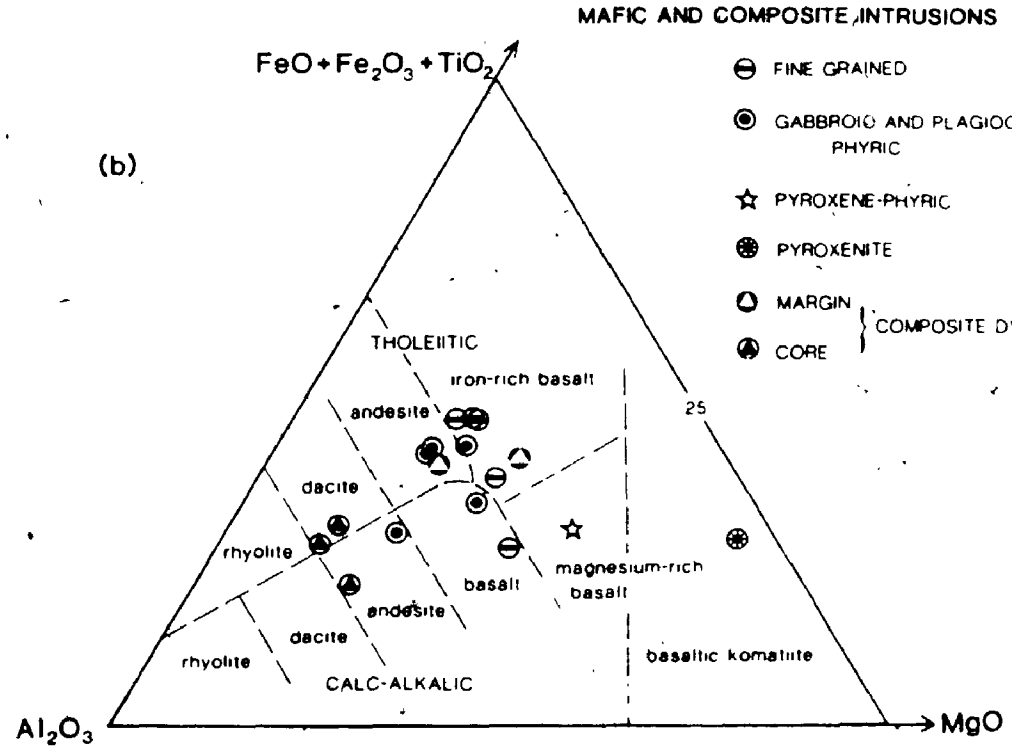


Figure 19. (a) AFM plot of least altered mafic flows. A = $Na_2O + K_2O$, F = FeO + 0.8998 $Fe_2O_3$, M = MgO, all in weight percent. Field boundary from Irvine & Baragar (1971).

(b) Jensen cation plot of least altered mafic intrusive rocks and composite dykes. Chemical components calculated as molecular proportions (Jensen, 1976).

Figure 20. Jensen cation plots of less altered and altered mafic and felsic rocks. Chemical components calculated as molecular proportions (Jensen, 1976).

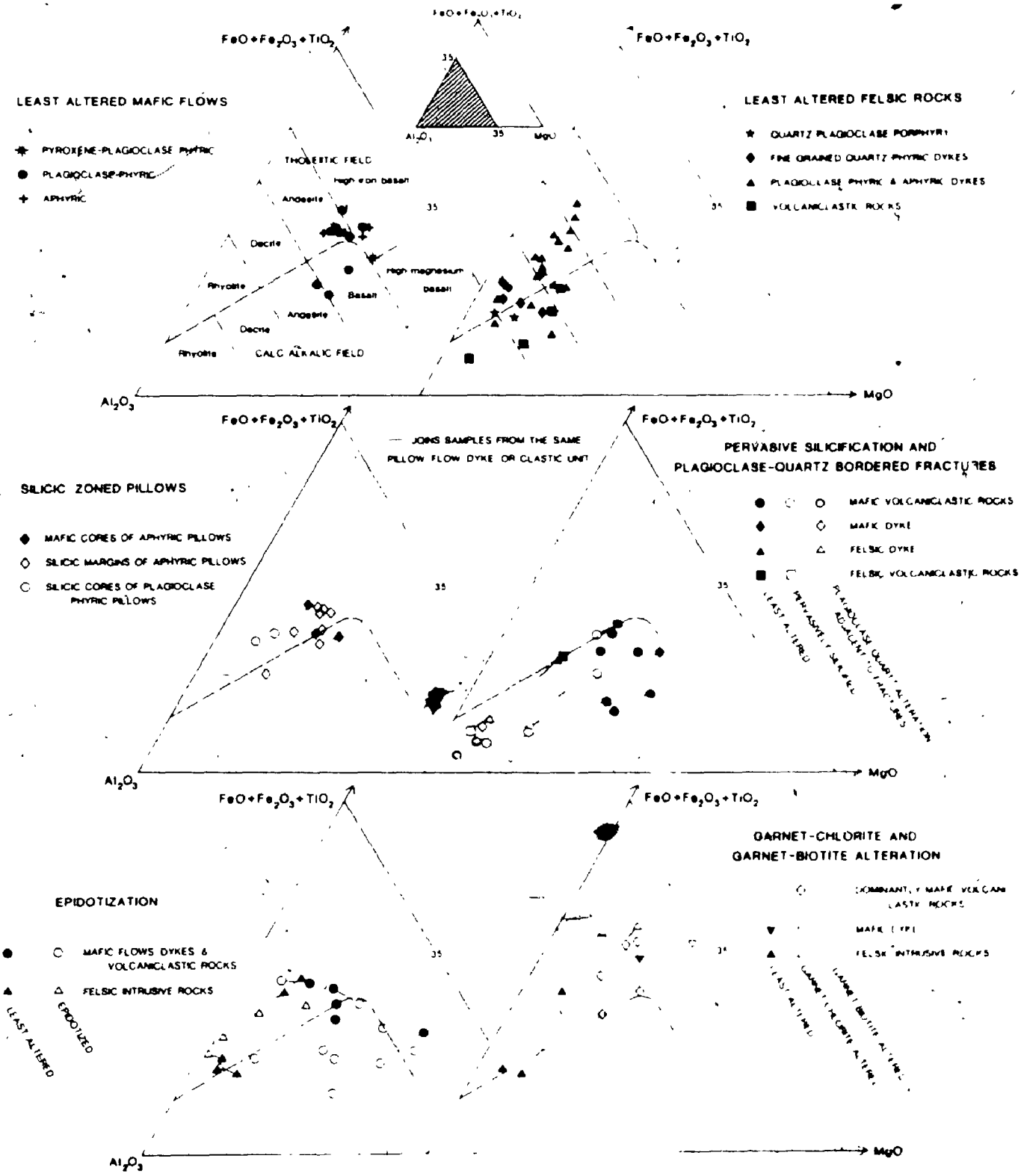
LEAST ALTERED MAFIC FLOWS
PYROXENE-PLAGIOCLASE PHYRIC
PLAGIOCLASE-PHYRIC
APHYRIC
LEAST ALTERED FELSIC ROCKS
QUARTZ PLAGIOCLASE PORPHYRY
FINE GRAINED QUARTZ PHYRIC DYKES
PLAGIOCLASE PHYRIC & APHYRIC DYKES
VOLCANICLASTIC ROCKS
THOLEIITIC FIELD
high iron basalt
Andesite
Dacite
Rhyolite
Basalt
high magnesium basalt
Andesite
Dacite
Rhyolite
CALC ALKALIC FIELD
$FeO+Fe_2O_3+TiO_2$
$Al_2O_3$
MgO
35
JOINS SAMPLES FROM THE SAME PILLOW FLOW DYKE OR CLASTIC UNIT
SILICIC ZONED PILLOWS
MAFIC CORES OF APHYRIC PILLOWS
SILICIC MARGINS OF APHYRIC PILLOWS
SILICIC CORES OF PLAGIOCLASE PHYRIC PILLOWS
PERVASIVE SILICIFICATION AND PLAGIOCLASE-QUARTZ BORDERED FRACTURES
MAFIC VOLCANICLASTIC ROCKS
MAFIC DYKE
FELSIC DYKE
FELSIC VOLCANICLASTIC ROCKS
LEAST ALTERED
PERVASIVELY SILICIFIED
PLAGIOCLASE-QUARTZ ALTERATION ADJACENT TO FRACTURES
EPIDOTIZATION
MAFIC FLOWS DYKES & VOLCANICLASTIC ROCKS
FELSIC INTRUSIVE ROCKS
LEAST ALTERED
EPIDOTIZED
GARNET-CHLORITE AND GARNET-BIOTITE ALTERATION
MAFIC INTRUSIVE ROCKS
LEAST ALTERED
GARNET-CHLORITE ALTERED
GARNET-BIOTITE ALTERED

in Threehouse basalt). The mafic volcanic wacke unit is more similar to the Threehouse Basalt, but these volcaniclastic rocks contain about half as much Zr.

### 5.1.2 Felsic rocks

Sampling of felsic volcanic rocks was restricted to volcaniclastic units because of the lack of exposed felsic flows, and consequently these analyses are not necessarily representative of magmatic compositions. Felsic volcanic wacke and clasts in felsic breccias contain 69% to 78% $SiO_2$ but a maximum of only 2.2% $K_2O$ is present (average = 0.9% $K_2O$; Appendix 3, Table 10). They are also notably low in Zr (average 47ppm), and one sample analyzed for REEs contains only 7-35 times as much REEs as chondrite (Appendix 3; Table 11). For comparison, rhyolites in the Proterozoic Lynn Lake belt typically contain 100-350 ppm Zr and between 15 and 100 times as much REEs as chondrite (Syme, 1985).

The various types of felsic intrusions are compositionally distinct from the volcaniclastic units and from each other, as illustrated in a $TiO_2$ vs Zr plot (Fig. 18). The intrusions contain about twice as much Zr as the volcanic wackes and breccias, and the aphyric and plagioclase-phyric phases have unusually high $TiO_2$ abundances, typically 0.4-0.6 %. $K_2O$ contents of the quartz-phenocryst-bearing intrusions reach only 2.1% (average = 1.1%), and are less than 1% in almost all aphyric and plagioclase-phyric felsic intrusions.

Following the definition of Barker (1979) that trondhjemites should contain greater than about 68% $SiO_2$, less than 3.4% (FeOT + MgO) and less than about 2.5% $K_2O$, all of the analyzed felsic volcaniclastic rocks and quartz-phenocryst-bearing intrusions are classified as trondhjemite, although their (FeOT + MgO) contents are in most cases

typical of tonalite. The aphyric and plagioclase-phyric felsic intrusions form a tonalite to trondhjemite suite, according to Barker's definition. The presence of biotite partially replacing plagioclase phenocrysts in some felsic rocks indicates that minor Fe-metasomatism has affected even the least altered felsic rocks, and may account for (FeOT + MgO) contents that are higher than expected for the corresponding $SiO_2$ abundances. Also, the possibility that K was leached during hydrothermal alteration cannot be dismissed.

Composite mafic-felsic dykes in the study area provide geochemical evidence, albeit limited, of a petrogenetic link between some of the mafic rocks and the high-$TiO_2$ felsic dykes. The mafic margins of the dykes have compositions which plot in the area of mafic volcanic and intrusive rocks in AFM, Jensen and $TiO_2$ vs Zr diagrams, whereas the felsic interiors of the dykes are compositionally similar to the high-$TiO_2$ tonalite to trondhjemite intrusions (Figs. 18, 19b, and 20). If the mafic and felsic magmas coexisted, as the field relationships suggest, then the simplist interpretation is that the two magmas possessed a common parent and are related through a process such as igneous differentiation, partial melting or magma mixing. However, the compositional gap between the high-$TiO_2$ felsic intrusions and the mafic rocks is not as broad as in bimodal suites (e.g Barker & Arth, 1976; Thurston et al., 1985).

Of possibly more direct relevance to the present study is the similarity in $TiO_2$, Zr and $Al_2O_3$ contents of the high-$TiO_2$ aphyric and plagioclase-phyric tonalite-trondhjemite intrusions to those in the plagioclase-phyric felsic volcaniclastic rocks that separate the Chisel Lake massive sulphide deposit from the heterolithic breccia unit HVC (Appendix 3, Table 10, analyses 16-33, 5 and 108). No other felsic volcanic units with a high-$TiO_2$ composition are known from the Chisel

Lake - Edwards Lake area. Although only two analyses were obtained, this felsic volcaniclastic unit is tentatively interpreted to represent the volcanic equivalent of the high-$TiO_2$ felsic intrusions because of their unusual, similar composition. As these dykes occur about 2 km stratigraphically below the Chisel Lake ore horizon, silicification that is spatially and probably temporally associated with the high-$TiO_2$ dykes can be inferred to have occurred at depths below the ore horizon of about 2 km. As discussed in Section 4.1.5, the minimum depth below the water-rock interface of silicification adjacent to high-$TiO_2$ felsic dykes is about 0.3 km and a maximum depth of 4-6 km is inferred.

Felsic rocks of the Anderson Lake area have $TiO_2$ contents that lie between those of the Edwards Lake felsic volcaniclastic rocks and high-$TiO_2$ tonalite-trondhjemite intrusions (Fig. 18), and generally contain more K. However, the quartz-phyric subvolcanic tonalite sill at Anderson Lake (Walford & Franklin, 1982) plots close to the field of high-$TiO_2$ felsic rocks in Figure 18 and has a similar major element composition (Table III of Walford & Franklin, 1982).

## 5.2 Geochemistry of alteration

The approach used to study the geochemistry of alteration focussed on comparison of less altered and altered rocks in order to determine mass gains and losses during metasomatism, and utilized the principles established by Akella (1966) and Gresens (1967). Because chemical components in whole rock data are conventionally summed to 100%, no component is independent of the others, so direct comparison of 'raw' data can lead to erroneous interpretations of gains and losses. If a geologically reasonable assumption can be made that metasomatism occurred at constant mass or constant volume, or that one component was conserved, then all of the remaining variables can be determined.

Grant (1986) determined a simple graphical solution to the equations of Gresens (1967) whereby components immobile during metasomatism, if any, can be readily identified. If two or more components were truly immobile, then their ratios should remain constant during metasomatism, despite possible changes in their absolute abundances. Hence, in a plot of concentrations in least altered rocks versus concentrations in the altered equivalent, the immobile components should plot on a line through the origin (the 'isocon'). The gains and losses of other components, or volume changes, can then be determined (Fig. 21). The following results were derived by Grant's method, and are presented for selected components in Figures 22 and 23; a complete tabulation of the gains and losses along with discussion of errors, can be found in Appendix 5.

Emphasis in the mapping was on tracing individual units into and through the alteration zones so that pairs of samples that were compared in the mass-balance calculations could be reliably chosen from the same pillow, flow, volcaniclastic unit (bed where possible) or intrusion. Small differences in trace element contents made comparison of even adjacent, texturally similar flows invalid in some cases, hence the necessity for careful sampling.

### 5.2.1 Alteration of pillows and massive flows

Figure 22 shows the calculated mass gains and losses of chemical components across a representative silicified pillow (Fig. 9) from near the base of aphyric flow unit MA. The profiles were constructed from comparison of four analyses of this pillow at the positions indicated in Figures 9 and 22, and from one selvage sample from another pillow in the same flow. Also shown are the maximum and minimum gains and losses found in other pillows, from a total of 19 samples. For some pillows,

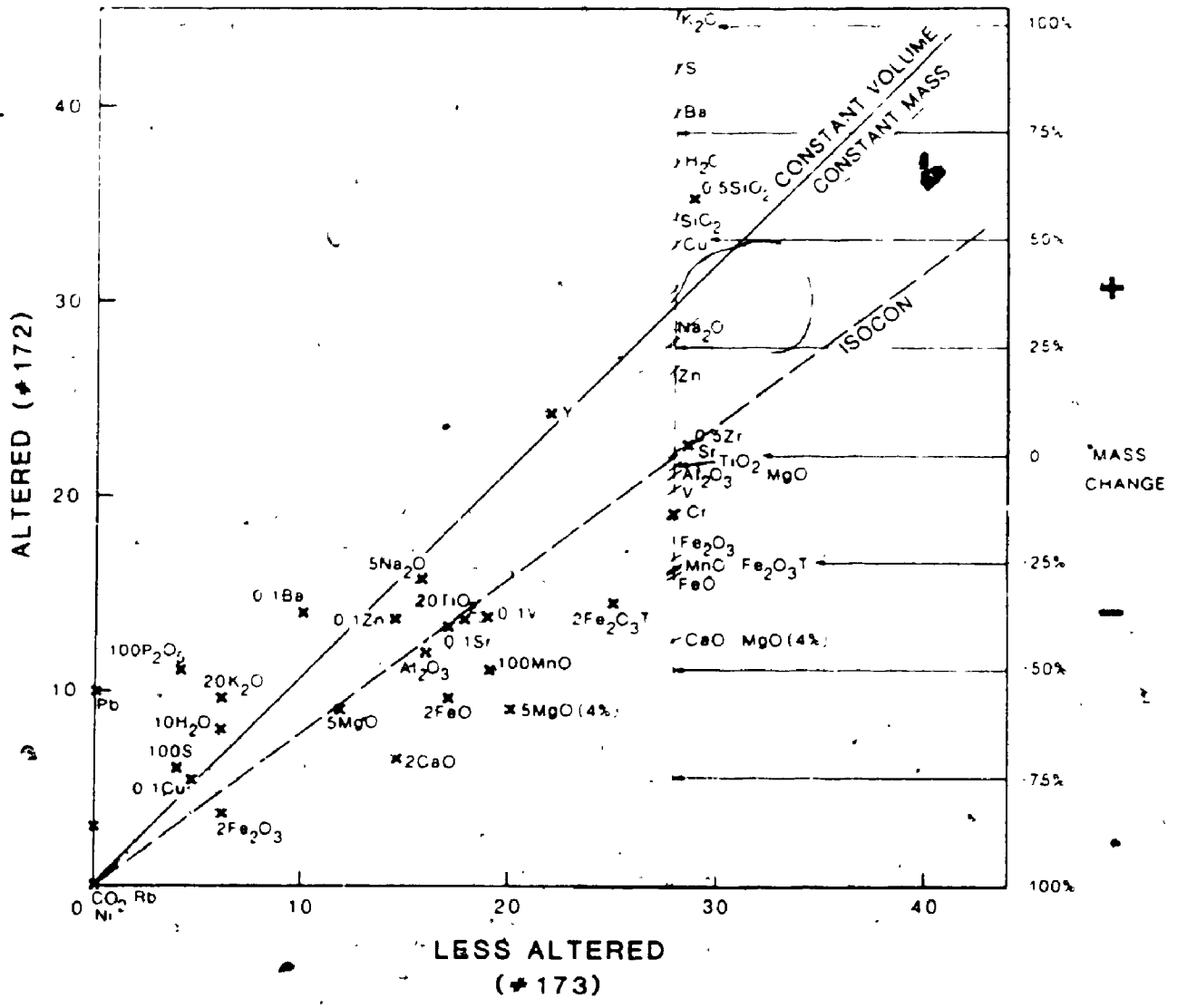


Figure 21. Isocon diagram illustrating the method of Grant (1986) for calculating mass and volume changes during metasomatism. The weight percent of each major element oxide and concentration in ppm of trace elements in the less altered rock are plotted against the same component in the altered rock, each multiplied by the same factor so that the points lie in the central parts of the diagram. The isocon in this example was chosen on the basis of the near-constant ratios of $TiO_2$, Zr and $Al_2O_3$. The difference in slope between the isocon and a line joining the origin to a point, is porportional to the mass change for that component represented by the point, subject to the errors discussed in Appendix 5. The 'constant volume' line has slope = (density of the less altered rock) / (density of the altered rock); volume changes are proportional to the difference of this slope to that of the isocon.

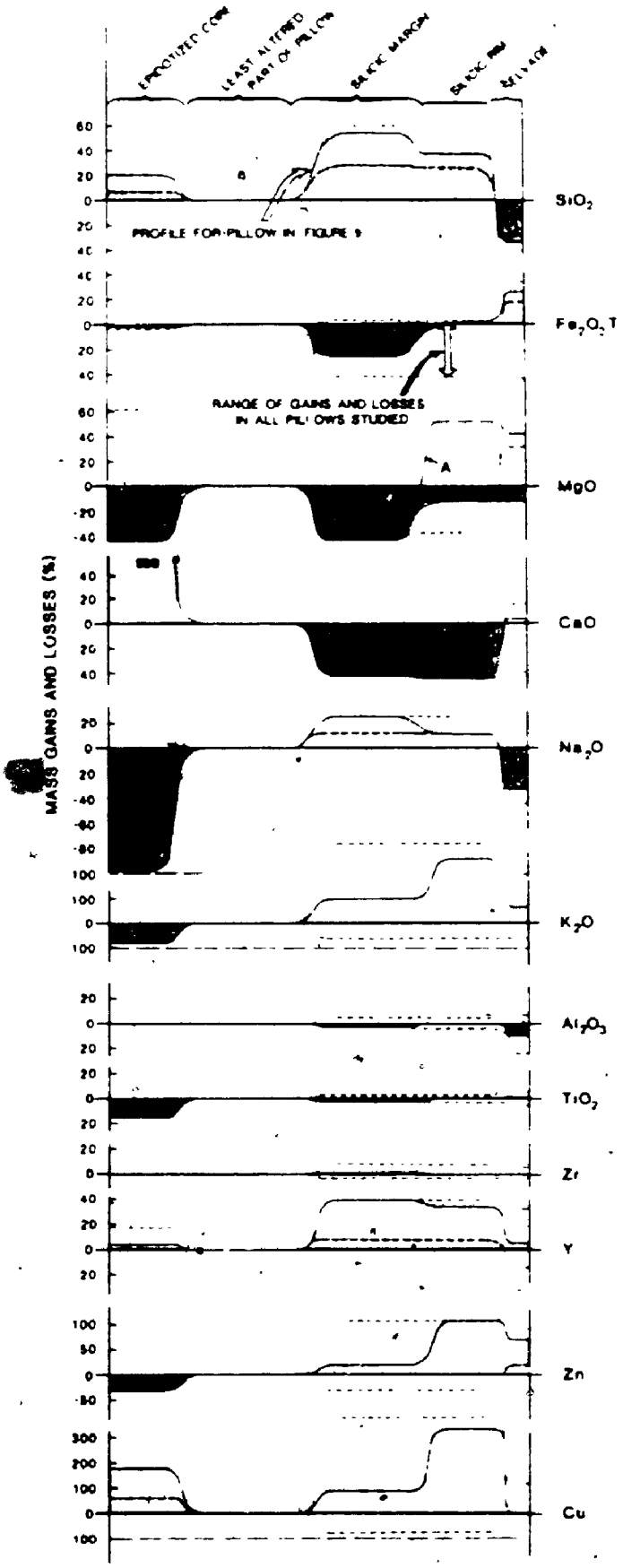


Figure 22. Mass gains and losses across the pillow shown in Figure 9, and the range of gains and losses in all pillows studied (19 samples). Mass changes were calculated by Grant's (1986) method as a percentage ~~of the mass~~ proportion of each chemical component in the least altered part of the pillow, and are subject to the errors discussed in Appendix 5. Curve A in the MgO profile is calculated assuming MgO=2.37% in sample 173; solid curve is for MgO=4% in sample 173 (see text).

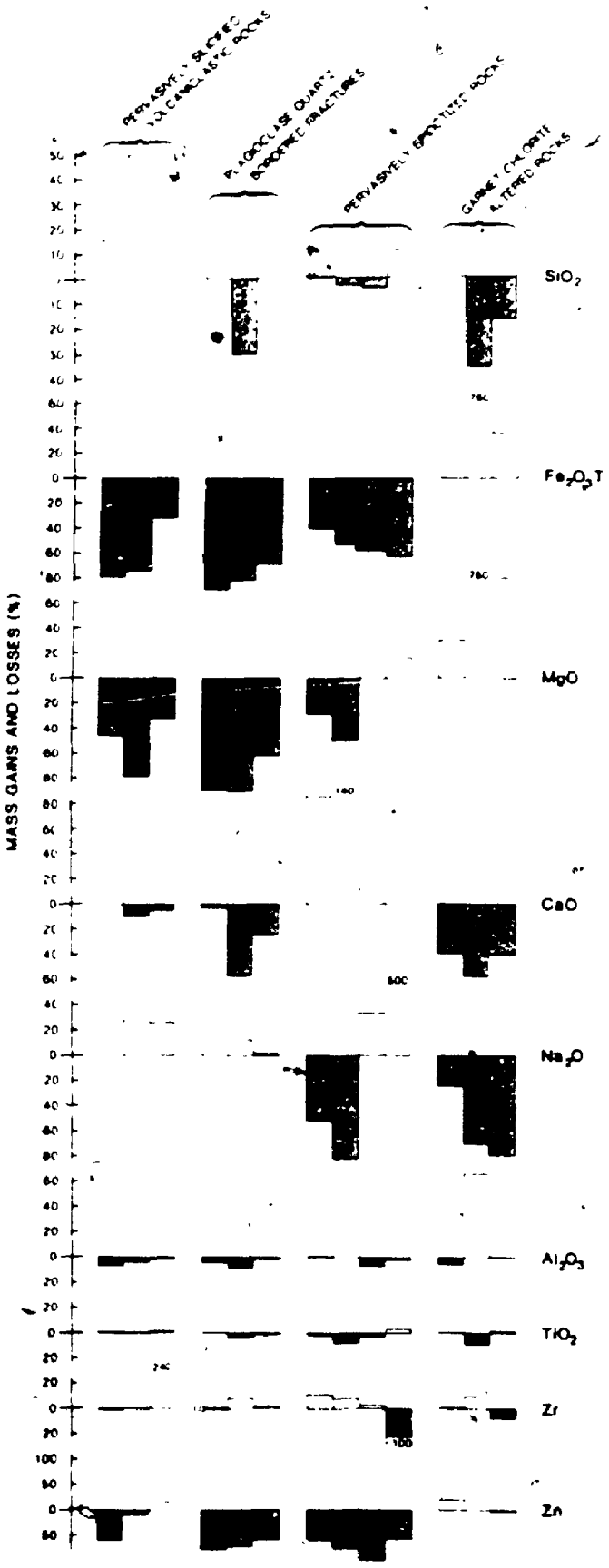


Figure 23. Mass gains and losses in pervasive silicification of volcaniclastic rocks, plagioclase-quartz-borders to fractures, pervasive epidotization and garnet-chlorite(-biotite) alteration. Mass changes in altered rocks were calculated by Grant's (1986) method as a percentage of the mass proportion of each chemical component in a less altered sample from the same bed, unit, intrusion or flow, and are subject to the errors discussed in Appendix 5.

such as the one shown in Figue 9, comparison was made between the altered and least altered parts of the pillow. However, analyses from the more completely altered pillows were compared with different but less altered pillows in the same flow. All least altered samples from silicified pillows have similar major element compositions to pillows in less altered flows of similar texture, except for the relatively low MgO content of #173 (2.37%), and the low $Fe_2O_3T$ content of #086 (9.55%; Appendix 3, Table 10, analyses 49 and 52). For the purposes of the mass-balance calculations MgO for #173 and $Fe_2O_3T$ for #086 were assigned values of 4 wt% and 12 wt%, respectively, which are approximately equal to the average MgO and $Fe_2O_3T$ contents of other least altered aphyric pillows. The results for MgO=2.37% and MgO=4% are both plotted in Figure 22, from which it is seen that the curve for MgO=4% is more typical of other pillows studied. The gains and losses of other components in the pillow in Figure 9 would appear to be representative of zoned pillows elsewhere in the study area.

Since $TiO_2$, Zr and $Al_2O_3$ lie close to a line through the origin in isocon plots of less altered versus altered samples in pillows (e.g. Fig. 21), these components are inferred to have been essentially immobile throughout the pillows, except possibly for Al loss from the selvages and Ti loss from epidotized cores. The gains and losses in Figure 22 were measured directly from isocon plots, so that immobile behaviour is indicated by very small deviations from the zero-change line.

The silicic margins of the pillows are strongly enriched in Si, Na, K, Rb, Y, Zn and Cu, whereas Fe, Mg, Ca, Mn and Sr were lost from this zone, based on plots such as Figure 21 in which $SiO_2$, $Na_2O$ etc. lie above the isocon defined by $TiO_2$, Zr and $Al_2O_3$, whereas $Fe_2O_3T$, etc. lie below the isocon. Again, these gains and losses are plotted in Figure

22; this procedure was used in determining all gains and losses described below. V is also lost from the silicic zone, but Cr shows relatively low mobility (Appendix 5).

In the selvages, Si, Fe, Mg and Na have opposite trends to those in the silicic margins. The epidotized cores of pillows display large gains of Ca and are extremely depleted in Na.

Silicification and epidotization of a massive, aphyric mafic flow probably led to similar gains and losses of components as in the pillows (Appendix 5), based on the similarities in composition of altered samples in the massive and pillowed flows (Appendix 3, Table 10, analyses 66-68). Analysis 66 represents the hornblendic periphery of a zoned alteration patch and is similar in composition to pillow selvage rock, whereas analysis 67 from the silicic part of a patch is similar in composition to the silicified margins of pillows.

Loss of Fe and Mg during silicifiction of the pillows is also illustrated qualitatively in a Jensen cation plot (Fig. 20): intensely silicified pillows form a trend towards the 'A' apex because Al was relatively immobile. On an AFM diagram the alteration trend is towards alkali enrichment, due to the addition of Na and loss of Fe and Mg, and thus resembles a calc-alkaline differentiation trend or the alkali-enrichment part of a tholeiitic differentiation trend.

The limited REE data are very interesting (Fig. 24 and Appendix 5, Table 17) and indicate that: (a) Based on the constancy of ratios of the heavy REEs (HREEs), $TiO_2$, Zr and $Al_2O_3$ in altered and less altered rock, the HREEs, and particularly Yb, were immobile (or nearly so) during silicification and epidotization, and were simply diluted. (b) The light REEs (LREEs) appear to have been more mobile, and may have been enriched in the silicified and epidotized parts of the pillow; (c) Eu was lost from the rock during silicification and epidotization; (d)

REE abundances in the least altered parts of a zoned pillow are significantly greater than in a less altered pillow from a different but nearby aphyric flow - an unrealistic mass loss of 70% would be required to effect such a change. This difference in REE abundances is probably due to differences in REE contents of the melts, and is supported by $TiO_2$-Zr data. Figure 25 shows the higher $Zr/TiO_2$ ratios of samples from silicified aphyric pillows, whether of least altered or of silicified portions of the pillows, compared to much less silicified aphyric and plagioclase-phyric flows. If silicification had led to a change in the $Zr/TiO_2$ ratio then a difference in this ratio between the least altered and silicified parts of pillows would be expected, but the observed differences are insignificant relative to those between silicified and less silicified flows. A similar argument can be made for $HREE/TiO_2$ ratios. Hence it is concluded that the silicified flows had greater $Zr/TiO_2$ and $HREE/TiO_2$ ratios in the melts than less silicified flows.

5.2.2 Gains and losses in other types of alteration.

Figure 23 presents the results of mass-balance computations for other alteration types, including **silicification** of volcaniclastic rocks. Apart from possible losses of Zn and low mobility of Ca, the gains and losses that occurred during silicification of volcaniclastic rocks are very similar to those observed in the silicified margins of pillows.

**Plagioclase-quartz borders to fractures** also share the patterns of enrithment and depletions that characterize the silicified pillows and volcaniclastic rocks, although Si apparently was lost in one of the three examples (Fig. 23). This particular comparison is between plagioclase-rich borders to fractures and a mafic dyke host rock, whereas, in the other cases of Si addition, quartz is more abundant in the alteration.

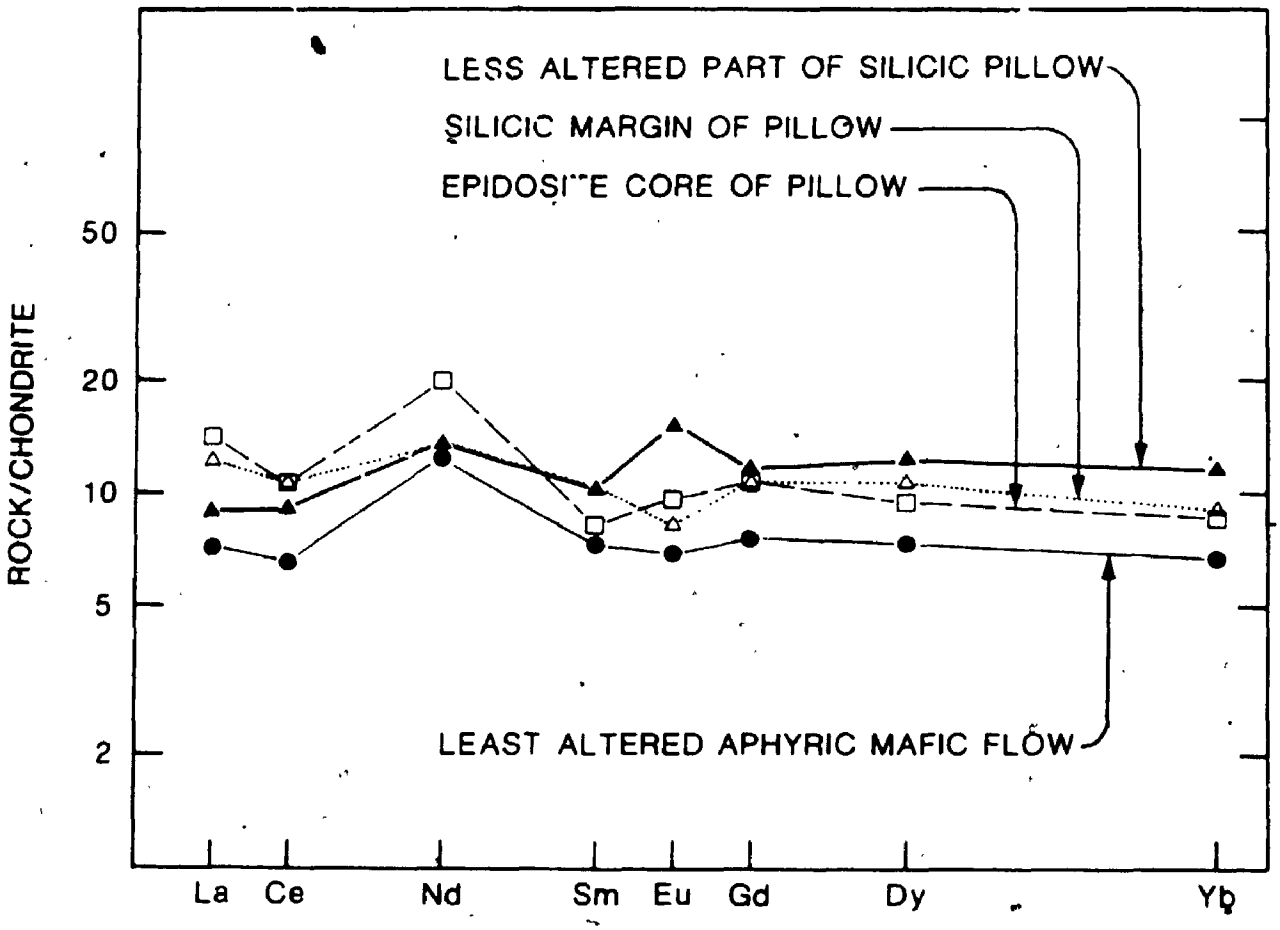


Figure 24. Chondrite-normalized REE abundances of samples in the altered pillow shown in Figure 9. Those of a less altered aphyric mafic flow nearby are also shown for comparison.

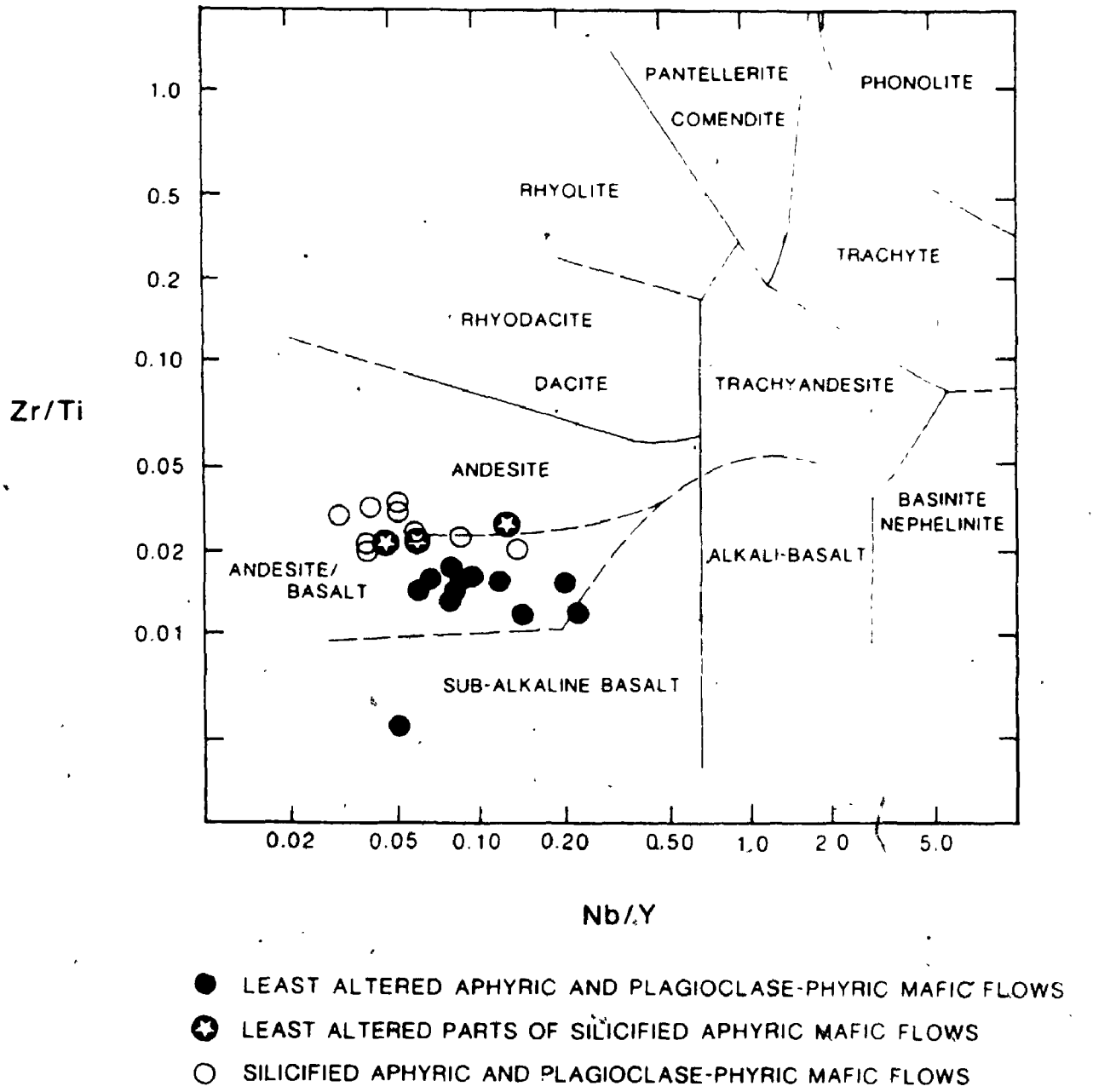


Figure 25. Plot of Zr/Ti versus Nb/Y (after Winchester & Floyd, 1977), comparing least altered mafic flows to silicified mafic flows. The higher Zr/Ti values of silicified flows are considered to be magmatic in origin (see text), but the trend towards lower Nb/Y values in silicified flows may in part be a result of alteration since these elements were more mobile.

On a Jensen cation plot (Fig. 20) the alteration trends for plagioclase-quartz borders to fractures and silicification of volcaniclastic rocks converge on the alumina apex, showing the generally greater percent mass losses of Fe and Mg during these alteration processes than in silicification of pillows (Fig. 20; compare also Figs. 22 and 23).

The gross patterns of gains and losses during both silicification and plagioclase-quartz alteration adjacent to fractures apparently are independent of rock type, with the possible exception of Si behaviour in the examples where plagioclase-quartz-bordered fractures cross from a fine grained mafic dyke to a felsic intrusion.

REE data for silicified volcaniclastic rocks is limited to a single comparison of silicified and less altered, although weakly Fe-metasomatized, felsic volcaniclastic rocks. The data are plotted in Figure 26 and show two significant features: (i) the pattern for the silicified rock is approximately parallel to that of the less altered sample, and (ii) the silicified rock contains about two thirds as much of each of the REEs as the less altered rock. Gains and losses calculated by Grant's method indicate that for this alteration most of the REEs were only slightly depleted, and Yb was essentially immobile, along with Ti, Zr and Al (Appendix 5, Table 17). The computations also suggest that a volume differential of about 20-30% between the less altered and silicified rocks could account for the differences in absolute concentrations of Yb, $TiO_2$, Zr and $Al_2O_3$. In other words the two features of the REE patterns noted above are consistent with the interpretation that Yb as well as Ti, Zr and Al were immobile or had low mobility and were diluted during alteration of the felsic volcaniclastic unit.

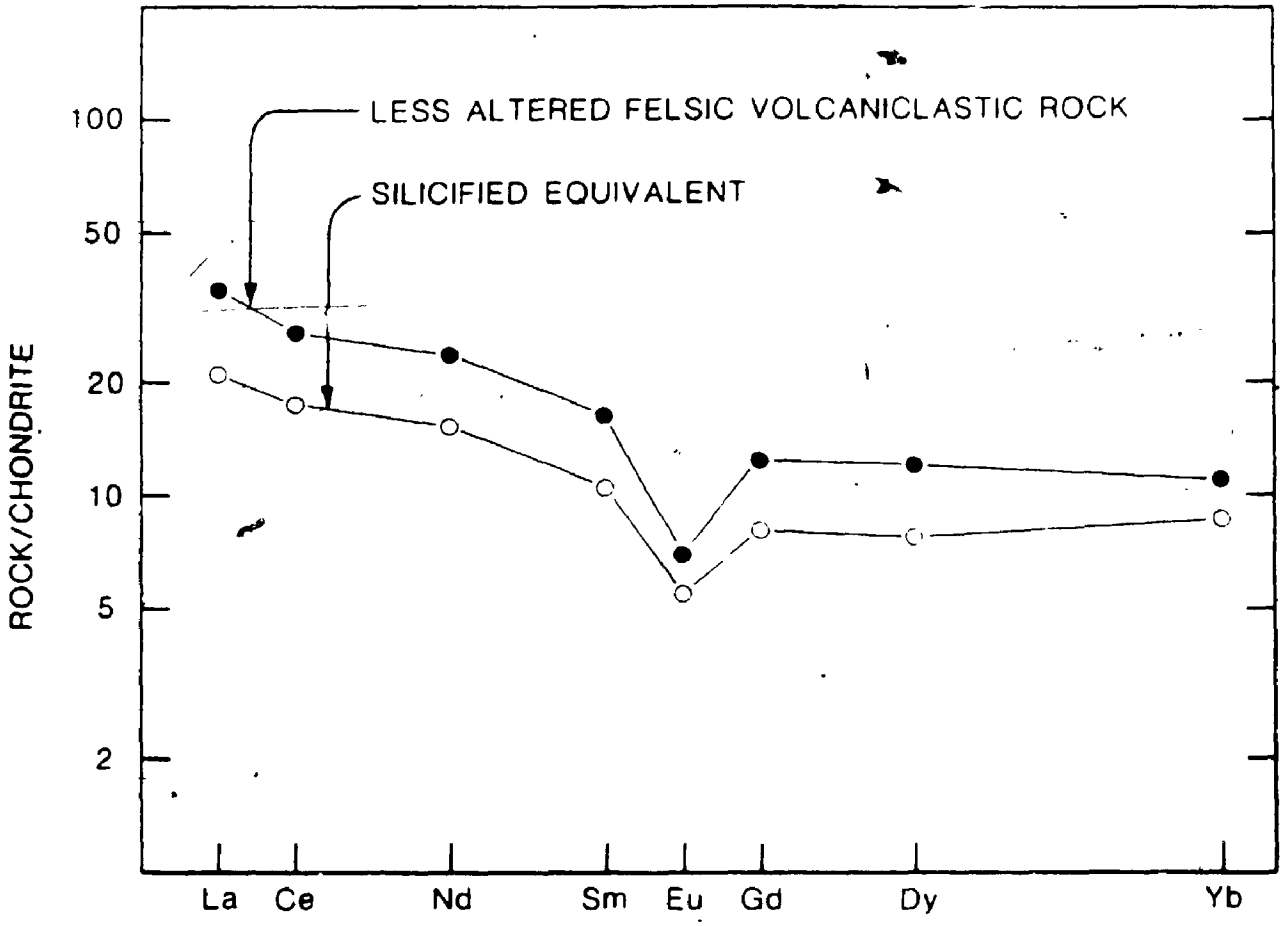


Figure 26. Chondrite-normalized REE abundances in a less altered felsic volcaniclastic rock (sample 270) and the silicified equivalent (sample 271).

**Pervasive epidotization** resulted in large losses of Fe and Zn, and addition of Ca, but only very small changes in Si and Ti. Al and Zr each show very small changes in three of the four examples, although addition of Al may have occurred in #015(ii), and an apparent depletion in Zr of 100% is shown in the comparison between #243 and #073. However, the Zr content of the least altered rock, a mafic volcanic wacke, is only 10 ppm and the combination of analytical errors (Appendix 4) and local variability in Zr abundance probably accounts for the apparent loss.

The behaviour of Na and Mg during epidotization was more variable than the other components shown in Figure 23. In specimens that have gained large amounts of Ca (#280 and #015(ii)) correspondingly large losses of Na occurred, along with depletion of Mg. Samples that gained less Ca, however, were enriched in Na and Mg, according to the calculations. Further illustration of the inconsistent gains and losses of Mg is afforded by a Jensen plot of epidotized rocks and their less altered equivalents (Fig. 20). The divergence of trends is due in large part to variability in the behaviour of Mg, because it has been shown (above) that Al was essentially immobile and Fe was leached.

In comparison to epidotization in zoned, silicified pillows, pervasive epidotization has resulted in much greater percentage mass losses of Fe, but the gains and losses of other components in the epidotized pillows are otherwise similar to those of the more Ca-enriched pervasively altered rocks.

**Garnet-chlorite-rich rocks** gained Fe, Mg and possibly Zn (in two of the three cases in Fig. 23), but lost Na. Si was leached in two of the examples shown in Figure 23. These results are strikingly opposed to the enrichments and depletions of the same components that occurred during pervasive silicification of volcaniclastic rocks, plagioclase-quartz alteration adjacent to fractures and, except for the behaviour of

Zn, during silicification of mafic flows. Ti, Zr and Al again show generally very low mobility, although Al evidently was gained in the extreme metasomatism that converted quartz-plagioclase porphyry to garnet-chlorite rock.

A Jensen cation plot (Fig. 20) of the three pairs of samples used in Figure 23 to calculate the gains and losses in garnet-chlorite alteration shows trends of alteration away from the 'alumina apex' for two of the three pairs of samples. These trends correspond to approximately equal percentage mass gains of $Fe_2O_3T$ and MgO during alteration. However, in terms of grams gained per 100 g of original rock, $Fe_2O_3T$ addition exceeded the gains of MgO in these two comparisons. The third pair of samples (#242 and #243) display an alteration trend of decreasing $Fe_2O_3T$/MgO ratio, but as in the first two comparisons, the alteration nevertheless was a process of dominantly Fe addition. For example, in the third comparison a 40% increase in the mass of $Fe_2O_3T$ is equivalent to a gain of about 5.9 g of $Fe_2O_3T$ per 100 g of original rock, whereas an 80% gain in MgO mass results in addition of only about 3 g of MgO because the MgO content of the less altered is less than the $Fe_2O_3T$ content.

Several volcaniclastic rocks marked by garnet-biotite-chlorite ± staurolite alteration were also analyzed. Quantitative assessment of gains and losses were not attempted because all these samples are from areas where no satisfactory least altered specimens were exposed. Qualitative changes, however, can be deduced by comparison of their compositions with those of inferred protoliths, which were determined from stratigraphic, textural and compositional characteristics ($TiO_2$, Zr). In general the garnet-biotite-chlorite ± staurolite rocks show similar gains and losses to those of garnet-chlorite rocks but have gained rather than lost K. Also, in the two samples that contained

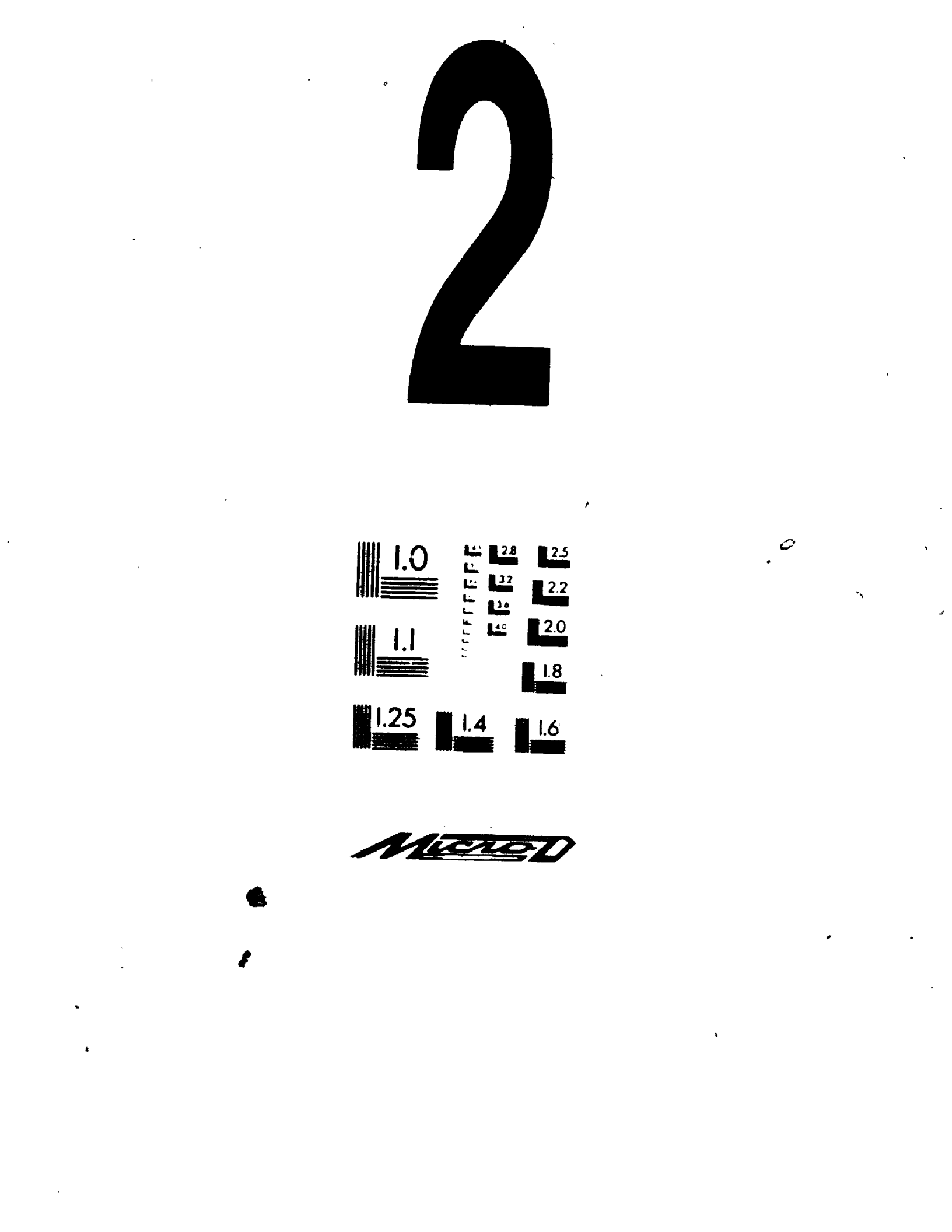
2
1.0
1.1
1.25
1.4
1.6
2.8
3.2
3.6
4.0
2.5
2.2
2.0
1.8
MICROCOPY

staurolite, Na was quantitatively removed. On a Jensen cation plot (Fig. 20) the biotitic rocks form a scatter of points which overlap the field of garnet-chlorite-rich rocks. The samples with relatively lower ($FeO + Fe_2O_3 + TiO_2$) contents all may contain a felsic detrital component, whereas those with relatively greater ($FeO + Fe_2O_3 + TiO_2$) contents were probably derived from either mafic or mixed mafic plus felsic protoliths. Comparison with the fields of less altered mafic and felsic rocks illustrates that most of the analyzed garnet-biotite-chlorite±staurolite rocks probably gained Fe.

### 5.2.3 Effects of alteration on $TiO_2$, Zr, $Al_2O_3$, and REEs.

A key finding of the present study is the lack of significant mobility of Ti, Zr, Al and HREEs (where analyzed) in almost all of the examples of alteration examined. This conclusion is based largely on the consistent ratios of these elements in less altered and altered rocks. To explain these results by a process of proportional dilution or loss of Ti, Zr, HREEs and Al in every type of alteration studied would require a highly contrived explanation because these elements have different diffusion rates and mineral/fluid partition coefficients, and enter a diversity of minerals which have different solubilities in a given fluid (Campbell et al., 1984).

Numerous other studies have found Ti and Zr to be immobile under conditions of low grade metamorphism and weak metasomatism, and even during intense hydrothermal alteration (e.g. Winchester & Floyd, 1977; Floyd & Winchester, 1978; Strong et al., 1979; Finlow-Bates & Stumpfl, 1981; Ludden et al., 1982; Costa et al., 1983; Lockwood, 1986). Ti and Zr do appear to have been mobile, however, where large $X_{CO2}$ gradients were present (Hynes, 1980; Murphy & Hynes, 1986), and in some cases where alteration was extreme (Campbell et al., 1984), and Zr mobility

during F-metasomatism was reported by Alderton et al. (1980). Conservation of Al is commonly assumed in low grade metamorphic rocks and in many types of hydrothermal alteration (e.g. MacGeehan, 1978; Strong et al. 1979; Costa et al., 1983; Morton & Nebel, 1984) because the solubility of aluminum in aqueous solutions is very low (~2 ppm) at temperatures below 500°C and at pressures of less than about 2 kbar (Ragnarsdottir & Walther, 1985). However, at temperatures of 600°C and above and at higher pressures, significant transport of Al may occur (Anderson et al., 1985). Aluminum solubility is also pH-dependent (Hem & Roberson, 1967).

The REEs, too, have been regarded as immobile under conditions of low grade metamorphism (Humphris et al., 1978; Ludden et al., 1982; Campbell et al., 1984) and during silicification (Dostal & Strong, 1983), but differential mobility of the REEs has been reported in several studies. For example, intense alteration in the footwall pipes beneath massive sulphide deposits has resulted in leaching of the LREEs and middle REEs (Campbell et al., 1984) or of all the REEs (MacGeehan & MacLean, 1980); low-temperature seafloor weathering of pillow selvages can lead to LREE enrichment (Ludden & Thompson, 1978), or depletion of all the REEs (Staudigel & Hart, 1983); and REE mobility evidently can occur where $X_{CO2}$ of the fluid was high (Martin et al., 1978; Ludden et al., 1982).

The few exceptions of mobility in the suite Al-Ti-Zr-HREEs at Edwards Lake may be related to some of the parameters discussed above: (a) The large gain of Al in sample #293 compared with #055 occurs in a fracture-controlled garnet-chlorite replacement zone of extreme metasomatism where fluid/rock ratios were probably very high. Loss of Al from pillow selvages may also have occurred during interaction at high fluid/rock ratios (Humphris & Thompson, 1978; Seyfried et al., 1978). Under such circumstances, low Al concentrations in the fluid may have been offset

by relatively large volumes of fluid involved in the metasomatism, permitting significant Al transport. (b) Epidotized sample #015(ii) has gained Al relative to #001, assuming Ti and Zr to be immobile. However, #015(ii) also contains more $CO_2$ (2.7 wt%) than in the other three pervasively epidotized rocks (<1.8 wt% $CO_2$) used in the mass balance calculations, and it is possible that Ti and Zr, rather than Al, were mobile in this case, due to locally high gradients in $X_{CO2}$ which are manifested in patchy concentrations of carbonate in the epidotized rock. An assumption of constant Al would not alter the main conclusions for major element mobility. Small Ti losses in the epidotized cores of pillows are also associated with relatively high $CO_2$ contents (3.3-4.1 wt %). (c) The apparent loss of Zr in sample #073 was previously ascribed to the combination of very low Zr contents, systematic analytical error and local variability in Zr abundances. (d) The 'gain' of Zr in sample 306 may reflect either local variability in Zr contents of the volcaniclastic rocks, or the influence of a $CO_2$ gradient, although $TiO_2$ and $Al_2O_3$ appear to have been immobile.

MacGeehan & MacLean (1980) considered the whole trace element suite and Ti to have been mobile during silicification of basalts at Matagami: Zr, Y and REEs show a positive correlation with $SiO_2$ content whereas $TiO_2$ decreases with increasing $SiO_2$ weight percent assuming Al to be immobile. This alteration, according to MacGeehan & MacLean (1980), produced rocks that are chemically similar to calc-alkaline andesites and dacites. At Noranda, Gibson (1979) and Gibson et al. (1983) suggest that, assuming constant volume metasomatism, Ti and Al (among other elements) were removed during silicification. Assessment of the results for silicified andesite (Gibson et al., 1983, Table 1) by Grant's method indicates that even if constant $Al_2O_3$ is assumed significant loss of $TiO_2$ is still indicated. Using the consistency of ratios between

elements in a single sample of less altered andesite and six samples of silicified andesite at Buttercup Hill, Noranda district, Lesher et al. (1986) determined that the REEs, Y, Zr, Th, U, Hf and Ta were relatively immobile during silicification as well as in epidotization, albitization, chloritization and sericitization. According to Lesher et al. (1986) Al and Ti were mobile, but consideration of sampling and analytical errors quoted by these workers suggests that the variations in the gains and losses of Al and Ti may not be significant relative to the errors involved.

In a third example of silicification of mafic volcanic rocks, Strong et al. (1979) and Dostal & Strong (1983) found Al, Ti, Zr and REEs to be relatively immobile along with Y, Hf, Th, Sc, P, Rb, Nb and Ga.

The suite of elements determined in the present study to be immobile is at variance with that of MacGeehan & MacLean (1980), Gibson (1979) and Gibson et al. (1983), although conservation of $Al_2O_3$ seems likely in all of the examples of silicification. The results of Strong et al. (1979), and Dostal & Strong (1983) and probably those of Lesher et al. (1986) for Al, Ti, Zr and HREEs concur with those of the present study, but in silicification at Edwards Lake Y was gained and $P_2O_5$, Rb and Nb display erratic interelement ratios, indicative of their mobility.

The consistently immobile behaviour of Ti and Zr in alteration at Edwards Lake implies that the ratio of these elements should represent magmatic values, and therefore they may be useful in discriminating magma types, or, for example, silicified mafic rocks and true felsic units. Based on this premise, the $TiO_2$ vs Zr plot used earlier (Fig. 18) can be justified as a means of distinguishing rock types, in conjunction with other field, petrographic and geochemical data, of course. The preservation of $Zr/TiO_2$ ratios during alteration is illustrated in this plot as well as in the isocon diagrams of Grant's

method. Altered samples lie on or very close to lines passing through the origin of the $TiO_2$ versus Zr diagram; igneous differentiation processes, on the other hand, produce trends that would not be expected to pass through the origin because of the differences in Ti and Zr partitioning during igneous differentiation (Finlow-Bates & Stumpfl, 1981). Thus, silicified mafic rocks can be distinguished by their much lower $Zr/TiO_2$ ratios from true felsic volcanic rocks.

# CHAPTER 6

# DISCUSSION

The principal aim of the study, to determine the origin of silicification in the Edwards Lake area, is discussed below in light of the field, mineralogic and mass balance evidence together with theoretical and experimental considerations. The secondary, but nonetheless important aims of establishing the relationships of silicification to other types of alteration in the area, and to massive sulphide deposits, are considered in the latter part of the chapter.

## 6.1 Origin of silicification

### 6.1.1 Evidence for alteration origin of silicific zones in pillows

Several lines of evidence suggest that the silicic margins in the zoned pillows are most likely the result of alteration, as opposed to primary (igneous) variations in composition or devitrification-related mass transfer. (i) The ratios of $TiO_2$, Zr and $Al_2O_3$ are very nearly constant in silicic and 'less altered' rock. This observation points to an alteration origin for the silicification in which these components were of very low mobility, and also demonstrates the difference between the silicic zoned pillows at Edwards Lake and variolitic pillows in the Rouyn-Noranda area; the latter have widely varying ratios of $TiO_2/Al_2O_3$ in varioles and matrix (Gelinas et al., 1976). (ii) Contacts between silicic and less altered rock are gradational, and no discrete variole-like bodies are present. (iii) The silicic zones are concentric around unequivocally altered (epidosite) pillow cores. (iv) Comparison with modern pillows, and (v) comparison with pillows in which similar compositional zoning is interpreted to have resulted from alteration,

add support to the proposed alteration origin of the silicification. The latter two points are discussed below.

(iv) The compositional variations across modern pillows that are pristine or have undergone only diagenetic modifications are relatively small. For example, a submarine basaltic pillow studied by Baragar et al. (1977) showed variations from rim to core of less than about 5% of the major element contents, except for MgO (about 15% variation). Furthermore, $SiO_2$ and $Na_2O$ were reported by Barager et al.(1977) to increase slightly towards the pillow core (from 47% to 49.5% $SiO_2$), an effect that these authors attributed to in situ crystal-liquid fractionation as the pillow crystallized from the rim to the centre. The very large variations in composition across Edwards Lake zoned pillows, and the fact that the margins of the pillows are relatively enriched in $SiO_2$ and $Na_2O$, suggest that the zoning is not of magmatic origin.

(v) $SiO_2$-$Na_2O$-rich pillow margins that most likely are alteration features are present in some greenschist facies Archean flows in the Yellowknife belt (Baragar et al., 1979). The increased $SiO_2$, $Na_2O$ and $K_2O$ and decreased FeOT contents of the Yellowknife pillow margin relative to its compositionally homogeneous core occur in equivalent parts of the pillow and over proportionally similar widths compared to the zone of $SiO_2$-$Na_2O$ addition in the Edwards Lake pillows. Baragar et al. (1979) demonstrate that elements enriched in the Yellowknife pillow margin (e.g. Si, Na) are almost exactly balanced by depletions of the same elements in the selvage, and vice versa. They contend that Si and Na from the pillow selvage were redistributed to the zone of incipient crystallization and the outer parts of the crystalline interior, where abundant plagioclase grains could accommodate these elements. Displaced Ca migrated to the selvage to form epidote, according to Baragar et al.

(1979). The similarities between zoning of Si, Na, Fe and Mg in the Yellowknife and Edwards Lake pillows suggest that alteration may have also caused the zoning in the latter. However, the positions of Ca enrichment differ, and the gains and losses in the Yellowknife pillow are not nearly as great, with the exception of Na, as in the Edwards Lake pillows.

Silicified mafic flows have also been documented from the Matagami Lake (MacGeehan, 1978; MacGeehan & MacLean, 1980), Noranda (Gibson, 1979; Gibson et al., 1983; Lesher et al., 1986) and St John, New Brunswick areas (Strong et al., 1979; Dostal & Strong, 1983). At Matagami, MacGeehan (1978) described silicified and quartz-veined pillow basalts adjacent to, and up to 10 m from, synvolcanic gabbro sills as well as more widespread quartz-epidote veinlets and patches mantled by 'spilitized' silicified rock. Superior exposure at Noranda allowed Gibson (1979) to delineate an extensive semiconformable zone of silicification and epidote-quartz ('mottled') alteration near the top of the Amulet formation. Silicification occurs in massive andesite flows as irregular-shaped patches, particularly adjacent to amygdales, and at the margins of andesite flow tongues. The latter form of alteration closely resembles silicification in pillows at Edwards Lake. Clasts in breccias commonly display silicified margins, and Gibson (pers. comm., 1986) has suggested that silica replaced earlier zeolites in some volcaniclastic rocks in the Amulet formation, as also observed by Dimroth & Lichtblau (1979). Silicification is found adjacent to felsic and mafic intrusions in a dyke swarm but timing relationships here are complex (H. Gibson, pers. comm., 1986). The presence of previously-silicified fragments of andesite in breccias that overlie the inferred source of the clasts (Gibson, 1979) indicates that silicification of some flows must have occurred very close to the seafloor. Direct

analogies of all of these features (except for the association with amygdales) have been described above at Edwards Lake and add weight to the contention of an alteration origin for silicification in both pillows and volcaniclastic rocks.

Strong et al. (1979) attribute pervasive silicification of mafic flows in Saint John, New Brunswick, to metamorphism under prehnite-pumpellyite facies conditions, possibly between 315° and 370°C and at 1 to 2.5 kbar. No evidence precluding a pre-metamorphic, hydrothermal, origin of silicification was presented, however.

### 6.1.2 Net gains and losses in the pillows

Net gains and losses of chemical components in a zoned pillow from Edwards Lake were estimated by summing the weighted percentage mass changes of each of the components across the pillow. The mass changes were weighted according to the cross-sectional areas of the alteration zones in the pillow, which would be proportional to the volumes of the zones if the reasonable approximation is made that the pillows are cylindrical or tubular in shape. The results (Table 3) indicate that for many components this pillow, and probably other zoned pillows, did not behave as a closed system for all elements. In particular, large amounts of Si were evidently added to the pillows, whereas Fe, Mg and Ca were probably lost. The calculations also suggest that Na can be modelled by closed-system exchange in the pillows, as in the Yellowknife example. In other words the mass of Na lost from the pillow selvages and epidotized pillow cores is approximately equal to the mass of Na gained by the silicified margins. Two implications of these findings are (i) a source of $SiO_2$ external to the pillows is required, and (ii) the transfer of large amounts of Si, Fe, Mg in an 'open system' (on the scale of the pillows) could most easily have been accomplished if

## Table 3

## Calculation of net gains and losses in a zoned pillow

Assumptions:

1. Pillow is ellipsoidal in cross-section with semimajor axis=60 cm and semiminor axis=30 cm, and is elongate in the third dimension.

2. Pillow was homogeneous and prior to zone development had the composition of sample # 173, except that the MgO content is assumed to be 4 wt. % (i.e. = MgO content of other less altered pillows).

3. Widths of the zones in the pillow are as follows:

| | | | | |
|---|---|---|---|---|
| selvage | 1.5 cm | at semiminor axis, | 3 cm | at semimajor axis |
| silicified rim | 6 | " | 12 | " |
| silicified margin | 8 | " | 16 | " |
| least altered part | 6.5 | " | 13 | " |
| epidosite core | 8 | " | 16 | " |

4. Only half of the area of the silicified margin is considered in the calculation, representing patches as opposed to rings of alteration.

5. Mass transfer is calculated for a cross-sectional slab of pillow, 1 cm in thickness, with density = 2.96 g/cm$^3$ (i.e. the density of # 173).

**Mass flux[1] (g) in zones of the pillow**

| Zone | Sample | $SiO_2$ | $Fe_2O_3T$ | MgO | CaO | $Na_2O$ | $K_2O$ |
|---|---|---|---|---|---|---|---|
| Selvage | 201 | -260 | +49 | -9 | +4 | -18 | -1 |
| Silicified rim | 171 | +1250 | +18 | -25 | -180 | +20 | +44 |
| Silicified margin | 172 | +870 | -90 | -48 | -85 | +22 | +9 |
| Least altered part | 173 | 0 | 0 | 0 | 0 | 0 | 0 |
| Epidosite core | 174 | +140 | -3 | -13 | +155 | -37 | -3 |
| Net flux for 1cm thick slab: | | +2000 | -26 | -95 | -106 | -13 | +49 |

[1] Mass flux (g) = $\left(\frac{\text{\% mass change of oxide}}{100}\right) \times \left(\frac{\text{wt \% of oxide in \# 173}}{100}\right) \times \left(\text{area of zone}\right) \times 2.96$

where % mass change of oxide are those in Table 16, and wt % oxide in # 173 are given in analysis 52, Table 10.

abundant fluid were present.

### 6.1.3 Porosity and permeability controls on silicification

Silicification of pillows appears to have proceeded in two stages: early exchange of Si and small quantities of Na for Ca, and later exchange of Si + Na for Fe + Mg + Ca. Evidence showing that these two processes may have occurred is shown in a plot of molar gains of Si + Na versus molar changes in Fe + Mg + Ca (Fig. 27). In the earlier stage of alteration of pillows (represented by the three comparisons with Si gains of about 0.3-0.4 moles per 100 g of less altered rock; in Fig. 27) little or no Fe + Mg was lost, and the molar gains of Si were far greater than the losses of Ca. Because abundant quartz-filled thermal contraction cracks are observed at the margins of zoned pillows it is likely that the earlier stage of alteration mainly involved infilling of such porosity by silica. The association of silicification with pillows that contain the greatest abundances of thermal contraction cracks, and with the margins of the pillows where the cracks are most abundant, is further evidence of the importance of porosity in controlling the sites of at least the initial stages of silicification.

Only where larger amounts of $SiO_2$ were added did significant loss of Fe and Mg occur (i.e. the two comparisons of pillow samples with the greatest Si + Na additions in Fig. 27). A similar dual process of initial infilling of pore space and later loss of Fe + Mg in the felsic volcaniclastic unit could account for the displacement of points representing this unit away from the 'mole-for-mole exchange' line in Figure 27.

In contrast, the molar gains of Si in the silicified mafic volcaniclastic rocks (Figure 27) were approximately balanced by the molar losses of Fe + Mg. The effects of Na and Ca exchange do not alter

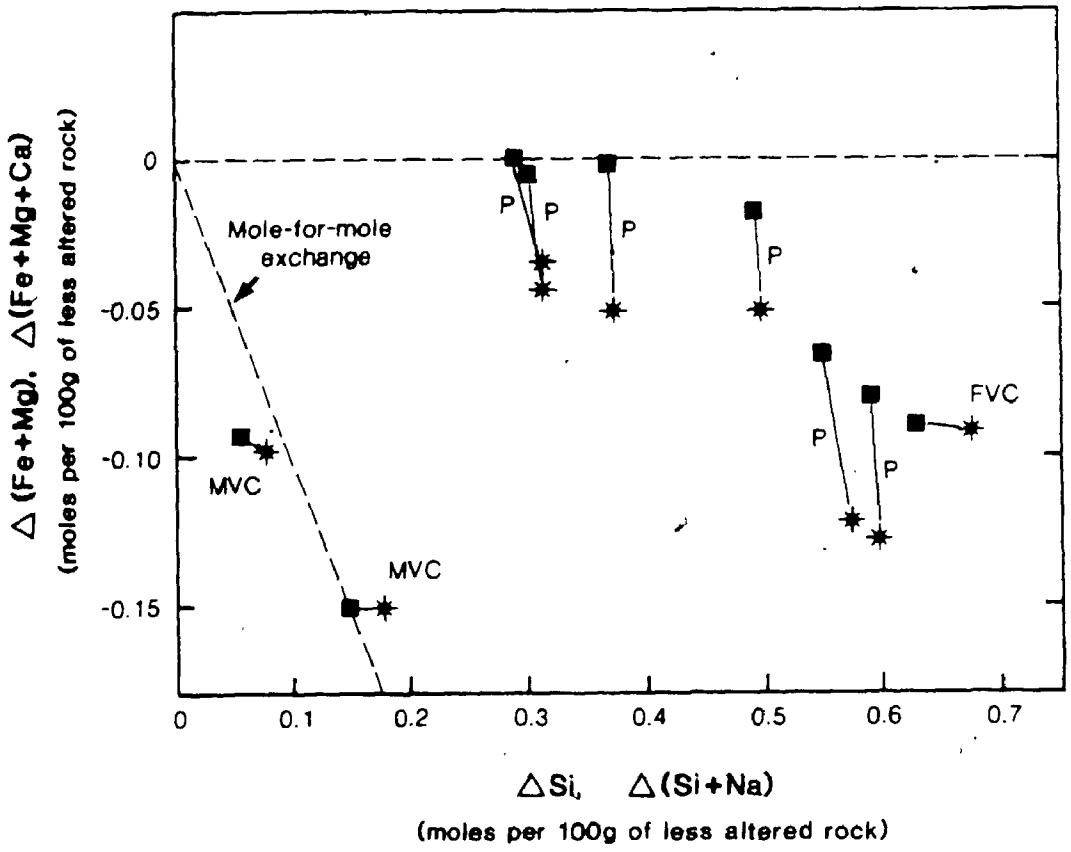


Figure 27. Molar changes of Si versus Fe + Mg (■) and Si + Na versus Fe + Mg + Ca (✱) during silicification of felsic volcaniclastic rock (FVC), mafic volcaniclastic rocks (MVC) and pillow margins (P). Each point represents the molar changes of cations calculated by comparing a less altered rock with an altered equivalent rock, using Grant's (1986) method. Thin lines join determinations of gains and losses from the same pair of samples.

this result significantly in this or in the other illustrated examples of silicification of volcaniclastic rocks. One explanation of these results is that if the porosity of the mafic volcaniclastic rocks was relatively low prior to silicification, then Si addition might be significant only if components such as Fe and Mg were lost, unless expansion of the rock occurred. In this mechanism porosity therefore would have influenced the relative amounts of silica gained and Fe and Mg lost.

A porosity and/or permeability control on the sites of silicification is also apparent in the breccias, where silicification evidently began at clast-matrix contacts and extended towards the centre of clasts as alteration progressed. The matrix and the margins of larger clasts both were silicified in preference to the centres of the larger clasts probably because these sites were in closer 'communication' with a pore fluid in the matrix. Variations in extent and intensity of silicification may result in part from primary bulk compositional or textural differences between clasts - in some places, pyroxene-phyric mafic clasts are more extensively silicified than other clast types, for example.

### 6.1.4 Metal leaching and Na addition

Much of the silicification in the Edwards Lake area involved both addition of Si and loss (interpreted as leaching) of Fe, Mg, Mn, and Ca and Zn in places. The other major element consistently added to the rock during silicification was Na. The clear association of Na- with Si-enrichment in both the margins of pillows and in silicified volcaniclastic rocks, and the magnitude of the Na gains, together suggest that Na was indeed added during silicification, although in the case of pillows the Na added in silicification may have been derived

from within the pillows themselves (see Section 6.1.2). It can reasonably be assumed that a silica mineral and one or more sodium silicates were precipitated during silicification. Unfortunately, recrystallization in the medium grade of regional metamorphism has obscured the nature of the alteration mineral assemblage, and the sodium silicate(s) could have been albitic plagioclase, analcime or a Na-mica, amongst others. This uncertainty also applies to other altered rocks in the study area, and prevents detailed interpretation of alteration reactions and mechanisms. However, this limitation can be circumvented to some extent by considering the physico-chemical conditions under which similar elemental gains and losses to those inferred at Edwards Lake are favoured in experimental and active, natural hydrothermal systems. Leaching of Fe, Mg, Zn and other metals and Na addition are treated in this section, followed by discussions of the source of silica and its precipitation.

Hydrothermal alteration processes during experimental rock-fluid interaction are controlled mainly by temperature, pressure, water/rock ratio, fluid composition, pH and rock composition and texture (Bischoff & Dickson, 1975; Seyfried & Bischoff, 1977; Mottl et al., 1979; Rosenbauer & Bischoff, 1984; Seyfried & Janecky, 1985). The water/rock ratio is defined by most experimentalists as the ratio of masses of fluid and rock in the experimental reaction chamber, but in many experiments only a portion of the sample is altered. Thus the actual amount of fluid that reacts with the rock may differ from that suggested by the 'water/rock' ratio. Until very recently (Seyfried, 1987) the experiments generally resulted in metastable mineral assemblages that differed from natural assemblages, mainly because of their relatively short duration (hours to months; see review by Rosenbauer & Bischoff, 1984). Also, the role of adsorption in experiments that used rock

powders is not clearly understood (J. Lydon, pers. comm., 1987). On the other hand, the success of the experiments in closely reproducing the compositions of seafloor vent fluids (e.g. Rosenbauer & Bischoff, 1984; see below) is supportive evidence of the importance of the variables listed above in controlling fluid-rock reactions.

In **seawater-basalt experiments** acidity is generated by hydrolysis of seawater Mg (Bischoff & Dickson, 1975). $Mg(OH)_2$ molecules are incorporated in smectite, mixed-layer smectite-chlorite or chlorite, and Mg hydroxy sulphate is also precipitated. Charge balance is maintained by dissolution of mainly $Ca^{2+}$ from the rock. At water/rock ratios of less than 50, low pH and relatively high Fe, Mn and Zn concentrations in the fluid occur only in the early stages of reaction; pH increases and heavy metal concentrations decrease to relatively low steady state values as the supply of Mg in the fluid is exhausted. Na addition to the rock is favoured at water/rock ratios of less than 5-10, and epidote-chlorite-albite-actinolite assemblages are predicted to result from basalt-seawater interaction at water/rock ratios of less than about 35 (Mottl, 1983). The gains and losses in the rock, assumed to be the opposite of those in the fluid, are summarized in Table 4a.

Under seawater-dominated conditions (water/rock >50) Mg-hydrolysis maintains pH at low values, resulting in relatively high steady state heavy metal concentrations in the fluid (3 to 10x those in the low water/rock experiments; Mottl & Seyfried, 1980). Chlorite-quartz rock may develop (without addition of Si) under these conditions (Mottl, 1983). At water/rock ratios of greater than 5-10 Na is leached from the rock in exchange for Mg when the supply of leachable Ca and K is exhausted (Mottl & Seyfried, 1980).

The results of seawater-basalt experiments conducted at temperatures of greater than 350°C and at low water/rock ratios resemble those of the

## Table 4a

### Comparison of elemental gains and losses (in the rock) and pH in fluid-rock experiments

| Fluid<br>Rock<br>Temp.<br>Fluid/rock | Fe,Mn | Zn | Cu | Mg | Ca | Si | pH | Na | K | Refs |
|---|---|---|---|---|---|---|---|---|---|---|
| seawater<br>basalt<br>150°-360°C<br>low w/r (<50) | - | - | - | ++ | - | - | - | +@<br>w/r<br><5-10 | - | 1 |
| seawater<br>basalt<br>150°-350°C<br>high w/r (>50) | = | = | = | ++ | = | = | = | = | - | 2 |
| seawater<br>basalt<br>>400°C<br>low w/r | = | = | = | ++;<br>+@<br>hi T | - | = | = | ? | - | 1 |
| evolved seawater<br>(Na-Ca-K-Cl)<br>basalt<br>300°-500°C<br>low w/r | =<br>↓<br>=@<br>hi T | =<br>max @<br>375-400°C | = | ? | ++<br>@<br>400°C;<br>+@<br>425°C | = | = | +<br>@<br>400°C;<br>++@<br>425°C | ? | 1 |
| 4 m NaCl<br>basalt<br>350°C<br>w/r=10 | - | O | O | O | - | O | O | + | - | 3 |
| 4 m NaCl<br>andesite<br>350°-500°C<br>high w/r | - | - | - | - | - | - | - | + | + | 4 |
| 4 m NaCl<br>greywacke<br>350°C<br>w/r=10 | - | - | - | - | - | - | - | + | - | 3 |
| natural brine<br>(contained Mg)<br>greywacke<br>350°C<br>w/r=10 | = | = | = | +? | ? | ? | = | ? | ? | 5 |

## Table 4b

**Comparison of elemental gains and losses (in the rock) in alteration at Edwards Lake and other natural systems**

| Alteration | Fe,Mn | Zn | Cu | Mg | Ca | Si | Na | K | Refs |
|---|---|---|---|---|---|---|---|---|---|
| halmyrolysis | + | | | - | - | - | | ++ | 6,7 |
| Svartsengi 240°C pH=5.4 | - | ? | ? | - | - | - | 0 | 0 | 8 |
| epidote-rich sea-floor basalts | - | ? | ? | - | - | - | + | 0 | 9 |
| chlorite-quartz seafloor basalts | + | | | ++ | = | = | 0 | 0 | 9 |
| **Edwards Lake alteration** | | | | | | | | | |
| silicification of volcani-clastic rocks | = | = | ? | = | 0 | +++ | ++ | + | |
| silicification in pillows | = | + | +? | = | - | +++ | ++ | + | |
| pervasive epi-dotization | = | = | ? | -,+ | +++ | 0 | -,+ | | |
| epidosite patches | 0 | - | + | - | +++ | 0 | = | = | |
| garnet-chlorite alteration | +++ | +,0 | ? | ++ | = | = | = | - | |

**Notes:** '-': loss from rock; '=': large loss from rock
'+': gain by rock: '++': large gain by rock
pH: '+' and '-' refer to increase and decrease of fluid pH
0: no net exchange between rock and fluid

**References:**

1 - Rosenbauer & Bischoff (1984)
2 - Seyfried & Mottl (1982)
3 - Rosenbauer et al. (1983)
4 - Ellis (1968)
5 - Bischoff et al. (1981)
6 - Scott & Hajash (1976)
7 - Thompson (1984)
8 - Ragnarsdottir et al. (1984)
9 - Humphris & Thompson (1978)

lower temperature experiments at low water/rock ratios, although some significant differences are apparent. For example: (a) Fe, Mn and Zn concentrations in the fluid are very high (up to 3 ppm Zn; 100-200 ppm Fe) at 400°C and increase strikingly (less so for Zn) with increasing temperature (Mottl et al., 1979); and (b) Mg-hydrolysis is followed by minor Ca-hydrolysis (Rosenbauer & Bischoff, 1984). The fluids generated in these experiments are almost identical to black smoker fluids at 21°N on the East Pacific Rise (Rosenbauer & Bischoff, 1984).

Experiments designed to simulate conditions deep within a sub-seafloor geothermal system have reacted 'evolved' seawater (Mg-depleted, Na-Ca-K-Cl solutions) with basalt at temperatures of 350°-500°C, pressures between 162 bars and 1000 bars and at water/rock ratios of 0.5-3 (Rosenbauer & Bischoff, 1984; Seyfried & Janecky, 1985). Ca- rather than Mg-hydrolysis is prominent, and clinozoisite and tremolite-actinolite alteration products were observed by Seyfried & Janecky (1985) in experiments at 350°-425°C. As in the seawater-basalt experiments, Fe and Mn removal from the rock is significant above 375°C and is greatest at the highest temperatures in response to the lowest pHs. Zn and Cu, however, generally reach maximum concentrations in the fluid at 375°-400°C. Silica leaching and Ca addition occur throughout the temperature range of these experiments whereas Na fixation is greatest at 400°C and above (Seyfried & Janecky, 1985; Seyfried 1987).

The behaviour of Mg in the evolved seawater experiments is not explicitly described by Rosenbauer & Bischoff (1984) or by Seyfried & Janecky (1985), but the fluids produced during interaction with basalt glass at 400°C, 292-1000 bars were noted to be very similar to vent fluids at 21°N on the East Pacific Rise, which contain no Mg (Rosenbauer & Bischoff, 1984). This suggests that Mg was neither leached nor added to the rock during the high temperature evolved seawater experiments,

because the starting fluid contained no Mg, although it is assumed that Mg was added to rocks in the cooler parts of the system.

Experiments that most closely reproduce the gains and losses in silicified rocks at Edwards Lake involve reaction of 4 m pure **NaCl brine with greywacke** at 350°C, 500 bars and at a fluid/rock ratio of 10 (Rosenbauer et al., 1983), and reaction of 2 m to 4 m **NaCl brine with andesite** at 350°-500°C, 1500 bars (Ellis, 1968). Although $SiO_2$ was leached rather than added to the rock in both of the experiments, all other major element fluxes were similar in direction to those deduced for silicificatiion. In the greywacke experiment $H^+$ was generated by albitization of illite and dedolomitization, despite the lack of Mg and Ca in the starting solution (Rosenbauer et al., 1983). Metals released in this process were maintained in solution by the combined effects of low pH and chloride complexing. In a separate experiment, Rosenbauer et al. (1983) reacted 4 m NaCl brine with basalt at 350°C and water/rock ratio of 10, and found that only very minor metal leaching had taken place. No acidity was produced because the fresh basalt, unlike greywacke used in the experiments, contained no $H^+$-bearing solid phases, and because Ca and Mg were absent from the starting brine (Rosenbauer et al., 1983). The results for basalt contrast with those for reaction of NaCl brine with devitrified andesite, in which strong leaching of Fe, Mg, Ca and Mn occurred along with intense Na-metasomatism (Ellis, 1968). Devitrification may have led to partial hydration of the rock, providing a source of $H^+$.

In some natural systems where basalt is interpreted to have reacted with an evolved fluid of seawater or mainly seawater composition, such as in the Icelandic Svartsengi geothermal system (Ragnarsdottir et al., 1984) and in epidote-rich seafloor basalt dredge samples (Humphris & Thompson, 1978), Fe, Mg and Ca have been leached, and small amounts of

Na added. $SiO_2$, however, is lost from the rock in each case (Table 4b and Fig. 28). The alteration mineral assemblage at Svartsengi was shown by Ragnarsdottir et al. (1984) to be in equilibrium with the coexisting fluid at the measured subsurface temperature of 240°C. The Svartsengi results suggest, therefore, that leaching of Fe, Mg and Ca from basalt can occur at temperatures of 240°C or less. However, the magnitudes of the gains and losses are significantly smaller than in silicified rocks at Edwards Lake (Fig. 28).

Intense metal leaching may also occur at low temperatures (<150°C). Opalized palagonite is described by Nayudu (1964), and some Archean hyaloclastites from the Noranda area that have undergone partial to complete replacement by microcrystalline quartz may have been silicified at an early diagenetic stage (Dimroth & Lichtblau, 1979). Paris et al. (1985) describe pervasive silicification of restricted portions of volcaniclastic rocks and pillow lavas, as well as more extensively silicified overlying sediments in the Barberton greenstone belt. Silica-filled fracture systems associated with the pervasively silicified rocks are inferred to have formed soon after sedimentation. However, no estimates of the temperature of alteration, nor chemical analyses, are presented in these studies. Infilling of porosity by silica at temperatures of up to 105°C was described by Elders & Bird (1974) in a near-surface geothermal environment, but no whole rock analyses were given.

Low temperature alteration of basalt by seawater (halmyrolysis) generally results in net addition of K, Rb, Cs, Fe, $H_2O$, U, B and Li, and a net loss of Ca, Mg and Si from the rock as well as oxidation (see summaries by Scott & Hajash, 1976; Thompson, 1984). The behaviour of Fe, Mn and Zn during halmyrolysis contrasts with the experimental and natural-system results of basalt-, andesite- and greywacke-fluid

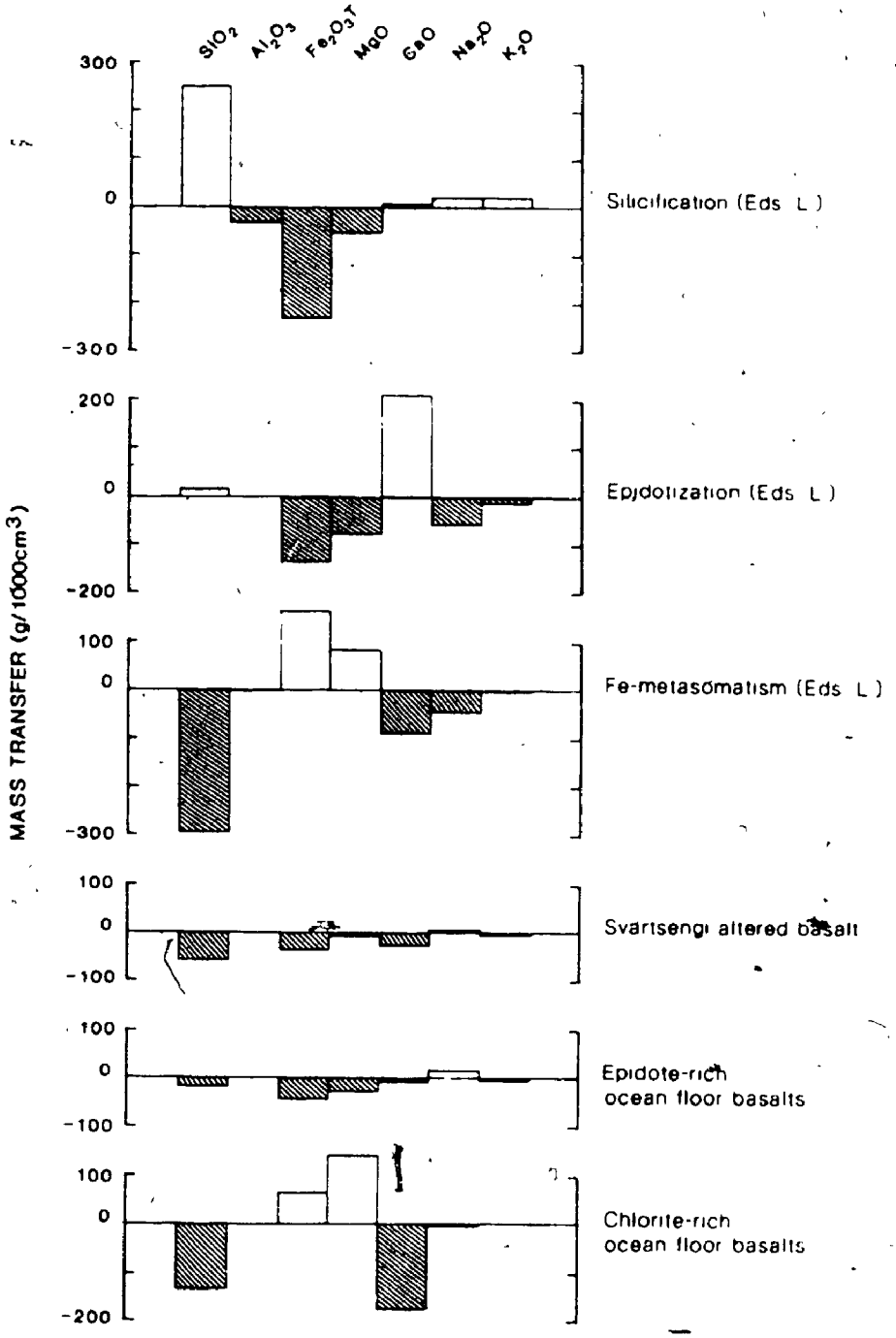


Figure 28. Comparison of the extent of mass transfer in g per 1000 $cm^3$ resulting from silicification, epidotization and Fe-metasomatism at Edwards Lake, with the extnet of mass transfer of altered tholeiitic basalt from the Svartsengi geothermal system (after Ragnarsdottir et al., 1984) and of epidote- and chlorite-rich altered ocean floor basalts (after Melson et al., 1968).

interaction at 150°C and above (Scott & Hajash, 1976; Rosenbauer & Bischoff, 1984; Ragnarsdottir et al., 1984; Humphris & Thompson, 1978; Rosenbauer et al., 1983; Ellis, 1968), and with the inferred behaviour of these elements during silicification at Edwards Lake.

Intense leaching of Fe, Zn and Cu from basalt within about 7 m of an acid hot spring (73-95°C, pH=1.5) in Iceland is reported by Sigvaldson (1959), and leaching also occurs near some alkaline hot springs (100°C, pH=9.4; Wedepohl, 1969).

Finally, oil field brines at 100-150°C and containing 360 ppm Zn and 100 ppm Pb were described by Carpenter et al. (1974). These data suggest that heavy metals were leached from rocks in the sedimentary basin, although the actual source rocks were not identified (Carpenter et al., 1974; Lydon, 1981).

From this brief review of the literature it is apparent that losses of Fe, Mg, Ca and Zn and gains of Na by the rock are favoured by interaction at low pH with a NaCl brine that is initially deficient in heavy metals. In the silicified parts of pillows Mg and Ca are both leached, so Mg- or Ca-hydrolysis at the site of silicification cannot be invoked as important $H^+$-producing reactions. The most likely alternative sources of acidity are: (a) albitization of a hydrous phase in the basaltic andesites, such as illite (by analogy to NaCl-greywacke experiments; Rosenbauer et al., 1983) or palagonite(?); (b) reaction of a neutral or alkaline fluid with volatiles such as $H_2S$, $SO_2$, HCl (Fournier, 1985); or (c) Mg- or Ca-hydrolysis elsewhere in the system, such as at pillow selvages, within interpillow volcaniclastic rock, in the epidotized cores of pillows or at more remote sites. In silicified volcaniclastic rocks Mg was leached but Ca shows only very small gains and losses, and thus Ca-hydrolysis as well as Na-metasomatism, or mechanisms (b) and (c) may have produced $H^+$ in these rocks. If

albitization of illite or palagonite(?) was the dominant process in generating $H^+$, then prior hydration of at least parts of the basaltic andesite pillows and of the volcaniclasitc units is implied. Another mechanism for producing acidity, by dedolomitization (Rosenbauer et al., 1983), is unlikely at Edwards Lake in view of the very low abundance, or lack, of primary or early carbonate in the less altered rocks.

Although leaching of Fe, Mn and Zn have been found to be strongly and positively correlated with temperature, particularly above about 350°C in fluid-rock experiments, it is evident from natural systems that leaching can also occur at much lower temperatures. Whether large and widespread losses of heavy metals, as occurred at Edwards Lake, can result from low temperature , low pH interaction, is not clear.

Na-fixation in the experimental systems is favoured at high temperatures, but is also strongly dependent on water/rock ratios and on the initial concentrations of Na in the fluid. Thus, although Na-fixation may reflect the finding of Rowe et al. (1967) that Na-silicate solubilities decrease with increasing temperature, Na-fixation does not conclusively indicate high temperatures of reaction. The temperature dependency of Ca and Mg leaching is not clear from the literature because all experiments that resulted in significant leaching of Ca and Mg as well as Fe, Mn and Zn either were conducted at the same temperature of 350°C (Bischoff et al., 1981; Rosenbauer et al., 1983), or indicated that temperature was less important than chlorinity in promoting leaching (Ellis, 1968). Removal of Ca and Mg from the rock in experimental systems occurs where a mechanism other than Ca- or Mg-hydrolysis is available to produce acidity, and where the fluid initially has very low concentrations of these metals but can supply other cations to the rock (e.g. $Na^+$) to balance charge in the reaction.

### 6.1.5 Source of Si

Three alternative sources of Si in silicification are: magmas, seawater or the surrounding strata. A direct magmatic source of at least some Si is possible in view of the presence of large synvolcanic felsic intrusions in the region, and the spatial association with high-$TiO_2$ felsic dykes. If silica also was derived from the quartz-plagioclase porphyry, however, it must have been removed from the magma before porphyry emplacement because silicification is cut by the intrusion.

Modern seawater is very undersaturated with respect to silica, and since there is no substantive evidence that Proterozoic and modern seawater differed significantly in composition (see review by Thompson, 1984), unmodified seawater probably was not the main source of Si. Alteration of mafic rocks to smectite- or chlorite-rich assemblages can release $SiO_2$ to solution, as shown in experiments that reacted seawater with basalt at temperatures of greater than about 150°C (e.g. Seyfried & Bischoff, 1977). In addition, fluids moving up a temperature gradient will acquire increasing amounts of silica, provided that the solution is in contact with free silica (Kennedy, 1950). Greater concentrations of silica in solution are possible where equilibrium with respect to amorphous silica or chalcedony, rather than quartz, is reached (see mechanism (2), below).

### 6.1.6 Precipitation of Si

The conditions under which silica precipitated in silicification at Edwards Lake are also difficult to ascertain, partly due to the lack of experimental data on the interaction between rock and silica saturated or supersaturated fluids, and partly because of the wide range of temperature, pressure and pH conditions within which silica can be

deposited. In order for silica to precipitate, supersaturation must be achieved (Rimstidt & Barnes, 1980); this could occur in several ways. (1) Heating of a fluid in equilibrium with quartz beyond the temperature of its solubility maximum (about 350°C at the vapour pressure of the solution; about 500°C at 800 bars; Fig. 29), either by imposition of a higher temperature thermal regime on a fluid-rock system, or by movement of a relatively cool fluid into a hotter region. The first process may account for the silicification aureoles adjacent to some felsic dykes in the Edwards Lake area. It is perhaps significant that in experimental systems large amounts of Fe, Mn and Zn can be leached from basalt at similar temperatures to those of retrograde solubility of silica (see foregoing discussion). Heating of fluids near intrusions was first suggested by MacGeehan (1978) as a mechanism for silicification in the Matagami area, Quebec. Fournier (1983a) and Bischoff & Rosenbauer (1984) also have predicted the presence of silicified zones near intrusions as a result of superheating of $SiO_2$-rich fluids.

The second process, movement up a thermal gradient of a relatively cool $SiO_2$-saturated fluid towards the centre of hot, newly erupted pillows, may account for silicification at the margins of pillows. However, in order for $SiO_2$-saturated fluids to have been in contact with pillows in a near-seafloor, high fluid flow regime, such as at the top of a volcanic pile, an insulating 'cap' of low-permeability rock may have been required. Less silicified massive flows overlying silicified pillows at the base of flow unit MA could represent such a 'cap'. One potential problem with this interpretation is that breccia unit HB, beneath the massive flows, contains silicified clasts of the underlying pillowed flow MP1. However, the possibility that the clasts were silicified after, rather than before, deposition in the breccia can not

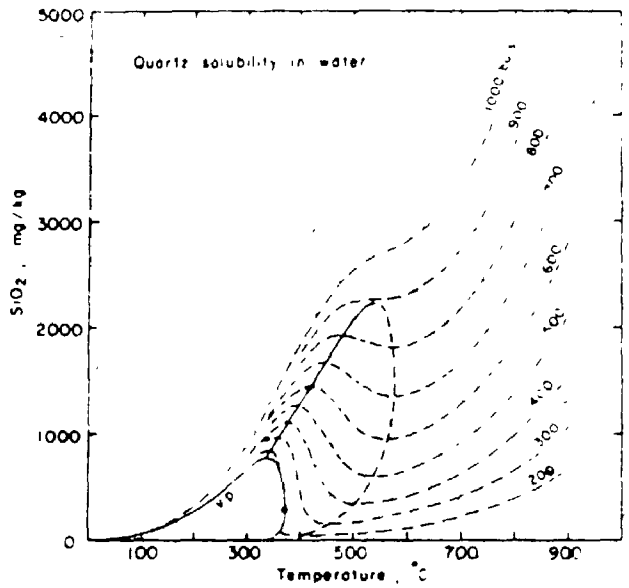


Figure 29. Calculated solubilities of quartz in water up to 900°C at the indicated pressures (v.p. = vapour pressure of the solution). The shaded area emphasizes the region of retrograde solubility (from Fournier, 1985).

be dismissed, in which case silicification of the pillows would not be constrained necessarily to the immediate vicinity of the seafloor.

The question arises as to why only some flows are strongly silicified, if heating of a $SiO_2$-rich fluid to high temperature was the mechanism of alteration. Ease of fluid access to the interiors of pillows may be part of the answer, as the pillows with the greatest proportions of thermal contraction cracks are generally the most silicified. The silicified flows also appear to have had slightly greater $Al_2O_3$, Zr and REE contents (see Section 5.1). The susceptibility to silicification conceivably could have been enhanced in a more aluminous rock if greater amounts of feldspar were present to act as nuclei for hydrothermal feldspar growth. The contention that abundant plagioclase may be necessary for silicification to occur at pillow margins was proposed by Baragar et al. (1979) from study of an altered Archean pillow in the Yellowknife belt. Differences in composition between Edwards Lake flows might also account for the variations in abundances of thermal contraction cracks, because cooling and crystallization histories of pillows should be dependent on composition, amongst other parameters.

The heat source required for silicification of large areas of volcaniclastic rocks in the absence of local felsic dykes at Edwards Lake is less obvious, however. The quartz-plagioclase porphyry postdates silicification in the volcaniclastic rocks and probably is too small to 'drive' a relatively large hydrothermal system such as at Edwards Lake (Cathles, 1983). The synvolcanic tonalite sill to the south (Bailes, 1986) is a more likely candidate as a 'heat engine', although the precise age relationships are unknown. Computer modelling of fluid flow in convecting submarine geothermal systems by Lister (1977), Cathles (1983) and Elders et al. (1984) has demonstrated that

temperatures of 350°C and above are restricted to within about 1-3 km of felsic and mafic intrusions that are in the order of 10-15 $km^2$ cross-sectional area - that is, of comparable dimensions to the tonalite sill. Consideration of fluid flow paths in the theoretical models suggests that silicification induced by heating of the fluid should occur where flow is toward the intrusion. The zone of silicified volcaniclastic rocks at Edwards Lake is about 1.5 to 3 km stratigraphically above the tonalite sill so temperatures of 350°C during alteration are not unreasonable. That such temperatures may have been achieved, is demonstrated in Middle Valley (Northeast Pacific Ocean) where there is no evidence of a sill, the basement volcanic rocks are about 100,000 years old, and yet temperatures of greater than 400°C at sub-seafloor depths of only a few hundred metres have been inferred from heat flow measurements (Davis et al., in press).

(2) Alternatively, silica precipitation in the volcaniclastic rocks, in the absence of local felsic dykes, may have occurred at temperatures below 350°C by the following mechanism, with heat contributed by a combination of the tonalite sill, cooling flows and dykes. Gibson (1979) contended that silica could be precipitated where a solution that had been in contact with fresh volcanic glass (which contributes $SiO_2$ to solution to a similar extent as amorphous silica; Fournier, 1985) moved into a higher temperature zone in which quartz was stable: $SiO_2$ would have been precipitated from the fluid to achieve equilibrium, since the solubility of quartz is less than that of amorphous silica. Even at constant temperature silica should eventually precipitate from such fluids because the solubility of quartz (at temperatures above about 140°C) and chalcedony (below about 140°C) which also has a solubility less than that of amorphous silica but greater than quartz, have been found to control dissolved silica where complete equilibrium is reached

in active hydrothermal systems (Fournier, 1985; Ragnarsdottir et al., 1984). Thus, solutions that have been in contact with fresh glass may be only capable of precipitating silica for relatively short periods of time (Fournier, 1985), unless supersaturation can be maintained by conditions of, for example, low pH, repeated exposure of fresh glass, or very low temperature (Seyfried & Janecky, 1985; Fournier, 1985; Rimstidt & Barnes, 1980).

The strong tendency towards equilibration with quartz at high temperature is apparent in experimental as well as in natural geothermal systems. Na- and Ca-metasomatism, in particular, evidently promote equilibrium with respect to quartz even where it is predicted that low pHs should cause supersaturation (Seyfried & Janecky, 1985; Seyfried, 1987). It is possible that precipitation from supersaturated fluids during silicification was aided by Na-fixing processes.

(3) Cooling of a solution in equilibrium with silica could lead to silica precipitation. Mixing with cooler waters, boiling, adiabatic expansion or simple conduction each could cool the fluid and cause silica deposition. The first three processes generally are operative in near-surface or near-seafloor environments where temperature gradients may be large, and typically result in quartz veining, as opposed to replacement-type silicification (Fournier, 1985). Lesher et al. (1986), however, propose that silicification in the Amulet formation at Noranda took place very close to the seafloor by cooling of the fluid.

(4) Silica solubility is strongly dependent on pressure (Fig. 29), and a decrease in pressure could result in silica precipitation.

(5) Silica solubility increases with pH in alkaline solutions (Fig. 30), and low-pH fluids can be grossly supersaturated with respect to silica. Neutralization of both high and low pH fluids could lead to deposition of silica (Fournier, 1985). High pH can be generated in

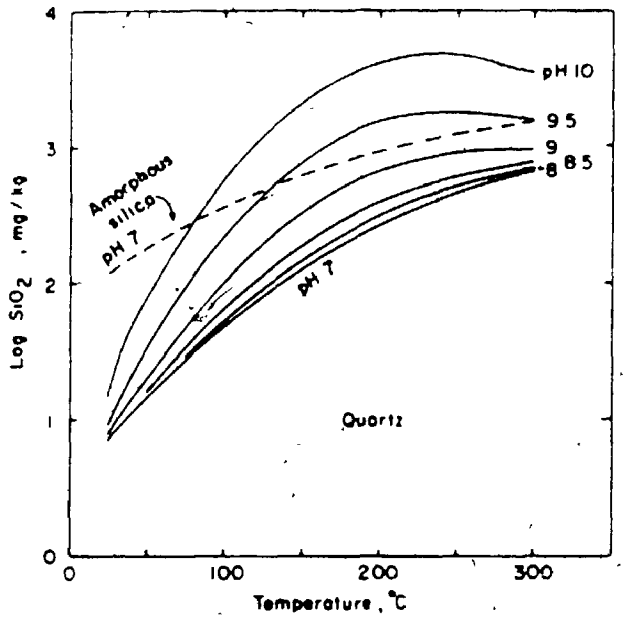


Figure 30. Solubility of quartz from 25°C to 300°C at pH values ranging from 7 to 10 (solid lines). The dashed line shows the solubility of amorphous silica at neutral pH (from Fournier, 1985).

systems where no phyllosilicates are present to buffer the pH, or where there is no quartz in the rock, or by subsurface boiling with removal of gas phases such as $CO_2$ (Fournier, 1985). Production of $H^+$ was discussed earlier but additionally may occur by interaction of water with gases evolved from a crystallizing magma, or from hydrolysis of NaCl at moderate to high temperatures and low pressures (Fournier, 1985).

Neutralization processes for low-pH fluids include acid-leaching reactions, mixing with higher-pH solutions or subsurface exsolution of $CO_2$ from the hydrothermal fluid, whereas for high-pH fluids neutralization may occur by mixing with lower-pH solutions, influx of $H_2S$, $SO_2$ or HCl or by oxidation of sulphides (Fournier, 1985).

The mass of silica precipitated per unit mass of solution is relatively small in all of the mechanisms listed above, however, compared to the gains of $SiO_2$ that accompany silicification at Edwards Lake. Gibson (1979) accounted for similar discrepancies at Noranda by proposing that water/rock ratios during silica addition were large. For example, to increase the mass of silica in a basaltic rock by 20% of its original value requires a water/rock mass ratio of about 200 if the fluid contained 1000 ppm $SiO_2$ and lost half of this quantity during alteration (e.g. by heating a quartz-saturated solution from 350°C to 400°C at 300 bars, or cooling from 300°C to 200°C at 300 bars). Greater concentrations of $SiO_2$ in the fluid at a given temperature and pressure are possible if contact with volcanic glass or amorphous silica has occurred, as noted earlier, or if a solution at a temperature of greater than about 300°C contains appreciable NaCl (Fournier, 1983b) or $Na_2SO_4$ (Chen & Marshall, 1982). However, these effects could, at most, reduce the water/rock ratio calculated by the method above by about half. Relatively low water/rock ratios may be consistent with the large mass fluxes if silica (and other components) diffused via pore fluids between

zones of high fluid flow and the sites of alteration. Interpillow rock, fractures or matrix in breccias could represent such zones of high water/rock ratio, and the pervasively altered rock adjacent to these pathways would correspond to sites where diffusion-controlled alteration occurred at low water/rock ratios.

### 6.1.7 Conclusions on silicification

Silicification of volcaniclastic rocks adjacent to some felsic dykes, and perhaps in pillows, may have resulted from interaction of Si-Na-Cl-rich, Fe-Mn-Zn-Ca-Mg-depleted fluids with the rocks as the fluids were locally heated to temperatures of 350°-450°C. Leaching of Fe, Mn and Zn is favoured in experimental rock-fluid systems at these temperatures, as is Na-metasomatism, although these elemental changes alone are not conclusive evidence of high temperatures during silicification. Si addition in the zones of metal leaching adjacent to felsic dykes and at pillow margins may have occurred when silica saturated fluids were heated to temperatures of 350°-450°C and entered the field of retrograde solubility of silica.

Silicification not associated with high-$TiO_2$ felsic intrusions, in volcaniclastic rocks, is of uncertain origin. High temperatures during alteration are probably not inconsistent with the synvolcanic tonalite sill to the south representing the heat source for the alteration process. Alternatively, metal leaching and Si-Na addition in the subconcordant zone could have occurred at lower temperature. In either case, intense and widespread leaching of metals would appear to have required relatively low pH conditions. At high temperatures $H^+$ could have been generated by Na-fixation reactions, interaction with acid-forming gases such as $CO_2$, or $SO_2$, or Ca- or Mg-hydrolysis reactions elsewhere in the geothermal system. At low temperatures, interaction of

the fluid with acid-forming gases is the most likely mechanism of $H^+$ generation.

The precise mechanism of silica precipitation in volcaniclastic rocks that are distant from felsic dykes is also problematic, but could have involved one or more of the following: heating, cooling or decompression of the fluid; reaction at constant temperature of a silica supersaturated fluid with rock to form phases such as albite, which promoted buffering of silica concentrations to near-saturation levels; or neutralization of either alkaline fluids in equilibrium with silica or of supersaturated low-pH solutions.

Plagioclase-quartz borders to fractures are geochemically similar to larger scale silicified zones, and the fluids involved may have been similar in composition. A permeability control on the sites of alteration is evident in fracture-related and other forms of silicification.

## 6.2 Origin of epidotization

Epidotized rocks at Edwards Lake that have gained both Ca and Na are remarkably similar in the direction of their gains and losses to those documented in reactions of 'evolved seawater' (Na-Ca-K-Cl solutions) with basalt (Table 4). The experiments showed that significant Ca- and Na-fixation as well as Fe, Mn, Zn and Cu leaching occurred at temperatures of about 375° and above, under conditions of low water/rock ratios and 375-400 bars (Rosenbauer & Bischoff, 1984; Seyfried & Janecky, 1985). Although tremolite-actinolite and clinozoisite are common to both the products of these reactions and some altered rocks at Edwards Lake, these minerals are also stable in Ca-Mg-rich, Fe-poor rocks at lower medium grade conditions (Winkler, 1979), which are inferred to have existed during regional metamorphism of the Edwards

Lake rocks. It is not clear whether tremolite-actinolite and clinozoisite, or other calcic phases which are stable at lower grade, such as calcite, gypsum, anhydrite, laumontite, prehnite or pumpellyite, formed during Ca-Na-metasomatism. Based on the temperature conditions deduced from the mass transfer evidence, however, clinozoisite and tremolite-actinolite are predicted to have crystallized during the Ca-Na-metasomatism. This is consistent with the temperatures at which epidote-group minerals and tremolite-actinolite occur in both active geothermal systems (i.e. greater than about 260°C for epidote: Keith et al., 1968; Tomasson & Kristmannsdottir, 1972; and greater than about 300°C for tremolite and actinolite: Kristmannsdottir, 1976; Keith et al., 1968) and in experiments to determine their stability (e.g. Bird & Helgeson, 1981).

Epidotized rocks that lost Na, Fe, Mg and Zn are suggested here to have formed by reaction of Ca-rich, Na-poor fluids with the mafic flows and volcaniclastic rocks at temperatures of greater than about 250°C. Epidote-quartz alteration has been described elsewhere by Harrigan & MacLean (1976), MacGeehan (1978), Gibson (1979), Gibson et al. (1983), Smith (1968), Evarts & Schiffman (1983), Condie et al. (1979) and Lydon & Jamieson (1984). Epidosite patches up to about 1 m in diameter appear to be common features in regionally metamorphosed rocks, but they differ in scale to the extensive zones of pervasive Ca-metasomatism at Edwards Lake, which were shown earlier to have formed prior to regional metamorphism.

Lydon & Jamieson (1984) proposed a model of epidote formation in the Troodos ophiolite complex in which chloritization of basalt or precursor low temperature minerals such as anhydrite or calcite supplied Ca. According to this model increasing temperature caused dissolution of these calcic minerals, locally enhancing the activity of Ca in solution

so that the evolved, Ca-rich pore waters in the chloritized basalt became sufficiently supersaturated with respect to Ca for epidote to nucleate. Epidote-quartz alteration occurred at low water/rock ratios in closed systems that were bounded by intersecting, low permeability dykes (Lydon & Jamieson, 1984).

Controls on the sites of alteration such as dykes and calcic vein minerals were not observed in epidotized zones at Edwards Lake. Supersaturation of a Ca-rich fluid with respect to epidote might have been achieved in the absence of calcic vein minerals if the fluid had moved relatively rapidly into zones of fresh or weakly altered rock, such as the centres of pillows or much larger bodies of rock (corresponding to zones of pervasive epidotization). This process may be analogous to the formation of clinozoisite in evolved seawater - basalt experiments: the Na-Ca-K-Cl solutions initially were grossly out of equilibrium with the rock, but lost Ca as clinozoisite crystallized (Seyfried & Janecky, 1985).

## 6.3 Origin of garnet-chlorite and garnet-biotite alteration

The compositions of garnet-chlorite- and garnet-biotite-rich rocks indicate that considerble amounts of Fe and lesser Mg were gained compared to less altered mafic rocks in the study area. Ca, Na, K and Si generally were depleted, although garnet-biotite±chlorite±staurolite rocks gained K. Three features of the alteration point to a tentative link between Fe-metasomatism and silicification. First, garnet-chlorite alteration is intimately associated with silicification in parts of the breccia unit HVC, affecting the matrix to silicified, zoned clasts. Second, with the exception of Ca, the elements gained during Fe-metasomatism are precisely those lost during silicification of clasts. However, Fe-metasomatism appears to have postdated silicification in the

vicinity of the Chisel Lake massive sulphide deposit, where it is the predominant alteration type, and continued after silicification in the Edwards Lake area. These observations can be reconciled in a model which involves initial release of Fe, Mg and possibly Zn to a fluid during silicification, and both local precipitation of some of these metals in alteration phases, and transport of a portion of these metals away from the silicified rocks to form separate zones of Fe-Mg-Zn(?)-enriched rocks. In this model regional metamorphism then converted minerals such as Fe-rich chlorite or smectite to almandine-chlorite assemblages (E. Froese, pers. comm., 1986). The garnet-chlorite rocks differ from chlorite-rich altered basalts (Humphris & Thompson, 1978) and from experimentally-produced chlorite- or smectite-rich altered basalts (e.g. Hajash, 1975; Seyfried & Bischoff, 1977) in the dominance of Fe- over Mg-addition. Thus if seawater was involved it probably was evolved, as opposed to unmodified, in composition.

In order for metals to precipitate from fluids that may have already partially equilibrated with silicified rocks, a change in the physico-chemical conditions would be required. Conductive cooling of the system, for example, or increase of solution pH upon exhaustion of $H^+$-producing hydrolysis reactions, as in some low water/rock ratio experimental seawater-basalt reactions (e.g. Seyfried & Bischoff, 1981), could cause deposition of some Fe, Mg and Zn in alteration phases. On the other hand, maintenance of metals in solution so that the separate zones of Fe-enrichment could form would have been facilitated by sustained low pH and high chlorinity, according to Rosenbauer et al. (1983).

For the proposed model to be viable the total mass of Fe and Mg leached during silicification should be roughly equal to, or greater than, the total mass of these elements added to the rocks that now

contain abundant garnet and chlorite. The 'greater than' condition would apply if some Fe and Mg had been 'lost' from the system. A very approximate estimate of the gains and losses can be deduced as follows: the percentage mass gains of Fe and Mg in pervasively Fe-metasomatized rocks (as opposed to garnet-chlorite veins) are of the same order of magnitude as the percentage mass losses of these elements in silicified rocks. Mass changes of 30-80% are typical in both cases for Fe and Mg. Approximately equal areas of silicified and garnet-chlorite altered rocks should therefore be present, assuming that the existing surface is a representative section through the alteration, and that the outcrop allowed realistic delineation of the spatial extent of the alteration zones. The results of the present study and of Bailes (1986) do indeed suggest that subequal areas of silicified and Fe-metasomatized rocks exist in the Edwards Lake - Chisel Lake area. It is open to speculation whether the three-dimensional extensions of the silicified zones were adequate in volume to provide the metals for the Chisel-Lost-Ghost Lakes Fe-Zn-Cu massive sulphide deposits. The mass of Fe in the deposits is about $2 \times 10^6$ tonnes, so only about 0.1 cubic kilometres of rock in excess of the volume of Fe-metasomatized rocks would need to be leached of 1% Fe to supply the deposits. A volume of about 5 $km^3$ of rock, leached of 50 ppm Zn, would be required to account for the $7.6 \times 10^5$ tonnes, or so, of Zn in the deposits (Walford & Franklin, 1982), assuming that very little of the leached Zn was precipitated en route to the deposits. In view of the scale of alteration beneath the deposits (i.e. about 1,5 $km^2$ of exposed silicification and Fe-enriched rocks) it would seem plausible that volumes of several cubic kilometres of leached rock may have existed, and that the metals could have been derived from silicified zones. Overprinting of silicification by Fe-metasomatism would be consistent with the interpretation if Fe, Mg, Zn etc. were

derived during silicification and were in places re-deposited after cessation of silica deposition.

Alternatively the metal source may have been a much larger volume of rock, and the silicified zones could represent the regions from which the ore fluids began their rapid ascent to the seafloor, as suggested by Bischoff & Rosenbauer (1984). Silica precipitation and fluid upflow should occur almost simultaneously if the fluid was heated to supercritical temperatures because the density of the fluid and silica solubility both decrease rapidly with increasing temperature near the critical point of a seawater-like fluid (Bischoff & Rosenbauer, 1984).

## 6.4 Model of alteration and comparison with other areas

Figure 31 schematically depicts the spatial distribution of the alteration zones, and their relationships to stratigraphy and felsic intrusions. Also shown is the speculated mass transfer in the fossil geothermal system, including the directions of fluid flow. It must be stressed that in order to more confidently establish the relationship of alteration to the Chisel Lake massive sulphide deposit, further detailed mapping and geochemical sampling between the deposit and the Edwards Lake area is required.

The large Fe-enriched, Na-depleted alteration zone in the heterolithic breccia unit is very similar in composition, mineralogy and extent to the 'lower semiconformable' alteration zone beneath the Anderson and Stall Lakes Zn-Cu massive sulphide deposits (Walford & Franklin, 1982). Magnesian footwall alteration 'pipes' may represent zones of fluid ascent from a reservoir now manifested by the lower alteration zone; magnesium in the footwall pipes was probably supplied by local downdraw of cold seawater near the inferred hydrothermal vents (Walford & Franklin, 1982; Franklin, 1986).

MacGeehan (1978) and MacGeehan & MacLean (1980) described zones of intense pervasive silicification of basalts adjacent to synvolcanic gabbro sills in the Matagami Lake district, and proposed a qualitative model in which some of the metals leached during silicification were transported to the seafloor to form the Garon Lake massive sulphide deposit. The similarities to the Edwards Lake model are clearly apparent. Extensive semiconformable zones of pervasive silicification and epidote-quartz alteration of andesites also occur in the Amulet 'Rhyolite' Formation in the Noranda area, but this alteration apparently preceded formation of the massive sulphide deposits and probably did not significantly contribute to metals in the deposits (Gibson, 1979; Gibson et al., 1983). The alteration is interpreted by Gibson (1979) and Gibson et al. (1983) to have formed in the medial parts of a shallow (less than 1 km in depth) sub-seafloor geothermal system, resulting in a low-permeability 'cap-rock'. Fracturing of the silicified seal promoted focussing of upflowing metalliferous fluids derived in other source regions, which ultimately may have vented at the seafloor to produce the massive sulphide deposits.

The Noranda and Matagami fossil systems both lack large, intensely Fe-enriched lower semiconformable zones between the footwall pipes and silicified rocks, although in the Amulet 'Rhyolite' Formation chlorite-sericite alteration of rhyolite does occur beneath the epidote-quartz alteration and silicification (Gibson, 1979). The speculated link between the Chisel Lake massive sulphide deposit and the Fe-enriched lower alteration zone in the footwall of the deposit; points to a possibly more direct relationship of silicification in the Edwards Lake area to massive sulphide deposition than at Noranda.

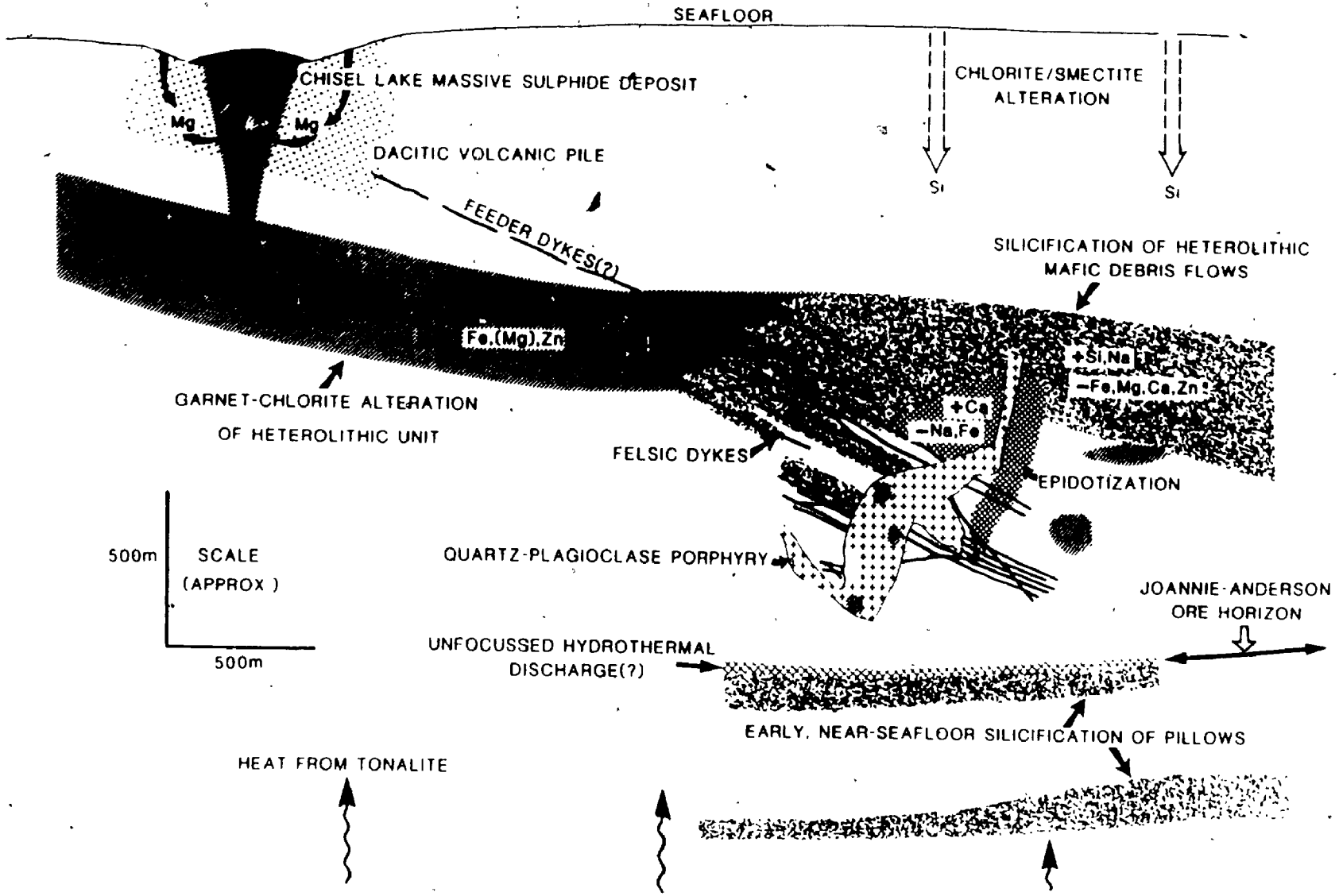


Figure 31. Schematic reconstruction of a cross-section through the alteration zones in the Edwards Lake area, showing generalized elemental gains and losses during alteration and spatial relationships to stratigraphy and intrusions. Also depicted is the speculated link between the silicified and Fe-metasomatized lower semi-conformable alteration zone and the Chisel Lake massive sulphide deposit.

## CHAPTER 7

## CONCLUSIONS

1. The strata in the Edwards Lake area form part of a subaqueously deposited volcanic succession, consisting of dominantly tholeiitic basaltic andesite and basalt flows overlain by mafic wacke and heterolithic, mainly mafic breccia. Intercalations of felsic volcanic breccia and wacke constitute less than 5% of the section. The volcanic breccias are interpreted as debris flow deposits.

2. Much of the volcaniclastic sequence has been hydrothermally altered. Silicification is prominent as a subconcordant zone in the heterolitic breccia unit, and grades laterally and upwards into Fe-metasomatized, garnet-chlorite±biotite-rich rocks in the direction of the Chisel Lake massive sulphide deposit. Pervasive epidotization occurs beneath the silicified zone in the eastern part of the study area.

3. Certain basaltic andesite flows, possibly those that had higher Al, Zr and REE contents, are intensely silicified in laterally extensive, subconcordant zones.

4. Silicification in mafic flows is interpreted to have occurred very soon after extrusion, close to the water-rock interface. However, silicification of volcaniclastic rocks adjacent to synvolcanic(?) felsic intrusions probably took place at depths of 0.3 to 2 km below the water-rock interface, coeval with deposition of the felsic volcaniclastic unit that underlies the Chisel Lake massive sulphide deposit, 1-2 km stratigraphically above the silicification. Broad zones of silicification in the heterolithic breccia are of less certain timing,

but formed prior to regional metamorphism and very likely are of synvolcanic age.

5. Fe-metasomatism continued after silicification near the Chisel Lake deposit, but is intimately associated with silicification in the Edwards Lake area, where these processes initially may have been contemporaneous.

6. Mass-balance calculations demonstrate that large quantities of Si and lesser Na were added to the rocks, and Fe, Mg and Mn leached. Losses of Zn from volcaniclastic rocks occurred in places, and Ca leaching characterized silicification of pillows. Mole-for-mole exchange took place in some cases, but Si additions far in excess of molar losses of cations are evident in other examples.

7. Clinozoisite-rich rocks lost Fe, Na, Mg, Mn, K, Ba and Zn, and gained Ca and Sr relative to less altered equivalent rocks.

8. Fe-metasomatism resulted in large mass additions of Fe, lesser gains of Mg and Mn; and patchy gains of Zn. Mass losses of Ca, Na and Si accompanied these gains.

9. Ti, Zr, Al and HREEs had very low mobility on decimetre and larger scale in almost all examined cases of alteration. Significant Ti and Zr mobility may have occurred where $P_{CO2}$ gradients were high. Al redistribution is apparent in zones where extreme fluid/rock ratios are inferred to have existed, such as in pillow selvages and veins.

10. The mechanism of silicification remains unclear, but probably involved interaction of Si supersaturated, Na-Cl-rich fluids (evolved seawater?) with the rock. Intense cation leaching would have been facilitated by sustained low pH and high temperature, but the loss of metals in silicified rocks is not conclusive evidence of high temperature alteration because heavy metal leaching can also occur at lower temperatures. Heating of the Si-rich fluids near felsic intrusions

or during incursion into more permeable hot pillows may have led to silica precipitation where temperature-pressure conditions appropriate to retrograde silica solubility were reached (i.e. greater than 350°C). The broad zone of silicification in the breccia unit lacks local heat sources, however, and the temperature at which this alteration occurred is unclear. Possible mechanisms of silica precipitation in the semiconformable zone include: decrease of Si concentrations in supersaturated fluids to near saturation levels with respect to quartz by reaction with the rock at nearly constant temperature, promoted by Na-fixation reactions; cooling or decompression of the fluid; or neutralization of low- or (less likely) high-pH fluids.

11. The Fe-metasomatized zone bears a strong resemblance, both chemically and in its position with respect to the Chisel Lake deposit, to the lower semiconformable zone beneath the Anderson and Stall Lakes deposits (Walford & Franklin, 1982). Similarities in the chemical character and spatial relationship of silicification zones to massive sulphide deposits in the Noranda and Matagami areas are also striking. The zonal arrangement of alteration in the lower semiconformable zone from distal, deeper silicification to Fe-metasomatism towards nearby massive sulphide deposits is not present in other documented lower semiconformable zones, however.

12. The areal extent of exposed silicification, inferred timing and stratigraphic position of the alteration are compatible with a model in which the metals in the Chisel Lake deposit and in the Fe-enriched alteration were derived from the silicified rocks, although a more passive role of silicification in ore formation as a low-permeability, insulating cap rock which was breached, promoting focussing of the ore fluids (e.g. at Noranda; Gibson et al., 1983), cannot be dismissed.

13. Large silicified zones, particularly in association with Fe-

metasomatized rocks, provide potentially important guides for locating favourable environments of volcanic-associated massive sulphide deposition.

## REFERENCES


Abbey, S.
1980: Studies in 'standard samples' for use in the general analysis of silicate rocks and minerals - Part 6: 1979 edition of 'usable' values; Geological Survey of Canada Paper 80-14.

Akella, J.
1966: Calculation of material transport in some metasomatic processes; N. Jahrbuch f. Mineralogie Abhandlungen, v. 104, no. 3, p. 316-329.

Alderton, D.H.M., Pearce, J.A. & Potts, P.J.
1980: Rare earth element mobility during granite alteration: Evidence from Southwest England; Earth and Planetary Science Letters, v. 49, p. 149-165.

Anderson, G.M., Pascal, M.L. & Rao, J.
1985: Aluminum speciation in metamorphic fluids; Proceedings of 2nd International Symposium on Hydrothermal Reactions, Pennsylvania State University, University Park.

Bailes, A.H.
1986: Chisel-Morgan Lakes Project. Manitoba Energy and Mines, Report of field activities, p. 70-76.

Bailes, A.H., Syme, E.C., Galley, A., Skirrow, R.G.
1987: Early Proterozoic volcanism, hydrothermal activity, and associated ore deposits at Flin Flon and Snow Lake, Manitoba; Field Trip Guidebook, Geological Association of Canada - Mineralogical Association of Canada Joint Annual Meeting, Saskatoon, May 1987 (in press).

Baragar, W.R.A., Plant, A.G., Pringle, G.J. & Schau, M.
1977: Petrology and alteration of selected units of Mid-Atlantic Ridge basalts sampled from sites 332 and 335, DSDP; Canadian Journal of Earth Sciences, v. 14, p. 837-874.

Baragar, W.R.A., Plant, A.G., Pringle, G.J., and Schau, M.
1979: Diagenetic and postdiagenetic changes in the composition of an Archean pillow; Canadian Journal of Earth Sciences, v. 16, p. 2102-2121.

Barker, F.,
1979: Trondhjemite: Definition, environment and hypotheses of origin, in Barker, F. (ed.), Trondhjemites, dacites and related rocks; Developments in Petrology, 6. Elsevier, p. 1-12.

Barker, F. & Arth, J.C.
1976: Generation of trondhjemitic-tonalitic liquids and Archean bimodal trondhjemite-basalt suites; Geology, v. 4, p. 596-

600.

Bird, D.K. & Helgeson, H.C.
1981: Chemical interaction of aqueous solutions with epidote-feldspar mineral assemblages in geologic systems. II. Equilibrium constraints in metamorphic/geothermal processes; American Journal of Science, v. 281, p. 576-614.

Bischoff, J.L. & Dickson, F.W.
1975: Seawater-basalt interaction at 200°C and 500 bars: Implications for the origin of sea-floor heavy-metal deposits and regulation of seawater chemistry; Earth and Planetary Science Letters, v. 25, p. 385-397.

Bischoff, J.L., Radtke, A.S. & Rosenbauer, R.J.
1981: Hydrothermal alteration of graywacke by brine and seawater: Roles of alteration and chloride complexing on metal solubilization at 200° and 350°C; Economic Geology, v. 76, p. 659-676.

Bischoff, J.L. & Rosenbauer, R.J.
1984: The critical point and two phase boundary of seawater, 200-500°C; Earth and Planetary Science Letters, v. 68, p. 172-180.

Campbell, I.H., Lesher, C.M., Coad, P., Franklin, J.M., Gorton, M.P. & Thurston, P.C.
1984: Rare-earth element mobility in alteration pipes below massive Cu-Zn sulphide deposits; Chemical Geology, v. 45, p. 181-202.

Carpenter, A.B., Trout, M.L. & Pickett, E.W.
1974: Preliminary report on the origin and chemical evolution of lead- and zinc-rich oil field brines in Central Mississippi: Economic Geology, v. 69, p. 1191-1206.

Cas, R.A.F.
1979: Mass-flow arenites from a Paleozoic interarc basin, New South Wales, Australia: mode and environment of emplacement; Journal of Sedimentary Petrology, v. 49, p. 29-44.

Cas, R.A.F. & Wright, J.V.
1982: Modern and ancient volcanic successions: An approach to analysis of facies, environments of deposition and tectonic setting; Course Notes, Monash University, Melbourne.

Cathles, L.M.
1983: An analysis of the hydrothermal system responsible for massive sulphide deposition in the Hokuroku Basin of Japan; Economic Geology, Monograph 5, p. 439-487.

Chen, C.T.A. & Marshall, W.L.
1982: Amorphous silica solubilities - IV. Behaviour in pure water and aqueous sodium chloride, sodium sulfate, magnesium chloride, and magnesium sulfate up to 350°C; Geochimica

et Cosmochimica Acta, v. 46, p. 279-287.

Condie, K.C., Vijoen, M.J. & Kable, E.J.D.
1977: Effects of alteration on element distributions in Archean tholeiites from the Barberton greenstone belt, South Africa: Contributions to Mineralogy nad Petrology, v. 64, p. 75-89.

Costa, U.R., Barnett, R.L., & Kerrich, R.,
1983: The Matagami Lake Mine Archean Zn-Cu sulphide deposit, Quebec: hydrothermal coprecipitation of talc and sulfides in a sea-floor brine pool - evidence from geochemistry, $^{18}O/^{16}O$, and mineral chemistry; Economic Geology, v. 78, p. 1144-1203.

Davis, E.E., Goodfellow, W.D., Bornhold, B.D., Adshead, J., Blaise, B., Villinger, H. & Le Cheminant, G.M.
In press: Massive sulphides in a sedimented rift valley, northern Juan de Fuca Ridge; Geology 17p.

Deer, W.A., Howie, R.A. & Zussman, J.
1966: An introduction to the rock-forming minerals; Longman, London.

Dimroth, E., Cousineau, P., Leduc, M., & Sanschagrin, Y.
1978: Structure and organization of Archean subaqueous basalt flows, Rouyn-Noranda Area, Quebec, Canada; Canadian Journal of Earth Sciences, v. 15, p. 902-918.

Dimroth, E. & Lichtblau, A.P.
1979: Metamorphic evolution of Archean hyaloclastites, Noranda area, Quebec, Canada. PartI: Comparison of Archean and Cenozoic sea-floor metamorphism; Canadian Journal of Earth Sciences, v. 16, no. 7, p. 1315-1340.

Dimroth, E. & Rocheleau, M.
1979: Volcanology and sedimentology of Rouyn-Noranda area, Quebec; Geological Association of Canada, Guidebook A-1.

Dostal, J. & Strong, D.F.
1983: Trace-element mobility during low-grade metamorphism and silicification of basaltic rocks from Saint John, New Brunswick; Canadian Journal of Earth Sciences, v. 20, p. 431 - 435.

Elders, W.A., Bird, D.K., Williams, A.E. & Schiffman, P.
1984: Hydrothermal flow regime and magmatic heat source of the Cerro Prieto Geothermal System, Baja California, Mexico; Geothermics, v. 13, no. 1/2, p. 27-47.

Elders, W.A. & Bird, D.K.
1974: Active formation of silicified cap rocks in arenaceous sands in a low-temperature, near-surface geothermal environment, in the Salton Trough of California, U.S.A.; International Symposium on water-rock Interaction; abstracts, Geological Survey of Czechoslovakia, Prague, p. 150-157.

Ellis, A.J.
1968: Natural hydrothermal systems and experimental hot-water/rock interaction: Reactions with NaCl solutions and trace metal extraction; Geochimica et Cosmochimica Acta, v. 32, p. 1356-1363.

Evarts, R.C. & Schiffman, P.
1983: Submarine hydrothermal metamorphism of the Del Puerto ophiolite, California; American Journal of Science, v. 283, p. 289-340.

Finlow-Bates, T. & Stumpfl, E.F.
1981: The behaviour of so-called immobile elements in hydrothermally altered rocks associated with volcanogenic submarine exhalative ore deposits; Mineralium Deposita, v. 16, p. 319-328.

Floyd, P.A. & Winchester, J.A.
1978: Identification and discriminatiion of altered and metamorphosed volcanic rocks using immobile elements; Chemical Geology, v. 21, p. 291-306.

Fournier, R.O.
1968: Depths of intrusion and conditions of hydrothermal alteration in porphyry copper deposits; Geological Society of America, Program with Abstracts 1968 Annual Meeting, p. 101.

Fournier, R.O.
1983a: Active hydrothermal systems as analogues of fossil systems; Geothermal Resources Council, Special Report, No. 13, p. 263-284.

Fournier, R.O.
1983b: A method of calculating quartz solubilities in aqueous sodium chloride solutions; Geochimica et Cosmochimica Acta, v. 47, p. 579-586.

Fournier, R.O.
1985: The behaviour of silica in hydrothermal solutions; in Berger, B.R. & Bethke, P.M. (eds.), Geology and Geochemistry of Epithermal Systems, Reviews in Economic Geology, v. 2, p. 45-61.

Franklin, J.M.
1986: Volcanic-associated massive sulphide deposits - an update; in Andrew, C.J., Crowe, R.W.A., Finlay, S., Pennell, W.M & Pyne J.F. (eds.), Geology and genesis of mineral deposits in Ireland, Irish Association for Economic Geology.

Franklin J.M., Sangster, D.F. & Lydon, J.W.
1981: Volcanic-associated massive sulphide deposits; Economic Geology 75th Anniversary Volume, p. 485-627.

Froese, E. & Gasparrini, E.
1975: Metamorphic zones in the Snow Lake area, Manitoba; Canadian Mineralogist, v. 13, p. 162-167.

Froese, E. & Moore, J.M.
1980: Metamorphism in the Snow Lake area, Manitoba; Geological Survey of Canada, Paper 78-27.

Gelinas, L., Brooks, C. & Trzcienski, W.E.
1976: Archean variolites - quenched immiscible liquids; Canadian Journal of Earth Sciences, v. 13, p. 210-230.

Gibson, H
1979: Geology of the Amulet Rhyolite formantion, Turcotte Lake section, Noranda area, Quebec; Unpublished M.Sc thesis, Carleton University.

Gibson, H.L., Watkinson, D.H., & Comba, C.D.A.
1983: Silicification: Hydrothermal alteration in an Archean geothermal system within the Amulet Rhyolite Formation, Noranda, Quebec: Economic Geology, v. 78, p. 954-971.

Gibson, I.L. & Walker, P.L.
1963: Some composite rhyolite/basalt lavas and related composite dykes in Eastern Iceland; Proceedings of the Geologists Association, v. 74, no. 3, p. 301-318.

Goodwin, A.M.
1977: Archean volcanism in Superior Province, Canadian Shield; in Baragar, W.R.A., Coleman, L.C. & Hall, J.M. (eds.), Volcanic regimes in Canada, Geological Association of Canada Special Paper No. 16, p. 205-241.

Grant, J.A.
1986: The isocon diagram - A simple solution to Gresens' equation for metasomatic alteration; Economic Geology, in press.

Gregory, S.
1963: Statistical methods and the geographer; Longmans, London.

Gresens, R.
1967: Composition-volume relationships of metasomatism. Chemical Geology, v. 2, p. 47-65.

Hajash, A.
1975: Hydrothermal processes along mid-ocean ridges: An experimental investigation; Contributions to Mineralogy and Petrology, v. 53, no. 3, p. 205-226.

Hampton, M.A.
1972: The role of subaqueous debris flow in generating turbidity currents; Journal of Sedimentary Petrology, v. 42, p. 725-793.

Harrigan, D.B. & MacLean, W.H.
1976: Petrography and geochemistry of epidote alteration patches in gabbro dykes at Matagami, Quebec; Canadian Journal of Earth Sciences, v. 13, p. 500-511.

Harrison, J.M.
1949: Geology and mineral deposits of File- Tramping Lakes area, Manitoba; Geological Survey of Canada, Memoir 250.

Hedenquist, J.W. & Henley, R.W.
1985: Hydrothermal eruptions in the Waiotapu Geothermal System, New Zealand: Their origin, associated breccias, and relation to precious metal mineralization; Economic Geology, v. 80, p. 1640-1668.

Hem, J.D. & Roberson, C.E.
1967: Form and stability of aluminum hydroxide complexes in dilute solutions; U.S. Geological Survey Water-Supply Paper 1827-A.

Hey, M.H.
1954: A new review of the chlorites; Mineralogical Magazine, v. 30, p. 277-

Hodgson, C.J. & Lydon, J.W.
1977: The geologic setting of volcanogenic massive sulphide deposits and active hydrothermal systems: Some implications for exploration; Canadian Mining and Mettallurgy Bulletin, v.70, p.95-106.

Holdaway, M.J.
1966: Hydrothermal stability of clinozoisite plus quartz; American Journal of Science v.264, p.643-667.

Humphris, S.E., Morrison, M.A. & Thompson, R.N.
1978: Influence of rock crystallization history upon subsequent lanthanide mobility during hydrothermal alteration of basalts; Chemical Geology, v. 23, p. 125-137.

Humphris, S.E. & Thompson, G.
1978: Hydrothermal alteration of oceanic basalts by seawater; Geochimica et Cosmochimica Acta, v. 42, p. 107-125.

Hynes, A.
1980: Carbonatization and mobility of Ti, Y and Zr in Ascot Formation metabasalts, S.E. Quebec; Contributions to Mineralogy and Petrology, v. 75, p. 79-87.

Irvine, T.N. & Baragar, W.R.A.
1971: A guide to the classification of the common volcanic rocks; Canadian Journal of Earth Sciences, v. 8, p. 523-549.

Jensen, L.S.
1976: A new cation plot for classifying subalkalic volcanic rocks; Ontario Division of Mines, Miscellaneous Paper 66, 22p.

Keith, T.E.C., Muffler, L.J.P. & Cremer, M.
1968: Hydrothermal epidote formed in the Salton Sea geothermal system, California; American Mineralogist, v. 53, p. 1653-1644.

Kennedy, G.C.
1950: A portion of the system silica-water; Economic Geology, v. 45, p. 629-653.

Kretz, R., Hartree, R., Garrett., D. & Cermignani, C.
1985: Petrology of the Grenville swarm of gabbro dikes, Canadian Precambrian Shield; Canadian Journal of Earth Sciences, v. 22, p. 53-71.

Kristmannsdottir, H.
1976: Hydrothermal alteration of basaltic rocks in Icelandic geothermal areas; Proceedings, Second United Nations Symposium on the Development and Use of Geothermal Resources, San Francisco, May 1975, v. 1. U.S. Government Printing Office, Washington, D.C., p. 441-445.

Leake, B.E.
1978: Nomenclature of amphiboles; Canadain Mineralogist, v. 16, p. 501-520.

Le Maitre, R.W.
1976: The chemical variability of some common igneous rocks; Journal of Petrology, v. 17, p. 589-637.

Lesher, C.M., Gibson, H.L. & Campbell, I.H.
1986: Composition-volume changes during hydrothermal alteration of andesite at Buttercup Hill, Noranda District, Quebec; Geochimica et Cosmochimica Acta, v. 50, p. 2693-2705.

Lister, C.R.B.
1977: Qualitative models of spreading-center processes, including hydrothermal penetration; Tectonophysics, v. 37, p. 203-218.

Lockwood, M.B.
1986: The petrogenetic and economic significance of chloritoid in the Wawa greenstone belt; unpublished M.Sc. thesis, Carleton University.

Ludden, J., Gelinas, L. & Trudel, P.
1982: Archean metavolcanics from the Rouyn-Noranda district, Abitibi Greenstone Belt, Quebec - 2. Mobility of trace elements and petrogenetic constraints; Canadian Journal of Earth Sciences, v. 19, p. 2276-2287.

Ludden, J.N. & Thompson,G.
1978: Behaviour of rare earth elements during submarine weathering of tholeiitic basalt; Nature, v. 274, p. 147-149.

Lydon, J.W.
1983: Chemical parameters controlling the origin and deposition of

sediment-hosted stratiform lead-zince deposits; in Sangster, D.F. (ed.): Short course handbook on sediment-hosted stratiform lead-zince deposits; Minerological Association of Canada, V. 8, p. 175-250.

Lydon, J.W. & Jamieson, H.E.
1984: The generation of ore-froming hydrothermal solutions in the Troodos ophiolite complex: Some hydrodynamic and mineralogical considerations; in Current Research, Part A, Geological Survey of Canada, Paper 84-1A, p. 617-625.

MacGeehan, P.J.
1978: The geochemistry of altered volcanic rocks at Matagami, Quebec: A geothermal model for massive sulphide genesis; Canadian Journal of Earth Sciences, v. 15, p. 551-570.

MacGeehan, P.J. & MacLean, W.H.
1980: An Archean sub-seafloor geothermal system, 'clac-alkali' trends, and massive sulphide genesis; Nature, v. 286, p. 767-771.

MacKenzie, W.S., Donaldson, C.H. & Guilford, C.
1982: Atlas of igneous rocks and their textures; Longman, London.

Martin, R.F., Whitley, J.E. & Wooley, A.R.
1978: An investigation of rare earth element mobility in fenitized quartzites, Borralen Complex, Scotland; Contributions to Mineralogy and Petrology, v. 66, p. 69-73.

Melson, W.G., Thompson, G. & van Andel, T.H.
1968: Volcanism and metamorphism in the Mid-Atlantic ridge, 22°N latitude. Journal of Geophysical Research, v. 73, p. 5925-5941.

Middleton, G.V. & Hampton, M.A.
1976: Subaqueous sediment transport and deposition by sediment gravity flows; in Stanley, D.J. & Swift, D.J.P. (eds.), Marine sediment transport and environmental management. J. Wiley & Sons, p. 197-218.

Moore, J.M.
1977: Orogenic volcanism in the Proterozoic of Canada; in Baragar, W.R.A., Coleman, L.C. & Hall, J.M. (eds.), Volcanic Regimes in Canada, Geological Association of Canada Special Paper No. 16, p. 127-148.

Morton, R.L. & Nebel, M.L.
1984: Hydrothermal alteration of felsic volcanic rocks at the Helen siderite deposit, Wawa, Ontario; Economic Geology, v. 79, p. 1318-1333.

Mottl, M.J.
1983: Metabasalts, axial hot springs, and the structure of hydrothermal systems at mid-ocean ridges; Geological Society of America Bulletin, v. 94, p. 161-180.

Mottl, M.J., Holland, H.D., & Corr, R.F.
1979: Chemical exchange during hydrothermal alteration of basalt by seawater - II. Experimental results for Fe, Mn and sulfur species; Geochimica et Cosmochimica Acta. v. 43, p. 869-884.

Mottl, M.J. & Seyfried, W.E.
1980: Sub-seafloor hydrothermal systems: Rock- vs. seawater-dominated; in Rona, P.A & Lowell, R.P. (eds.), Seafloor spreading centers - Hydrothermal systems; Dowden Hutchinson and Ross, Inc., Stroudsburg, Pennsylvania, 424 p.

Murphy, J.B. & Hynes, A.J.
1986: Contrasting secondary mobility of Ti, P, Zr, Nb and Y in two metabasaltic suites in the Appalachians; Canadian Journal of Earth Sciences, v. 23, p. 1138-1144.

Nayudu, Y. R.
1964: Palagonite tuffs (hyaloclastites) and the products of post-eruptive processes; Bulletin Volcanologique, v. 27, p. 391-410.

Ohmoto, H & Skinner, B.J.
1983: The Kuroko and related volcanogenic massive sulphide deposits: Introduction and summary of new findings; in Ohmoto, H. & Skinner, B.J. (eds.), The Kuroko and related volcanogenic massive sulphide deposits, Economic Geology Monograph 5, p.1-8.

Paris, I., Stanistreet, I.G. & Hughes, M.J.
1985: Cherts of the Barberton Greenstone Belt interpreted as products of submarine exhalative activity; Journal of Geology, v. 93, p. 111-129.

Ragnarsdottir, K.V., Walther, J.V. & Arnorsson, S.
1984: Description and interpretation of the composition of fluid and alteration mineralogy in the geothermal system, at Svartsengi, Iceland; Geochimica et Cosmochimica Acta, v. 48, p. 1535-1553.

Ragnarsdottir, K.V. & Walther, J.V.
1985: Experimental determination of corundum solubilities in pure water between 400-700°C and 1-3 kbar; Geochimica et Cosmochimica Acta, v. 49, p. 2109-2115.

Rimstidt, J.D. & Barnes, H.L.
1980: The kinetics of silica-water reactions; Geochimica et Cosmochimica Acta, v. 44, p. 1683-1699.

Rosenbauer, R.J. & Bischoff, J.L.
1984: Uptake and transport of heavy metals by heated seawater: A summary of the experimental results; in Rona, P.A., Bostrom, K., Laubier, L., Smith, K.L. Jr. (eds), Hydrothermal processes at seafloor spreading centers, Plenum, New York.

Rosenbauer, R.J., Bischoff, J.L. & Radtke, A.S.
1983: Hydrothermnal alteration of graywacke and basalt by 4 molal NaCl; Economic Geology, v. 78, p. 1701-1710.

Rowe, J.J., Fournier, R.O., & Morey, G.W.
1967: The system water - sodium oxide - silicon dioxide at 200, 250 and 300°; Inorganic Chemistry, v. 6, p. 1183-1188.

Sangster, D.F.
1972: Precambrian volcanogenic massive sulphide deposits in Canada: A review; Geological Survey of Canada Paper 72-22, 44p.

Spooner, E.T.C.
1977: Hydrodynamic model for the origin of the ophiolitic cupriferous pyrite ore deposits of Cyprus; in Volcanic processes in ore genesis, Geological Society of London, Special Publication 7, p.58-71.

Spooner, E.T.C. & Fyfe, W.S.
1973: Sub-seafloor metamorphism, heat and mass transfer; Contributions to Mineralogy and Petrology, v.42, p.287-304.

Scott, R.B. & Hajash, A. Jr
1976: Initial submarine alteration of basaltic pillow lavas: A microprobe study; American Journal of Science, v. 276, p. 480-501.

Seyfried, W.E. Jr.
1987: Experimental and theoretical constraints on hydrothermal alteration processes at mid-ocean ridges; Recent hydrothermal mineralization of seafloor spreading centres: Tectonic, petrologic and geochemical constraints; Mineral Exploration Research Institute conference program and abstracts, Montreal Quebec, February 1987.

Seyfried W.E. Jr. & Bischoff, J.L.
1977: Hydrothermal transport of heavy metals by seawater: the role of seawater/basalt ratio. Earth and Planetary Science Letters v. 34, p. 71-77.

Seyfried, W.E. Jr., Mottl, M.J. & Bischoff, J.L.
1978: Seawwater/basalt ratio effects on the chemistry and mineralogy of spilites from the ocean floor. Nature, v. 275, p. 211-213.

Seyfried, W.E. Jr. & Bischoff, J.L.
1981: Experimental seawater-basalt interaction at 300°C, 500 bars: Chemical exchange. secondary mineral formation, and implications for the transport of heavy metals; Geochimica et Cosmochimica Acta, v.45, p. 135-147.

Seyfried, W.E. Jr. & Janecky, D.R.
1985: Heavy metal and sulfur transport during subcritical and supercritical hydrothermal alteration of basalt: Influence of fluid pressure and basalt composition and crystallinity;

Geochimica et Cosmochimica Acta, v. 49, p. 2545-2560.

Sigvaldson, G.E.
1959: Mineralogische untersuchungen uber gesteinszersetzung durch postvolkanische akivitat in island; Beitr. Mineralogie Petrologie, v. 6, p. 405-427.

Smith, R.E.
1968: Redistribution of major elements in the alteration of some basic lavas during burial metamorphism; Journal of Petrology, v. 9, p. 191-219.

Spry, A.
1969: Metamorphic textures. Pergamon, London.

Staudigel, H. & Hart, S.R.
1983: Alteration of basaltic glass: Mechanisms and significance for the oceanic crust-seawater budget; Geochimica et Cosmochimica Acta, v. 47, p. 337-350.

Strong, D.F., Dickson, W.L., & Pickerill, R.K.
1979: Chemistry and prehnite-pumpellyite facies metamorphism of calc-alkaline Carboniferous volcanic rocks of southeastern New Brunswick; Canadian Journal of Earth Sciences, v. 16, p. 1071-1085.

Syme, E.C., Bailes, A.H., Price, D.P. & Ziehlke, D.V.
1982: Flin Flon volcanic belt: Geology and ore deposits at Flin Flon and Snow Lake Manitoba; Field Trip Guidebook, Geological Association of Canada - Mineralogical Association of Canada Joint Annual Meeting, Winnipeg, May 1982.

Syme, E.C.
1985: Geochemistry of metavolcanic rocks in the Lynn Lake Belt; Manitoba Energy and Mines, Geological Report GR84-1.

Taylor, S.R. & Gorton, M.P.
1977: Geochemical application of spark source mass spectrography - III. Element sensitivity, precision and accuracy; Geochimica et Cosmochimica Acta, v. 41, p. 1375-1380.

Thompson, G.
1984: Basalt-seawater interaction; in Rona, P.A., Bostrom, K., Laubier, L., Smith, K.L. Jr. (eds.), Hydrothermal processes at seafloor spreading centers, Plenum, New York, p. 225-277.

Thurston, P.C., Ayers, L.D., Edwards, G.R., Gelinas, L., Ludden, J.N. & Verpaelst, P.
1985: Archean bimodal volcanism; in Ayers, L.D., Thurston, P.C., Card, K.D., & Weber, W. (eds.), Evolution of Archean supracrustal sequences, Geological Association of Canada Special Paper 28, p.7-21.

The remaining samples were analyzed by XRF at the University of Ottawa by Ron Hartree, using a Phillips PW10-80 X-ray fluorescence spectrometer with a rhodium tube. Splits of these samples were analyzed at X-Ray Assay Laboratories Limited, Dons Mills, for Cu and Pb by DCP, and for $H_2O$, $CO_2$ and FeO by chemical methods.

Standards used during XRF analysis were DRN, SY-2 and RGM. Standards sent to X-Ray Laboratories Limited were AGV-1, G-1 and W-1.

(a) **Precision and accuracy of XRF and ICP analysis**

The precision of XRF determinations at the University of Ottawa laboratory is given in Table 12, and ws checked in the present study by analysing several samples repeatedly (DR-N, SY-2, and RGM). The mean and range for three analyses of the same fusd disc of sample DR-N are presented in Table 13. The precision of XRF and ICP analysis at the G.S.C. laboratory is also given in Table 12.

The accuracy of the XRF technique was tested by comparing the analyses of the standards DR-N, SY-2 and RGM with the 'usable' values of Abbey (1980). The results for DR-N, shown in Table 13, indicate departures of less than 6% of the concentrations of major components except $P_2O_5$, and less than 16% of trace element concentrations.

Detection limits for trace elements, $H_2O$, $CO_2$ and FeO are listed in Table 14.

(b) **Precision or reproducibility of sample and fused pellet preparation procedures**

To test the homogeneity of powdered samples and the reproducibility of the fusion method, two fused pellets were made from each of 14 different powder samples. The duplicate analyses are compared to the original analyses using the T-statistic on paired observations (Table 15). Using the coefficient of variation at the 95% confidence interval

# APPENDIX 1

## MINERAL ASSEMBLAGES OF SAMPLES ANALYZED FOR MAJOR AND TRACE ELEMENTS

### Codes used in subsequent tables

| | Code | Rock Type |
|---|---|---|
| Felsic | Fa | Volcaniclastic rock |
| | Fb | Quartz-plagioclase porphyry intrusion |
| | Fe | Fine quartz ± plagioclase-phyric dyke |
| | Fd | Aphyric and plagioclase-phyric dyke |
| Mafic | Ma | Aphyric flow |
| | Mb | Plagioclase-phyric flow |
| | Mc | Pyroxene-phyric flow |
| | Md | Pyroxene-phyric volcaniclastic rock |
| | Me | Plagioclase-phyric volcaniclastic rock |
| | Mf | Volcaniclastic, including heterolithic |
| | Mg | Fine-grained dyke |
| | Mh | Gabbroic and plagioclase-phyric intrusion |
| | Mi | Pyroxene-phyric intrusion |
| | Mj | Pyroxenite intrusion |

### Alteration Codes

| | |
|---|---|
| S | Silicified |
| E | Epidotized |
| P | Plagioclase-quartz borders to fractures |
| G | Garnet-chlorite alteration |
| B | Garnet-biotite and biotite alteration |
| Y | Pyritic or pyrrhotitic |

### Codes following sample number

C = pillow core
M = pillow margin
V = pillow selvage

Table 5

Mineral assemblages of samples analyzed for major and trace elements

| Sample | C | A | qtz | pla | hb | bt | chl | gt | mv | cum | st | ep | cc | ap | mt/ilm | sph | py/po |
|---|---|---|---|---|---|---|---|---|---|---|---|---|---|---|---|---|---|
| 001 | Mb | 70 | + | ++ | ++ | + | | | | | | | | | + | | |
| 002 | Fd | 22 | ++ | ++ | + | tr | | tr | tr | | | tr | | tr | + | | |
| 0031 | Fd | 23 | + | ++ | ++ | | | tr | tr | | | + | | tr | + | tr | |
| 00311 | FdE | 36 | + | ++ | ++ | | | tr | tr | | | + | | tr | + | tr | |
| 0051 | Mb | 71 | + | ++ | ++ | tr | | | | | | | | | + | | |
| 00511 | Fd | 16 | ++ | ++ | ++ | + | | + | | | | tr | | tr | tr | | |
| 006 | FbE | 35 | ++ | ++ | + | + | tr | + | | | | tr | | | tr | | |
| 007 | Mh | 120 | + | ++ | ++ | | | + | | | | | | | + | | |
| 009 | Fb | 8 | ++ | ++ | | + | tr | | + | | | | tr | | tr | | |
| 010 | Fd | 24 | ++ | ++ | + | | tr | | | | | | | | + | | |
| 011 | MgE | 134 | + | + | ++ | tr | | | | | | ++ | | | | tr | |
| 012 | Mb | 75 | + | ++ | ++ | | | | | | | tr | tr | | tr | + | |
| 013 | MbE | 83 | ++ | + | + | | tr | | | | | ++ | + | | tr | + | |
| 014 | Mg | 114 | tr | ++ | ++ | | | | | | | | | | + | | |
| 0151 | MbE | 84 | + | tr | ++ | | | | | | | ++ | + | | tr | + | |
| 01511 | MbE | 85 | + | | tr | | | | | | | ++ | + | | | + | |
| 016 | Mb | 76 | tr | ++ | ++ | tr | tr | | tr | | | | tr | | + | | |
| 0171 | MbS | 79 | ++ | | + | | tr | | | tr | | | tr | | | | |
| 01711 | Mb | 72 | + | ++ | ++ | | + | | | | | | tr | | + | | |
| 01811 | FdE | 37 | ++ | ++ | tr | | | | | | | ++ | | | | tr | |
| 020 | Fd | 25 | ++ | ++ | ++ | + | | + | | | | + | | | + | | |
| 036 | Fe | 11 | ++ | ++ | ++ | | | | | | | tr | | tr | tr | tr | |
| 042 | Fe | 12 | ++ | ++ | | + | + | tr | + | | | | tr | | + | | |
| 046 | Fa | 2 | ++ | ++ | | + | + | | ++ | | | | + | | tr | | |
| 048 | Mh | 121 | ++ | ++ | ++ | | | | | | | + | | | + | | |
| 051 | Fe | 13 | ++ | ++ | + | + | | + | | | | | | tr | tr | | |
| 052 | Mh | 122 | ++ | ++ | ++ | tr | | | + | | | | tr | + | tr | | |
| 055 | Fb | 9 | + | + | | + | + | | + | | | | + | + | + | | |
| 062 | Md | 89 | + | + | + | | | | | | | | | | + | | |

Table 5 (cont.)

| Sample | C | A | qtz | pla | hb | bt | chl | gt | mv | cum | st | ep | cc | ap | mt/ilm | sph | py/po |
|---|---|---|---|---|---|---|---|---|---|---|---|---|---|---|---|---|---|
| 063 | Mc | 88 | ++ | ++ | ++ | | | | | | | tr | | | tr | | |
| 064 | Md | 90 | ++ | ++ | ++ | tr | tr | | | | | | | | + | | |
| 073 | MeE | 103 | | + | trem | | | | | | | + | + | | | + | |
| 077 | Mh | 123 | + | + | + | + | + | | | | | | | tr | tr | | |
| 080 | Mj | 129 | | + | ++ | | | | | | | | + | | + | | |
| 083 | Fc | 14 | ++ | ++ | | ++ | | | + | | | tr | tr | | + | | |
| 0841 | MaS | 50 | ++ | ++ | ++ | + | tr | | | | | tr | + | | | | |
| 08411 | Ma | 51 | ++ | ++ | ++ | + | + | | | | | | + | tr | + | | |
| 086 | Ma | 49 | ++ | ++ | ++ | + | | | | | | | tr | | + | | |
| 088 | Ma | 43 | ++ | ++ | ++ | | | | | | | tr | + | | + | tr | |
| 089 | Fa | 3 | ++ | ++ | | + | + | + | tr | | | tr | tr | | tr | | |
| 091 | FaB | 42 | ++ | ++ | | ++ | ++ | | + | | | tr | tr | tr | tr | | |
| 093 | Mg | 115 | ++ | ++ | ++ | | | + | | + | | | | | + | | |
| 094 | Fd | 26 | | | | | | | | | | | | | | | |
| 095 | Fa | 4 | ++ | ++ | tr | + | | | | ++ | | | | | tr | | |
| 098 | Mh | 124 | | ++ | ++ | | | | | | | | | | + | | |
| 102 | Mb | 73 | + | ++ | ++ | | | | | | | | | | + | | |
| 104 | MbE | 86 | + | ++ | ++ | | | | | | | ++ | ++ | | tr | + | |
| 105 | Mb | 74 | + | ++ | ++ | | | | | | | | | | + | | |
| 106 | MbB | 87 | ++ | ++ | | ++ | | | | | | | | tr | tr | tr | |
| 109 | FdE | 38 | + | + | + | | + | | | | | | | | + | + | |
| 111 | Mh | 125 | + | ++ | ++ | tr | tr | + | | | | tr | | | + | | |
| 114 | FdG | 40 | + | + | | + | ++ | + | | | | | | | + | | |
| 115 | Fd | 27 | ++ | ++ | + | | + | + | | | | | | tr | + | | |
| 116 | Fd | 28 | ++ | ++ | ++ | | | | | | | + | | tr | tr | + | |
| 119 | Fd | 17 | ++ | ++ | + | + | + | + | | | | tr | | tr | + | | |
| 122 | Mg | 116 | | ++ | ++ | ++ | | tr | | | | | | | tr | | |
| 123 | Fd | 18 | ++ | ++ | ++ | + | | + | | | | | | tr | tr | | |

Table 5 (cont.)

| Sample | C | A | qtz | pla | hb | bt | chl | gt | mv | cum | st | ep | cc | ap | mt/ilm | sph | py/po |
|---|---|---|---|---|---|---|---|---|---|---|---|---|---|---|---|---|---|
| 063 | Mc | 88 | ++ | ++ | ++ | | | | | | | tr | | | tr | | |
| 064 | Md | 90 | ++ | ++ | ++ | tr | tr | | | | | | | | + | | |
| 073 | MeE | 103 | | + | trem | | | | | | | + | + | | | + | |
| 077 | Mh | 123 | + | + | + | + | + | | | | | | | tr | tr | | |
| 080 | Mj | 129 | | + | ++ | | | | | | | | + | | + | | |
| 083 | Fc | 14 | ++ | ++ | | ++ | | | + | | | tr | tr | | + | | |
| 0841 | MaS | 50 | ++ | ++ | ++ | + | tr | | | | | tr | + | | | | |
| 08411 | Ma | 51 | ++ | ++ | ++ | + | + | | | | | | + | tr | + | | |
| 086 | Ma | 49 | ++ | ++ | ++ | + | | | | | | | tr | | + | | |
| 088 | Ma | 43 | ++ | ++ | ++ | | | | | | | tr | + | | + | tr | |
| 089 | Fa | 3 | ++ | ++ | | + | + | + | tr | | | tr | tr | | tr | | |
| 091 | FaB | 42 | ++ | ++ | | ++ | ++ | | + | | | tr | tr | tr | tr | | |
| 093 | Mg | 115 | ++ | ++ | ++ | | | + | | + | | | | | + | | |
| 094 | Fd | 26 | | | | | | | | | | | | | | | |
| 095 | Fa | 4 | ++ | ++ | tr | + | | | | ++ | | | | | tr | | |
| 098 | Mh | 124 | | ++ | ++ | | | | | | | | | | + | | |
| 102 | Mb | 73 | + | ++ | ++ | | | | | | | | | | + | | |
| 104 | MbE | 86 | + | ++ | ++ | | | | | | | ++ | ++ | | tr | + | |
| 105 | Mb | 74 | + | ++ | ++ | | | | | | | | | | + | | |
| 106 | MbB | 87 | ++ | ++ | | ++ | | | | | | | | tr | tr | tr | |
| 109 | FdE | 38 | + | + | + | | + | | | | | + | | | + | + | |
| 111 | Mh | 125 | + | ++ | ++ | tr | tr | + | | | | tr | | | + | | |
| 114 | FdG | 40 | + | + | | + | ++ | + | | | | | | | + | | |
| 115 | Fd | 27 | ++ | ++ | + | | + | + | | | | | | tr | + | | |
| 116 | Fd | 28 | ++ | ++ | ++ | | | | | | | + | | tr | tr | + | |
| 119 | Fd | 17 | ++ | ++ | + | + | + | + | | | | tr | | tr | + | | |
| 122 | Mg | 116 | | ++ | ++ | ++ | | tr | | | | | | | tr | | |
| 123 | Fd | 18 | ++ | ++ | ++ | + | | + | | | | | | tr | tr | | |

Table 5 (cont.)

| Sample | C | A | qtz | pla | hb | bt | chl | gt | mv | cum | st | ep | cc | ap | mt/ilm | sph | py/po |
|---|---|---|---|---|---|---|---|---|---|---|---|---|---|---|---|---|---|
| 124 | Mb | 78 | | ++ | ++ | | | | | | | tr | tr | | + | | |
| 132 | Mg | 117 | ++ | ++ | ++ | + | | | | | | | | tr | + | | |
| 134 | Fd | 29 | ++ | ++ | | + | + | tr | | | | | | tr | + | tr | |
| 138 | Fd | 30 | ++ | ++ | ++ | | | | | tr | | | | tr | + | | |
| 140 | FdP | 41 | ++ | ++ | + | | | | | | | tr | tr | tr | + | | |
| 1411 | Mg | 118 | + | ++ | ++ | | | | | | | | | | + | | |
| 14111 | MgP | 137 | ++ | ++ | + | tr | | | | | | | | | + | tr | |
| 142 | Mb | 77 | + | ++ | ++ | | | | | | | tr | | | + | tr | |
| 146 | Fd | 31 | ++ | ++ | ++ | | | | | | | tr | + | tr | + | + | |
| 151 | Md | 91 | + | ++ | ++ | | | | | | | | | tr | + | | |
| 155 | Fd | 19 | ++ | ++ | ++ | tr | | | | tr | | | tr | tr | + | | |
| 156 | Mh | 126 | + | ++ | ++ | | | | | | | | tr | | tr | tr | |
| 160 | Fd | 20 | ++ | ++ | | ++ | ++ | + | tr | | | | tr | tr | | | |
| 161 | Fd | 32 | ++ | ++ | tr | + | + | | | | | | + | tr | tr | tr | |
| 171 | MaS | 55 | + | ++ | ++ | + | tr | | | | | tr | tr | | + | | |
| 172 | MaS | 54 | ++ | ++ | ++ | | tr | tr | | | | tr | tr | | + | tr | tr |
| 173 | Ma | 52 | ++ | ++ | ++ | | tr | | | | | | tr | | + | tr | tr |
| 174 | MaE | 64 | + | | + | | | | | | | ++ | + | | + | | |
| 175 | Ma | 45 | + | ++ | ++ | | | | | | | | tr | | + | tr | tr |
| 176 | Ma | 44 | ++ | ++ | ++ | | | | | | | tr | tr | | + | tr | tr |
| 177 | MaE | 65 | ++ | | ++ | | | | | | | ++ | ++ | | tr | + | |
| 186 | MfG | 104 | + | | + | + | + | + | | + | | | + | | + | + | |
| 192 | Fc | 15 | ++ | ++ | | | | | | | | | | | | | |
| 196 | MfB | 107 | ++ | ++ | | + | + | ++ | | | | | | | tr | | |
| 198 | Ma | 46 | ++ | + | + | + | + | | | | | | | | + | | |
| 200 | MaS | 56 | ++ | ++ | ++ | + | + | | | | | | | | | + | + |
| 201 | Ma | 59 | + | ++ | ++ | | | | | | | | | | + | | |
| 202 | MaS | 57 | ++ | ++ | ++ | + | + | | | | | | | | | + | + |
| 205 | MaS | 58 | ++ | ++ | ++ | tr | tr | | | | | | | | | + | + |

Table 5 (cont.)

| Sample | C | A | qtz | pla | hb | bt | chl | gt | mv | cum | st | ep | cc | ap | mt/ilm | sph | py/po |
|---|---|---|---|---|---|---|---|---|---|---|---|---|---|---|---|---|---|
| 206 | MbS | 80 | ++ | ++ | + | + | tr | + | | | | | | | + | | |
| 210 | Mb | 82 | + | ++ | ++ | + | | | | | | | | | tr | | |
| 211 | MbS | 81 | ++ | ++ | ++ | | | | | | | | | | + | | |
| 212 | Ma | 66 | tr | ++ | ++ | | | | | | | | | | + | | |
| 213 | MaS | 67 | ++ | ++ | ++ | | | | | | | | | | + | | |
| 215 | MaE | 68 | + | | + | | | | | | | ++ | ++ | | + | | tr |
| 216 | Ma | 47 | + | ++ | ++ | | | | | | | | | | | + | |
| 217 | Ma | 48 | ++ | ++ | ++ | ++ | | | | | | | | | + | + | |
| 220 | MaS | 61 | ++ | ++ | ++ | | | | | | | + | + | | + | tr | |
| 221 | MaS | 62 | ++ | ++ | ++ | | + | | | | | ++ | tr | | + | | |
| 222 | Ma | 63 | | + | ++ | + | | tr | | | | | tr | | + | | tr |
| 223 | Ma | 60 | + | ++ | ++ | | | | | | | | | | + | | |
| 229 | MfG | 105 | ++ | ++ | | + | + | ++ | | | | | | | tr | | |
| 235 | MfG | 106 | + | | | + | + | + | + | | + | | | | + | | |
| 237 | Fa | 5 | ++ | ++ | + | ++ | tr | tr | tr | | | ++ | | | tr | | |
| 242 | Mg | 119 | ++ | ++ | ++ | | | + | | | | | | | + | | |
| 243 | MgG | 136 | ++ | + | ++ | | ++ | ++ | | | | | | | + | | |
| 245 | MfB | 108 | ++ | + | | ++ | + | + | + | | + | | | | | | |
| 246 | MfB | 109 | + | ++ | | ++ | ++ | ++ | | | | | | | + | | |
| 247 | MfB | 110 | ++ | ++ | | ++ | + | ++ | | | | | | | + | | |
| 248 | Me | 92 | ++ | ++ | ++ | | | + | | | | | | | + | | |
| 250 | Fa | 6 | ++ | ++ | | + | + | + | | | | | | | tr | | |
| 254 | Fd | 33 | ++ | ++ | | + | + | + | + | | | | tr | tr | tr | | |
| 255 | Fd | 21 | + | + | | + | + | + | | | | | | | + | | |
| 256 | Me | 93 | + | ++ | ++ | + | tr | | | | | | tr | | tr | | |
| 257 | MfB | 101 | ++ | ++ | ++ | ++ | + | + | | | | | | | tr | | |
| 258 | Mf | 97 | ++ | ++ | ++ | ++ | + | | | | | | tr | tr | tr | | |
| 262 | Mf | 98 | | ++ | ++ | ++ | | | | | | tr | | tr | tr | + | |
| 263 | MfP | 111 | + | ++ | + | + | | | | | | ++ | ++ | | | + | |

**Table 5 (cont.)**

| Sample | C | A | qtz | pla | hb | bt | chl | gt | mv | cum | st | ep | cc | ap | mt/ilm | sph | py/po |
|---|---|---|---|---|---|---|---|---|---|---|---|---|---|---|---|---|---|
| 270 | Fa | 7 | ++ | ++ | tr | + | ++ | tr | | | | | | | + | | tr |
| 271 | FaS | 34 | ++ | ++ | | + | | | tr | | | | tr | tr | tr | | |
| 273 | Mg | 129 | + | ++ | ++ | | + | + | | | | | | | + | | |
| 274 | Fd | 131 | ++ | ++ | + | + | + | + | | | | | | | + | | |
| 280 | MiE | 135 | ++ | ++ | trem | | | | | | | ++ | + | | | + | |
| 282 | Mi | 127 | + | ++ | ++ | + | + | | | | | | | | + | | |
| 283 | Mf | 99 | + | ++ | | + | ++ | + | | | | | | | + | | |
| 284 | MfS | 102 | ++ | ++ | | ++ | tr | | | | | | | tr | | rutile | |
| 288 | Mg | 130 | | ++ | ++ | | | | | | | | | | + | | |
| 289 | FdE | 132 | ++ | | | + | + | | | | | ++ | ++ | | | + | |
| 291 | FdE | 133 | ++ | ++ | ++ | tr | | | | | | ++ | | | + | tr | |
| 293 | FbG | 39 | + | ++ | | + | ++ | ++ | + | | | | | | tr | | |
| 294 | Fb | 10 | ++ | ++ | | tr | + | | + | | | | + | | tr | tr | |
| 305 | Me | 95 | + | ++ | ++ | + | | | | | | tr | | | + | | |
| 306 | MeS | 100 | ++ | ++ | ++ | | | | | | | + | | | tr | | |
| 3071 | Me | 95 | + | ++ | ++ | ++ | | | | | | + | | | tr | tr | |
| 30711 | MeP | 112 | ++ | ++ | + | + | | | | | | tr | tr | | | + | |
| 3081 | Me | 96 | + | ++ | | ++ | | | | | | | tr | | | | |
| 30811 | MeP | 113 | ++ | ++ | tr | ++ | | | | | | + | tr | | | + | |

**Abbreviations:** C = rock type code; A = analysis number; qtz = quartz; pla = plagioclase; hb = hornblende; bt = biotite; chl = chlorite; gt = garnet; mv = muscovite; cum = cummingtonite; st=staurolite; ep = epidote or clinozoisite; cc = carbonate; ap = apatite; mt/ilm = Fe-Ti oxides; sph = sphene; py/po = pyrite or pyrrhotite; trem = tremolite-actinolite.

**Symbols:** ++ = major mineral, greater than or equal to 10 vol. %;
+ = minor mineral, 1-9 vol. %;
tr = trace mineral, less than 1 vol. % (visual estimates).

## APPENDIX 2
## MINERAL COMPOSITIONS

All mineral compositions were determined on polished thin sections by electron microprobe analysis (PDS) at Carleton University (by P. Jones).

### Table 6

### Plagioclase compositions

| Sample | Code | Anorthite contents | Comments on plagioclase texture |
|---|---|---|---|
| 014 | Mg | 40,43,41 | interstitial to hornblende |
| 141 | Mg, MgP | 20,20 | very fine, in less altered rock |
| | | 21,22,21,20,20 | very fine, in altered rock |
| 171 | MaS | 24,24, | in silicified pillow margin |
| 217 | Ma | 25,24 | in less altered flow near sample 171 |
| 255 | Fd | 24,28,30,29,29, 24,26,25 | 1 mm-width plagioclase vein, grains up to 0.5 mm diam., twinned |
| | | 26,25 | fine grained, in plagioclase-quartz border to vein |
| | | 25,24,24 | in less altered rock |
| 270 | Fa | 4,2,3 | very fine, in less altered rock |
| | | 3,3,4 | very fine, in silicified rock |
| 282 | Mi | 23,25 | fine grained, twinned |
| | | 25,21 | plagioclase phenocryst |
| 284 | MfS | 25,27,26,26,24,27 | fine grained |
| | | 27,26,24,23,23,23 | phenocryst |
| | | 25,21 | fine grained |
| 298 | MiS | 36,28,36,29,31 | fine, polygonal, zoned plagioclase insilicic 'halo' aroundhornblende aggregate |
| | | 32,37,37 | fine, polygonal, some zoned |
| 307 | MeP | 34,36 | twinned phenocryst in plagioclase-quartz border to fracture, with clinozoisite |
| | | 40,37,39 | fine grained in altered border to fracture with clinozoisite |
| 308 | MeP | 40,40,39,32,40, 38,39,40,38 | fine grained, in plagioclase-quartz border to a fracture, with clinozoisite |

**Table 7**

**Representative analyses of amphiboles**

| Sample Code | 014 Mg | 186 MfG | 217 Ma | 262 Mf | 280 MiE | 282 Mi | 282 Mi |
|---|---|---|---|---|---|---|---|
| $SiO_2$ (%) | 41.64 | 41.10 | 41.31 | 43.37 | 53.89 | 52.86 | 50.30 |
| $Al_2O_3$ | 17.84 | 15.04 | 16.46 | 14.32 | 2.86 | 4.07 | 7.94 |
| FeOT[a] | 17.76 | 18.22 | 19.67 | 12.64 | 10.23 | 14.15 | 14.98 |
| MgO | 7.36 | 7.28 | 7.21 | 12.29 | 17.50 | 15.64 | 14.60 |
| CaO | 11.49 | 11.24 | 11.12 | 12.31 | 12.97 | 8.51 | 10.16 |
| $Na_2O$ | 1.46 | 1.84 | 1.58 | 1.66 | 0.25 | 0.85 | 1.01 |
| $K_2O$ | 0.16 | 0.27 | 0.32 | 0.28 | 0.08 | 0.11 | 0.18 |
| $TiO_2$ | 0.28 | 0.41 | 0.36 | 0.24 | 0.06 | 0.10 | 0.20 |
| MnO | 0.30 | 0.16 | 0.31 | 0.25 | 0.34 | 0.28 | 0.26 |
| TOTAL | 98.29 | 95.55 | 98.35 | 97.45 | 98.17 | 98.57 | 99.63 |

Notes: [a] total iron calulated as FeO

014 = ferro - tschermakite
217 = ferroan pargasitic hornblende
186 = ferroan pargasite
262 = ferroan pargasitic hornblende
280 = tremolite - actinolite
282 (first column) = actinolite
282 (second column) = magnesio-hornblende
(classified after Leake, 1978)

Table 8

**Representative analyses of chlorite and garnet**

| Sample Code | chlorite 186 MfG | chlorite 270 Fa | chlorite 285 MfG | garnet 186 MfG | garnet 285 MfG | garnet 285 MfG |
|---|---|---|---|---|---|---|
| $SiO_2$ (%) | 23.79 | 23.54 | 23.05 | 36.96 | 36.79 | 36.77 |
| $Al_2O_3$ | 21.27 | 23.71 | 22.95 | 20.88 | 21.19 | 21.41 |
| FeOT[a] | 25.77 | 27.27 | 30.34 | 34.99 | 36.62 | 29.99 |
| MgO | 14.04 | 12.29 | 10.69 | 2.48 | 1.20 | 0.48 |
| CaO | 0.02 | 0.05 | 0.01 | 3.46 | 3.79 | 5.74 |
| $Na_2O$ | 0.00 | 0.03 | 0.00 | 0.00 | 0.01 | 0.04 |
| $K_2O$ | 0.00 | 0.02 | 0.00 | 0.00 | 0.00 | 0.00 |
| $TiO_2$ | 0.03 | 0.05 | 0.05 | 0.05 | 0.06 | 0.09 |
| MnO | 0.12 | 0.51 | 0.06 | 0.58 | 0.35 | 6.40 |
| TOTAL | 85.03 | 87.47 | 87.14 | 99.41 | 100.00 | 100.91 |

Note: [a] total iron calculated as FeO
Chlorites in samples 186, 270 and 285 are repidolite (classified after Hey, 1954).
Garnets in samples 186 and 285 are almandine (classified after Deer et al., 1966).

Table 9

**Representative analyses of epidote-group minerals**

| Sample Code | 013 MbE | 174 MaE | 280 MiE |
|---|---|---|---|
| $SiO_2$ (%) | 38.60 | 37.66 | 39.49 |
| $Al_2O_3$ | 29.15 | 23.93 | 29.99 |
| FeT[a] | 5.85 | 12.33 | 5.61 |
| MgO | 0.06 | 0.03 | 0.05 |
| CaO | 23.73 | 23.09 | 24.14 |
| MnO | 0.08 | 0.04 | 0.08 |
| TOTAL | 97.47 | 97.07 | 98.80 |

Note: [a] total iron calculated as $Fe_2O_3$
Epidote mineral in sample:
013 = $Cz_{89}$; 174 = $Cz_{75}$; 280 = $Cz_{89}$.

# APPENDIX 3

# WHOLE ROCK MAJOR AND TRACE ELEMENT COMPOSITIONS

Table 10

Whole rock major and trace element compositions

Felsic rocks

| | Volcaniclastic rocks (Fa) | | | | | | | Quartz-plagioclase porphyry (Fb) | | | Fine quartz-phyric dykes (Fc) | | | |
|---|---|---|---|---|---|---|---|---|---|---|---|---|---|---|
| Analysis | 1 | 2 | 3 | 4 | 5 | 6 | 7 | 8 | 9 | 10 | 11 | 12 | 13 | 14 |
| Sample | 035 | 046 | 089 | 095 | 237 | 250 | 270 | 009 | 055 | 294 | 036 | 042 | 051 | 083 |
| $SiO_2$(%) | 69.82 | 73.23 | 77.56 | 71.55 | 65.46 | 68.21 | 73.28 | 75.8 | 75.52 | 79.04 | 74.67 | 68.72 | 74.27 | 75.1 |
| $Al_2O_3$ | 13.36 | 11.87 | 12.58 | 13.58 | 14.49 | 16.64 | 12.45 | 11.40 | 1.49 | 10.97 | 11.40 | 11.50 | 12.46 | 12.40 |
| $Fe_2O_3T$ | 5.89 | 2.20 | 1.35 | 4.56 | 8.32 | 4.43 | 6.07 | 3.29 | 3.24 | 0.62 | 3.58 | 4.46 | 5.00 | 4.25 |
| FeO | 4.2 | 1.4 | 0.9 | 3.4 | | 3.2 | 3.5 | 2.3 | 1.6 | 0.2 | 2.0 | 2.7 | 3.6 | 2.8 |
| $Fe_2O_3$ | 1.2 | .6 | .4 | .8 | | .9 | 2.2 | 0.7 | 1.5 | .4 | 1.4 | 1.5 | 1.0 | 1.2 |
| MgO | 1.97 | 1.38 | 0.47 | 1.98 | 1.43 | 1.58 | 1.68 | 0.88 | 0.48 | 0.77 | 1.43 | 0.48 | 0.47 | 0.59 |
| CaO | 3.89 | 1.39 | 3.15 | 1.88 | 5.99 | 5.75 | 0.60 | 1.02 | 1.86 | 1.32 | 5.13 | 1.91 | 1.78 | 2.18 |
| $Na_2O$ | 3.85 | 2.92 | 3.50 | 5.96 | 1.77 | 1.85 | 5.08 | 3.82 | 4.33 | 5.20 | 2.67 | 3.79 | 4.00 | 3.55 |
| $K_2O$ | 0.68 | 2.24 | 0.80 | 0.40 | 1.72 | 0.77 | 0.49 | 2.13 | 0.89 | 0.52 | 0.16 | 1.21 | 1.39 | 1.71 |
| $TiO_2$ | 0.26 | 0.15 | 0.14 | 0.15 | 0.45 | 0.25 | 0.17 | 0.14 | 0.18 | 0.15 | 0.20 | 0.21 | 0.24 | 0.21 |
| $P_2O_5$ | 0.01 | 0.0 | 0.0 | 0.04 | 0.08 | 0.03 | 0.07 | 0.04 | 0.02 | 0.00 | 0.0 | 0.01 | 0.03 | 0.0 |
| MnO | 0.09 | 0.03 | 0.05 | 0.10 | 0.16 | 0.07 | 0.11 | 0.02 | 0.04 | 0.05 | 0.05 | 0.05 | 0.15 | 0.07 |
| $H_2O$ | 0.7 | 0.9 | 0.5 | 0.4 | | 0.6 | 1.1 | 0.6 | 0.8 | 0.3 | 0.4 | 1.0 | 0.6 | 0.5 |
| S | 0.0 | 0.0 | 0.01 | 0.0 | 0.0 | 0.0 | 0.02 | 0.09 | 0.0 | 0.0 | 0.01 | 0.03 | 0.05 | 0.01 |
| $CO_2$ | 0.17 | 0.54 | 0.27 | <0.01 | | <0.01 | <0.01 | 0.8 | 1.02 | 0.88 | 0.01 | 0.87 | 0.05 | 0.03 |
| Ba (ppm) | 116 | 186 | 163 | 70 | 729 | 113 | 130 | 200 | 210 | 101 | 70 | 248 | 609 | 478 |
| Cr | 23 | 18 | 26 | 26 | 3 | 31 | 23 | 140 | 17 | 21 | 14 | 8 | 2 | 16 |
| Zr | 22 | 41 | 45 | 59 | 116 | 18 | 98 | 140 | 89 | 93 | 120 | 128 | 128 | 109 |
| Sr | 193 | 123 | 134 | 171 | 292 | 287 | 65 | 120 | 177 | 92 | 121 | 190 | 148 | 134 |
| Rb | 3 | 28 | 4 | 0 | 24 | 7 | 0 | 32 | 6 | 0 | 0 | 8 | 22 | 33 |
| Y | 19 | 8 | 22 | 22 | 31 | 11 | 28 | 37 | 34 | 29 | 36 | 36 | 38 | 35 |
| Nb | 2 | 0 | 1 | 0 | 11 | 0 | 0 | 10 | 4 | 7 | 7 | 10 | 7 | 5 |
| Zn | 56 | 55 | 29 | 55 | 170 | 63 | 60 | 39 | 42 | 24 | 39 | 78 | 150 | 91 |
| Cu | 5.5 | 1.5 | 210 | 5.5 | | 8.5 | 9 | 8 | 2 | 1 | 2.5 | 16 | 18 | 3 |
| Ni | 4 | 10 | 0 | 0 | 21 | 16 | 0 | 33 | 9 | 0 | 0 | 5 | 0 | 0 |
| Pb | <2 | 2 | 4 | <2 | | <2 | <2 | 3 | 2 | <2 | 4 | 4 | 6 | 7 |
| V | 54 | 4 | 4 | 5 | 105 | 81 | 20 | 13 | 0 | 11 | 0 | 0 | 0 | 18 |
| TOTAL | 100.22 | 96.69 | 100.28 | 100.23 | 100.04 | 99.82 | 100.73 | 99.9 | 99.69 | 99.76 | 99.49 | 93.94 | 100.09 | 100.1 |
| Density | 2.76 | 2.69 | 2.68 | 2.73 | | 2.76 | 2.73 | 2.64 | 2.69 | 2.64 | 2.73 | 2.66 | 2.72 | 2. |

Table 10 (cont.)

**Felsic rocks**

| | Aphyric intrusions (Fd) | | | | | | Plagioclase - phyric intrusions (Fd) | | | | | | |
|---|---|---|---|---|---|---|---|---|---|---|---|---|---|
| Analysis | 16 | 17 | 18 | 19 | 20 | 21 | 22 | 23 | 24 | 25 | 26 | 27 | 28 |
| Sample | 00511 | 119 | 123 | 155 | 160 | 255 | 002 | 0031 | 010 | 020 | 094 | 115 | 116 |
| $SiO_2$ (%) | 66.5 | 67.11 | 65.98 | 67.65 | 67.86 | 72.74 | 69.1 | 69.5 | 70.6 | 68.9 | 69.42 | 68.44 | 68.15 |
| $Al_2O_3$ | 12.4 | 13.84 | 13.07 | 13.90 | 13.23 | 12.51 | 12.9 | 11.6 | 12.6 | 14.2 | 13.71 | 13.04 | 13.93 |
| $Fe_2O_3T$ | 10.4 | 9.18 | 9.77 | 5.80 | 8.52 | 6.43 | 6.97 | 9.24 | 5.79 | 7.19 | 6.42 | 9.16 | 6.18 |
| FeO | 7.6 | 4.1 | 6.5 | 3.9 | 6.3 | 4.4 | 4.8 | 6.2 | 4.6 | 5.2 | 4.2 | 4.6 | 2.9 |
| $Fe_2O_3$ | 2.0 | 4.6 | 2.5 | 1.5 | 1.5 | 1.5 | 1.6 | 2.4 | 0.7 | 2.1 | 1.8 | 4.0 | 3.0 |
| MgO | 1.44 | 1.35 | 1.55 | 2.19 | 1.71 | 1.08 | 1.05 | 1.42 | 1.10 | 0.93 | 1.28 | 1.11 | 1.19 |
| CaO | 5.15 | 4.13 | 4.68 | 4.31 | 2.96 | 2.65 | 5.70 | 4.43 | 3.42 | 5.43 | 5.13 | 3.96 | 5.33 |
| $Na_2O$ | 2.67 | 3.26 | 3.05 | 5.55 | 2.00 | 2.99 | 2.94 | 2.86 | 4.49 | 3.18 | 3.97 | 3.03 | 4.67 |
| $K_2O$ | 0.62 | 0.51 | 0.96 | 0.17 | 2.42 | 0.93 | 0.55 | 0.54 | 0.44 | 0.54 | 0.21 | 0.81 | 0.22 |
| $TiO_2$ | 0.55 | 0.63 | 0.60 | 0.71 | 0.53 | 0.42 | 0.62 | 0.62 | 0.51 | 0.42 | 0.62 | 0.40 | 0.62 |
| $P_2O_5$ | 0.19 | 0.12 | 0.16 | 0.21 | 0.12 | 0.08 | 0.22 | 0.22 | 0.14 | 0.10 | 0.21 | 0.0 | 0.06 |
| MnO | 0.14 | 0.12 | 0.16 | 0.10 | 0.09 | 0.10 | 0.10 | 0.13 | 0.06 | 0.13 | 0.09 | 0.26 | 0.09 |
| $H_2O$ | 0.7 | 0.7 | 0.9 | 0.4 | 0.8 | 0.4 | 0.6 | 0.6 | 0.4 | 0.5 | 0.4 | 0.4 | 0.2 |
| S | 0.05 | 0.0 | 0.0 | 0.0 | 0.0 | 0.0 | 0.03 | 0.0 | 0.02 | 0.2 | 0.0 | 0.0 | 0.0 |
| $CO_2$ | 0.0 | <0.01 | <0.01 | 0.08 | 0.28 | <0.01 | 0.2 | 0.1 | 0.1 | 0.1 | 0.01 | <0.01 | 0.01 |
| Ba (%) | 200 | 117 | 585 | 91 | 654 | 187 | 200 | 200 | 30 | 100 | 52 | 508 | 111 |
| Cr | 78 | 20 | 11 | 25 | 22 | 7 | 100 | 87 | 150 | 92 | 12 | 19 | 21 |
| Zr | 120 | 107 | 100 | 103 | 112 | 113 | 120 | 130 | 130 | 170 | 111 | 158 | 109 |
| Sr | 210 | 282 | 212 | 157 | 114 | 138 | 360 | 210 | 120 | 190 | 283 | 195 | 122 |
| Rb | 12 | 0 | 12 | 0 | 38 | 10 | 8 | 8 | 5 | 5 | 0 | 9 | 0 |
| Y | 31 | 40 | 36 | 33 | 35 | 30 | 39 | 31 | 30 | 34 | 30 | 22 | 31 |
| Nb | 11 | 6 | 9 | 6 | 9 | 8 | 7 | 8 | 10 | 11 | 6 | 6 | 6 |
| Zn | 74 | 55 | 107 | 35 | 78 | 57 | 44 | 55 | 34 | 76 | 39 | 34 | 32 |
| Cu | 260 | 25 | 94 | 9 | 1.5 | 1 | 400 | 9 | 11 | 81 | 5.5 | 32 | 19 |
| Ni | 27 | 4 | 0 | 6 | 0 | 0 | 27 | 25 | 20 | 21 | 0 | 0 | 0 |
| Pb | 0 | 2 | <2 | <2 | 6 | <2 | 2 | 1 | 1 | 1 | 2 | <2 | 2 |
| V | 29 | 7 | 0 | 0 | 6 | 0 | 28 | 27 | 22 | 22 | 0 | 6 | 2 |
| TOTAL | 100.0 | 100.50 | 100.17 | 100.04 | 99.82 | 99.84 | 100.5 | 100.6 | 99.2 | 101.8 | 101.0 | 100.11 | 100.33 |
| Density | 2.90 | 2.79 | 2.85 | 2.76 | 2.78 | 2.76 | 2.82 | | 2.64 | 2.79 | 2.79 | 2.81 | 2.74 |

Table 10 (cont.)

Felsic rocks (cont.)

| | Plagioclase-phyric intrusions (cont.) | | | | | Silic[d] | Epidotized | | | | Gt-chl→ | Pl- | Bt → | |
|---|---|---|---|---|---|---|---|---|---|---|---|---|---|---|
| Analysis | Fd 29 | Fd 30 | Fd 31 | Fd 32 | Fd 33 | FaS 34 | FbE 35 | FdE 36 | FdE 37 | FdE 38 | FbC 39 | FdC 40 | FdP 41 | FaR 42 |
| Sample | 134 | 138 | 146 | 161 | 254 | 271 | 006 | 00311 | 01811 | 109 | 293 | 115 | 140 | 091 |
| $SiO_2$(Z) | 60.34 | 68.15 | 66.38 | 72.79 | 74.89 | 83.22 | 79.0 | 53.3 | 71.2 | 69.28 | 47.20 | 68.90 | 74.05 | 70.39 |
| $Al_2O_3$ | 12.91 | 14.01 | 12.78 | 12.84 | 12.82 | 9.10 | 9.7 | 19.0 | 12.5 | 10.22 | 18.62 | 11.25 | 13.46 | 13.42 |
| $Fe_2O_3T$ | 12.10 | 5.91 | 4.02 | 2.53 | 2.95 | 1.18 | 2.89 | 7.71 | 4.16 | 6.73 | 25.99 | 13.27 | 1.82 | 5.63 |
| FeO | 4.8 | 3.7 | 2.5 | 1.5 | 1.9 | 0.4 | 2.4 | 1.2 | 0.5 | 2.4 | 16.2 | 6.3 | 1.0 | 4.2 |
| $Fe_2O_3$ | 6.8 | 1.8 | 1.2 | .9 | .8 | 0.7 | 0.2 | 6.4 | 3.6 | 4.1 | 8.0 | 6.3 | 0.71 | 1.0 |
| MgO | 1.33 | 1.86 | 1.27 | 2.14 | 0.67 | 0.27 | 0.41 | 0.51 | 0.15 | 1.69 | 4.03 | 1.32 | 0.70 | 1.11 |
| CaO | 3.21 | 4.43 | 5.27 | 2.34 | 2.75 | 0.41 | 2.84 | 16.5 | 11.7 | 9.62 | 0.77 | 2.19 | 3.35 | 2.61 |
| $Na_2O$ | 3.35 | 4.67 | 5.37 | 5.42 | 3.50 | 4.88 | 2.99 | 0.51 | 0.09 | 0.01 | 1.32 | 2.09 | 4.65 | 3.33 |
| $K_2O$ | 0.47 | 0.35 | 0.23 | 0.80 | 1.05 | 0.27 | 0.33 | 0.32 | 0.09 | 0.11 | 1.45 | 0.38 | 0.56 | 2.19 |
| $TiO_2$ | 0.60 | 0.63 | 0.57 | 0.50 | 0.42 | 0.13 | 0.18 | 0.58 | 0.31 | 0.51 | 0.16 | 0.36 | 0.61 | 0.23 |
| $P_2O_5$ | 0.09 | 0.18 | 0.06 | 0.11 | 0.12 | 0.03 | 0.06 | 0.20 | 0.07 | 0.00 | 0.01 | 0.00 | 0.11 | 0.03 |
| MnO | 0.08 | 0.11 | 0.07 | 0.05 | 0.06 | 0.01 | 0.05 | 0.11 | 0.12 | 0.11 | 0.36 | 0.09 | 0.05 | 0.07 |
| $H_2O$ | 0.9 | 0.5 | 0.3 | 0.3 | 0.6 | 0.2 | 0.3 | 1.5 | 0.7 | 0.8 | 3.5 | 1.1 | 0.3 | 0.8 |
| S | 0.0 | 0.0 | 0.0 | 0.00 | 0.00 | 0.00 | 0.03 | 0.0 | 0.0 | 0.0 | 0.01 | 0.00 | 0.0 | 0.01 |
| $CO_2$ | 0.01 | 0.01 | 1.68 | 0.24 | 0.27 | 0.05 | 0.1 | 0.1 | 0.1 | <0.01 | 0.01 | 0.01 | 0.08 | 0.33 |
| Ba (ppm) | 157 | 105 | 94 | 298 | 245 | 65 | 40 | 70 | 10 | 77 | 254 | 93 | 107 | 328 |
| Cr | 19 | 16 | 13 | 17 | 7 | 21 | 170 | 150 | 150 | 21 | 39 | 15 | 14 | 33 |
| Zr | 96 | 103 | 100 | 111 | 117 | 74 | 97 | 100 | 140 | 82 | 96 | 143 | 104 | 75 |
| Sr | 167 | 257 | 146 | 139 | 252 | 52 | 140 | 1200 | 200 | 323 | 36 | 279 | 284 | 107 |
| Rb | 0 | 0 | 0 | 10 | 11 | 0 | 2 | 3 | 2 | 0 | 11 | 3 | 0 | 20 |
| Y | 23 | 38 | 43 | 37 | 32 | 20 | 23 | 46 | 26 | 30 | 26 | 31 | 26 | 56 |
| Nb | 8 | 7 | 3 | 7 | 10 | 0 | 6 | 14 | 10 | 6 | 4 | 0 | 9 | 7 |
| Zn | 38 | 66 | 35 | 36 | 47 | 41 | 19 | 18 | 17 | 86 | 83 | 91 | 27 | 77 |
| Cu | 10 | 2 | 2.5 | 1.5 | 0.5 | 1 | 28 | 10 | 14 | 43 | 1.5 | 58 | 2.5 | 14 |
| Ni | 0 | 0 | 0 | 0 | 0 | 0 | 14 | 29 | 19 | 0 | 0 | 0 | 2 | 0 |
| Pb | <2 | <2 | <2 | 10 | <2 | <2 | 2 | 3 | 0 | <2 | <2 | <2 | 4 | <2 |
| V | 0 | 0 | 5 | 0 | 0 | 7 | 13 | 31 | 17 | 17 | 11 | 0 | 0 | 43 |
| TOTAL | 94.86 | 100.40 | 97.72 | 99.89 | 99.89 | 99.71 | 98.6 | 100.2 | 101.2 | 98.93 | 101.63 | 100.26 | 99.63 | 100.01 |
| Density | 2.80 | 2.79 | 2.72 | 2.70 | 2.68 | 2.64 | 2.67 | | | 2.91 | 3.11 | 2.88 | 2.69 | 2.71 |

Table 10 (cont.)

**Aphyric mafic flows**

| | Less altered pillowed flows | | | | | | Silicified pillowed flows | | | | | | | |
|---|---|---|---|---|---|---|---|---|---|---|---|---|---|---|
| Analysis | Ma 43 | Ma 44 | Ma 45 | Ma 46 | Ma 47 | Ma 48 | Ma 49 | MaS 50 | Ma 51 | Ma 52 | Ma 53 | MaS 54 | MaS 55 | MaS 56 |
| Sample | 088C | 176C | 175V | 198V | 216M | 217M | 086C | 0841M | 0841IV | 173C | 173C | 172M | 171M | 200M |
| $SiO_2$(%) | 57.58 | 59.48 | 46.01 | 53.15 | 58.84 | 57.33 | 56.95 | 73.06 | 44.80 | 57.65 | 57.70 | 70.46 | 64.31 | 6..1 |
| $Al_2O_3$ | 14.41 | 14.62 | 16.72 | 15.21 | 13.71 | 13.85 | 14.88 | 11.77 | 18.13 | 15.87 | 15.94 | 11.97 | 12.88 | 14.1 |
| $Fe_2O_3T$ | 12.61 | 11.92 | 18.48 | 15.39 | 12.42 | 13.60 | 9.55 | 4.33 | 17.20 | 12.51 | 12.54 | 7.18 | 10.27 | 10.7 |
| FeO | 9.0 | 8.2 | 13.0 | 10.7 | 8.5 | 9.6 | 6.5 | 2.9 | 12.1 | 8.5 | | 4.8 | 7.5 | 8.2 |
| $Fe_2O_3$ | 2.7 | 2.8 | 4.0 | 3.5 | 3.0 | 2.9 | 2.3 | 1.1 | 3.8 | 3.1 | -1 | 1.9 | 1.9 | 1.6 |
| MgO | 4.13 | 3.16 | 5.59 | 5.10 | 4.64 | 4.91 | 3.04 | 1.46 | 6.03 | 2.37 | 2.44 | 1.79 | 2.87 | 2.7 |
| CaO | 7.83 | 7.15 | 9.68 | 7.14 | 7.08 | 6.49 | 8.54 | 4.63 | 7.27 | 7.25 | 7.28 | 3.26 | 3.24 | 4.5 |
| $Na_2O$ | 2.63 | 3.03 | 2.30 | 2.76 | 2.53 | 2.52 | 3.58 | 3.31 | 2.80 | 3.13 | 3.28 | 3.14 | 2.80 | 3.. |
| $K_2O$ | 0.27 | 0.25 | 0.52 | 0.68 | 0.27 | 0.69 | 0.83 | 0.63 | 2.69 | 0.30 | 0.30 | 0.48 | 0.88 | 1. |
| $TiO_2$ | 0.69 | 0.75 | 0.92 | 0.76 | 0.64 | 0.71 | 0.59 | 0.45 | 0.85 | 0.89 | 0.90 | 0.68 | 0.72 | 0.9 |
| $P_2O_5$ | 0.0 | 0.00 | 0.00 | 0.00 | 0.00 | 0.00 | 0.0 | 0.02 | 0.06 | 0.04 | 0.03 | 0.11 | 0.06 | 0.1 |
| MnO | 0.19 | 0.16 | 0.25 | 0.21 | 0.19 | 0.18 | 0.17 | 0.08 | 0.22 | 0.19 | 0.19 | 0.11 | 0.12 | 0.1 |
| $H_2O$ | 0.6 | 0.5 | 0.9 | 0.9 | 0.7 | 0.9 | 0.7 | 0.4 | 1.7 | 0.6 | -1 | 0.8 | 1.4 | 0.7 |
| S | 0.01 | 0.01 | 0.00 | 0.00 | 0.00 | 0.01 | 0.02 | 0.00 | 0.01 | 0.04 | 0.04 | 0.06 | 0.17 | 0.05 |
| $CO_2$ | 0.05 | <0.01 | 0.02 | 0.03 | <0.01 | 0.02 | 2.16 | 0.96 | 0.13 | <0.01 | -1 | <0.01 | 0.04 | <0.01 |
| Ba (ppm) | 82 | 98 | 105 | 140 | 96 | 220 | 365 | 223 | 1052 | 99 | 62 | 140 | 201 | 252 |
| Cr | 8 | 18 | 8 | 14 | 15 | 11 | 53 | 44 | 65 | 28 | 29 | 19 | 32 | 19 |
| Zr | 32 | 29 | 33 | 27 | 27 | 25 | 38 | 33 | 61 | 57 | 56 | 65 | 60 | 67 |
| Sr | 61 | 183 | 112 | 98 | 135 | 122 | 108 | 88 | 77 | 170 | 175 | 132 | 122 | 134 |
| Rb | 0 | 0 | 0 | 8 | 0 | 7 | 6 | 5 | 36 | 0 | 0 | 0 | 10 | 12 |
| Y | 16 | 14 | 19 | 18 | 13 | 13 | 17 | 16 | 26 | 22 | 23 | 24 | 21 | 24 |
| Nb | 0 | 3 | 0 | 0 | 0 | 1 | 0 | 1 | <0 | 0 | 0 | 1 | 2 | 2 |
| Zn | 121 | 92 | 161 | 235 | 116 | 132 | 104 | 56 | 167 | 135 | 134 | 137 | 235 | |
| Cu | 84 | 150 | 260 | 140 | 24 | 68 | 160 | 17 | 53 | 46 | -1 | 54 | 160 | |
| Ni | <2 | 0 | 3 | 0 | 0 | 0 | 17 | 3 | 29 | 0 | 0 | 0 | 13 | |
| Pb | <2 | 6 | 2 | <2 | 4 | 2 | 4 | 4 | <2 | <2 | -1 | 10 | 6 | 7 |
| V | 530 | 407 | 560 | 447 | 393 | 417 | 360 | 252 | 596 | 189 | 191 | 137 | 145 | 172 |
| TOTAL | 100.05 | 100.12 | 99.94 | 100.14 | 100.07 | 100.14 | 100.29 | 100.78 | 100.54 | 99.89 | 100.73 | 99.51 | 99.93 | 99.1 |
| Density | 2.98 | 2.92 | 3.09 | 3.02 | 2.96 | 2.98 | 2.87 | 2.75 | 3.03 | 2.96 | | 2.76 | 2.93 | |

**Table 10 (cont.)**

**Aphyric mafic flows (cont.)**

| | Silicified pillowed flows (cont.) | | | | | | | Epidotized pillows | | Massive flows | | | |
|---|---|---|---|---|---|---|---|---|---|---|---|---|---|
| Analysis | MaS 57 | MaS 58 | Ma 59 | Ma 60 | MaS 61 | MaS 62 | Ma 63 | MaE 64 | MaE 65 | Ma 66 | MaS 67 | MaT 68 | MaY 69 |
| Sample | 202M | 205M | 201V | 223C | 220M | 221M | 222V | 174 | 177 | 212 | 213 | 215 | 033 |
| $SiO_2$(%) | 66.34 | 63.91 | 48.22 | 53.26 | 60.29 | 61.28 | 45.85 | 54.91 | 52.16 | 44.24 | 67.38 | 60.01 | 55.27 |
| $Al_2O_3$ | 12.66 | 13.76 | 15.96 | 17.70 | 13.84 | 13.92 | 17.95 | 12.52 | 12.59 | 17.81 | 13.68 | 11.05 | 14.66 |
| $FE_2O_3T$ | 10.04 | 10.96 | 18.46 | 11.82 | 9.27 | 8.26 | 16.40 | 9.60 | 9.93 | 18.28 | 7.88 | 7.16 | 13.82 |
| FeO | 6.8 | 8.3 | 12.7 | 8.6 | 6.4 | 6.1 | 12.6 | 3.6 | 4.0 | 14.3 | | 2.2 | 10.2 |
| $Fe_2O_3$ | 2.5 | 1.7 | 4.3 | 2.3 | 2.2 | 1.5 | 2.4 | 5.6 | 5.5 | 2.4 | | 4.7 | 2.5 |
| MgO | 2.32 | 2.81 | 4.03 | 4.78 | 2.97 | 3.09 | 5.28 | 1.02 | 3.89 | 5.72 | 2.07 | 3.36 | 2.05 |
| CaO | 4.09 | 4.34 | 8.86 | 7.06 | 10.15 | 7.27 | 9.24 | 15.70 | 14.22 | 9.34 | 5.99 | 11.91 | 9.29 |
| $Na_2O$ | 2.73 | 3.04 | 2.35 | 3.70 | 1.29 | 2.05 | 2.96 | 0.03 | 0.10 | 2.55 | 2.78 | 0.09 | 1.31 |
| $K_2O$ | 1.12 | 0.23 | 0.30 | 0.67 | 0.22 | 0.84 | 0.33 | 0.05 | 0.08 | 0.34 | 0.17 | 0.11 | 0.79 |
| $TiO_2$ | 0.71 | 0.78 | 1.10 | 0.70 | 0.54 | 0.53 | 0.90 | 0.59 | 0.56 | 0.91 | 0.65 | 0.51 | 0.60 |
| $P_2O_5$ | 0.04 | 0.03 | 0.02 | 0.02 | 0.00 | 0.00 | 0.00 | 0.00 | 0.00 | 0.02 | 0.00 | 0.00 | 0.33 |
| MnO | 0.15 | 0.14 | 0.30 | 0.19 | 0.13 | 0.14 | 0.24 | 0.14 | 0.13 | 0.25 | 0.11 | 0.10 | 0.22 |
| $H_2O$ | 0.5 | 1.1 | 1.0 | 1.4 | 0.5 | 2.1 | 1.0 | 0.4 | 0.7 | 1.0 | | 0.7 | 1.0 |
| S | 0.01 | 0.06 | 0.01 | 0.00 | 0.00 | 0.06 | 0.15 | 0.06 | 0.02 | 0.21 | 0.00 | 0.01 | 0.05 |
| $CO_2$ | <0.01 | <0.01 | <0.01 | <0.01 | 1.19 | 0.47 | 0.01 | 3.26 | 4.06 | <0.01 | | 3.98 | 0.06 |
| Ba (ppm) | 223 | 57 | 66 | 141 | 85 | 131 | 104 | 51 | 49 | 120 | 18 | 70 | 377 |
| Cr | 19 | 27 | 27 | 60 | 55 | 52 | 375 | 16 | 14 | 81 | 2 | 18 | 14 |
| Zr | 43 | 48 | 65 | 55 | 44 | 45 | 75 | 45 | 25 | 69 | 24 | 22 | 49 |
| Sr | 113 | 143 | 81 | 164 | 88 | 171 | 171 | 448 | 218 | 150 | 196 | 224 | 371 |
| Rb | 14 | 0 | 0 | 5 | 0 | 0 | 0 | 0 | 0 | 0 | 0 | 0 | 6 |
| Y | 23 | 23 | 26 | 23 | 20 | 20 | 26 | 18 | 14 | 23 | 14 | 11 | 21 |
| Nb | 3 | 0 | 0 | 3 | 0 | 0 | 0 | 0 | 2 | 0 | 1 | 0 | 10 |
| Zn | 160 | 178 | 235 | 103 | 97 | 105 | 241 | 38 | 52 | 201 | 57 | 53 | 159 |
| Cu | 11 | 190 | 25 | 88 | 17 | 140 | 260 | 100 | 200 | 300 | | 140 | 150 |
| Ni | 0 | 0 | 0 | 14 | 0 | 22 | 37 | 0 | 0 | 33 | 2 | 0 | 0 |
| Pb | 2 | 6 | <2 | 6 | <2 | <2 | 2 | 10 | <2 | 4 | | 4 | 2 |
| V | 154 | 112 | 239 | 395 | 286 | 272 | 516 | 165 | 365 | 538 | 412 | 310 | 104 |
| TOTAL | 99.97 | 100.24 | 99.20 | 100.34 | 99.68 | 99.33 | 98.91 | 97.88 | 97.96 | 99.08 | 100.82 | 99.66 | 98.31 |
| Density | 2.84 | 2.85 | 3.20 | 2.91 | 2.92 | 2.83 | | 3.03 | 30.5 | 3.13 | | 2.97 | 3.03 |

Table 10 (cont.)

**Plagioclase-phyric mafic flows**

| | Less altered flows | | | | | | | | Silicified flows | | | | |
|---|---|---|---|---|---|---|---|---|---|---|---|---|---|
| Analysis # | Mb 70 | Mb 71 | Mb 72 | Mb 73 | Mb 74 | Mb 75 | Mb 76 | Mb 77 | Mb 78 | MbS 79 | MbS 80 | MbS 81 | Mb 82 |
| Sample | 001 | 0051 | 01711 | 102 | 105 | 012 | 016 | 142 | 124 | 0171 | 206M | 211M | 210V |
| $SiO_2$ (%) | 53.6 | 55.0 | 53.5 | 53.84 | 54.47 | 56.4 | 55.6 | 53.95 | 51.75 | 69.2 | 66.95 | 71.06 | 58.79 |
| $Al_2O_3$ | 16.2 | 15.4 | 14.0 | 16.44 | 15.69 | 15.5 | 17.6 | 16.31 | 15.04 | 8.67 | 14.11 | 12.82 | 14.07 |
| $Fe_2O_3T$ | 14.1 | 13.6 | 15.0 | 14.65 | 13.81 | 7.08 | 8.57 | 10.74 | 14.94 | 10.3 | 8.06 | 6.39 | 12.93 |
| FeO | 10.2 | 9.8 | 10.5 | 10.5 | 9.8 | 5.2 | 6.3 | 7.1 | 10.0 | 7.2 | 5.3 | 4.8 | 9.0 |
| $Fe_2O_3$ | 2.8 | 2.7 | 3.3 | 3.0 | 2.9 | 1.3 | 1.6 | 2.8 | 3.8 | 2.3 | 7.2 | 1.1 | 2.9 |
| MgO | 3.78 | 4.03 | 3.46 | 4.01 | 4.66 | 4.37 | 4.23 | 5.30 | 5.07 | 2.33 | 1.49 | 0.98 | 3.81 |
| CaO | 9.01 | 8.21 | 7.18 | 7.76 | 8.64 | 8.88 | 6.50 | 8.79 | 8.49 | 5.04 | 3.49 | 4.66 | 6.72 |
| $Na_2O$ | 3.20 | 2.56 | 3.37 | 3.53 | 3.11 | 5.05 | 5.49 | 4.08 | 3.87 | 2.00 | 4.05 | 3.29 | 2.59 |
| $K_2O$ | 0.47 | 0.79 | 0.32 | 0.39 | 0.36 | 0.37 | 0.77 | 0.29 | 0.39 | 0.22 | 1.00 | 0.23 | 0.60 |
| $TiO_2$ | 0.59 | 0.56 | 0.51 | 0.60 | 0.52 | 0.58 | 0.70 | 0.43 | 0.51 | 0.32 | 0.71 | 0.65 | 0.65 |
| $P_2O_5$ | 0.10 | 0.10 | 0.07 | 0.02 | 0.0 | 0.06 | 0.11 | 0.0 | 0.0 | 0.06 | 0.13 | 0.13 | 0.03 |
| MnO | 0.25 | 0.27 | 0.28 | 0.18 | 0.23 | 0.13 | 0.10 | 0.11 | 0.20 | 0.19 | 0.18 | 0.12 | 0.23 |
| $H_2O$ | 0.8 | 1.3 | 1.0 | 1.0 | 0.6 | 0.6 | 0.8 | 0.5 | 0.6 | 0.8 | 0.5 | 0.2 | 0.6 |
| S | 0.0 | 0.0 | 0.0 | 0.00 | 0.00 | <0.01 | 0.0 | 0.0 | 0.0 | 0.0 | 0.08 | 0.10 | 0.00 |
| $CO_2$ | 0.1 | 0.1 | 0.1 | <0.01 | 0.11 | 1.3 | 0.4 | <0.01 | <0.01 | 0.7 | <0.01 | <0.01 | <0.01 |
| Ba (ppm) | 200 | 300 | 70 | 81 | 130 | 40 | 200 | 105 | 104 | 50 | 163 | 138 | 120 |
| Cr | 49 | 62 | 71 | 24 | 36 | 66 | 62 | 42 | 60 | 120 | 31 | 27 | 33 |
| Zr | 25 | 25 | 23 | 26 | 24 | 29 | 32 | 6 | 14 | 17 | 57 | 56 | 53 |
| Sr | 260 | 220 | 240 | 158 | 137 | 190 | 230 | 173 | 197 | 130 | 121 | 169 | 105 |
| Rb | 4 | 8 | 2 | 0 | 0 | 2 | 15 | 0 | 0 | 2 | 20 | 0 | 3 |
| Y | 13 | 8 | 10 | 16 | 12 | 13 | 11 | 20 | 18 | 6 | 31 | 24 | 26 |
| Nb | 0 | 0 | 2 | 0 | 0 | 1 | 3 | 0 | 0 | 3 | 0 | 0 | 4 |
| Zn | 120 | 130 | 240 | 75 | 50 | 56 | 72 | 69 | 171 | 160 | 109 | 92 | 145 |
| Cu | 17 | 38 | 68 | 25 | <0.5 | 6 | 0 | 40 | <0.5 | 140 | 86 | 300 | 7 |
| Ni | 45 | 47 | 40 | 0 | 0 | 32 | 57 | 4 | 1 | 30 | 0 | 0 | 0 |
| Pb | 0 | 0 | 1 | <2 | <2 | 2 | 2 | 2 | <2 | 1 | 8 | 2 | <2 |
| V | 390 | 370 | 330 | 498 | 369 | 370 | 430 | 423 | 433 | 220 | 37 | 47 | 70 |
| TOTAL | 101.1 | 100.9 | 97.7 | 101.26 | 101.01 | 99.8 | 100.3 | 99.72 | 99.76 | 99.1 | 100.09 | 101.10 | 100.03 |
| Density | 3.00 | 3.01 | | 3.02 | 3.02 | 2.80 | 2.86 | 2.96 | 3.03 | | 2.77 | 2.78 | 2.97 |

Table 10 (Cont.)

| | Aphyric mafic flows (cont.) | | | | | | Mafic volcaniclastic rocks | | | | | | | |
|---|---|---|---|---|---|---|---|---|---|---|---|---|---|---|
| | Pervasive Epidotized flows | | | | Bt | Px-phyr flow | Pyroxene-phyric wacke | | | Plagioclase-phyric wacke & breccia | | | | |
| | MbE | MbE | MbE | MbE | MbB | Mc | Md | Md | Md | Me | Me | Me | Me | Me |
| Analysis | 83 | 84 | 85 | 86 | 87 | 88 | 89 | 90 | 91 | 92 | 93 | 94 | 95 | 96 |
| Sample | 013 | 0151 | 01511 | 104 | 016 | 063 | 062 | 064 | 151 | 248 | 256 | 305 | 3071 | 3081 |
| $SiO_2$ (%) | 53.0 | 50.0 | 50.1 | 55.44 | 66.98 | 49.16 | 53.24 | 53.28 | 57.21 | 53.21 | 49.98 | 51.16 | 52.79 | 54.07 |
| $Al_2O_3$ | 15.8 | 13.1 | 18.1 | 16.49 | 14.18 | 16.41 | 14.37 | 14.28 | 14.71 | 18.44 | 18.50 | 18.19 | 20.40 | 20.63 |
| $Fe_2O_3T$ | 7.20 | 8.94 | 6.28 | 6.60 | 5.83 | 12.88 | 14.06 | 14.15 | 11.22 | 12.20 | 13.90 | 11.33 | 5.88 | 4.95 |
| FeO | 2.3 | 5.4 | 1.4 | 4.0 | 4.3 | 9.2 | 10.5 | 10.2 | 8.0 | 9.0 | 10.2 | | | |
| $Fe_2O_3$ | 4.6 | 2.9 | 4.7 | 2.2 | 1.1 | 2.7 | 2.4 | 2.8 | 2.9 | 2.2 | 2.6 | | | |
| MgO | 3.86 | 5.50 | 1.80 | 4.64 | 3.54 | 6.42 | 5.82 | 6.36 | 4.14 | 4.63 | 4.49 | 6.07 | 5.56 | 5.89 |
| CaO | 16.5 | 15.7 | 20.1 | 9.46 | 2.25 | 10.00 | 8.48 | 7.75 | 7.45 | 8.70 | 8.06 | 8.45 | 8.97 | 6.55 |
| $Na_2O$ | 0.41 | 1.81 | 0.56 | 5.14 | 3.35 | 3.83 | 2.53 | 2.50 | 4.45 | 0.95 | 3.01 | 2.71 | 4.05 | 3.57 |
| $K_2O$ | 0.23 | 0.48 | 0.22 | 0.37 | 2.91 | .49 | 0.37 | 0.32 | 0.24 | 0.24 | 1.58 | 1.74 | 1.32 | 3.28 |
| $TiO_2$ | 0.50 | 0.52 | 0.52 | 0.63 | 0.47 | 0.38 | 0.66 | 0.62 | 0.69 | 0.32 | 0.46 | 0.43 | 0.39 | 0.52 |
| $P_2O_5$ | 0.08 | 0.09 | 0.10 | 0.00 | 0.0 | 0.0 | 0.19 | 0.20 | 0.16 | 0.00 | 0.00 | 0.00 | 0.00 | 0.02 |
| MnO | 0.13 | 0.15 | 0.11 | 0.09 | 0.06 | 0.12 | 0.21 | 0.23 | 0.15 | 0.25 | 0.20 | 0.15 | 0.09 | 0.09 |
| $H_2O$ | 1.4 | .13 | .12 | 0.6 | 0.8 | 0.7 | 0.7 | 0.6 | 0.6 | 1.2 | 0.9 | | | |
| S | 0.0 | 0.01 | 0.01 | 0.00 | 0.0 | 0.01 | 0.00 | 0.00 | 0.0 | 0.01 | 0.00 | 0.00 | 0.00 | 0.00 |
| $CO_2$ | 2.1 | 3.6 | 2.7 | 1.81 | <0.01 | 0.03 | 0.01 | <0.01 | 0.02 | 0.02 | 0.32 | | | |
| Ba (ppm) | 20 | 30 | 20 | 106 | 1077 | 152 | 93 | 166 | 0 | 247 | 241 | 261 | 705 | |
| Cr | 120 | 91 | 100 | 20 | 43 | 182 | 91 | 155 | 74 | 43 | 32 | 22 | 25 | 13 |
| Zr | 23 | 234 | 26 | 29 | 18 | 0 | 19 | 18 | 28 | 10 | 11 | 14 | 9 | 14 |
| Sr | 460 | 260 | 420 | 207 | 159 | 186 | 153 | 193 | 290 | 167 | 230 | 207 | 315 | 242 |
| Rb | 3 | 3 | 2 | 0 | 56 | 0 | 0 | 0 | 0 | 0 | 29 | 35 | 21 | 68 |
| Y | 14 | 13 | 12 | 20 | 9 | 14 | 17 | 19 | 20 | 9 | 8 | 9 | 12 | 13 |
| Nb | 2 | 1 | 1 | 1 | 0 | 0 | 0 | 0 | 3 | 0 | 0 | 0 | 0 | 0 |
| Zn | 33 | 67 | 28 | 0 | 92 | 63 | 85 | 61 | 49 | 94 | 98 | 47 | 38 | 125 |
| Cu | 2 | 3 | 1 | <0.5 | <0.5 | <0.5 | <0.5 | 4.5 | 1 | 9.0 | <0.5 | | | |
| Ni | 34 | 44 | 31 | 2 | 0 | 54 | 16 | 41 | 11 | 11 | 0 | 30 | 1 | 0 |
| Pb | 0 | 3 | 5 | <2 | <2 | <2 | <2 | <2 | <2 | <2 | <2 | | | |
| V | 350 | 460 | 330 | 381 | 325 | 371 | 263 | 247 | 150 | 219 | 387 | 340 | 398 | 485 |
| TOTAL | 101.0 | 100.7 | 101.7 | 100.83 | 99.90 | 99.41 | 99.47 | 99.31 | 100.15 | 9.16 | 100.26 | 100.37 | 99.59 | 99.78 |
| Density | 3.02 | | | 2.85 | 2.75 | 3.04 | 3.02 | 3.00 | 2.94 | 2.94 | 2.98 | | | |

Table 10 (Cont.)

Mafic volcaniclastic rocks (Cont.)

| | Other wacke, incl. mixed maf + fel | | | Silicified | | | Ep | Gt-chl | | | Garnet-biotite alteration | | | |
|---|---|---|---|---|---|---|---|---|---|---|---|---|---|---|
| | Mf | Mf | Mf | MeS | MfS | MfS | MeE | MfG | MfG | MfG | MfB | MfB | MfB | MfB |
| Analysis | 97 | 98 | 99 | 10 | 101 | 102 | 103 | 104 | 105 | 106 | 107 | 108 | 109 | 110 |
| Sample | 258 | 262 | 283 | 306 | 257 | 284 | 073 | 186 | 229 | 235 | 196 | 245 | 246 | 247 |
| $SiO_2$ (%) | 68.11 | 54.17 | 56.23 | 55.86 | 65.77 | 66.41 | 55.48 | 51.86 | 68.47 | 61.14 | 64.25 | 66.63 | 55.38 | 60.25 |
| $Al_2O_3$ | 13.84 | 17.80 | 18.86 | 18.44 | 13.88 | 17.91 | 16.69 | 15.21 | 12.15 | 13.08 | 13.14 | 13.26 | 15.22 | 16.29 |
| $Fe_2O_3T$ | 6.02 | 6.58 | 10.55 | 7.91 | 8.85 | 2.28 | 4.16 | 21.68 | 14.15 | 18.19 | 15.53 | 11.65 | 18.61 | 14.46 |
| FeO | 4.1 | 4.5 | 7.2 | | 6.2 | 1.5 | 2.4 | 16.3 | 10.1 | 12.5 | 9.3 | 7.7 | 13.6 | 10.7 |
| $Fe_2O_3$ | 1.5 | 1.6 | 2.6 | | 2.0 | 0.6 | 1.5 | 3.6 | 2.9 | 4.2 | 5.2 | 3.1 | 3.5 | 2.6 |
| MgO | 2.43 | 7.11 | 4.16 | 4.26 | 2.71 | 2.26 | 4.98 | 6.28 | 1.41 | 3.49 | 2.60 | 3.78 | 3.52 | 2.55 |
| CaO | 3.47 | 8.24 | 2.59 | 8.31 | 4.11 | 2.79 | 10.25 | 1.86 | 1.11 | 0.96 | 2.06 | 0.32 | 2.82 | 2.29 |
| $Na_2O$ | 3.41 | 4.08 | 4.29 | 3.53 | 3.07 | 5.23 | 5.31 | 0.77 | 2.05 | 0.00 | 1.22 | 0.01 | 1.25 | 2.77 |
| $K_2O$ | 1.52 | 1.31 | 1.51 | 0.88 | 1.18 | 2.20 | 0.28 | 0.71 | 1.14 | 1.40 | 1.24 | 2.25 | 1.03 | 1.61 |
| $TiO_2$ | 0.42 | 0.54 | 0.40 | 0.45 | 0.39 | 0.41 | 0.31 | 0.37 | 0.31 | 0.59 | 0.37 | 0.40 | 0.96 | 0.35 |
| $P_2O_5$ | 0.16 | 0.00 | 0.06 | 0.00 | 0.11 | 0.04 | 0.0 | 0.04 | 0.12 | 0.39 | 0.11 | 0.08 | 0.88 | 0.07 |
| MnO | 0.07 | 0.10 | 0.17 | 0.14 | 0.14 | 0.06 | 0.08 | 0.48 | 0.19 | 0.57 | 0.24 | 0.07 | 0.37 | 0.21 |
| $H_2O$ | 0.7 | 0.6 | 2.6 | | 0.6 | 0.6 | 0.4 | 3.1 | 0.9 | 1.7 | 0.8 | 1.7 | 1.9 | 0.7 |
| S | 0.00 | 0.00 | 0.00 | 0.00 | 0.00 | 0.00 | 0.00 | 0.00 | 0.00 | 0.00 | 0.00 | 0.00 | 0.00 | 0.00 |
| $CO_2$ | 0.13 | 0.05 | 0.01 | | <0.01 | 0.11 | 1.3 | <0.01 | 0.02 | 0.03 | <0.01 | 0.04 | 0.07 | <0.01 |
| Ba (ppm) | 380 | 245 | 181 | 178 | 254 | 301 | 143 | 161 | 447 | 913 | 517 | 287 | 318 | 431 |
| Cr | 31 | 14 | 36 | 21 | 28 | 30 | 58 | 83 | 30 | 107 | 43 | 13 | 20 | 39 |
| Zr | 49 | 12 | 16 | 48 | 37 | 16 | 0 | 18 | 50 | 44 | 34 | 134 | 84 | 33 |
| Sr | 143 | 241 | 152 | 276 | 197 | 87 | 239 | 58 | 32 | 6 | 52 | 8 | 71 | 107 |
| Rb | 18 | 22 | 18 | 8 | 25 | 31 | 0 | 6 | 19 | 9 | 16 | 41 | 17 | 24 |
| Y | 29 | 22 | 16 | 24 | 20 | 11 | 16 | 12 | 19 | 20 | 21 | 26 | 37 | 16 |
| Nb | 0 | 0 | 0 | 5 | 0 | 0 | 0 | 0 | 0 | 0 | 0 | 9 | 11 | 3 |
| Zn | 50 | 97 | 78 | 56 | 82 | 31 | 46 | 198 | 89 | 339 | 61 | 121 | 63 | 116 |
| Cu | 1.5 | 0.5 | 0.5 | | 1.5 | 0.5 | <0.5 | 11 | 1.5 | 7.5 | 0.5 | 1.5 | 1.5 | 0.5 |
| Ni | 0 | 0 | 0 | 3 | 0 | 0 | 9 | 3 | 0 | 0 | 0 | 0 | 0 | 0 |
| Pb | <2 | <2 | 4 | | <2 | 6 | 2 | <2 | <2 | <2 | 10 | <2 | <2 | <2 |
| V | 38 | 537 | 272 | 187 | 103 | 254 | 257 | 271 | 6 | 37 | 77 | 16 | 30 | 129 |
| TOTAL | 99.82 | 100.08 | 100.63 | 99.88 | 100.12 | 100.13 | 98.97 | 100.55 | 100.30 | 100.07 | 100.53 | 99.33 | 100.45 | 100.1 |
| Density | 2.96 | 2.88 | 2.77 | | 2.84 | 2.70 | 2.92 | 3.06 | 2.92 | 3.06 | 3.02 | 2.88 | 3.05 | 2.9 |

Table 10 (Cont.)

| | Mafic volc rocks (Cont.) Plag-qtz borders to fractures | | | Mafic intrusions Fine grained dykes | | | | | | Gabbroic and plagioclase-ph intrusions | | | | |
|---|---|---|---|---|---|---|---|---|---|---|---|---|---|---|
| | MfP | MeP | MeP | Mg | Mg | Mg | Mg | Mg | Mg | Mh | Mh | Mh | Mh | Mh |
| Analysis | 111 | 112 | 113 | 114 | 115 | 116 | 117 | 118 | 119 | 120 | 121 | 122 | 123 | 124 |
| Sample | 263 | 30711 | 30811 | 014 | 093 | 122 | 132 | 1411 | 242 | 007 | 048 | 052 | 077 | 098 |
| $SiO_2$ (%) | 47.05 | 62.30 | 66.95 | 51.0 | 54.15 | 57.30 | 55.57 | 54.01 | 57.44 | 55.1 | 49.42 | 50.87 | 48.06 | 50.0 |
| $Al_2O_3$ | 19.92 | 21.99 | 19.58 | 15.7 | 14.22 | 13.42 | 13.89 | 14.36 | 13.55 | 15.5 | 17.11 | 16.67 | 21.04 | 16.9 |
| $Fe_2O_3T$ | 1.59 | 1.30 | 0.57 | 14.3 | 16.08 | 14.51 | 16.03 | 9.31 | 14.78 | 14.0 | 15.82 | 12.65 | 11.63 | 14.3 |
| FeO | 0.1 | | | 10.7 | 11.5 | 10.5 | 9.4 | 5.9 | 10.3 | 10.2 | 10.6 | 8.9 | 7.6 | 10.3 |
| $Fe_2O_3$ | 1.3 | | | 10.7 | 3.3 | 2.8 | 5.5 | 2.8 | 3.3 | 2.7 | 4.0 | 2.8 | 3.2 | 2.9 |
| MgO | 1.26 | 1.20 | 0.65 | 5.80 | 4.14 | 4.22 | 4.00 | 5.88 | 3.42 | 3.41 | 3.84 | 5.63 | 4.46 | 6.0 |
| CaO | 22.04 | 6.89 | 6.34 | 10.2 | 6.79 | 7.22 | 7.23 | 7.25 | 7.26 | 8.21 | 10.72 | 9.99 | 10.27 | 9.9 |
| $Na_2O$ | 0.16 | 5.30 | 4.60 | 2.14 | 3.12 | 1.90 | 2.37 | 4.39 | 1.91 | 3.16 | 2.23 | 1.48 | 3.00 | 2.5 |
| $K_2O$ | 0.16 | 1.08 | 0.76 | 0.18 | -.20 | 1.11 | 0.44 | 0.43 | 0.14 | 0.26 | 0.33 | 1.07 | 1.08 | 0.2 |
| $TiO_2$ | 0.44 | 0.44 | 0.52 | 0.14 | 0.88 | 0.46 | 0.68 | 0.47 | 0.91 | 0.57 | 0.58 | 0.38 | 0.41 | 0.3 |
| $P_2O_5$ | 0.00 | 0.00 | 0.00 | 0.05 | 0.93 | 0.0 | 0.0 | 0.0 | 0.53 | 0.11 | 0.07 | 0.0 | 0.06 | 0.0 |
| MnO | 0.06 | 0.02 | 0.01 | 0.22 | 0.18 | 0.27 | 0.17 | 0.13 | 0.24 | 0.23 | 0.16 | 0.21 | 0.19 | 0.1 |
| $H_2O$ | 0.6 | | | 1.0 | 1.4 | 1.0 | 0.7 | 0.8 | 0.5 | 0.8 | 0.7 | 1.1 | 1.1 | 0.7 |
| S | 0.00 | 0.00 | 0.00 | 0.02 | 0.00 | 0.0 | 0.0 | 0.0 | 0.01 | 0.0 | 0.05 | 0.01 | 0.01 | 0.00 |
| $CO_2$ | 5.4 | | | 0.1 | 0.01 | <0.01 | <0.01 | 0.01 | 0.06 | 0.1 | <0.01 | 0.54 | 0.13 | <0.01 |
| Ba (ppm) | 76 | 165 | 124 | 40 | 79 | 569 | 154 | 165 | 64 | 50 | 57 | 419 | 494 | 93 |
| Cr | 23 | 26 | 17 | 51 | 14 | 31 | 128 | 136 | 7 | 43 | 17 | 70 | 52 | 37 |
| Zr | 11 | 15 | 14 | 12 | 47 | 21 | 19 | 8 | 113 | 21 | 21 | 0 | 4 | 15 |
| Sr | 308 | 426 | 286 | 300 | 113 | 121 | 225 | 215 | 290 | 230 | 302 | 247 | 523 | 229 |
| Rb | 3 | 6 | 5 | 1 | 0 | 20 | 5 | 0 | 0 | 1 | 0 | 17 | 14 | 0 |
| Y | 12 | 7 | 9 | 7 | 65 | 16 | 21 | 44 | 25 | 6 | 12 | 11 | 14 | 11 |
| Nb | 0 | 2 | 2 | 1 | 10 | 0 | 0 | 0 | 5 | 0 | 8 | 4 | 5 | 0 |
| Zn | 11 | 19 | 29 | 98 | 100 | 126 | 72 | 68 | 139 | 100 | 67 | 109 | 94 | 92 |
| Cu | 2.5 | | 100 | 1 | 4.5 | 45 | 2 | 310 | 44 | 30 | 93 | 160 | 37 | 1.5 |
| Ni | 0 | 0 | 0 | 44 | 0 | 0 | 8 | 5 | 0 | 39 | 0 | 18 | 6 | 0 |
| Pb | <2 | | | 1 | <2 | <2 | <2 | <2 | <2 | 1 | 2 | 2 | 4 | <2 |
| V | 186 | 135 | 120 | 350 | 192 | 314 | 438 | 405 | 211 | 360 | 319 | 389 | 287 | 360 |
| TOTAL | 99.67 | 100.63 | 100.06 | 100.0 | 100.82 | 100.25 | 100.01 | 96.38 | 99.60 | 100.4 | 99.86 | 99.61 | 100.58 | 100.2 |
| Density | 3.04 | | | 3.07 | 3.01 | 2.99 | 2.95 | 2.95 | 3.04 | 2.96 | 3.11 | 3.03 | 2.99 | 3.08 |

Table 10 (cont.)

| | Clast | Px-phy | Pxen-ite | Mafic margin of zoned dykes | | Silicic core of zoned dykes | | | Epidotized | | Gt-chl | Pl qtz |
|---|---|---|---|---|---|---|---|---|---|---|---|---|
| | Mafic intrusions (Cont.) | | | | | | | | | | | |
| Analysis | 126 | 127 | 128 | 129 | 130 | 131 | 132 | 133 | 134 | 135 | 136 | 137 |
| Sample | 156 | 282 | 080 | 273 | 288 | 274 | 289 | 291 | 011 | 280 | 243 | 14111 |
| $SiO_2$ | 47.74 | 51.15 | 48.00 | 45.54 | 43.83 | 63.62 | 65.88 | 64.89 | 50.0 | 51.81 | 49.99 | 56.68 |
| $Al_2O_3$ | 23.15 | 15.04 | 10.24 | 19.23 | 16.67 | 16.42 | 12.59 | 14.50 | 15.5 | 15.0 | 114.27 | 19.96 |
| $Fe_2O_3T$ | 8.92 | 11.36 | 11.55 | 16.65 | 16.82 | 8.48 | 4.19 | 6.37 | 9.19 | 6.80 | 21.11 | 2.36 |
| FeO | 6.6 | 8.2 | 8.8 | 12.2 | 11.8 | 6.1 | 0.7 | 3.3 | 6.3 | 2.9 | 15.2 | 1.3 |
| $Fe_2O_3$ | 1.6 | 2.3 | 1.8 | 3.1 | 3.7 | 1.7 | 3.4 | 2.7 | 2.2 | 3.6 | 4.2 | 0.91 |
| MgO | 4.11 | 8.90 | 13.85 | 4.78 | 7.04 | 2.02 | 2.*7 | 1.64 | 8.42 | 6.37 | 6.46 | 0.90 |
| CaO | 12.79 | 8.18 | 12.56 | 9.88 | 10.95 | 4.02 | 10.74 | 9.65 | 14.1 | 15.16 | 4.57 | 4.75 |
| $Na_2O$ | 2.65 | 3.70 | 1.17 | 2.50 | 2.37 | 3.27 | 0.12 | 0.78 | 2.03 | 1.79 | 0.42 | 7.34 |
| $K_2O$ | 0.29 | 0.66 | 0.25 | 0.37 | 0.56 | 0.46 | 0.33 | 0.24 | 0.25 | 0.20 | 0.09 | 0.49 |
| $TiO_2$ | 0.26 | 0.49 | 0.32 | 0.57 | 0.96 | 0.52 | 0.47 | 0.57 | 0.38 | 0.48 | 0.98 | 0.68 |
| $P_2O_5$ | 0.0 | 0.00 | 0.0 | 0.14 | 0.40 | 0.33 | 0.17 | 0.21 | 0.04 | 0.00 | 0.65 | 0.0 |
| MnO | 0.16 | 0.13 | 0.22 | 0.26 | 0.23 | 0.13 | 0.05 | 0.08 | 0.15 | 0.13 | 0.46 | 0.09 |
| $H_2O$ | 0.7 | 1.0 | 0.8 | 1.1 | 1.0 | 1.3 | 0.9 | 0.4 | 1.0 | 0.8 | 3.0 | 0.2 |
| S | 0.0 | 0.00 | 0.00 | 0.00 | 0.01 | 0.01 | 0.00 | 0.00 | 0.0 | 0.00 | 0.00 | 0.0 |
| $CO_2$ | 0.61 | 0.02 | 1.27 | 0.03 | 0.03 | <0.01 | 1.36 | 0.01 | 0.1 | 1.19 | 0.04 | 0.02 |
| Ba | 102 | 102 | 78 | 80 | 68 | 107 | 91 | 116 | 70 | 69 | 49 | 144 |
| Cr | 52 | 256 | 525 | 49 | 17 | 18 | 7 | 9 | 190 | 275 | 12 | 92 |
| Zr | 0 | 18 | 0 | 51 | 45 | 122 | 87 | 112 | 6 | 20 | 109 | 13 |
| Sr | 494 | 159 | 127 | 127 | 86 | 199 | 231 | 290 | 230 | 273 | 10 | 461 |
| Rb | 0 | 4 | 0 | 0 | 0 | 0 | 1 | 0 | 2 | 0 | 0 | 0 |
| Y | 13 | 25 | 12 | 14 | 19 | 25 | 34 | 33 | 4 | 21 | 33 | 12 |
| Nb | 0 | 0 | 0 | 3 | 4 | 10 | 4 | 7 | 0 | 0 | 4 | 4 |
| Zn | 52 | 173 | 89 | 114 | 77 | 76 | 9 | 15 | 68 | 74 | 140 | 29 |
| Cu | 1 | 2 | 0.5 | 1 | 1 | 24 | 2 | 1.5 | 13 | 1 | 1.5 | 3.5 |
| Ni | 9 | 5 | 97 | 0 | 0 | 0 | 0 | 0 | 92 | 13 | 0 | 0 |
| Pb | 4 | 4 | <2 | 4 | <2 | 2 | <2 | <2 | 1 | 6 | <2 | 2 |
| V | 171 | 270 | 336 | 382 | 449 | 95 | 10 | 6 | 320 | 270 | 208 | 27 |
| TOTAL | 100.65 | 99.72 | 99.25 | 99.69 | 99.56 | 99.90 | 98.89 | 98.97 | 101.0 | 99.41 | 100.36 | 93.[illegible] |
| Density | 2.93 | 2.97 | 3.11 | 3.12 | 3.13 | 2.8 | 2.92 | 2.90 | 3.02 | 3.02 | 3.17 | 2.76 |

## Table 11

### Rare earth element abundances

| Code | MaS | MaS | Ma | MaE | Ma | Fa | FaS |
|---|---|---|---|---|---|---|---|
| Analysis | 55 | 54 | 52 | 64 | 48 | 7 | 34 |
| Sample | 171M | 172M | 173C | 174 | 217M | 270 | 271 |
| La | 4.0 (12.7)[a] | 3.9 (12.4) | 2.8 (8.9) | 4.5 (14.3) | 2.3 (7.3) | 11 (34.9) | 6.6 (21.0) |
| Ce | 9.3 (11.4) | 8.8 (10.8) | 7.4 (9.1) | 8.7 (10.7) | 5.4 (6.6) | 22 (27.1) | 14 (17.2) |
| Nd | 8.8 (14.7) | 8.1 (13.6) | 8.2 (13.7) | 12 (20.1) | 7.5 (12.6) | 14 (23.5) | 9.0 (15.1) |
| Sm | 2.1 (10.9) | 2.0 (10.4) | 2.0 (10.4) | 1.6 (8.3) | 1.4 (7.3) | 3.1 (16.1) | 2.0 (10.4) |
| Eu | 0.6 (8.3) | 0.6 (8.3) | 1.1 (15.2) | 0.7 (9.7) | 0.5 (6.9) | 0.5 (6.9) | 0.4 (5.5) |
| Gd | 2.9 (11.2) | 2.8 (10.8) | 3.0 (11.6) | 2.8 (10.8) | 2.0 (7.7) | 3.2 (12.4) | 2.1 (8.1) |
| Dy | 3.6 (11.1) | 3.5 (10.8) | 4.0 (12.3) | 3.1 (9.5) | 2.4 (7.4) | 3.9 (12.0) | 2.5 (7.7) |
| Yb | 1.9 (9.1) | 1.9 (9.1) | 2.4 (11.5) | 1.8 (8.7) | 1.4 (6.9) | 2.3 (11.1) | 1.8 (8.7) |

Note: [a] Figure in parentheses is the chondrite-normalized value, using the REE data of Taylor & Gorton (1977).
Samples 171, 172, 173 and 174 are from the same zoned pillow (shown in Figure 9).
Sample 217 is from a less altered flow close to the zoned pillow.
Sample 271 is the silicified equivalent of sample 270.

# APPENDIX 4

## SAMPLE PREPARATION AND ANALYTICAL PROCEDURES

### (1) Sample preparation for whole rock analysis

0.1-1 kg hand samples were trimmed of weathering rinds and large veins, crushed to -1/4 inch in a jaw crusher, and ground to powder in a tungsten carbide dish and puck 'shatterbox'. The sample was then homogenized by mixing on a paper sheet.

Fused pellets for XRF analysis were prepared in platinum crucibles from a mixture of 1.3 g of sample, 0.433 g of lithium carbonate and 3.9 g of lithium tetraborate.

Powder samples 001-020 were submitted to the Analytical Chemistry Section at the Geological Survey of Canada for ICP analysis. Data for major elements were obtained on 0.5 g of sample fused with lithium metaborate, dissolved in 5% $HNO_3$ and diluted to 250 ml. Trace element data were obtained on 1.0 g of sample (acid + fusion of residue) dissolved in 10% HCl and diluted to 100 ml; rare earth elements were determined on trace solution after XIO pre-concentration and separation of major elements using iron exchange resin.

### (2) Analysis

Samples 001-020 were analyzed for major and trace elements by ICP at the G.S.C., except for (a) Pb which was determined by Atomic Absorption analysis, (b) Nb, Rb, Sr Y and Zr which were determined by XRF (EDS) analysis, and (c) $H_2O$, $CO_2$, S and FeO which were determined by chemical methods. Rare earth element data for six samples was obtained by ICP at the G.S.C.

The remaining samples were analyzed by XRF at the University of Ottawa by Ron Hartree, using a Phillips PW10-80 X-ray fluorescence spectrometer with a rhodium tube. Splits of these samples were analyzed at X-Ray Assay Laboratories Limited, Dons Mills, for Cu and Pb by DCP, and for $H_2O$, $CO_2$ and FeO by chemical methods.

Standards used during XRF analysis were DRN, SY-2 and RGM. Standards sent to X-Ray Laboratories Limited were AGV-1, G-1 and W-1.

(a) **Precision and accuracy of XRF and ICP analysis**

The precision of XRF determinations at the University of Ottawa laboratory is given in Table 12, and ws checked in the present study by analysing several samples repeatedly (DR-N, SY-2, and RGM). The mean and range for three analyses of the same fusd disc of sample DR-N are presented in Table 13. The precision of XRF and ICP analysis at the G.S.C. laboratory is also given in Table 12.

The accuracy of the XRF technique was tested by comparing the analyses of the standards DR-N, SY-2 and RGM with the 'usable' values of Abbey (1980). The results for DR-N, shown in Table 13, indicate departures of less than 6% of the concentrations of major components except $P_2O_5$, and less than 16% of trace element concentrations.

Detection limits for trace elements, $H_2O$, $CO_2$ and FeO are listed in Table 14.

(b) **Precision or reproducibility of sample and fused pellet preparation procedures**

To test the homogeneity of powdered samples and the reproducibility of the fusion method, two fused pellets were made from each of 14 different powder samples. The duplicate analyses are compared to the original analyses using the T-statistic on paired observations (Table 15). Using the coefficient of variation at the 95% confidence interval

as a measure of precision (Gregory, 1963) the reproducibility of the sample preparation procedure is within 5% of the concentration of most elements (Table 15), and generally is close to or within the precision of the XRF technique itself.

Table 12

**Routine precision of XRF and ICP analyses at the University of Ottawa and Geological Survey of Canada laboratories**

| | U.O. (XRF) | | | | | | G.S.C.(ICP) |
|---|---|---|---|---|---|---|---|
| | Concentration range (%) | | | | | | |
| | 0.1-1.0 | 0.1-2.0 | 1.0-3.0 | 2.0-5.0 | 1.0-20 | 50-100 | |
| $SiO_2$ | | | | | | ±1.0 | ±1 |
| $Al_2O_3$ | ±10(%) | | ±1.5 | ±1.5 | ±1.5 | | ±1 |
| $Fe_2O_3T$ | ±5 | | | | ±2 | | ±1 |
| MgO | ±25 | | | | ±3 | | ±1 |
| CaO | ±5 | | | | ±2 | | ±1 |
| $Na_2O$ | | ±15 | ±3 | | | | ±1 |
| $K_2O$ | ±5 | | | | ±1 | | ±1 |
| $TiO_2$ | ±2 | | ±1 | | | | ±1 |
| $P_2O_5$ | ±10 | | ±1 | | | | ±1 |
| MnO | ±10 | | | | | | ±1 |
| S | ±10 | | | | | | ±5 |

| | U.O. (XRF) | | | G.S.C. |
|---|---|---|---|---|
| | Concentration range (ppm) | | | |
| | <10 | 10-30 | >30 | |
| Ba | <10(%) | ±50 | ±30 | ±5 (ICP) |
| Cr | " | " | " | ±5 (ICP) |
| Zr | " | " | " | ±10 (XRF) |
| Sr | " | " | " | ±10 (XRF) |
| Rb | " | " | " | ±10 (XRF) |
| Y | " | " | " | ±10 (XRF) |
| Nb | " | " | " | ±10 (XRF) |
| Zn | " | " | " | ±5 (ICP) |
| Ni | " | " | " | ±5 (ICP) |
| Cu | | | | ±5 (ICP) |
| Pb | | | | ±10 (ICP) |
| V | | | | ±5 (ICP) |
| REE | | | | ±5 (ICP) |

Table 13

XRF major and trace element composition of ANRT standard DR-N

| | X (n=3) | Range | 'Usable' (Abbey, 1980) |
|---|---|---|---|
| $SiO_2$ (%) | 52.7 | 0.33 | 52.88 |
| $Al_2O_3$ | 17.51 | 0.20 | 17.56 |
| $Fe_2O_3T$ | 9.69 | 0.08 | 9.69 |
| MgO | 4.24 | 0.06 | 4.47 |
| CaO | 7.13 | 0.14 | 7.09 |
| $Na_2O$ | 3.03 | 0.09 | 3.00 |
| $K_2O$ | 1.83 | 0.05 | 1.73 |
| $TiO_2$ | 1.06 | 0.01 | 1.11 |
| $P_2O_5$ | 0.18 | 0.06 | 0.25 |
| MnO | 0.22 | 0 | 0.21 |
| S | 0.02 | 0 | ? |
| Ba (ppm) | 428 | 11 | 380 |
| Cr | 42 | 8 | 45 |
| Zr | 112 | 4 | 125? |
| Sr | 385 | 4 | 400 |
| Rb | 68 | 2 | 75 |
| Y | 31 | 2 | ? |
| Nb | 2 | 6 | ? |
| Zn | 160 | 13 | 150 |
| Ni | 17 | 9 | 22 |
| V | 255 | 14 | 220 |
| Total | 97.87 | | 97.59 |

Table 14

Detection limits for trace elements, $H_2O$, $CO_2$ and FeO

| | Ba | Cr | Zr | Sr | Rb | Y | Nb | Zn | Cu | Ni | Pb | V | $H_2O$ | $CO_2$ | FeO |
|---|---|---|---|---|---|---|---|---|---|---|---|---|---|---|---|
| | ppm | | | | | | | | | | | | | | |
| Samples 301-320 | 100 | 10 | 10 | 10 | 10 | 10 | 10 | 5 | 10 | 10 | 20 | | | | |
| Samples 033-308b | 10 | 10 | 10 | 10 | 10 | 10 | 10 | 10 | 0.2 | 10 | 2 | 0 | | | |

| | Ce | Dy | Eu | Gd | La | Nd | Sm | Yb |
|---|---|---|---|---|---|---|---|---|
| REE samples (ppm) | 0.5 | 0.2 | 0.1 | 0.2 | 0.5 | 0.5 | 0.3 | 0.1 |

Table 15

Precision or reproducibility of sample add fused pellet preparation procedures

| | $SiO_2$ | $Al_2O_3$ | $Fe_2O_3T$ | MgO | CaO | $Na_2O$ | $K_2O$ | $TiO_2$ | $P_2O_5$ | MnO |
|---|---|---|---|---|---|---|---|---|---|---|
| **Mean of paired observations, (Xa - Xb)/2** | | | | | | | | | | |
| n=14 X = | 58.48 | 15.46 | 9.79 | 3.25 | 7.93 | 2.45 | 0.83 | 0.61 | 0.09 | 0.15 |
| Sd = | 10.07 | 3.13 | 6.42 | 2.06 | 4.54 | 1.71 | 0.91 | 0.22 | 0.14 | 0.14 |
| **Difference between paired observations, (Xa - Xb)** | | | | | | | | | | |
| n=14 X = | -0.028 | 0.031 | 0.029 | -0.014 | 0.014 | 0.010 | 0.006 | -0.001 | -0.002 | 0 |
| Sd = | 0.243 | 0.090 | 0.142 | 0.084 | 0.119 | 0.100 | 0.025 | 0.012 | 0.020 | 0 |
| Sd/ 14 = | 0.064 | 0.024 | 0.038 | 0.022 | 0.032 | 0.027 | 0.007 | 0.003 | 0.005 | |
| $t_{.05}$ (13 d.f.) = 1.77 | | | | | | | | | | |
| t(Sd/ 14) = | 0.115 | 0.043 | 0.067 | 0.040 | 0.056 | 0.047 | 0.012 | 0.005 | 0.009 | |
| $U_L$ = Sd + t(Sd/ 14) = | 0.358 | 0.133 | 0.209 | 0.124 | 0.175 | 0.147 | 0.037 | 0.018 | 0.029 | |
| $L_L$ = Sd - t(Sd/ 14) = | 0.128 | 0.047 | 0.075 | 0.044 | 0.063 | 0.053 | 0.013 | 0.006 | 0.011 | |
| $V_{.025} = (U_L/X) \times 100$ = | 0.60% | 0.86% | 2.1% | 3.8% | 2.2% | 5.2% | 4.4% | 2.9% | 3.0% | |

# APPENDIX 5

## ELEMENTAL GAINS AND LOSSES

### Error in gains and losses

Possible sources of error in determining mass gains and losses are local variability in composition (over distances of cm's to tens of cm's) of less altered and altered rocks, and analytical error including that introduced during sample preparation. Estimates of volume changes are additionally affected by error in determining rock density (±2%). The cumulative error is probably less than about 10% of the contents of most elements, based on the difference in compositions of nearby samples of less altered rock (e.g. # 216 and # 217; # 001 and # 005i), although errors for K, Pb, Ba, Cu and Pb are larger.

In using Grant's method to compute metasomatic changes, a clustering of the ratios of individual elements in altered and less altered rock is generally apparent. Ratios of $TiO_2$, Zr and $Al_2O_3$ in almost every case occur near the 'centre' of the cluster, and for this reason the isocon was chosen (by inspection) to lie between the ratios of $TiO_2$, Zr and $Al_2O_3$. Where only two of these three components have similar ratios, an isocon bisecting the points representing the two elements in the isocon diagram was chosen. Taking into account the error on individual points in the diagrams, the position of the isocon may lie anywhere within an 'envelope' defined by the 'outer' error bounds of the individual points.

Since in many cases the ratios of $TiO_2$, Zr and $Al_2O_3$ are within 10% of one another, the 'envelope' of error in the position of the isocon is estimated to be ± 15-20% of the slope of the isocon. Thus, the actual gains and losses of individual components (except K, Rb, Ba, Cu and Pb) probably are within 20-25% of the values calculated with respect to the isocon.

Table 16

**Mass gains and losses (%) between less altered and altered rocks**

| | Silicification of pillow margins | | | | | | | |
|---|---|---|---|---|---|---|---|---|
| Altered | 171 | 172 | 200 | 202 | 205 | 0841 | 221 | 220 |
| Less alt. | 173 | 173 | 173 | 173 | 173 | 086 | 223 | 223 |
| $SiO_2$ | +38[a] | +55 | +29 | +49 | +30 | +60 | +40 | +43 |
| $Al_2O_3$ | 0 | -4.5 | +5.0 | +3.0 | +1.5 | -1 | 0 | -2 |
| $Fe_2O_3T$ | +2.5 | -26 | +1.9 | +3.0 | +2.5 | -43 | -10 | -1 |
| $Fe_2O_3$ | -22 | -22 | -36 | +3.0 | -33 | -40 | -17 | +23 |
| FeO | +9.5 | -28 | +14 | +3.0 | +14 | -45 | -9 | -6 |
| MgO | +52 (-11)[b] | -4.5 (-43) | +39 (-1.7) | +27 (-24) | +38 (-18) | -39 | -12 | -17 |
| CaO | -44 | -43 | -27 | -27 | -30 | -32 | +26 | +81 |
| $Na_2O$ | +11 | +26 | +24 | +12 | +14 | +15 | -28 | -56 |
| $K_2O$ | +260 | +103 | +320 | +310 | -12 | -6 | +52 | -59 |
| $TiO_2$ | 0 | -2.7 | +1.5 | +3.0 | +2.5 | -4 | -4 | -2.5 |
| $P_2O_5$ | +87 | +250 | +140 | +27 | -12 | +1 | -100 | -100 |
| MnO | -22 | -25 | -18 | +2.0 | -14 | -41 | -6 | -14 |
| $H_2O$ | +190 | +68 | +39 | +7.0 | +115 | -29 | +81 | -55 |
| S | +430 | +91 | +140 | -68 | +76 | -100 | +i | BD |
| $CO_2$ | BD | BD | BD | BD | BD | -40 | +i | +i |
| Ba | +150 | +80 | +200 | +190 | -33 | -17 | +15 | -24 |
| Cr | +63 | -14 | -19 | -13 | +12 | +4 | +8 | +15 |
| Zr | 0 | +0.9 | -1.9 | -3.0 | -1.5 | +8 | +3 | +0.5 |
| Sr | +78 | 0 | -12 | -14 | -2.5 | +1.5 | +31 | -31 |
| Rb | +i | BD | +i | +i | BD | +4 | -100 | -100 |
| Y | +35 | +39 | +30 | +35 | +22 | +18 | +8 | +9 |
| Nb | +i | +i | BD | +i | BD | +i | -100 | -100 |
| Zn | +110 | +20 | +41 | +43 | +43 | -33 | +26 | +19 |
| Cu | +340 | +49 | +190 | -69 | +380 | -99 | +92 | -76 |
| Ni | +i | BD | BD | BD | BD | -78 | +92 | -100 |
| Pb | +i | +i | +i | +i | +i | -40 | -100 | -100 |
| V | -5.0 | -8.2 | -4.2 | 0 | -31 | -12 | -12 | -9 |
| Δ Vol. | +30 | +35 | +23 | +34 | +23 | +31 | +26 | +30 |

[a] +38 indicates that sample 171 gained a mass of $SiO_2$ equivalent to 38% of the mass of $SiO_2$ in sample 173, determined by Grant's method and subject to the errors discussed in this Appendix.

[b] figure in parentheses represents mass change assuming 4 wt % MgO in sample 173.

BD = element abundance below detection limit.

+i = very large gain, due to concentrations near zero in less altered rock.

Table 16 (cont.)

**Mass gains and losses (Z)**

| | Epid. of pillow cores | | Selvages of pillows | | | | Silicified volcaniclastic rocks | | |
|---|---|---|---|---|---|---|---|---|---|
| Altered | 177 | 174 | 175 | 198 | 201 | 0841i | 284 | 271 | 306 |
| Less alt. | 176 | 173 | 176 | 176 | 173 | 086 | 283 | 270 | 305 |
| $SiO_2$ | +6 | +21 | -34 | -7.1 | -28 | -44 | +16 | +50 | +6 |
| $Al_2O_3$ | 0 | 0 | -1.4 | +7.5 | -13 | -18 | -7 | -4 | -2 |
| $Fe_2O_3T$ | -3 | -2 | +34 | +33 | +24 | +18 | -79 | -74 | -32 |
| $Fe_2O_3$ | +130 | +130 | +26 | +27 | +15 | +7 | -77 | -56 | |
| FeO | -43 | -46 | +39 | +35 | +25 | +20 | -80 | -85 | |
| MgO | +62 | -45 | +51 | +87 | +42 (-13) | +31 | -46 | -79 | -32 |
| CaO | +130 | +180 | +16 | +2.9 | +3.2 | -40 | +6 | -10 | -4 |
| $Na_2O$ | -96 | -99 | -36 | -6.2 | -35 | -44 | +19 | +27 | +26 |
| $K_2O$ | -65 | -79 | +80 | +190 | -15 | +105 | +43 | -28 | -51 |
| $TiO_2$ | -13 | -15 | +5.4 | +4.6 | +4.7 | -4.6 | +1 | 0 | +2 |
| $P_2O_5$ | BD | -100 | BD | BD | -54 | +i | -35 | -43 | BD |
| MnO | -5 | -6 | +34 | +35 | +32 | -13 | -65 | -89 | -9 |
| $H_2O$ | +63 | -15 | +54 | +87 | +40 | +58 | -77 | -76 | |
| S | +140 | +92 | -100 | -100 | -75 | -62 | BD | -100 | BD |
| $CO_2$ | +i | +i | BD | BD | BD | -97 | +i | -37 | |
| Ba | -35 | -34 | -7.1 | +49 | -41 | +85 | +64 | -34 | -28 |
| Cr | -9 | -27 | -62 | -19 | -18 | -18 | -18 | +20 | -7 |
| Zr | 0 | 0 | -2.5 | -4.2 | -2.9 | +5.4 | -1 | 0 | +240 |
| Sr | +39 | +230 | -48 | -45 | -56 | -52 | -43 | +7 | +29 |
| Rb | BD | BD | BD | +i | BD | +280 | +70 | BD | -78 |
| Y | +17 | +4 | +16 | +32 | +0.6 | +0.8 | -32 | -6 | +160 |
| Nb | -22 | BD | -100 | -100 | BD | BD | BD | BD | +i |
| Zn | -33 | -66 | +51 | +169 | +35 | +18 | -61 | -10 | +16 |
| Cu | +56 | +180 | +49 | -100 | -52 | -71 | +49 | -85 | |
| Ni | BD | BD | +i | BD | BD | +11 | BD | BD | -90 |
| Pb | -100 | +i | -71 | -100 | BD | -100 | +49 | BD | |
| V | +5 | -27 | -41 | +13 | +6.5 | +9.2 | -8 | -54 | -47 |
| $\Delta$ Vol. | +12 | +24 | -19 | -1 | -21 | -35 | +2 | +37 | |

Table 16 (cont.)

**Mass gains and losses (%)**

| | Plag-qtz borders to fractures | | | Pervasive epidotization | | | | garnet-chl alteration | | |
|---|---|---|---|---|---|---|---|---|---|---|
| Altered | 3081i | 1411i | 140 | 280 | 0151i | 104 | 073 | 114 | 293 | 243 |
| Less alt. | 3081 | 1411 | 138 | 282 | 001 | 102 | 248 | 115 | 055 | 242 |
| $SiO_2$ | +24 | -30 | +10 | +1 | -3 | -4 | +11 | +11 | -36 | -17 |
| $Al_2O_3$ | -4 | -8 | -2 | 0 | +33 | -7 | -3 | -5 | +66 | 0 |
| $Fe_2O_3T$ | -90 | -82 | -69 | -40 | -53 | -58 | -63 | +61 | +760 | +36 |
| $Fe_2O_3$ | | -80 | -61 | +61 | +75 | -33 | -27 | +77 | +600 | +21 |
| FeO | | -86 | -74 | -65 | -86 | -65 | -72 | +53 | +800 | +41 |
| MgO | -90 | -90 | -62 | -29 | -50 | +7 | +15 | +31 | +760 | +80 |
| CaO | -3 | -57 | -24 | +86 | +140 | +12 | +26 | -39 | -57 | -40 |
| $Na_2O$ | +33 | +11 | +1 | -52 | -82 | +34 | +500 | -24 | -70 | -79 |
| $K_2O$ | -77 | -25 | +62 | -70 | -51 | -12 | +26 | -48 | +68 | -39 |
| $TiO_2$ | 0 | -4 | -2 | -2 | -8 | -3 | +3 | 0 | -9 | +2 |
| $P_2O_5$ | +1 | BD | -38 | BD | +4 | -100 | BD | BD | -51 | +17 |
| MnO | -90 | -85 | -55 | 0 | -54 | -54 | -66 | -62 | +760 | +84 |
| $H_2O$ | [redacted] | -81 | -40 | -20 | +58 | -45 | -64 | +210 | +350 | +500 |
| S | BD | BD | BD | BD | BD | BD | -100 | BD | BD | -100 |
| $CO_2$ | | +30 | +1 | +1 | +1 | +1 | +400 | BD | -100 | -36 |
| Ba | -82 | -42 | +3 | -32 | -100 | +21 | +1 | -80 | +24 | -27 |
| Cr | +31 | -55 | -11 | +8 | +115 | -23 | +32 | -13 | +130 | +65 |
| Zr | 0 | +8 | +2 | +11 | +8 | +3 | -100 | 0 | +10 | -8 |
| Sr | +18 | +43 | +12 | +72 | +70 | +21 | +54 | +67 | -79 | -100 |
| Rb | -92 | BD | BD | -100 | -48 | BD | BD | -64 | +90 | BD |
| Y | -30 | -82 | -31 | -16 | -3 | +15 | +90 | +55 | -22 | +26 |
| Nb | +1 | +1 | +30 | BD | BD | BD | BD | BD | +2 | -23 |
| Zn | -77 | -72 | -59 | -57 | -75 | -100 | -58 | +20 | +108 | -4 |
| Cu | | +13 | +24 | -50 | -94 | -100 | -100 | +100 | -100 | BD |
| Ni | BD | -100 | +1 | +160 | -28 | BD | -12 | BD | -100 | BD |
| Pb | | +1 | +1 | +52 | BD | BD | +1 | BD | BD | BD |
| V | -75 | -95 | BD | 0 | -12 | -14 | +24 | BD | +1 | -10 |
| $\Delta$ Vol. | | -30 | +5 | +3 | | -3 | +2 | +12 | +12 | -1 |

Table 17

Mass gains and losses (%) of REE

| Altered / Less altered | 171 / 173 | 172 / 173 | 174 / 173 | 271 / 270 |
|---|---|---|---|---|
| La | +77 | +79 | +110 | -20 |
| Ce | +55 | +52 | +54 | -16 |
| Nd | +32 | +27 | +93 | -15 |
| Sm | +30 | +28 | +4 | -15 |
| Eu | -33 | -30 | -17 | +7 |
| Gd | +19 | +19 | +21 | -14 |
| Dy | +11 | +12 | 0 | -13 |
| Yb | -3 | +1 | -1 | +4 |

Note: Samples from the same zoned pillow (shown in Fig. 9):
171: silicified rim
172: silicified margin
173: least altered part of pillow
174: epidotized core
Sample 271 is the silicified equivalent of sample 270.

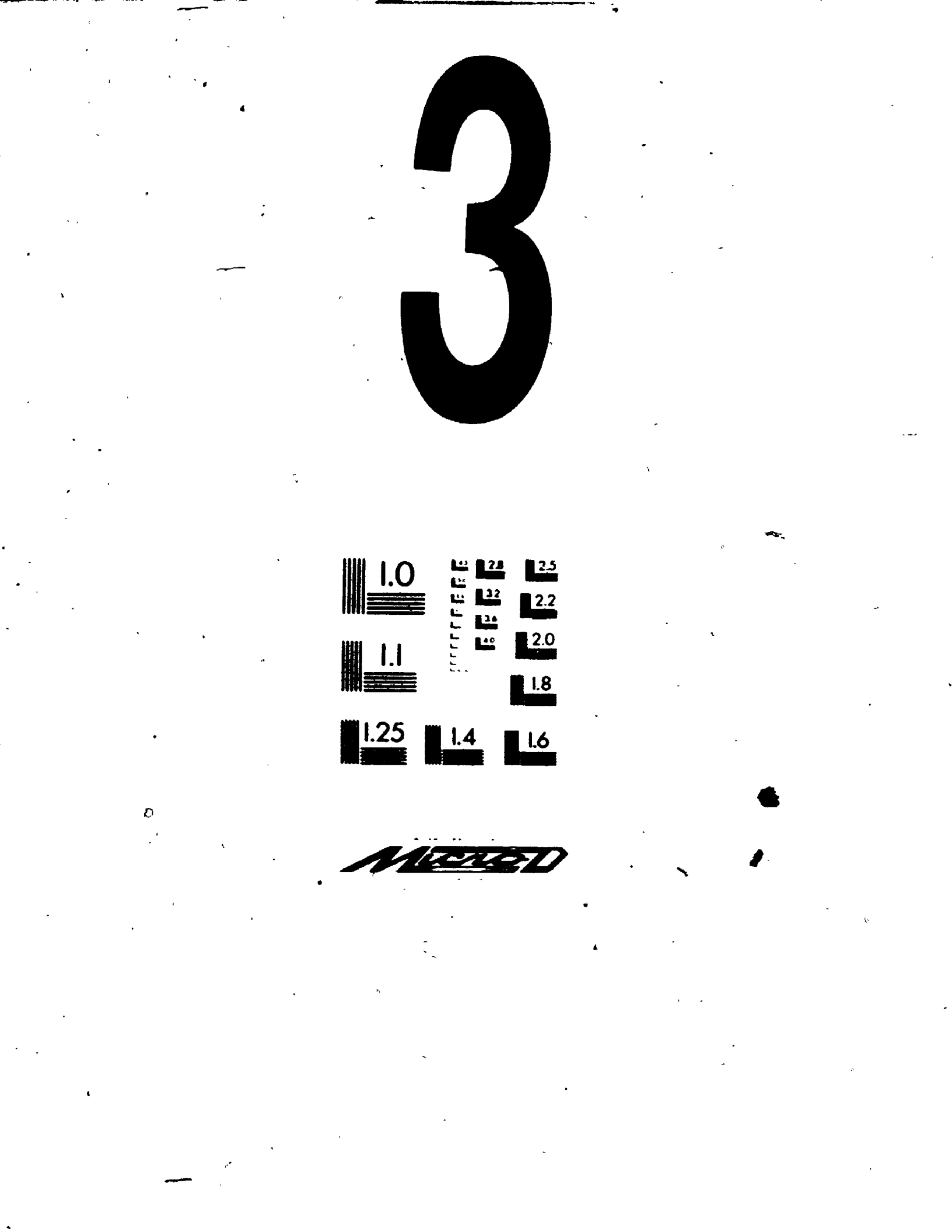
3
1.0
1.1
1.25
1.4
1.6
2.8
3.2
3.6
2.5
2.2
2.0
1.8

100°06'52"

06'30"

06'10"

54°48'28"

48'20"

Chisel Lake Mine 1.8 km

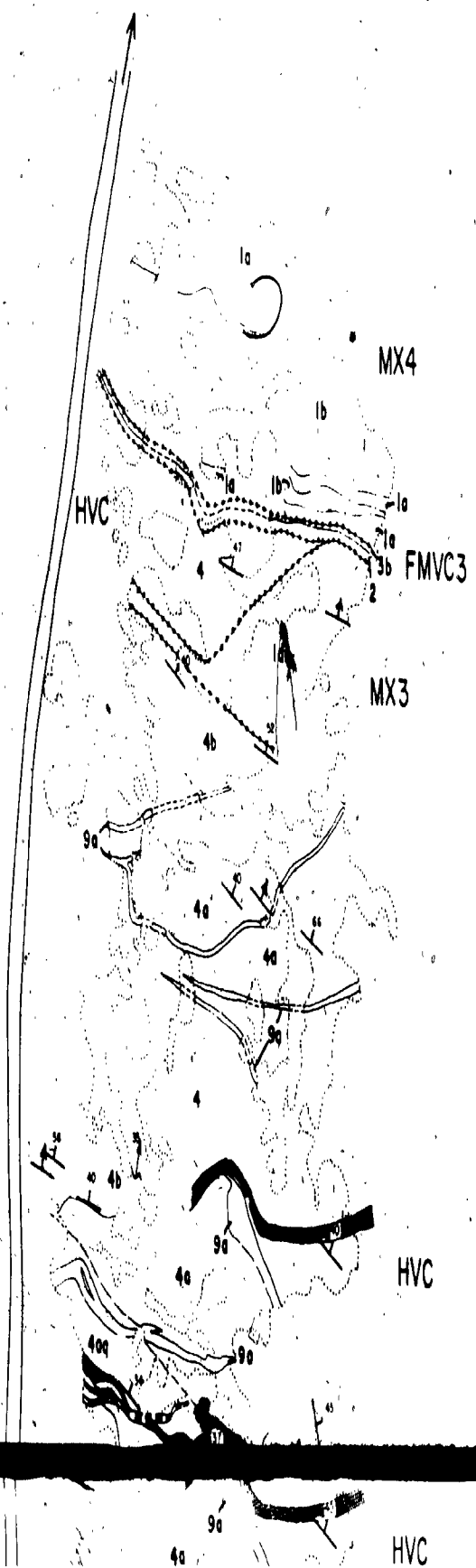


# GEOLOGY OF THE EDWARD

## LOWE

Amisk intrusive rocks, intrusions of unknown a

9 Mafic intrusions

9a a) fine grained, medium grained and plagioclase

9b b) pyroxene-phyric

9c c) composite: mafic margin, felsic core

8 Pyroxenite

7 Quartz-plagioclase porphyry, phenocrysts up to 6 mm in diameter

6 Fine grained quartz-phyric intrusions, phenocrysts up to 2 mm in diameter

5 Aphyric and plagioclase-phyric felsic intrusions

5 Aphyric and plagioclase-phyric felsic intrusions

06'10" 05'50" 100°05'38"

54°48'28"

Figure 2a

# GEOLOGY OF THE EDWARDS LAKE AREA

## Legend

### LOWER PROTEROZOIC

#### Amisk intrusive rocks, intrusions of unknown age

9 Mafic intrusions

9a a) fine grained, medium grained and plagioclase-phyric

9b b) pyroxene-phyric

9c c) composite: mafic margin, felsic core

8 Pyroxenite

7 Quartz-plagioclase porphyry, phenocrysts up to 6 mm in diameter

6 Fine grained quartz-phyric intrusions, phenocrysts up to 2 mm in diameter

5 Aphyric and plagioclase-phyric felsic intrusions

#### Amisk Group

4 Heterolithic, mixed mafic and felsic volcaniclastic rocks

a) breccia of mainly mafic clasts,
q quartz phenoclasts up to 1 cm in diameter

b) wacke, bedded

3 Mafic volcaniclastic rocks

a) pyroxene-phenocryst-rich wacke, massive

b) fine grained, massive and bedded

c) plagioclase-phenocryst rich wacke and breccia

2 Felsic volcanic breccia and wacke

1 Mafic flows

1a a) pyroxene plagioclase-phyric, pillowed and massive

1b b) pyroxene-phyric, pillow-fragment breccia

48'20"

1 Mafic flows

Chisel Lake Mine 1.8 km

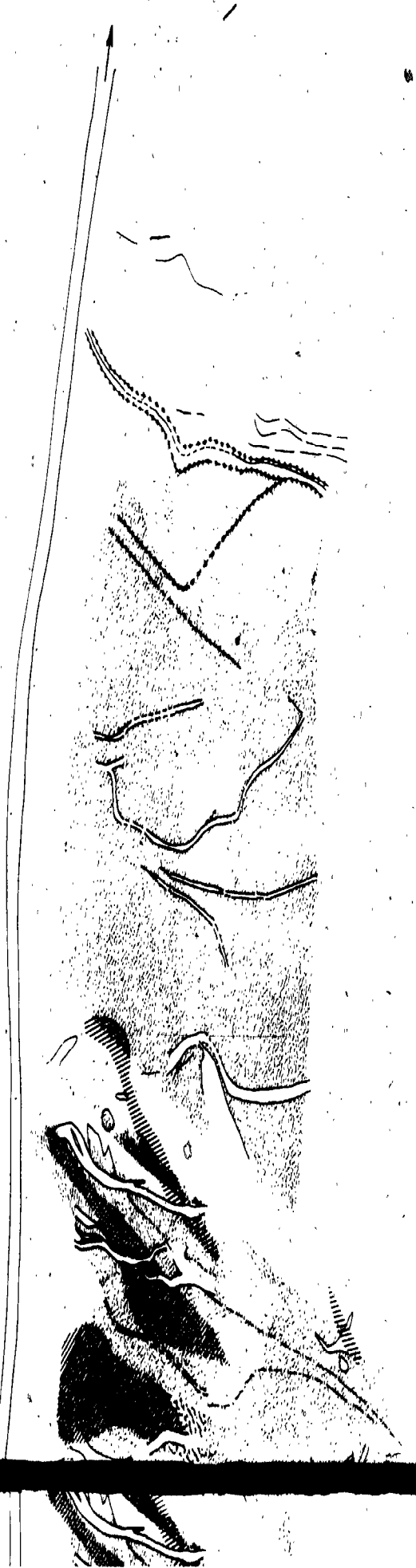

# ALTERATION IN THE EDWARDS LAK

Iron sulphidic alteration

Plagioclase-quartz-bordered fractures; b: biotitic envelo

Garnet-chlorite (-biotite) alteration

Pervasive epidotization; epidosite patches

Intense pervasive silicification

Low and moderate intensity pervasive silicification

SCALE 1:2 000

0 50 100 150

Figure 3a

# ALTERATION IN THE EDWARDS LAKE AREA

Iron sulphidic alteration

Plagioclase-quartz-bordered fractures; b: biotitic envelope, m: muscovitic envelope

Garnet-chlorite (-biotite) alteration

Pervasive epidotization; epidosite patches

Intense pervasive silicification

Low and moderate intensity pervasive silicification

## Symbols

SCALE 1:2 000

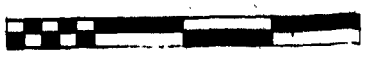

Geological contact: accurate; approximate; inferred

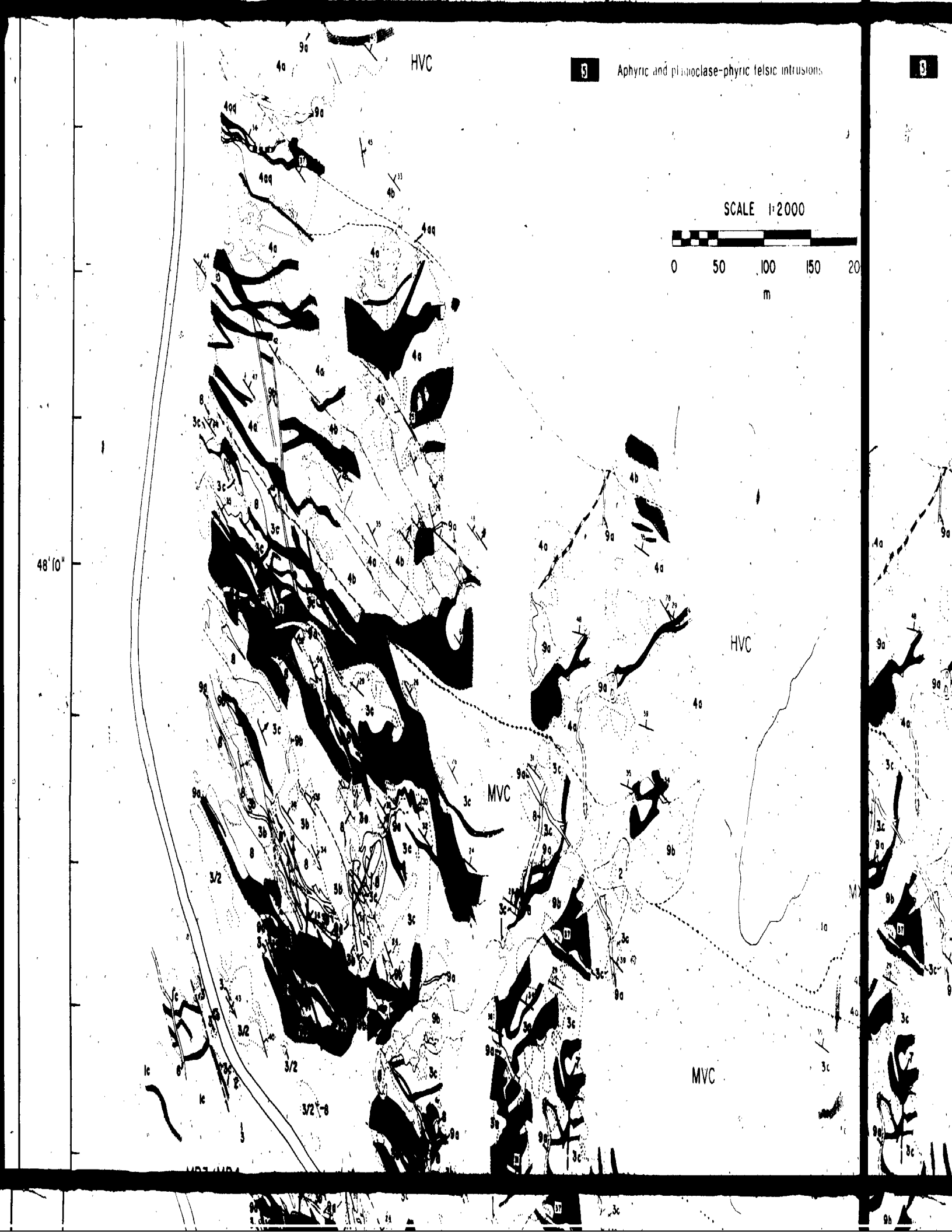

3 Aphyric and plagioclase-phyric felsic intrusions
SCALE 1:2000
0 50 100 150 20
m
HVC
MVC
48'10"

9 Aphyric and plagioclase-phyric felsic intrusions

1 Mafic flows

1a a) pyroxene plagioclase-phyric, pillowed and massive

1b b) pyroxene-phyric, pillow-fragment breccia

9 Aphyric and plagioclase-phyric felsic intrusions

1 Mafic flows

1a a) pyroxene plagioclase-phyric, pillowed and massive

1b b) pyroxene-phyric, pillow-fragment breccia

1c c) plagioclase-phyric, pillowed and massive

1d d) aphyric, pillowed

1e e) aphyric, massive

1f f) aphyric, pillow-fragment and isolated-pillow breccias

SCALE 1:2000

0 50 100 150 200

m

Geology by R. G. Skirrow, 1985-1986

Magnetic declination approximately 11° 56' East, decreasing 5' annually

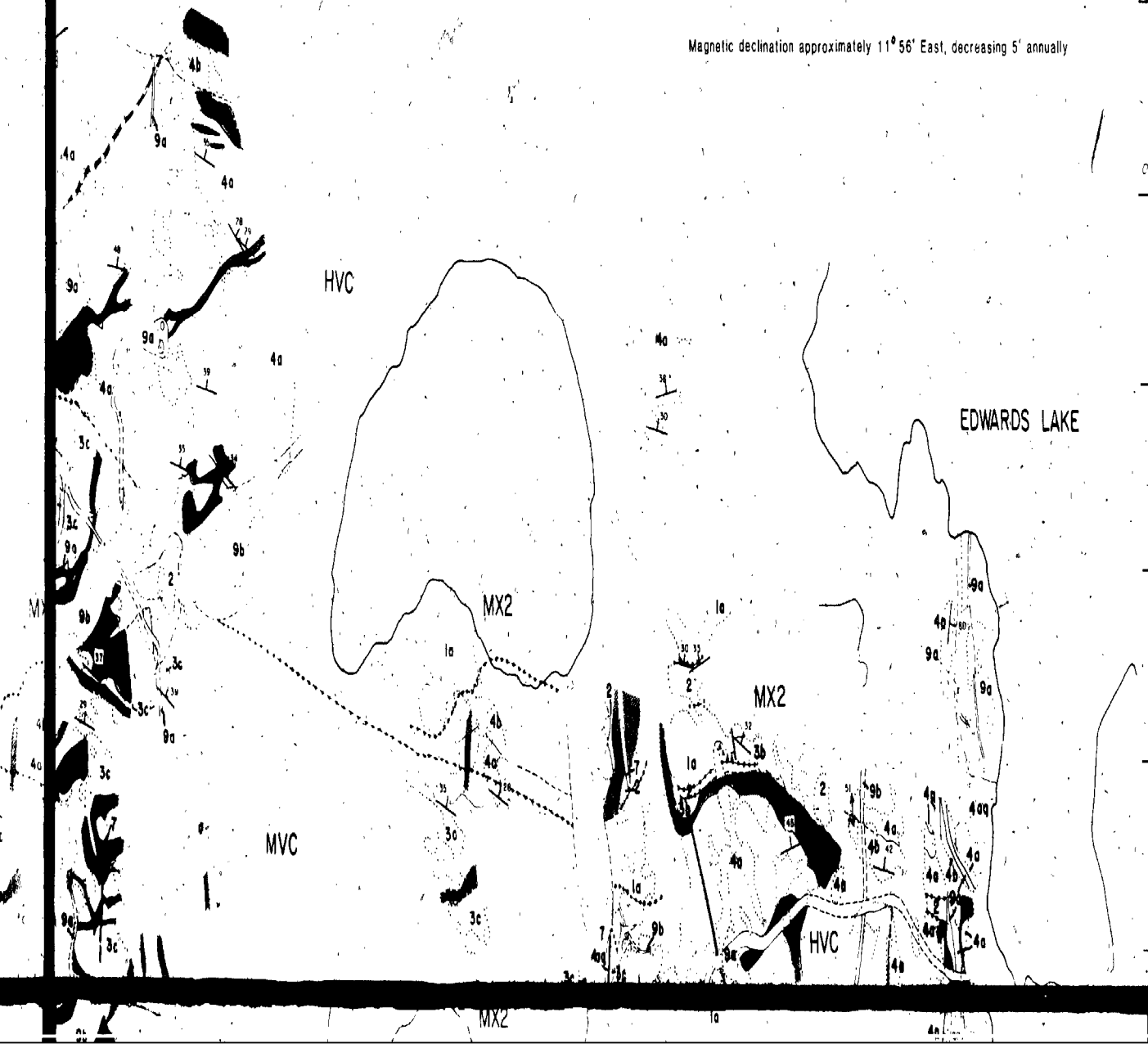

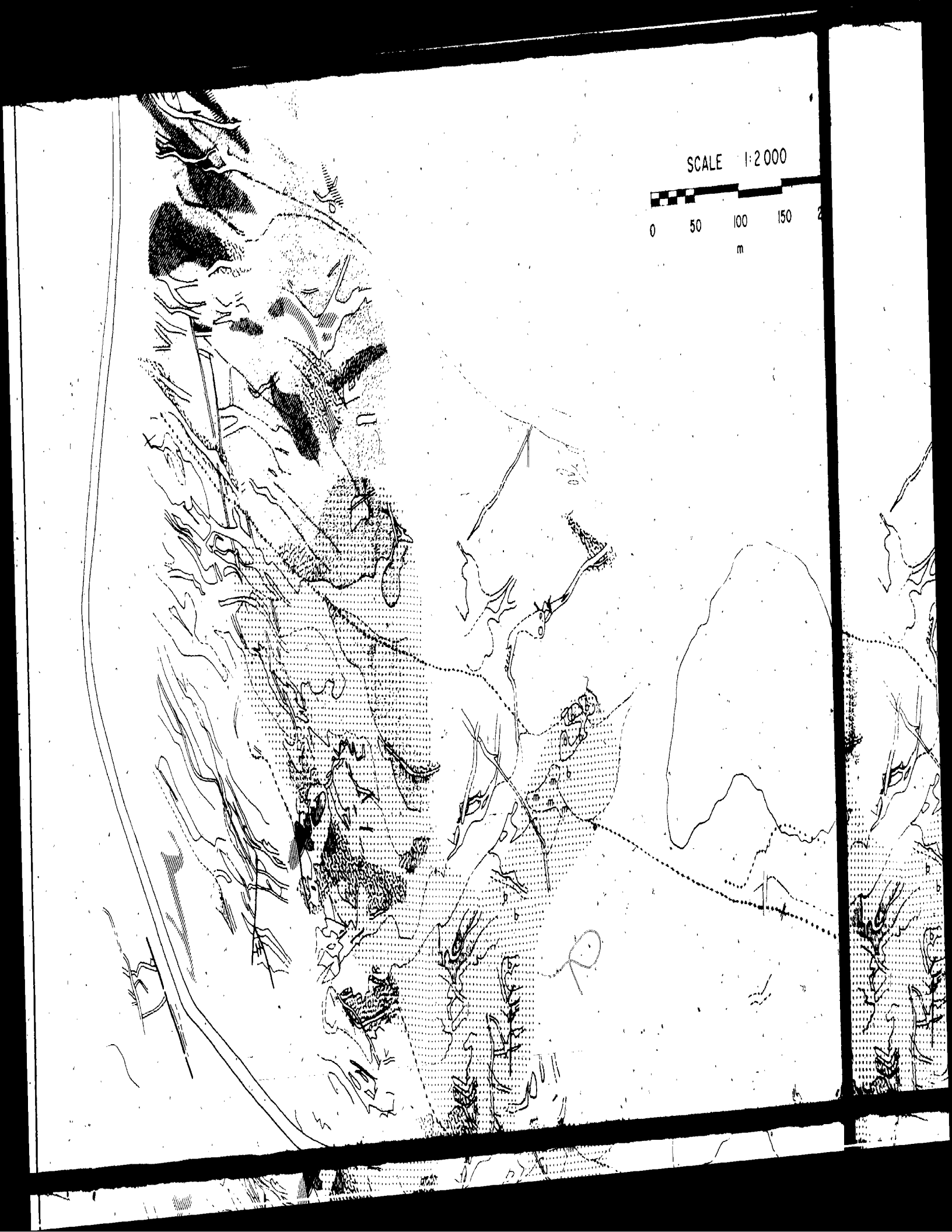
SCALE 1:2 000
0 50 100 150
m

## Symbols

SCALE 1:2 000

0 50 100 150 200

m

Geological contact, accurate; approximate; inferred

Stratigraphic division boundary

Fault: accurate; inferred

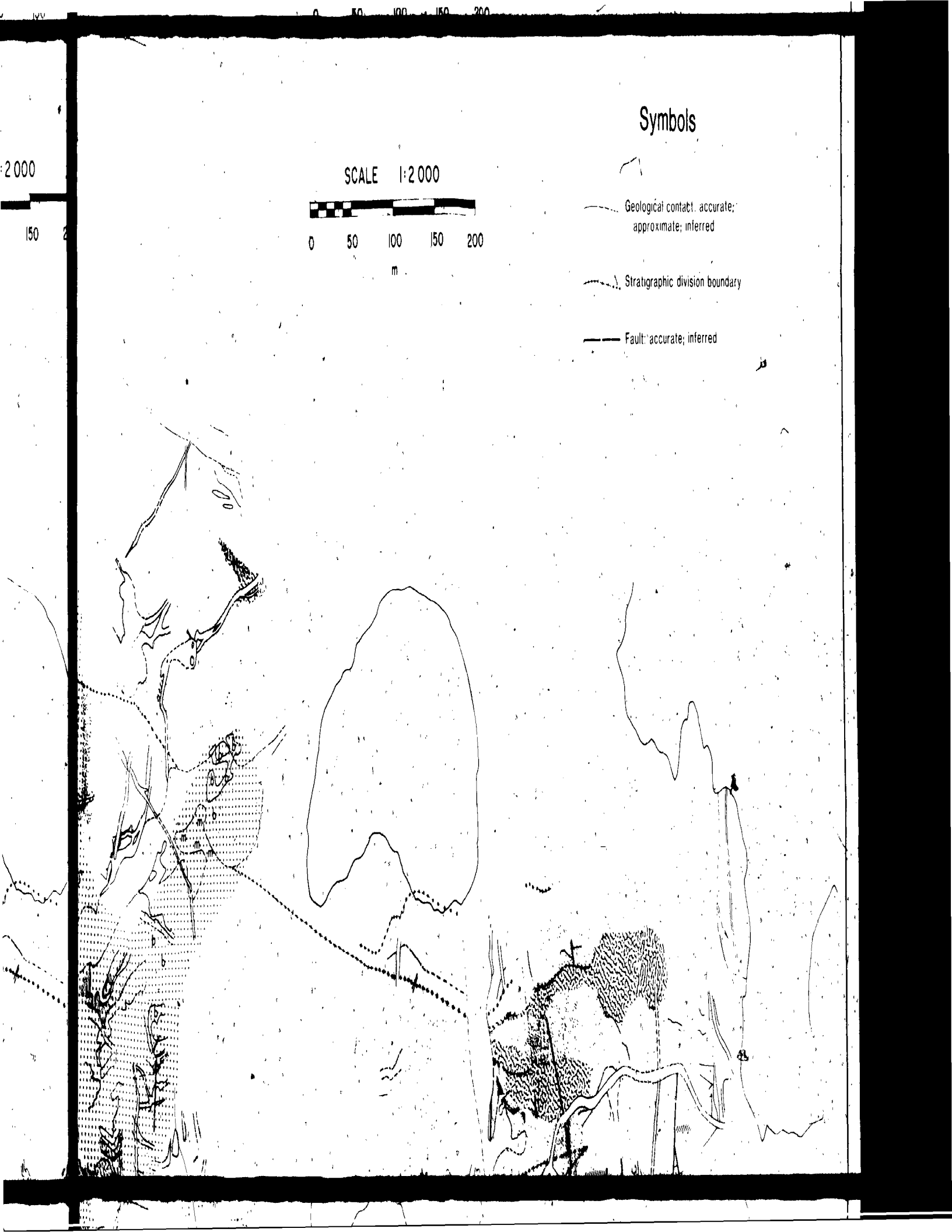

MP3/MP4
MVC
MVC
MXI
MVC
MVC
MP5
48'00"
47'50"

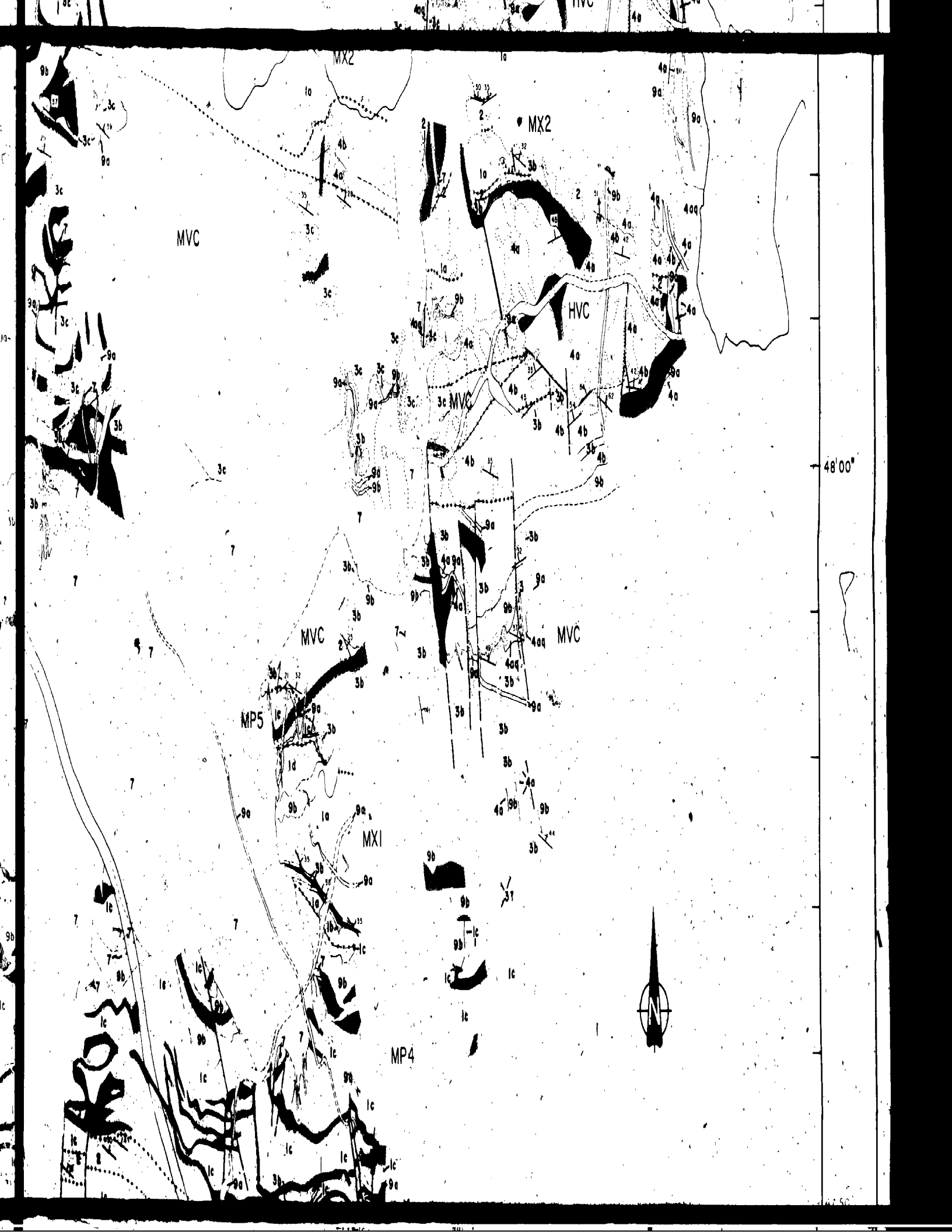
MX2
MVC
HVC
MVC
MVC
MVC
MP5
MXI
MP4
48'00"
N

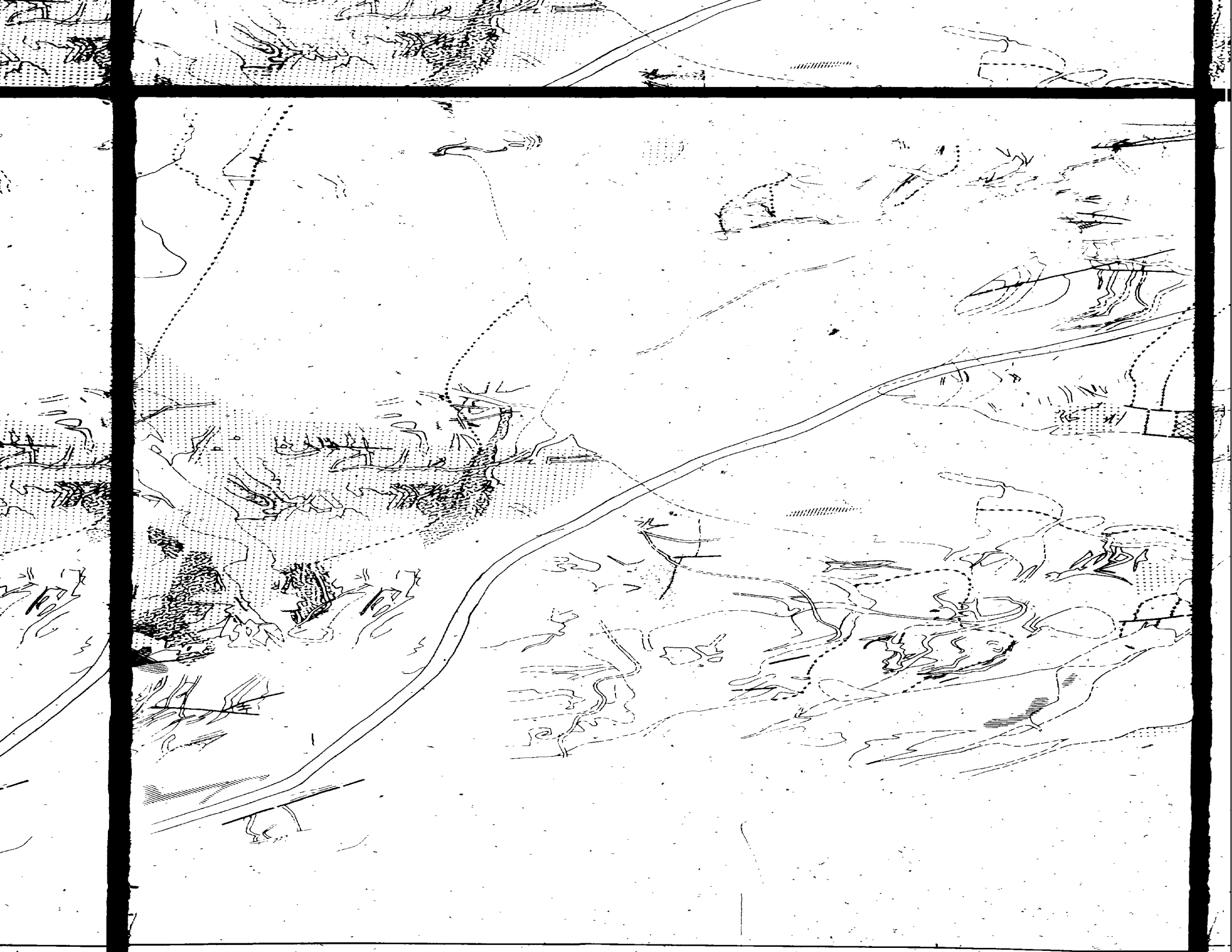

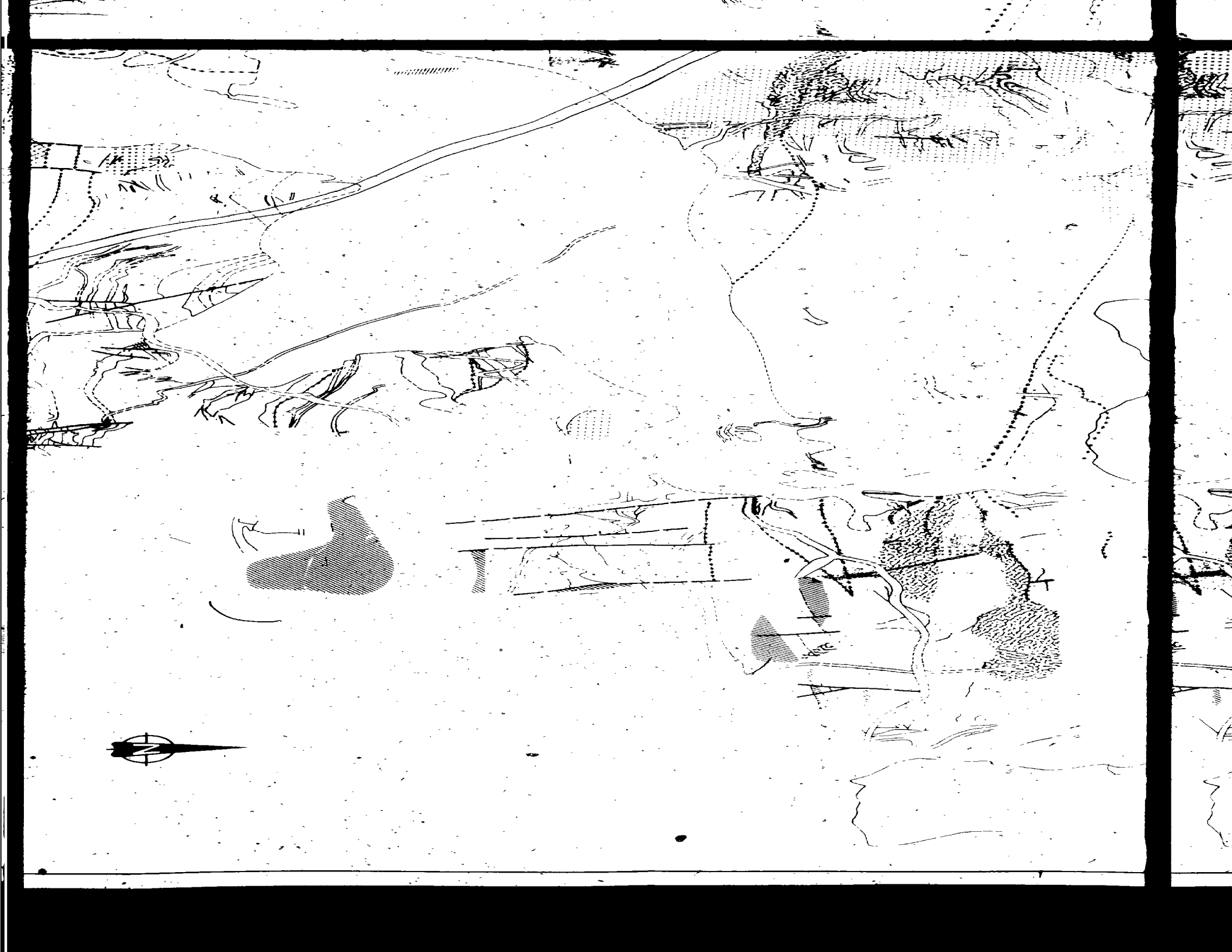

47'50"
47'50"
47'40"
FMVCI
FMVCI
MP2
MP2
MA
MA

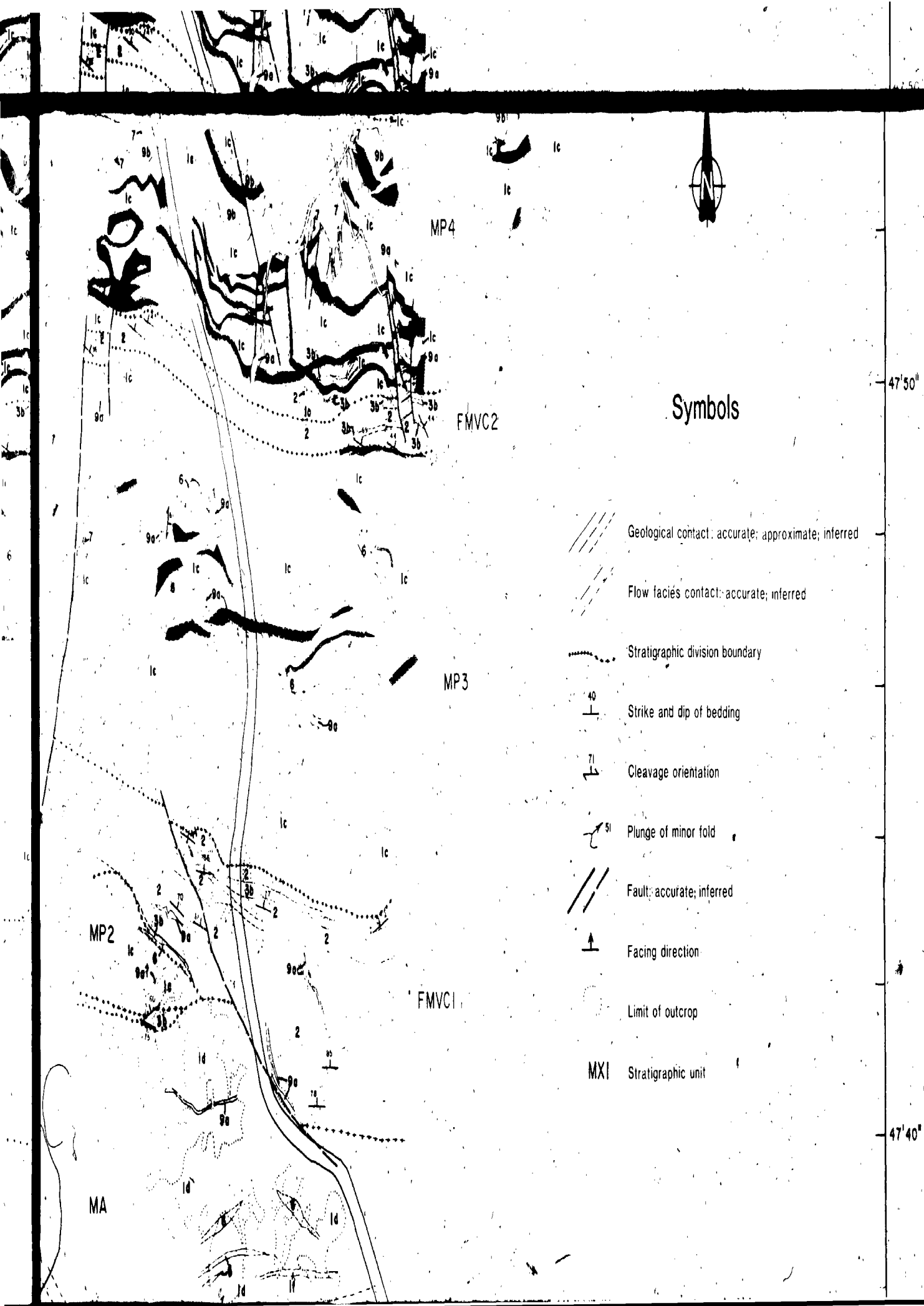
MP4
FMVC2
MP3
MP2
FMVC1
MA
47°50"
47°40"
Symbols
Geological contact: accurate; approximate; inferred
Flow facies contact: accurate; inferred
Stratigraphic division boundary
Strike and dip of bedding
Cleavage orientation
Plunge of minor fold
Fault: accurate; inferred
Facing direction
Limit of outcrop
MXI Stratigraphic unit

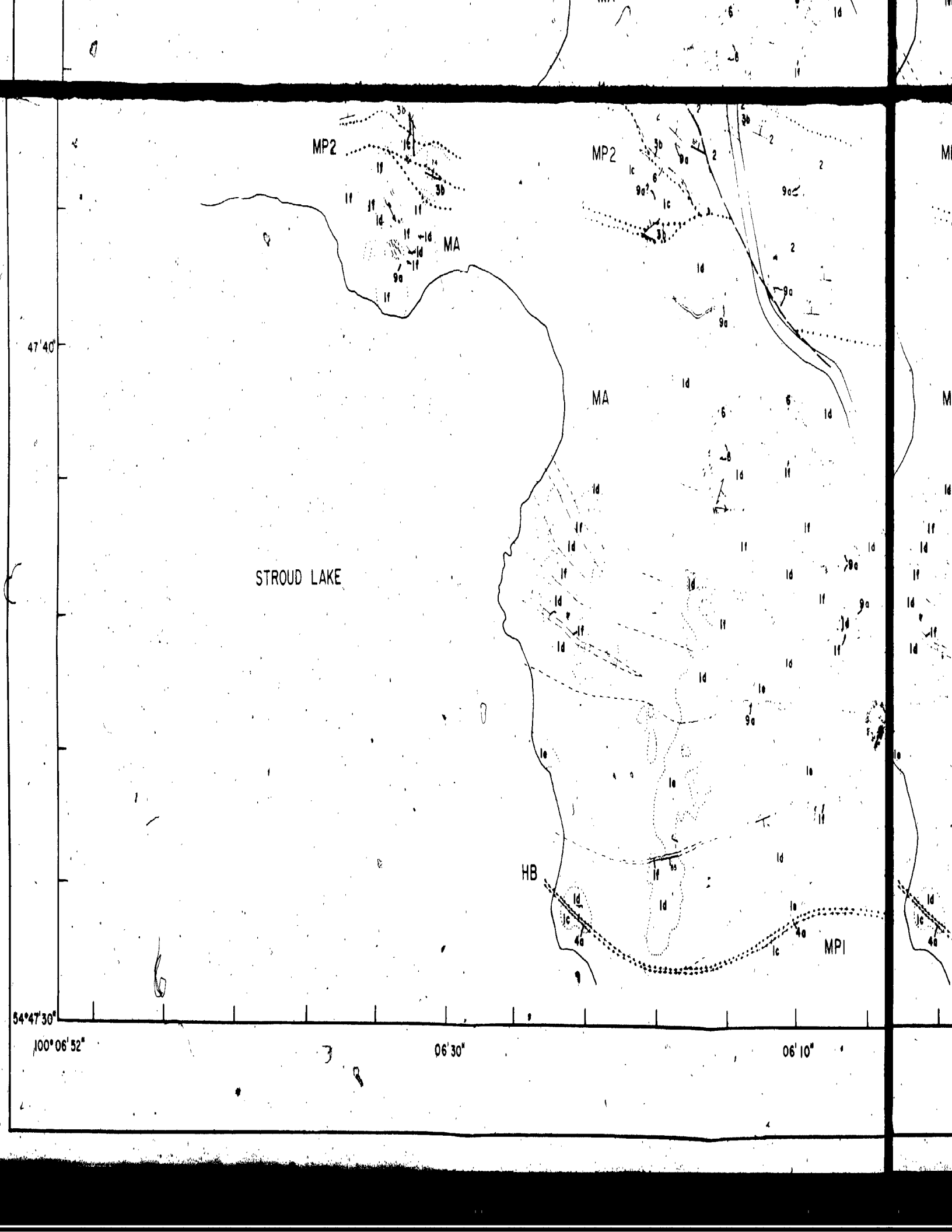
MP2
MP2
MA
MA
STROUD LAKE
HB
MPI
47'40"
54°47'30"
100°06'52"
06'30"
06'10"

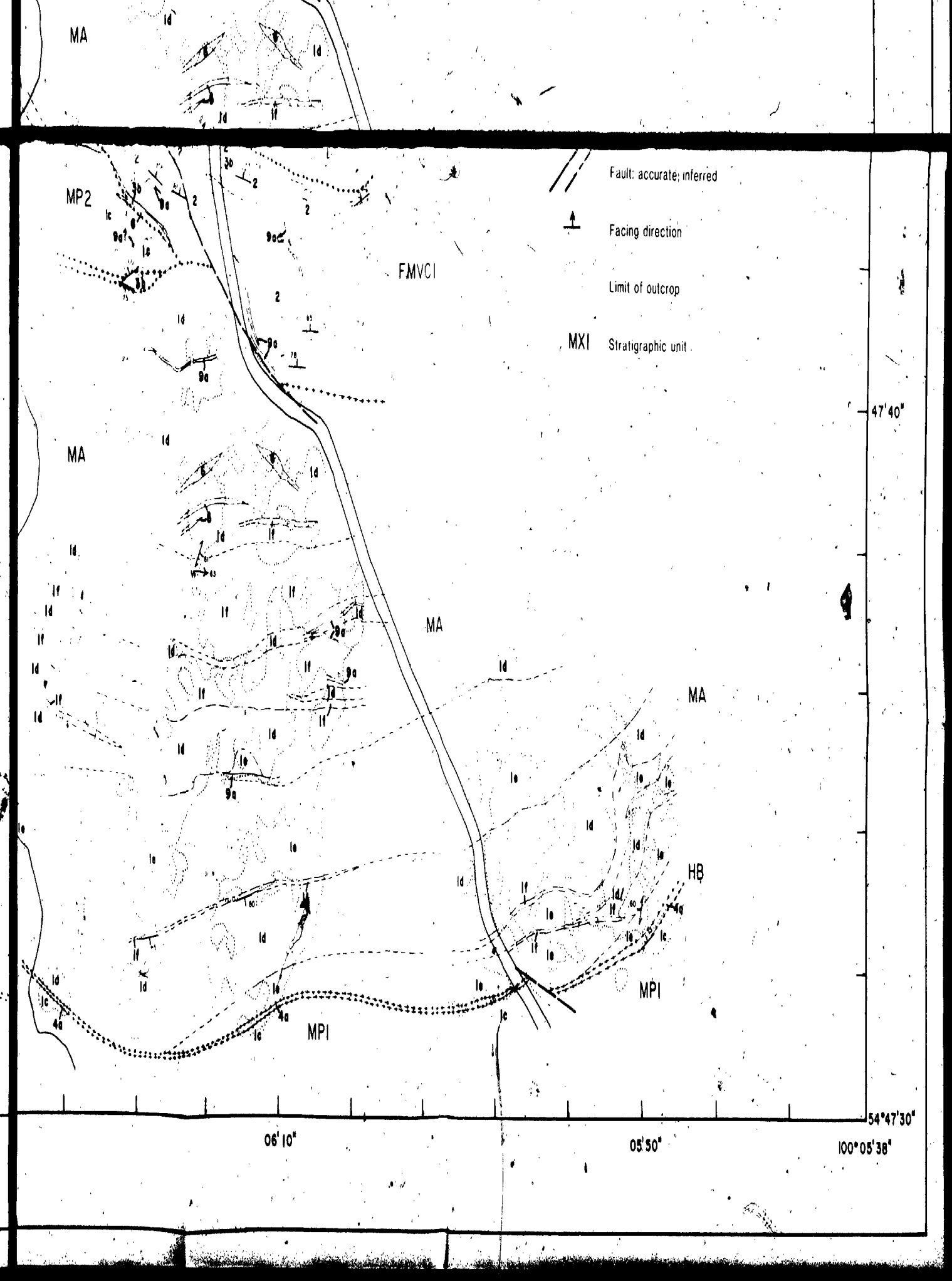
MA
MP2
FMVC1
MA
MA
MA
HB
MPI
MPI
Fault: accurate; inferred
Facing direction
Limit of outcrop
MXI Stratigraphic unit
47'40"
54°47'30"
06'10"
05'50"
100°05'38"

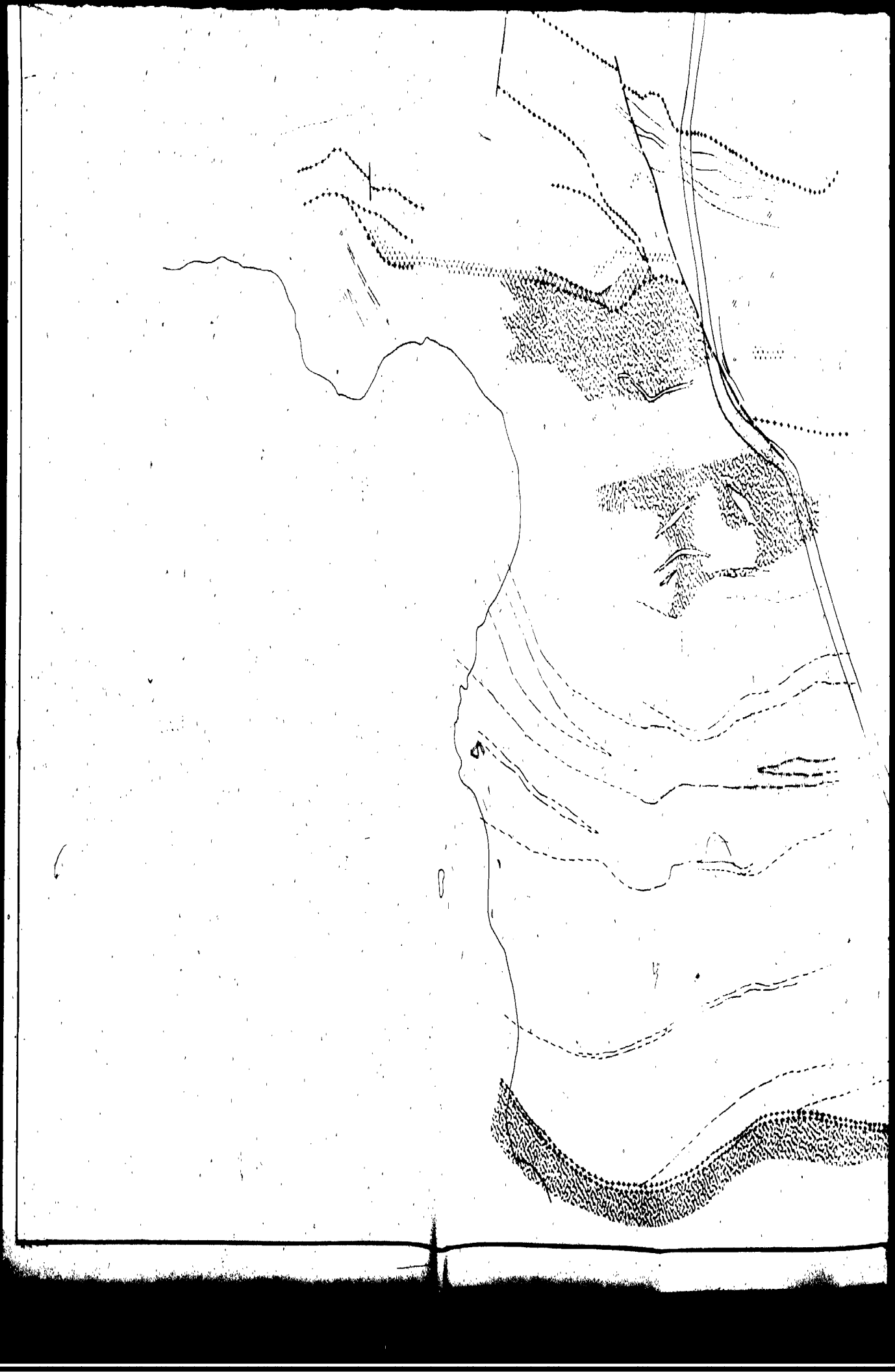

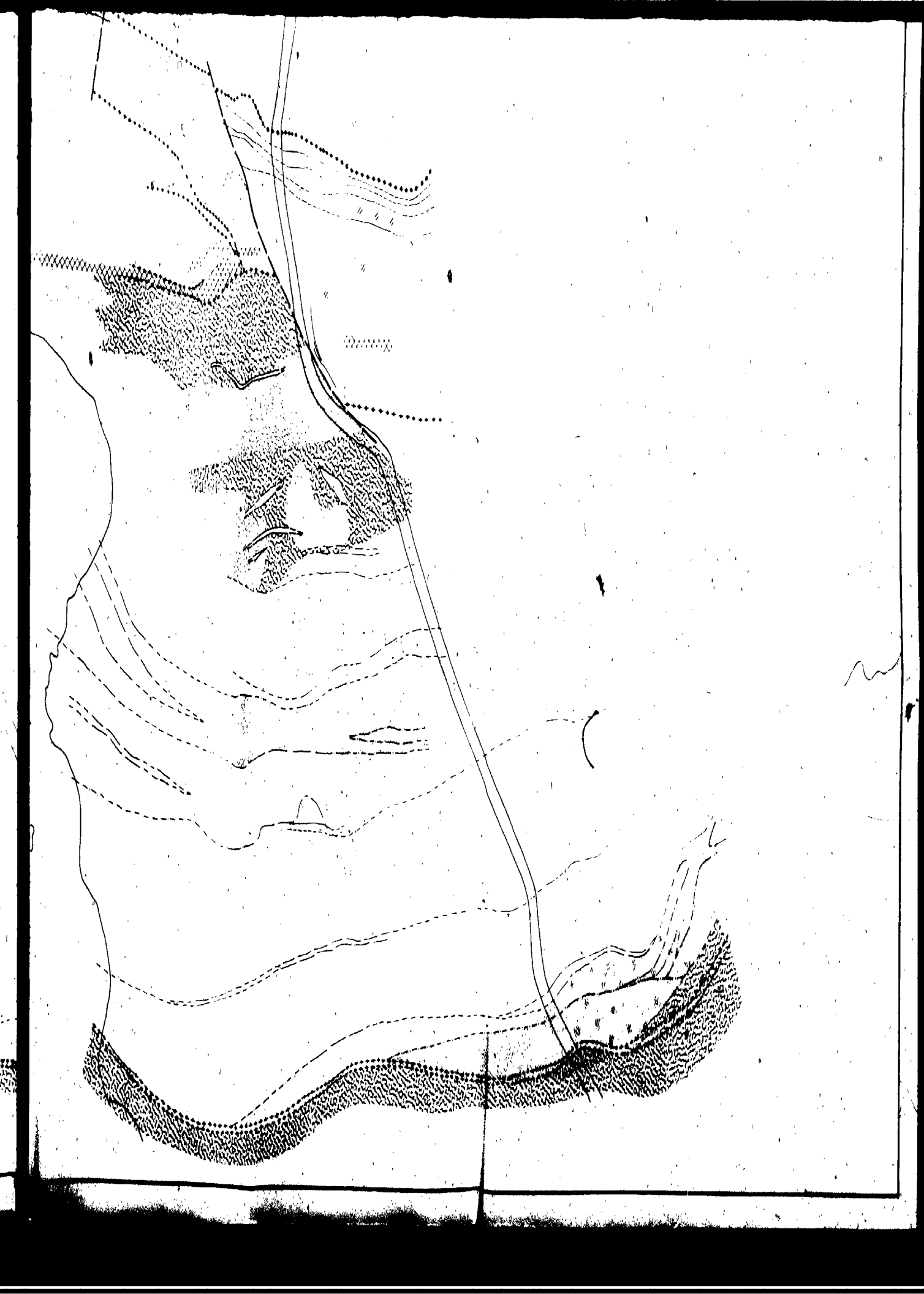

# 4 of/de 4

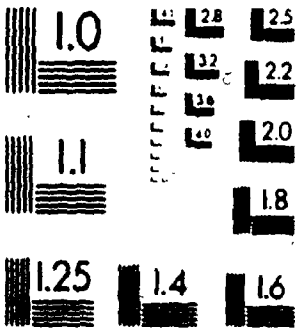


MicroR

Figure 4

# SAMPLE LOCATION MAP

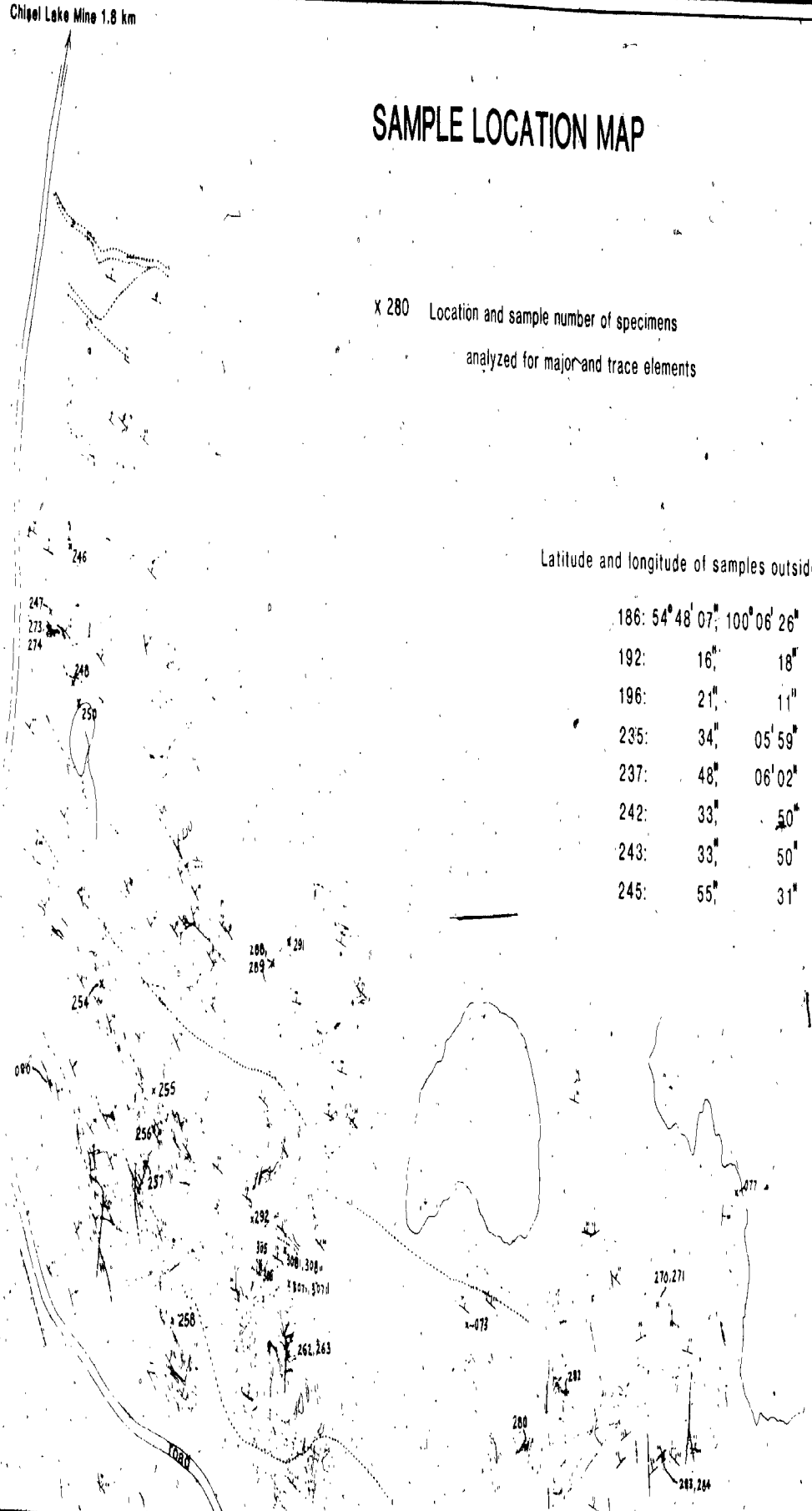


250
235: 34"; 05' 59"
237: 48"; 06' 02"

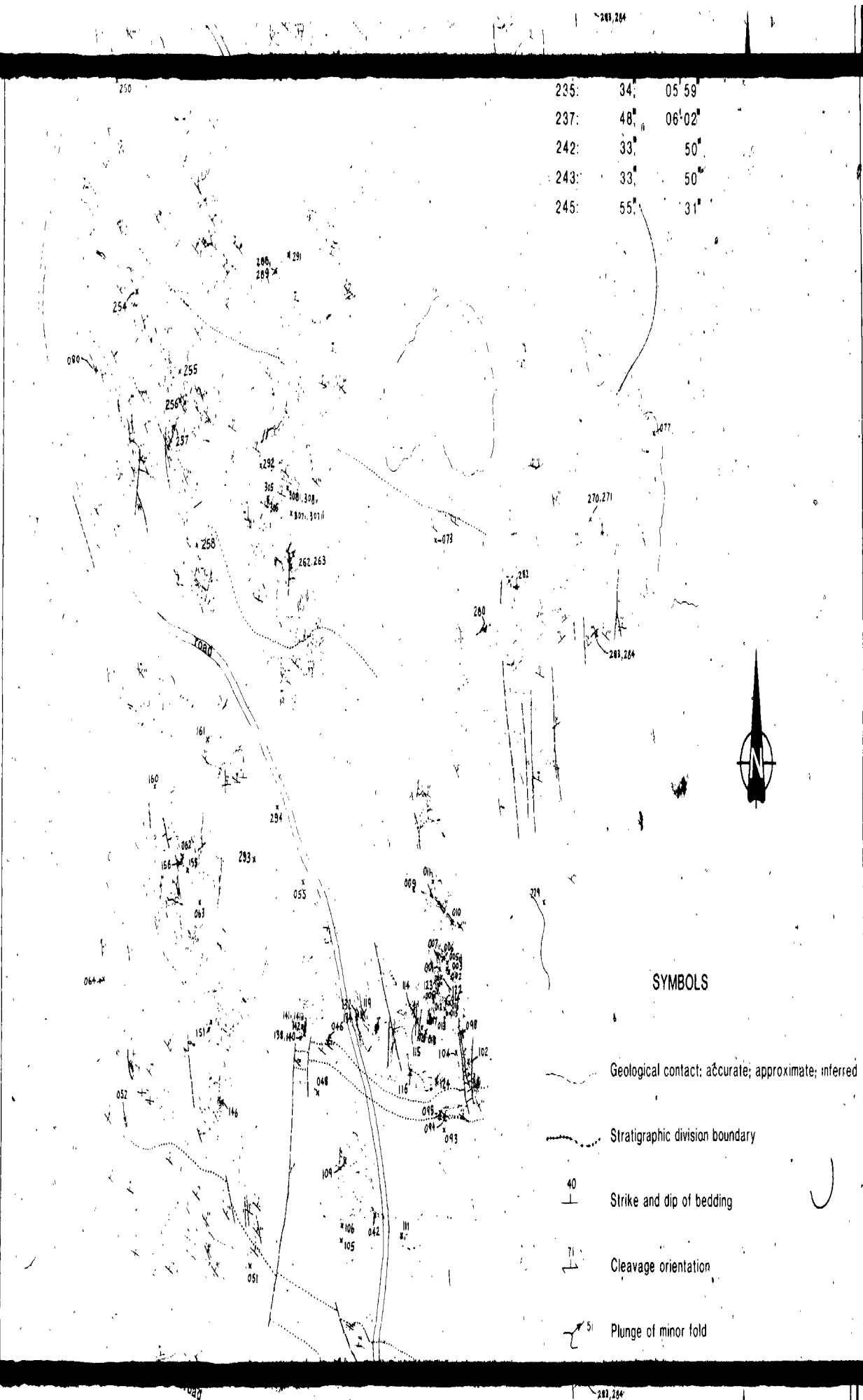
283,284
235: 34" 05 59"
237: 48" 06 02"
242: 33" 50"
243: 33" 50"
245: 55" 31"
road
262,263
270,271
SYMBOLS
Geological contact: accurate; approximate; inferred
Stratigraphic division boundary
40
Strike and dip of bedding
71
Cleavage orientation
51
Plunge of minor fold

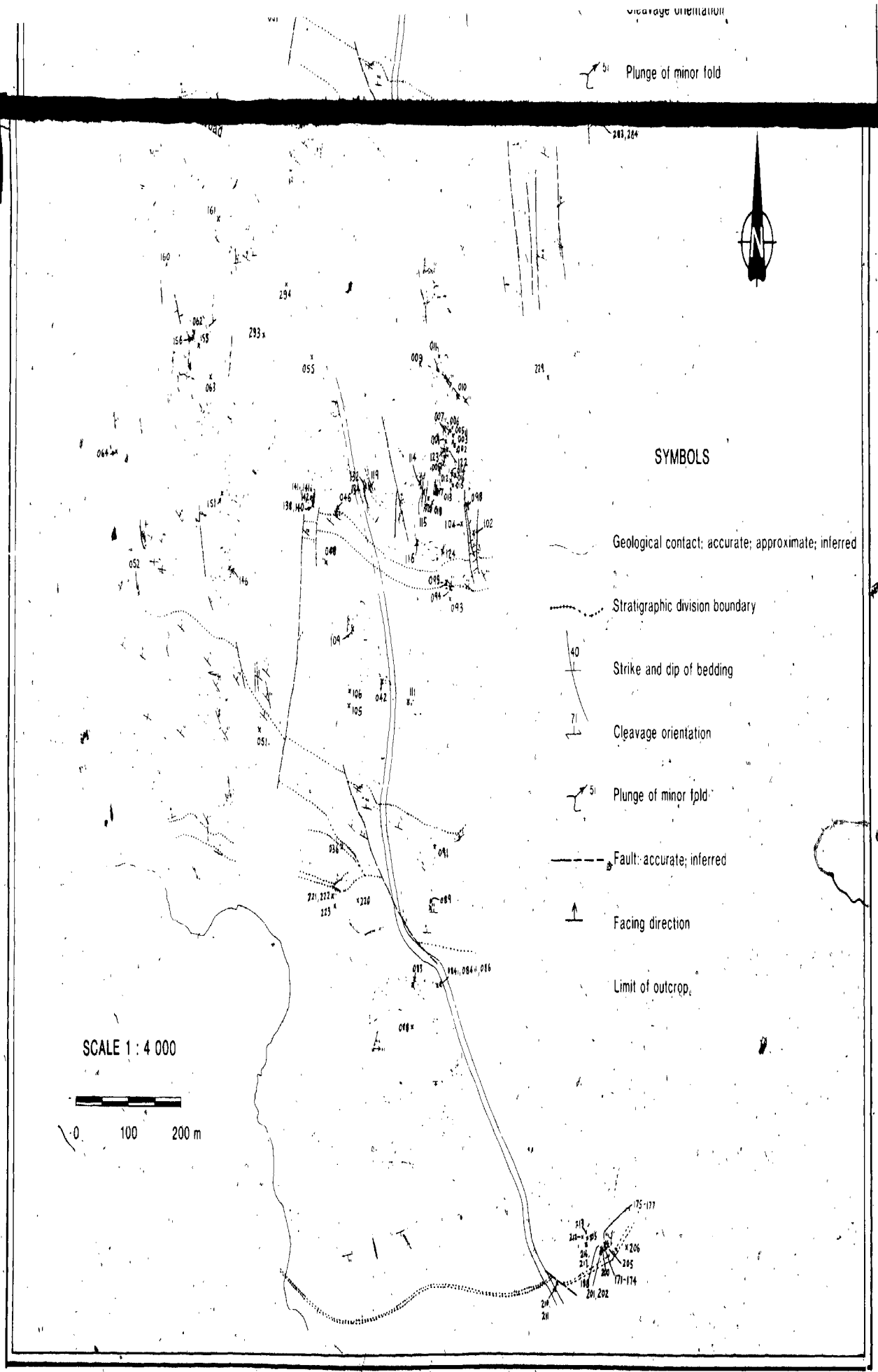
Cleavage orientation
Plunge of minor fold
SYMBOLS
Geological contact; accurate; approximate; inferred
Stratigraphic division boundary
Strike and dip of bedding
Cleavage orientation
Plunge of minor fold
Fault: accurate; inferred
Facing direction
Limit of outcrop
SCALE 1 : 4 000
0
100
200 m

# END

# 05·01·88

# EIN